Control and management strategies of smart grids with high penetration of renewable energy

Elvira Amicarelli

Communauté
UNIVERSITÉ Grenoble Alpes

THÈSE

Pour obtenir le grade de

DOCTEUR DE LA COMMUNAUTE UNIVERSITE GRENOBLE ALPES

Spécialité : **Génie électrique**

Arrêté ministériel : 7 août 2006

Présentée par

Elvira Amicarelli

Thèse dirigée par **Quoc Tuan TRAN** et
codirigée par **Seddik BACHA**

préparée au sein du **Laboratoire de Systèmes Electriques Intelligentes du CEA-INES** et **du Laboratoire de Génie Electrique de Grenoble INP**
dans **l'École Doctorale Electronique, Electrotechnique, Automatique & Traitement du Signal.**

Stratégie de gestion des réseaux électriques à fort taux de production renouvelable distribuée

Thèse soutenue publiquement le **16 Octobre 2017**,
devant le jury composé de :

M. Jean Paul GAUBERT
Professeur, Université de Poitier, Président

Mme Zita VALE
Professeur, Institut Polytechnique de Porto, Rapporteur

Mme Manuela SECHILARIU
Professeur, Université de Technologie de Compiègne, Rapporteur

M. Phuong NGUYEN
Assistant Professeur, Université technique d'Eindhoven, Examinateur

M. Quoc Tuan TRAN
Professeur, INSTN, CEA-INES, Directeur de thèse

M. Seddik BACHA
Professeur, Université de Grenoble-Alpes, Co-Directeur de thèse

M. Nicolas MARTIN
Ingénieur de Recherche, CEA-INES, Invité

CONTENT

LIST OF FIGURE

LIST OF TABLE

ABSTRACT

In 2007 with the renewable energy directive, the European Union established the development of a low-carbon economy. This directive aims to decrease greenhouse gas emissions by increasing the energy produced by renewable energy. Already today, the massive diffusion of renewable systems is tangible in the European electricity mix. However, in spite of their potential benefits, their large-scale integration leads to new technical and regulatory questions. Consequently, new management strategies need to be developed and applied in order to ensure a reliable and economical operation of the system. Microgrids are considered to be one of the most effective and flexible solutions able to meet these new needs.

The main goals of this thesis are the conceptualization, development and implementation of different management strategies for microgrids. The algorithms developed aim to facilitate the massive integration of renewables and at the same time lead to an effective and economic operation of the systems. A new architecture of distribution grids based on cluster of microgrids was proposed. Each microgrid is composed of a number of renewable-based and conventional generation systems, storage systems and consumption. An optimal and distributed energy management strategy was then defined and developed. This strategy allows to manage the short-term energy management and real-time control of microgrids by using the connected sources in a smart and cost-efficient way. A multi-agent system and the mixed integer linear optimization technique were used for the implementation of this strategy.

From a global point of view, each microgrid is seen as a coherent entity, which can support network operation by using its flexible and aggregated sources. Hence, the second part of this thesis aims to understand how distribution grids can exploit these cluster of microgrids and their properties. Different mechanisms for the active management of distribution grids are conceptualized from the technical and economical point of view. A new strategy based on hierarchical management of different smart levels allow to reduce the complexity of the system and to implement a more flexible and extensible system, thanks to a more local use of model knowledge and users behaviour. On the end, the theoretical work were tested on an experimental test-bed in order to show the effectiveness of the proposed theories.

RESUME

En 2007 avec la directive sur les énergies renouvelables, l'Union Européen s'est engagée à développer une économie à faible intensité de carbone. Cette directive amène à réduire les émissions de gaz à effet de serre en augmentant entre autres la partie d'énergie produite par des sources renouvelables. Le processus d'insertion massive d'énergies renouvelables dans le mix électrique européen, est d'ores et déjà un fait acquis et ses effets sont tangibles. Cependant, à côté de ses effets environnementaux bénéfiques, l'intégration à large échelle du renouvelable ne va pas sans causer des interrogations techniques et réglementaires. Par conséquent, de nouvelles stratégies de gestion du système électrique doivent être pensées et actées pour garantir un fonctionnement fiable et économiquement acceptable. Les microréseaux sont à cet effet, un réceptacle intégrateur avec suffisamment de flexibilité pour accueillir un système de gestion capable de répondre aux exigences ci-dessus.

Les travaux de cette thèse sont centrés sur la conception, le développement et l'implémentation de différentes stratégies de gestion des microréseaux. Les algorithmes développés visent, soit à faciliter l'intégration du renouvelable à large échelle, soit à garantir un fonctionnement efficace et économique du système électrique. Une nouvelle architecture de réseau de distribution composé de microréseaux clustérisés a été premièrement proposée. Chaque microréseau est composé de systèmes de production à base ou non de renouvelable, des systèmes de stockage et de charges. Une stratégie de gestion énergétique optimale a été ensuite définie et développée. Cette stratégie permet de gérer la planification à court-terme et le contrôle en temps-réel des microréseaux via un usage adéquat des sources et ce, tout en réduisant le coût du microréseau. Un système multi-agents et l'optimisation linéaire mixte en nombres entiers ont été utilisés pour le développement et l'implémentation de cette stratégie intelligente distribuée.

D'un point de vue extérieur, chaque microréseau est vu comme une entité cohérente capable de supporter le fonctionnement du réseau principal en utilisant un ensemble de ses sources flexibles. Ainsi, que la seconde partie de cette thèse exploitera les clusters des microréseaux et leurs propriétés pour gérer au mieux le réseau de distribution hôte. La conceptualisation technico-économique de différents mécanismes de gestion des réseaux de distribution a été abordée.

Le développement d'une architecture de gestion hiérarchisée en plusieurs niveaux d'intelligence a permis de réduire la complexité du système et faciliter l'implémentation d'un

réseau flexible, extensible et à fort taux de pénétration de renouvelables. Cette gestion distribuée a été possible grâce à une connaissance locale des modèles et des comportements des différentes systèmes connectés, et à un usage local des informations. Les travaux théoriques ont été ensuite testés sur une plateforme expérimentale conséquente et les résultats finaux ont corroboré les attentes de la théorie.

ACKNOWLEDGEMENT

In general, I would like to thank all people who encouraged and supported me from both technical and human point of view during these three years of intense work. I am thankful for all enriching and valuable conversions, which increased and contributed to my technical maturity and my ideas.

In particular, I want to thank both my supervisors M. TRAN Quoc Tuan and M. BACHA Seddik for choosing me as candidate for this thesis, for dedicating me their time and for guiding and advancing me with their valuable experience.

I am also grateful for the financial support received by the CEA – INES, where I conducted this work. I want to thank M. MARTIN Nicolas our leader in the group of Smart Energy System for the support and the enthusiasm who incited me to work hardly and serenely. A special thanks also for the leader of S3E, M.me PERRIN Marion for her precious support.

I also want to say thank to all members of jury. I am particularly grateful to professors M.me VALE Zita and M.me SECHILARIU Manuela for accepting to report my thesis and for their advices, comments and questions, and to M. GAUBERT Jean Paul to participate as president to my defence. A last thank to M. NGUYEN Hong Phuong for hosting and supporting me during my enriching exchange with the Technological University of Eindhoven and for examining my work.

And last but not least, I would like to thank my family, my friends and my collegues for their constant encouragement and presence.

I. GENERAL INTRODUCTION

I.1.Energy Scenarios: Opportunities and Challenges

The use of various forms of energy contributed to exponential development of the human quality of life during the last two centuries. During this societal growth, fossil fuels have driven all energy-based technologies. Since, the coal-era advent, the world's demand for electricity continued to escalate and has continued to do so till date. In fact, statistics affirm that during the next few decades the social and industrial development of China will induce a tremendous growth in China's electricity demand; greater than the total current demand in the United States of America and Japan taken together [1]. Furthermore, the diffusion of new electricity-based technologies, such as electrical vehicles, will increase the electricity demand in industrialized regions, such as Europe and United States as well which will lead to an overall proliferation of electricity demand in the world.

The increase in electricity consumption is an important factor which impels to think and plan judiciously the amount and the type of energy resources to use in the future. Moreover, increase in consumption combined with pressing topics like global warming, availability of resources and electricity costs are also driving politicians and scientists around the world to find solutions to these impending threats.

In fact, the use of conventional energy resources is repeatedly questioned because of its numerous harmful implications on the society and environment. The reliable and economical accessibility of these resources have become a cause of concern for many countries around the world. In fact, fossil fuels are located only in restricted regions in the earth and are subjected to political agreements and relations. Their availability and price often reflect political tensions between important geographical regions, and pose a huge risk for both developed and developing countries alike. Moreover over the last decades, extraction of conventional fuels have become increasingly harder and often led to huge debate between governments, environmentalists, extraction companies and health experts. Discussions on reserve-water pollution and man induced earthquakes due to shale gas extraction is a current example.

Furthermore, the analyses of the consequences of climatic change are generating huge public and political awareness and inciting in these actors the need to take actions in this aspect. Exclusion of environmental factors can no longer be afforded while taking political

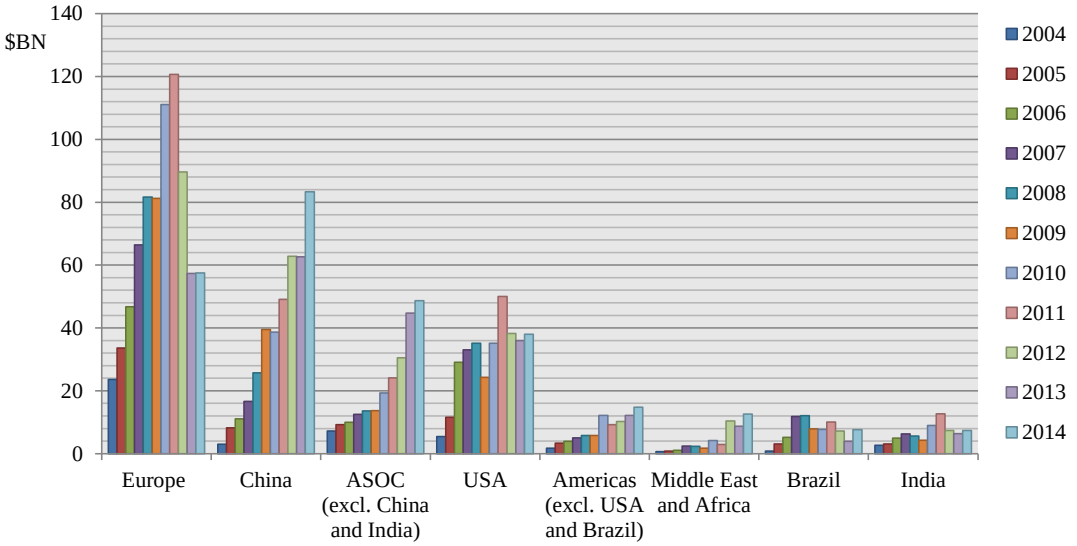

Fig. I.1 Total investments in RES by region between 2004 and 2014 [2]

and economic decisions. Hence, many developed countries have decided to fix a climate goal in order to limit the earth from warming more than 2 °C. In 2016, the carbon dioxide emissions from the electricity sector in USA alone had amounted to about 1 million and 800 thousand metric tons, which accounts for about 35% of the total emissions in USA [3]. Furthermore, statistics suggest that a huge part of these emissions originate from coal based technologies [3].

In Europe, critical scenarios in conventional energy resources and the frightful projections in climate change are subjects of great public concern. Hence in 2007, the EU established the development of a low-carbon economy in order to challenge this fuel-based economy and limit greenhouse gas emissions. The EU energy directive takes action not only on the increase in Renewable Energy Sources (RES) in the production mix but also focuses on the increase in energy efficiency. Between 2004 and 2013, the EU countries efforts can be seen by considering their investments. Statistics estimates that they had invested around 600 billion $ in renewables and fuels growth especially by policy support [4]. The amount of investments by region between 2004 and 2014 are resumed in Fig. I.1. These investments financed both utility-scale projects and small-scale distributed systems. So far, Europe has been the pioneer and leader in providing financial incentives for renewable energy. Europe reached its investment peaks in 2010 and 2011 by investing around 110 billion $ and 120 billion $, respectively [2]. During the last five years, Europe was followed and surpassed by China, which has experienced an unprecedented boom in its renewable energy sector and has invested more than 200 billion $ between 2012 and 2014 [5]. Chinese investments focused

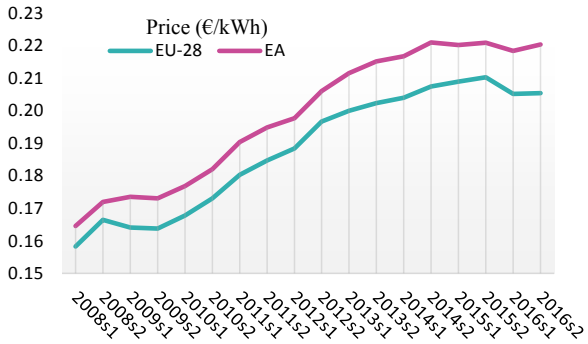

Fig. I.2 Evolution of EU-28 and EA electricity prices for household consumers [6]

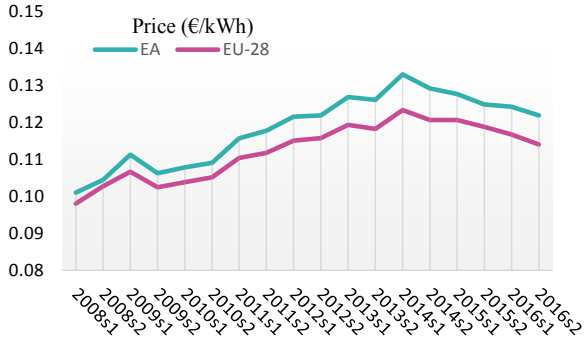

Fig. I.3 Evolution of EU-28 and EA electricity prices for industrial consumers [6]

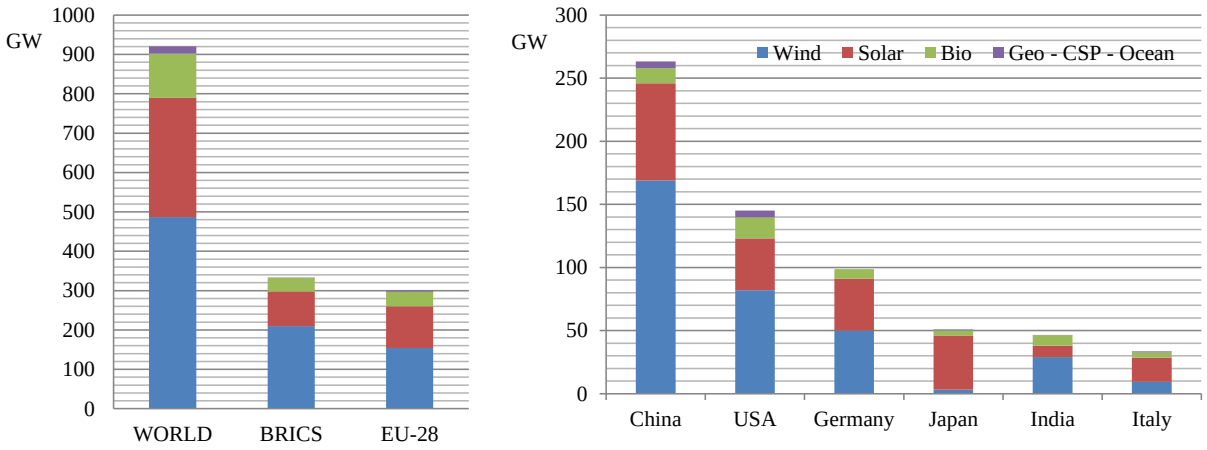

Fig. I.4 Statistics on renewable energy sources installed capacity in 2016 per sources in the world, in EU-28 and in BRICS [7]

more on utility-scale (more than 1MW) solar systems making about three quarters of the global solar investment [2].

However, in 2016, the European Commission roadmap fixed new targets to move towards a competitive green economy in order to decrease the total European greenhouse gas emissions to around 80 % - 95 % of the 1990 levels by 2050 [8].

During the last few decades, the factors and actions mentioned above have added to the increase in the electricity cost. In fact, European statistics, depicted in Fig. I.2 and Fig. I.3, highlight an increasing trend of electricity prices for both household and industrial consumers, which led to an increase of around 10 % in the price of electricity in the last five years.

The radical development in the energy sector has been given different names like “Energy Transition” in English, “Transition Energétique” in French and “Energiewende” in German. Since the beginning of the energy transition, these economic policies have allowed a huge increase in RES installed capacity whose growth has assumed an increasing trend by setting a new record of 921 GW in 2016 [7], as shown in Fig. I.4. During the last few decades, the lar-

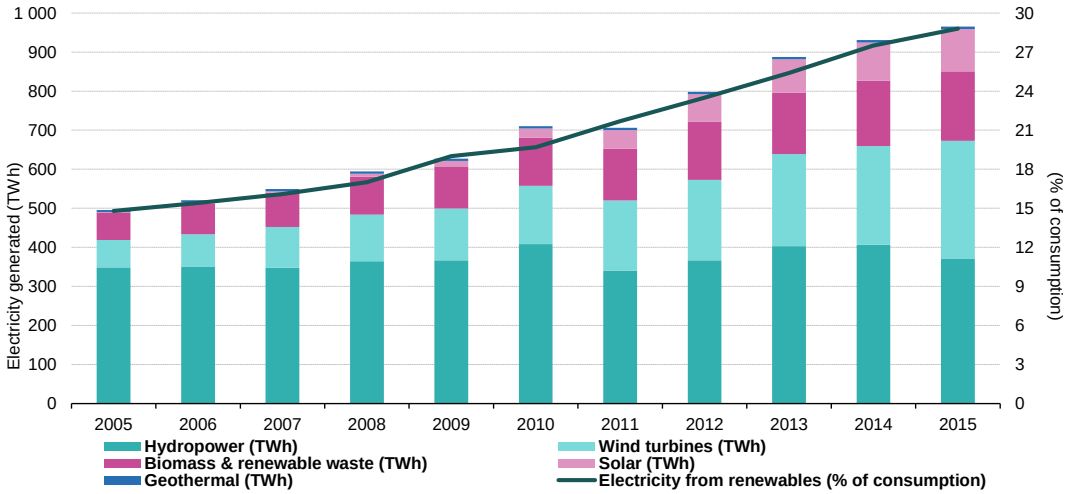

Fig. I.5 Trend in electricity generated by RES in EU-28 from 2005 to 2015 [9]

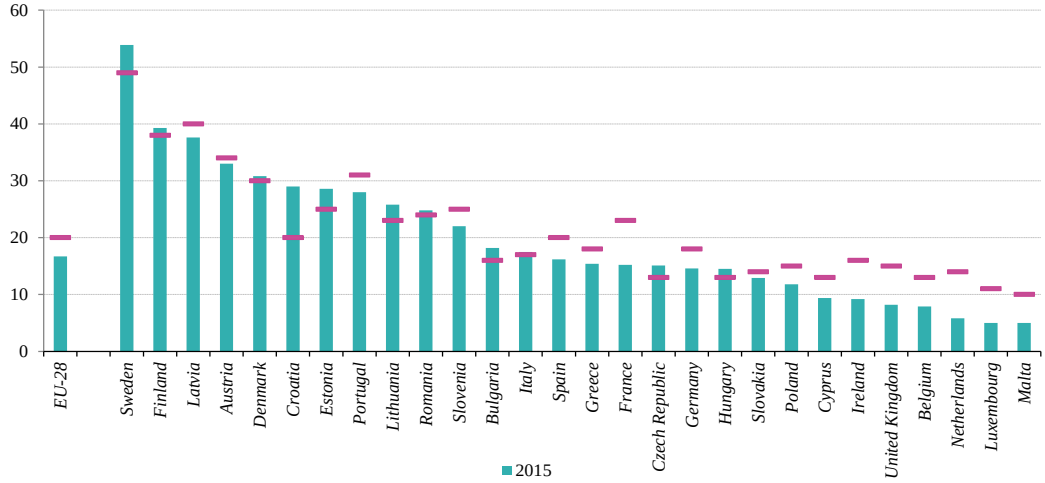

Fig. I.6 Percent share of renewable energies in gross final energy consumption in 2015 for European country and fixed targets for 2020 [9]

gest part of new annual installed capacity in the world is composed of RES. Already by the year 2016, the new installed power of RES has reached 161 GW, which is equal to around 62 % of the total added power plants [7]. It was estimated that this installed capacity would be able to supply about 24.5% of global electricity needs [7]. Statistics on RES as capacity per source in the world, in Europe and in BRICS[1] are resumed for the year 2016 in Fig. I.4. These statistics do not take into account hydroelectric technologies, but simply new emerging technologies (solar, wind, bio-fuel, geothermal and marine systems).

In Europe since 2005, the electricity generated by RES rapidly increased and in the year 2015, it increased by 14% (Fig. I.5). The 28 European countries participate with around the 32.6 % of the worldwide installed capacity (Fig. I.4). Furthermore, this graphic shows that

[1] BRICS is an English acronym used to refer to five major emerging national economies: Brazil, Russia, India, China and South Africa.

Germany and Italy RES in Europe had succeeded to satisfy 16.7% of the total gross consumption of the 28 European countries, which is very close to the 20% target fixed as objective for 2020. The amount of consumption supplied by RES increases to 28.8 % if hydro-power is added (see Fig. I.5). However, the situation is extremely heterogeneous among the various European Union member states. Hence, the participation of RES in the gross energy consumption for each European country in 2015 is resumed in Fig. I.6. This percent value is then compared with the fixed targets for 2020. Among the different EU member states, the highest RES participation in consumption supply is obtained in northern countries with a record of 53.9 % in Sweden [9]. In 2015, countries such as Sweden, Finland, Croatia and Estonia had already attained their targets for 2020. However countries like France, Netherlands and United Kingdoms are still to reach their targets and require to increase their share of renewables in gross final energy consumption by at least 7.8 %, 8.2 % and 6.8 % percentage points [9].

Also as underlined in Fig. I.4, the greatest interest was directed at solar and wind based technologies. In 2014, 92 % of the total global RES investments all over the world represent subsidies for these resources [5]. In the year 2005, the share of production RES in gross consumption of Europe was covered for more than 70% by hydroelectric power. Their exponential growth was essentially launched as a result of gigantic efforts in technological growth, which led to a reduction of installation cost.

Until now, wind turbines covered the main growth in installed RES power. More than 50 % of installed capacity worldwide was covered by wind-based systems (Fig. I.4). In the year 2015 in Europe, hydroelectric covered around 38.4 % of the gross consumption whereas solar and wind participated with 11.2 % and 32.3 %, respectively (Fig. I.5). However nowadays, photovoltaic systems (PVS) are considered to be the most up-and-coming solution in all energetic projection until 2050. In fact, the International Energy Agency (IEA) has envisioned in its roadmap for PV technology that the global photovoltaic electricity production in the world will rise up to 16% by 2050 [10].

Support-policies and the phenomenon of economies of scale are making these technologies more and more competitive with respect to conventional technologies for power plants applications. In fact, the cost of electricity produced by solar energy has been continuously dwindling in recent years. The costs of PV cells and modules were subjected to a rapid fall from 4 $/W in 2008 to 0.8 $/W in 2012 [10]. The IEA provided PV price scenarios up to 2050. In these scenarios the levelized cost of electricity (LCOE) is estimated to diminish by

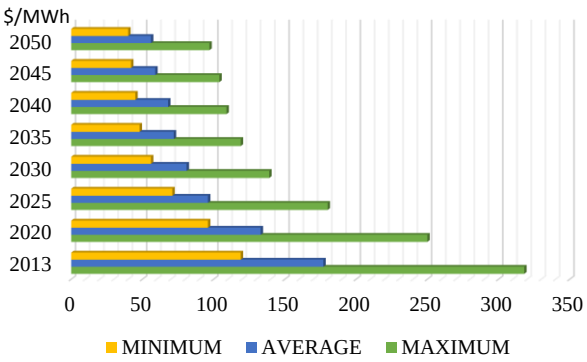

Fig. I.7 Levelized cost of electricity projections for utility-scale PV systems to 2050 (data from [10])

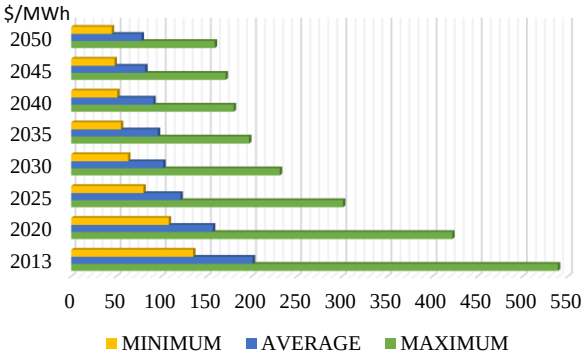

Fig. I.8 Levelized cost of electricity projections for rooftop PV systems to 2050 (data from [10])

around 65% from 2013 to 2050 for both utility and small scale consumers [10], as shown in Fig. I.7 and Fig. I.8. In the year 2014, an average levelized cost of electricity of 133.0 $/MWh was estimated for utility-scale PV plants for 2020 [10]. However, statistical studies show that the most optimistic estimations have already been met for large-sized PV systems as in the case of PV installations in south of Italy where an average LCOE of 55.0 $/MWh was attained by the end of 2016 [11], by suggesting a radical diffusion in next ten years.

I.2.Electrical Grids with High Penetration of RES

As discussed in section I.1, the massive penetration of RES into the electricity grid is already tangible in the European electricity mix and it has turned into a cause of concern for different European grid operators. Despite their potential environmental and economic benefits, large-scale integration of RES leads to new technical and regulatory issues in order to ensure a reliable and economical operation of the entire electrical system.

Often the variability, intermittency, and unpredictability of solar-driven resources, such as wind and irradiation have posed as constraints and decelerated the massive RES diffusion. However, their widespread availability and low energetic density, combined with the numerous economic incentives, have induced a diffusion throughout the sector of small and medium-sized RES. Consequently, a new term was coined to describe this new situation: Distributed Generation (DG).

Currently, no unique definition on how a DG should be exists in literature. However, researchers and industries have agreed on basic characteristics of DGs. They are small-sized power generators or storage systems, which typically range from a few kW to tens of MW,

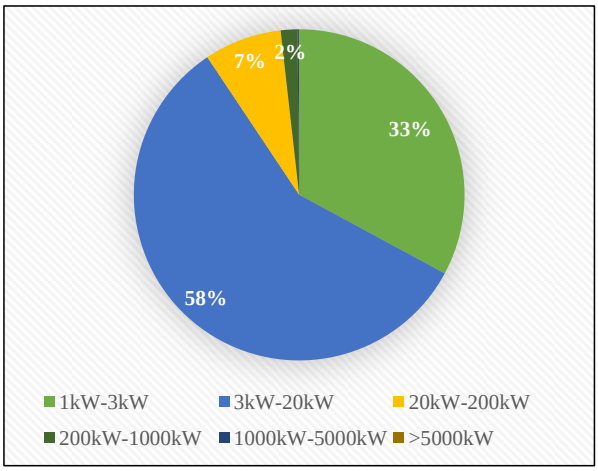

Fig. I.9 Number of PV plants per size in Italy [12]

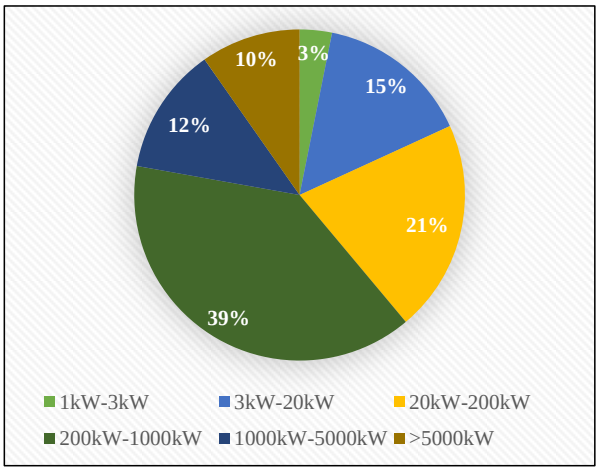

Fig. I.10 Installed capacity of PV plants in Italy [12]

and they are not part of a larger power system [13]. Moreover, they are typically installed close to the consumption and they can be operated connected or isolated from the main grid [13]. The CIGRE working group stated some robust and representative characteristics in order to classify a power system as a DG. In general, the power of a DG must be smaller than 10–50 MW [13].

Furthermore, due to their size they are usually connected to the distribution network and they are not planned or dispatched in a centralized way [13].

In fact, in Europe, more than 90% of solar and wind systems are connected to distribution grids [14]. Moreover, if analysis focuses especially on photovoltaic plants, this percentage is even higher. The Italian case could be taken as an example. In 2014, the number of installed photovoltaic plants accounted to 648,418, corresponding to a total power of 18.6 GW [12]. Furthermore, analysing in detail the statistics diffused by the *Gestore Sevizi Energetici* revealed that the PV systems with a power greater than 5 MW correspond around 0.03% of the total number PV systems installed which represents 9.7 % of the total installed power. On the contrary, systems with an installed power lower than 1 MW represent 99.8 % of the total number PV systems installed and constitute 77.8% of the total national installed power. Pie charts in Fig. I.9 and Fig. I.10 promptly show these statistics on both installed capacity and number of PV systems.

This large diffusion of small DG already places distribution system operators (DSO) at the core of the energy transition. Until now, DSOs have had the obligation to assure the grid access to RES-based DGs and also to absorb all the produced energy by RES (except in emergency cases) [15]. Hence, DSOs today are confronted by new tasks and roles. In fact traditionally, the role of distribution was to locally distribute electricity in order to feed small

and medium sized consumers through medium and low voltage networks. Medium and low voltage networks have traditionally been passive with unidirectional energy flux, leaving the TSOs the role to ensure energy balance between consumption and production. This distributed electricity was centrally produced by large-sized conventional systems, such as nuclear and coal power plants, and supplied by high voltage lines to distribution grids.

In theory, due to their proximal location to consumption, DG should positively contribute to an efficient system management. DG may reduce transmission and distribution power losses by limiting long-distance transport, help to improve power quality and security of supply, reduce grid investments by decreasing peak load and congestions, and so on. However, in practice, renewable-based DGs induce various negative impacts on distribution grids operation, such as feeders' voltage variation, issues in protection and automation systems, increase in short circuit currents, undesired islanding, etc.

In general, DGs confer an extremely heterogeneous architecture to distribution grids, due to their variability in type, size and location. Distribution grids are not passive anymore and are becoming bidirectional in terms of energy fluxes. Voltage variation is one of the most important impacts to be considered. DGs induce voltage profile variation in the supplied feeder, which no longer represents a linear descending line from the substation until the last supply point. Furthermore, this voltage variation can also be significant with respect to the point of power injection by DG as it could accelerate insulation damage in network components as well as exceed permissible technical standard limits.

In one of the first reviews on DG impacts, authors discussed a reasonable rule-of-thumb according to which shared feeders among DG and consumption in secondary level, even a small generator that injects about the 5% of current at the primary level could cause a voltage regulation risk to customers sharing the feeder [16]. Briefly, majority of the medium voltage radial grids are mainly regulated by using an on-load-tap-changer in the substation transformer, which responds to current variations and is able to increase/decrease the secondary voltage with steps of 1.5% of the rated nominal voltage and within a range of ±15% of the rated nominal voltage. The heterogeneous architecture does not assure the performance of this strategy. Cable reinforcement through wider cables could also be seen as the solution for voltage issues [17]. However in order to increase the utilization rate of grids, this centralized solution needs to be combined with local actions.

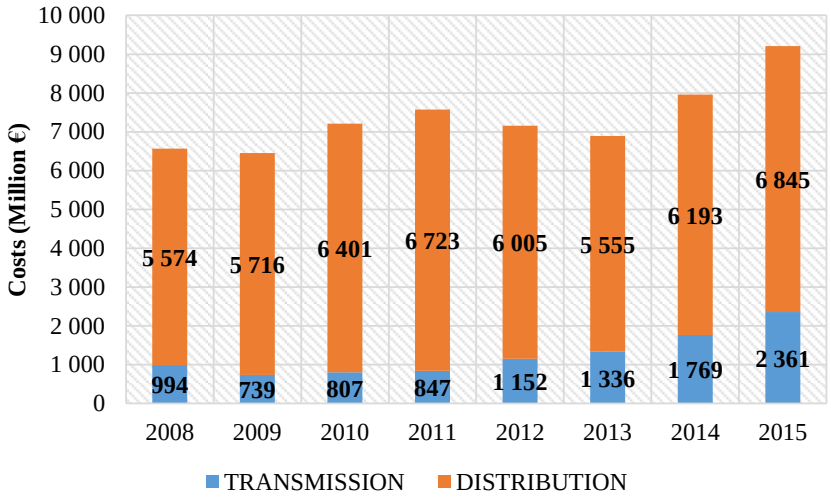

Fig. I.11 German investments in distribution and transmission power grids [14]

Another factor to be considered is that DGs are only partially dispatchable. This is mainly due to their variability and stochastic intermittence. Hence, although they are closer then power sources connected to the high voltage networks, they are not always located in close proximity to the elements that are consuming and often their production does not coincide with the local power demand. For example, the power peak of small and medium size of residential and commercial users occurs in the late afternoon hours when PV is not available or is simply at the end of its daily production cycle. The asynchronisation between load and generation, combined with their non-dispatchability, makes DGs hardly useful for constrained grids support and congestions might also occurs. Hence, the need to oversize the distribution grids for peak load remains and the capital expenditure for grid reinforcement also rapidly increases in case of densely populated feeders of DGs. Reinforcements and expansion of distribution grids in order to increase the hosting capacity of RES requires huge investment costs and extensive planning analysis.

Germany is undergoing a massive RES integration and the level of investment has risen in recent years and is estimated to continue to grow in the future [14]. As divulged by the Federal Network Agency in October 2016, Fig. I.11 shows the investments made in Germany for new constructions, expansions and maintenance for both transmission and distribution networks. In 2015, around 3.8 billion € [2] were invested for the expansion of distribution grids [14]. The increase in CAPEX may induce higher connection costs for DG's owners [17] and/or higher grid tariff for passive[3] users [14]. In general throughout Europe, the investment

[2] Expressed in short scale.

[3] In this thesis, the term passive is used to indicate users/systems that are absorbing energy. On the contrary, the term active is used to indicate users/systems that are injecting energy.

needs for the distribution sector will be much higher than for transmission grid and represents around 80% for the German case [8], as also observed in Fig. I.11.

The large-scale integration of RES into distribution grids is not the unique issue related to power system modernization. In recent years, RES subsidies, such as Feed-in Tariffs and quota obligations mainly based on Green Certificate, have been key support mechanisms to help foster RES and integrate them into the electricity system. Feed-in Tariff schemes acted as economic incentives to RES producers and were independent of the electricity market price fixing mechanism. New schemes, such as Feed-in Premiums, have also been introduced in order to test the introduction of high and medium sized RES in the electricity market. In fact, in the long term, large scale renewable-based plants have to be integrated into the electricity market, while maintaining an economically competitive structure. However, what will happen if the amount of energy produced by small and medium sized generators reaches a high value? Hence, solutions for market access (forward or wholesale) of these systems are discussed in the literature, e.g. in MASSIG Project [18].

In general, the integration process of intermittent, variable and partially dispatchable sources into the power system will first and foremost require the exploitation and development of new active strategies which exploit flexible elements, such as energy storage and demand-response. The revision and evolution of current regulations have to be carried out as well and the two solutions have to go hand in hand in order to ensure technical as well as economical robustness of the future electrical system.

Storage systems can facilitate the access of renewables into market and grid applications by addressing the uncertainty of availability of resources and providing capability to supply the contracted scheduled power and/or energy. Moreover, they can also mitigate the aforementioned asynchronisation between consumption and production. Both stationary energy storage systems (ESS), such as stationary batteries or fly-wheels, and mobile systems, such as electrical vehicles, are expected to play an important role in this energy transition. Currently in the overall European electricity system, only around 5 % of the installed production capacity is installed as storage capacity and the storage park is mainly composed of pumped hydroelectric energy storage [8]. The required storage capacity will change based on different scenarios of RES mix in the total production capacity. However, a range between 43 GW and 90 GW of storage capacity is expected to be introduced for European scenarios by 2050 with estimated investments between 80 Billion $ and 130 Billion $ [8].

For stationary applications, various systems are available in the current market. All these technologies have different characteristics and performances, costs, specific power and energy, maximal capacity, energy density, efficiency, lifetime, and so on. Electrochemical systems are considered to be the most interesting technology for small and large scale applications in the electrical system. In fact, they have high specific power and energy, high efficiency and they are modular, which allows a flexible use. Moreover, they have much shorter installation periods when compared to hydroelectric pumping stations, and they can be installed almost everywhere and especially in close proximity to many connection points of renewable power plants. Li-ion technology is the most promising technology among the various electrochemical systems, thanks to their performances. In the next few years, their large integration will depend on their economic competitiveness. The Li-ion based battery costs is expected to drastically decrease. Since 2007, it started to fall by about 14% each year [19]. Already by 2014, Li-ion pack costs were below the average projected costs for the year 2020 [19]. Authors in [19], projected optimistic and pessimistic scenarios in Li-ion costs trend for electrical vehicle applications by analysing data from multiple sources available in the literature. According to these scenario, the average cost will be between 150 $/kWh and 250 $/kWh in 2025.

The second core element of flexibility in this energy transition is the consumption. Traditionally, the consumption has been almost entirely considered inelastic. However in recent years, smart use of power demand is considered a helpful and efficient program to manage RES variability and intermittence. Hence, in the literature several studies are proposed. In Scotland, authors affirmed that the available demand capacity for power flexibility is around 5% of the global available demand for the evaluated scenario (1700 MW peak) [20]. Furthermore, up to 15% of the rated fan power of a HVAC system may be employed for grid services, without impacting the occupants' comfort [21]. More detailed studies have shown that the available flexibility can also be more than 15% if used for a limited timeframe. For example, results indicated that a reduction between 30% up to 60% in the air-supplied fan power could be applied for around 120 min without compromising indoor air quality [22]. In practice, the use of flexibility offered by power demand response has started to be reinforced into current regulations. For example in France through the new TURPE, new mechanisms were actuated in August 2017 in order to reinforce the temporal economic signals which aim to influence and control the consumption peaks. The first new

mechanism, the mobile tariff option on the HV network (20 kV), would encourage erasure of load during national peak load periods.

The combined use of distributed generators with these flexible systems by implementing advanced management and control functionalities is nonetheless a required capability in order to guarantee a reliable and economic integration of these multi-technology systems into the power system and in order to implement active management strategies for its operation. A promising way to implement these management and control capabilities on a national scale lies on a coordinated and systematic approach of sub-systems, known as the microgrid concept [15].

I.3. Research Approach and Thesis Contributions

This thesis draws its inspiration from the energy transition movement and its evolution context, one where electrical grids will be soon populated by numerous small and medium sized distributed sources.

In particular, this work is driven by many questions still open to be explored, such as:

- *Can the functional architecture of microgrids guarantee interoperability among various technologies? And how?*
- *Can users respect their self-interests and privacy and at the same time work in a collaborative way?*
- *Can a microgrid be seen as a coherent and controllable structure from the exterior?*
- *Are microgrids flexible and controllable elements?*
- *Can several microgrids collaborate by respecting their willingness to participate and different technical behaviours?*
- *How does microgrid react in real-time when participating in electricity or service markets?*
- *Can microgrids contribute to a smart and active management of grids?*
- *Which basic information are required to be shared?*
- *…*

Hence, this thesis aims to conceptualize, develop and implement new management strategies for electrical grids in order to facilitate the high penetration of RES. The massive

RES penetration requires development of technical solutions and to understand how the electrical system can exploit users' flexibilities. Actually, on one side, these solutions have to be able to manage the complexity of this new smart system and make it flexible and extensible and on the other side, these have to lead to an efficient and economic operation of the system.

The main contribution, which is also the main difference with other solutions proposed in the literature, lies on the decentralization of the decision-making process through the development of a distributed multi-level sling process. This process allows microgrids to integrate in electricity and/or services market by delocalizing tasks and information, while on the same time respecting the constraints imposed on each level. Hence, in this distributed framework various components are modelled and an optimal energy management strategy at microgrid level is defined and developed. This strategy allows to manage the short-term energy management and real-time control of microgrids by using the connected sources in a smart and cost-efficient way. In a second step this smartness is introduced also in the higher levels of the hierarchy in order to implement the mechanisms for the active management of distribution grids that were conceptualized.

I.4. Thesis Contents and Organization

The contents of this thesis are structured in five main chapters which follow this brief introduction, as resumed in Fig. I.12. Each chapter deals with different subjects, aspects and questions, as follow:

- Chapter II aims to introduce the current state of the art in the development of smart grids, with a strong emphasis on the concept of microgrid, its technical issues, dissemination and perspectives. Special attention is also given to discussions made on centralized and distributed strategies for microgrids' management and control. A distributed version of smart grids which proposes a multi-microgrid architecture is discussed as a solution for smart management of numerous distributed renewable systems, storage systems and flexible loads in a system. Finally, multi-agent systems are presented. Their main characteristics and benefits are discussed and their abilities to implement and simulate complex systems, such as multi-microgrid systems, are analysed.
- Chapter III focuses on energy management strategies for microgrids. Each microgrid is composed of a number of renewable-based and conventional

generation systems, storage systems and consumption. Hence first of all, a functional architecture to implement a distributed management is proposed and implemented. After that, two algorithms for an efficient and cost-efficient schedule of microgrid's energy resources are defined and developed, based respectively on logic-rules and optimization techniques. These strategies are implemented and discussed through case studies, in order to compare them and to underline the different advantages and disadvantages of both the strategies.

- Chapter IV focuses on the management strategies for a distributed multi-microgrid system. In particular, it aims to understand how distribution grids can exploit these clusters of microgrids, their properties and flexibilities. Two mechanisms for the active management of active distribution grids are conceptualized from both the technical and economical point of view. Also in this chapter, the implemented strategies are tested and discussed through simulations. Moreover, the distributed strategies proposed are then compared with a centralized strategy in order to test the effectiveness of the approach proposed.
- Chapter V concerns the implementation of a real-time control strategy for microgrids in order to manage all schedule uncertainty due to renewable sources and consumption. Finally, the implemented control strategy is tested on an experimental test-bed in order to validate and show the effectiveness of the algorithms proposed.
- Chapter VI is the conclusive chapter, in which global considerations, results and comparison between different developed strategies are discussed, and in particular with regard to prospective future research based on advantages and weakness of the conducted work.

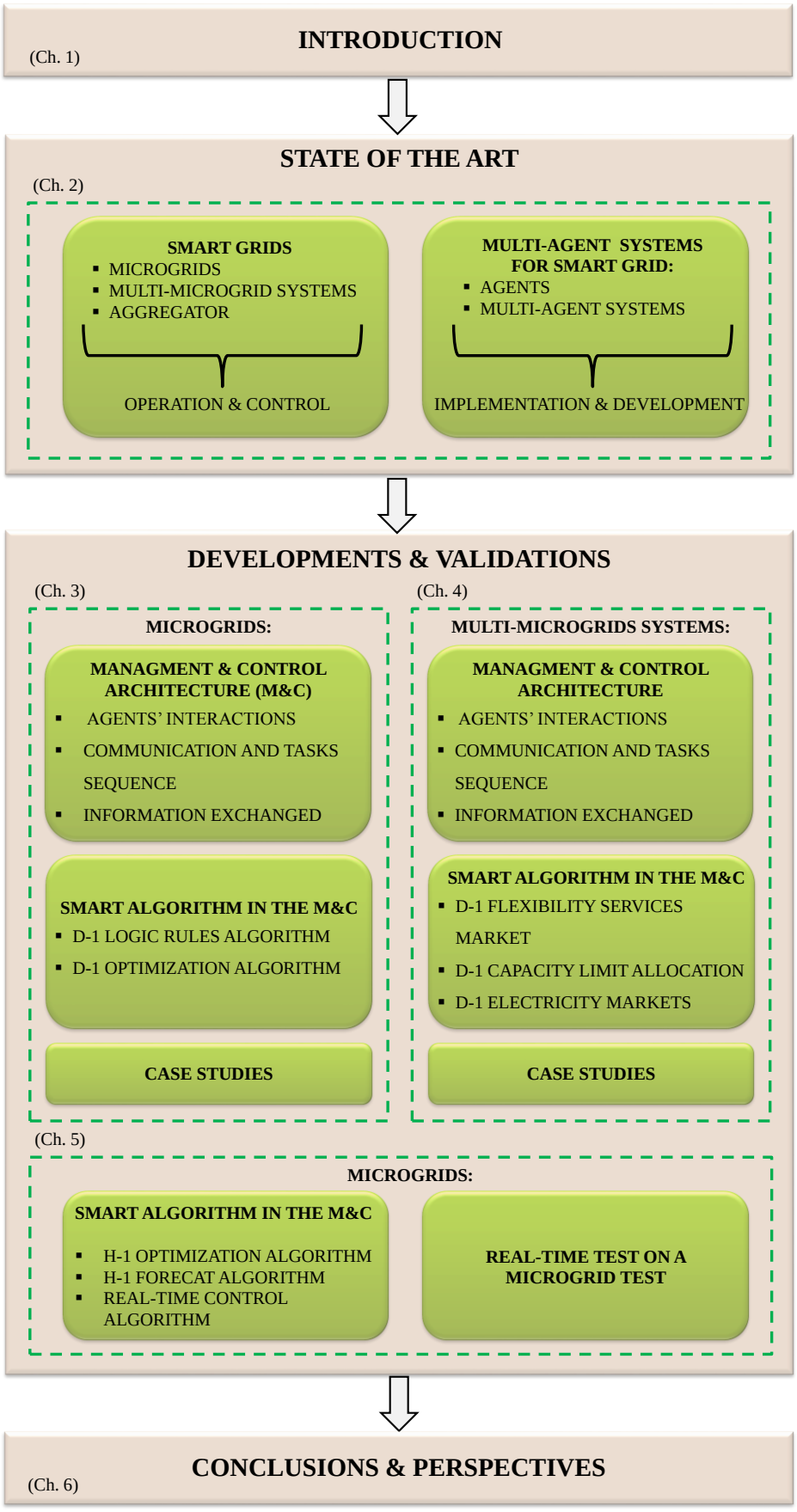

Fig. I.12 Summary of thesis organization

II. TOWARDS SMART AND FLEXIBLE ELECTRICAL GRIDS: ARCHITECTURE AND MANAGEMENT STRUCTURE OF MULTI-MICROGRID SYSTEMS

II.1. Introduction

Smart Grids are an emerging solution to meet the challenges of the current energy system by providing reliable electrical supply to end users, high power quality, and integrating distributed generation like solar, wind, combined heat and power, in electrical grids. The main idea on which the concept of smart grid is based and which distinguishes the smart grid from the current passive grid with penetration of DGs is the capability to manage, coordinate and control connected resources.

Small RES and consumers, such as households or commercial facilities, have not enough capacity to be directly traded in electricity markets or to be used as flexibilities to resolve critical grid situations. Moreover, consumption at this level and renewable sources are more variable and difficult to predict compared to higher size aggregated sources. Consequently, a coherent organization of a number of DERs, ESSs, flexible and inflexible loads needs to be defined.

Operation and control of this new grid structure, based on Microgrids and Aggregators, is a technical challenge that requires the development of new distributed, efficient and cost-effective strategies. These strategies have to be capable to support network operation by deploying user flexibilities and have to be apt for an extendable and scalable system. An up-and-coming approach to design and develop complex distributed system as smart grid is the multi-agent system.

The main objective of this chapter is to introduce and discuss main issues regarding development and key elements of smart grids implementation; i.e. its building blocks, its architecture and its management and control methods.

II.2. Microgrids: The backbone of Smart Grids

II.2.1. Concept and Characteristics

The development of active and intelligent networks requires the design and the development of new systems associated with the existing framework. Microgrids defined by

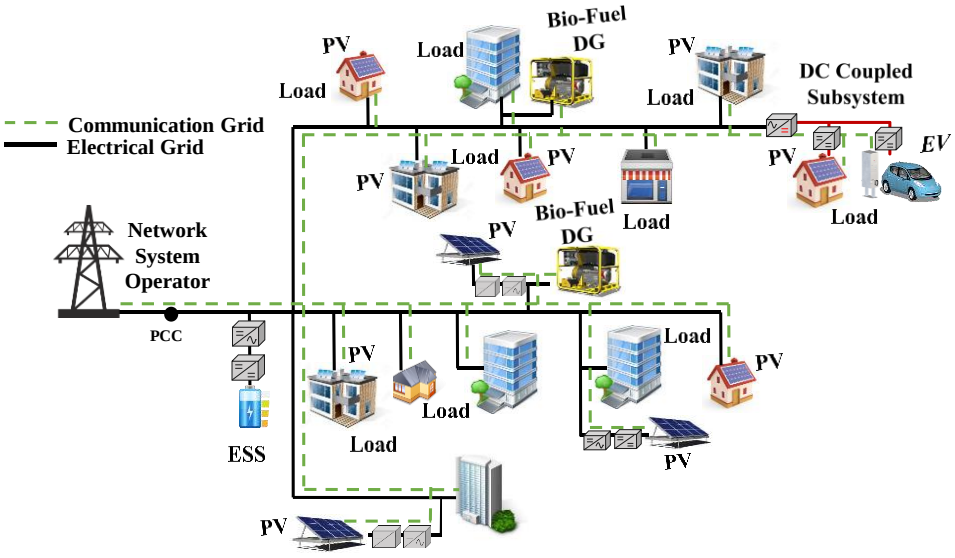

Fig. II.1 Example of microgrid

Schwaegerl and *Tao* in [15] as a fundamental "building block of smart grid", are probably the most promising novel structure of grids. Microgrids and their characteristics are still an open subject of research.

Nowadays, a lot of definitions are proposed in various reports and journals by research organizations all over the world. A significant one that can clarify some important questions about components, architecture and operation of microgrids, was proposed by researchers and industrials working in two EU projects [23] [24]:

"Microgrids comprise low voltage distribution systems with distributed energy resources (micro-turbines, fuel cells, PV, etc.) together with storage devices (flywheels, energy capacitors and batteries) and flexible loads. Such systems can be operated in a non-autonomous way, if interconnected to the grid, or in an autonomous way, if disconnected from the main grid. The operation of micro-sources in the network can provide distinct benefits to the overall system performance, if managed and coordinated efficiently."

A microgrid is a powerful tool for the integration of DGs, ESSs and DR, while continuing to serve the satisfaction of local inflexible demand as its primary goal. The mix and the size of components installed in a microgrid is a complex issue that depends on user's needs, choices, regulation and economics issues. Both renewable and conventional sources can be used in microgrids. The primary and secondary transducers of generators can be connected either directly to the grid by electrical rotating machines or can be interfaced by inverters. The

components of a microgrid need to be located close or within the same local network which can be more or less large.

In general microgrids are operated at the Low Voltage (LV) level. However, there are no limits on its maximal size and its components. Although there can be exceptions and parts of Medium Voltage (MV) network can belong to a microgrid [15]. In fact at the "Innovative Smart Grid Technologies Conference", authors proposed that [25]:

"Microgrid can be defined as a low to medium voltage network that contains aggregation of certain loads and distribution generation units, which is connected to the main grid system through a point of common coupling. It can operate in either grid-connected or islanded mode. In grid mode it remains connected to the main grid and is seen as a single aggregate load or source, while in the islanded mode it separates from the main grid, due to a major disturbance, becoming self-sustained and continues to serve certain loads."

Consequently, majority of the DGs are constituted of small-sized units with power less than 200 kW[4]. Otherwise, a Microgrid can have a large variety of sizes, starting from an entire MV/LV grid, to a LV feeder or just a single LV house. At European level, the maximum capacity of a microgrid (in terms of peak load demand) is limited to few MW [15]. It is clear that microgrids with numerous heterogeneous components need to be more intelligent and use more sophisticated equipment and management and control strategies. At higher voltage and power levels, the concept of multi-microgrid systems is applied and discussed in section II.3.

Microgrids may be able to work in two modes of operation: grid-connected and islanded mode. During grid-connected mode, flexible users are expected to supply or consume pre-specified amount of energy to rationally dispatch their resources in a cost-effective way. Power balance between consumption and generation, as well as frequency control, are guaranteed by the main grid. Whereas in islanded-mode, DGs production and ESS injections have to meet the load demand at every time instant by fast and flexible voltage and frequency control strategies. These strategies need to be implemented as well via the active and reactive power management of flexible resources. Except for microgrids built far away from the main grid, such as military fields, physical islands or remote areas, microgrids with main grid access operate in normal functioning in grid-connected mode for economic and reliability

[4] In many regulations, such as in Italy, the power of 200 kW corresponds to the maximal power that can be connected in LV grid, according to the technical reference rules for the connection of active and passive users to the grid [196].

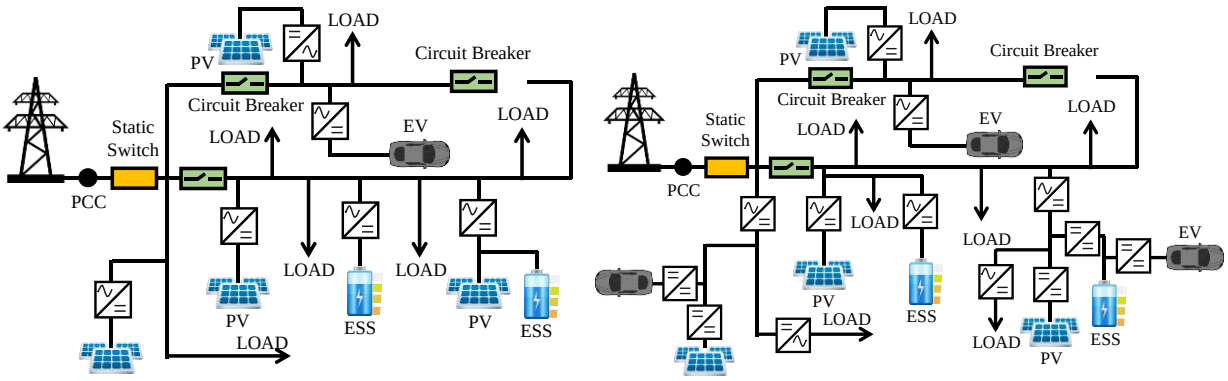

(a) AC Architecture *(b) Hybrid AC–DC Architecture*

Fig. II.2 Examples of microgrid architectures

reasons and the islanded mode is employed only in emergency case [15]. However, the choice of mainly operating mode will influence the components sizing, requiring frequent oversizing of DGs, ESSs and DR to ensure continuity of operation.

Another fundamental parameter to be discussed is the architecture of microgrids. In general, microgrid's architectures can be essentially classified into three main groups based on the way in which components are connected: AC-microgrid, DC-microgrid and hybrid AC–DC microgrid [26] [27]. The choice of architecture is influenced by different factors:

- Generators output signals
- Economic factors
- Microgrid services
- Quality constraints.

In fact in microgrids, various generation systems are connected. These systems can differs from the types of output power, such as direct current (DC) for PV systems and alternating current (AC) for bio-diesel generators, which influence grid characteristics and architecture. As mentioned previously, the mode of operation strongly impacts the economic expense and influences the choice of components and their sizing. Furthermore, microgrid objectives and services provided to users and grid operators are important factors which influence the type and size of installed components, and indirectly the architecture. Microgrid architectures are also influenced by the type of applications, such as military, industrial, residential or commercial purposes. Several architectures are proposed and discussed in the literature.

The AC-microgrid architecture is the most discussed and tested in industrial and research applications. This configuration allows an easy integration with existing distribution networks. These microgrids consist of radial structures with one or several AC feeders where all components are connected to. DGs, such as PV, and ESS need to be connected through DC/AC power electronic interfaces such as inverters as depicted in Fig. II.2. During normal operating conditions, microgrids and the main grid are interconnected at the Point of Common Coupling (PCC). The static switch is in charge of microgrid transition from grid-connected operation to islanded operation and circuit breakers deals with microgrid reconfiguration [26]. This architecture was proposed and tested by the Consortium for Electric Reliability Technology Solutions (CERTS) [28] in Cleveland (Ohio). During their studies and tests based on a radial three-feeder grid with loads, RES-based DGs and combined heat and power, CERTS demonstrated the economic benefits, reliability and robustness of microgrids operating in islanded mode. Moreover, microgrids like Holiday Park in Bronsbergen (Netherlands) developed in the framework of several European projects, such as MOREMICROGRIDS [24] [29] and INCREASE [30], and University of Genoa Smart Polygeneration Microgrid in Genova (Italy) [31], proved the technical feasibility of this concept and opened doors to a massive deployment.

On the contrary, microgrids containing one or more feeders in DC constitute DC-microgrids. Normally, the main grid continues to be fed in AC and this requires an AC-DC converter to be installed between the microgrid and the main grid at the PCC. This configuration may need less conversion stages reducing energy losses, providing higher overall efficiency, and there is no circulation of reactive power in the microgrid [32]. Moreover, there is no need for synchronization of DG that leads to simpler control strategies [32]. However, depending on their technical characteristics and on the voltage level of the main DC bus, DC/DC or AC/DC power electronic converters may be required to ensure the correct operation of various loads, generators and storage devices. Generally, most of the household appliances, such as microwaves, ovens, washing machines and dishwashers, need to be fed in AC. Because of efficiency and economic reasons, this kind of architecture is more suitable for industrial applications with DC loads, such as refrigeration industry or EV fleets, or for multi-source production centres, such as hybrid wind and solar electric systems. In the framework of MOREMICROGRIDS project, CESI RICERCA proposed a test DC microgrid in low voltage (400 V) DC connected to the medium voltage network (23 kV) to monitor

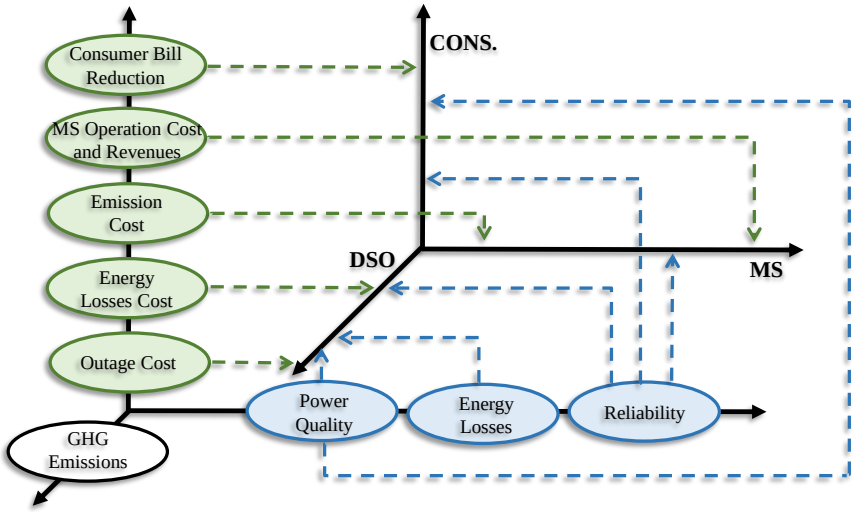

*__Legend__: DSO: Distribution System Operator; MS: Micro-Sources; CONS: Consumption

Fig. II.3 Benefits of Microgrids Diffusion and Impacts on Electricity Sector Stakeholders (inspired by picture in chapter 7 in [15])

power quality and to test control and management strategies for DC configurations [33].

Hybrid AC–DC configuration, as that of in Fig. II.2 (b), inherits characteristics and advantages from both architectures analysed above. In fact, this kind of architecture allows increasing efficiency by reducing multistage conversions and facilitates the direct insertion of DC-based technologies. Moreover, when the number of DC components is substantial, the economic feasibility of hybrid microgrids results higher than AC configuration [32]. On the other hand, this architecture requires a more complex management, because of the simultaneous control of AC and DC devices [32].

II.2.2. Operation and Control

Optimal operation of resources in microgrids can have several economic and technical benefits for all stakeholders in the electrical system: consumers, suppliers and network operators. At the same time, the optimal operation of resources plays an important role in the reduction of Greenhouse Gas (GHG) emissions [15]. For briefly, all these possible benefits are summarised in Fig. II.3. From the user's point of view, microgrids may provide both electrical and thermal needs using efficiently and cost-effectively all local resources while supporting an eco-friendly production and enhancing local reliability and power quality.

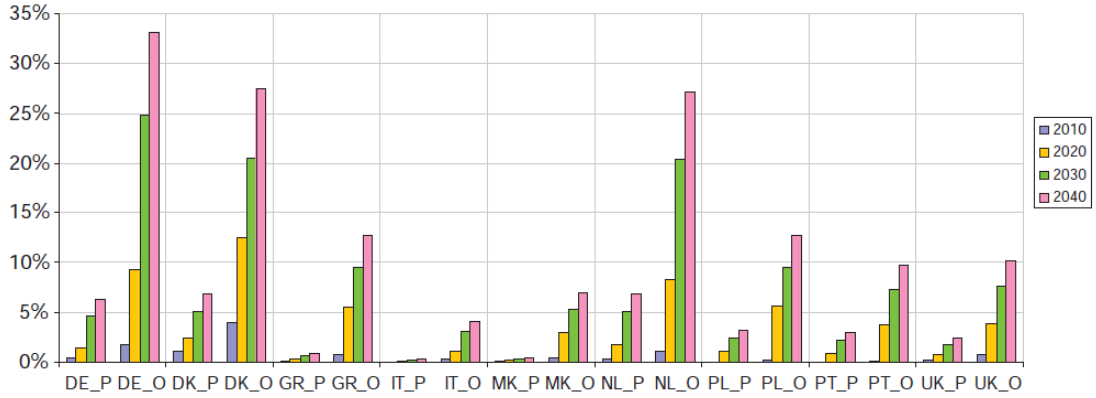

*__Legend__: O = optimistic assumptions, P = pessimistic assumptions). (DE=Germany, DK=Denmark, GR=Greece, IT=Italy, MK=FYROM, NL=The Netherlands, PL=Poland, PT=Portugal, UK=United Kingdom

Fig. II.4 Evolution of microgrids scenarios for years 2010, 2020, 2030 and 2040 and for country [15]

Moreover, island mode of operation enhances supply reliability during periods of fault in the main grid. From the grid operator's and aggregator's point of view, a microgrid can be seen as a coherent controlled entity that can be operated as a single units supporting network operation, e.g. using flexible components such as demand response and micro-sources, to decrease energy loss, increase network hosting capacity or support congested grids.

All these benefits will push DSOs, consumers and energy suppliers to install more and more microgrids. Statistics estimates their rapid diffusion in power systems in some European country, such as Germany and Netherlands, for the next coming years. Schwaegerl and Tao in [15] propose scenarios about microgrid dissemination for years 2010, 2020, 2030 and 2040 satisfying 10%, 20%, 30% and 40% of their own demands by RES and bio-fuelled heat-driven combined heat and power units, respectively (reported for simplicity in Fig. II.4).

However, the implementation, management and control of microgrids remain a challenge due to technical, regulatory and market challenges. From a technical point of view, each microgrid is a complex system which contains not only small-sized components using different technologies, but also multiple decision makers, with interests and needs that conflict and compete. This leads to a challenging management with high communication requirements and computational complexities. Another important challenge concerns the design of protection systems which need to respond to both main grid and microgrid commands in case of fault to move from grid-connected to islanded operation. From regulatory and market point of view, it is fundamental to reorganize roles and responsibilities in the electrical system. Small-sized systems need to be more aware of the impact of their

activities and be integrated into markets. Market mechanisms have to be extended to microgrids increasing competitiveness which will decrease costs, and these mechanisms will also create new services markets.

Operation of microgrids is one of the most crucial challenges these days in terms of the Smart Grid concept. New management and control capabilities have to be developed. These smart capabilities will be the key feature that distinguishes microgrids from distribution networks with DGs. The study of microgrid optimal management and control approaches have to take into account different parameters and constraints proper of the microgrid, such as operation mode, users' goals and needs, and sometimes also limits due to existing infrastructure. The primary elements to consider are how and where the decisions are made, the applied strategy (collaborative or competitive) and the information shared among the elements in the system. The control and managment configurations can be categorized in: Centralized, Decentralized and Hybrid approaches.

A centralized configuration is suitable in case of collaboration among microgrids elements where they have one or more common goals. A typical example is an industrial microgrid with a single owner that aims to operate the system in the most economical way. In this case, the central controller is able to continuously monitor the system, knows all the constraints about its process and can entirely control all its micro-sources and consumptions. This configuration relies on a central manager and controller that gathers data through smart meters and has a global knowledge about affiliated components. The central manager is the decision maker, which performs the required calculations and determines the control actions for all the units in the microgrid. This approach requires extensive communication between the central manager and controlled units [34]. The strong coupling among components permits to reach the overall optimal management and control of the microgrid, minimizing the overall operational costs and controlling the more appropriate resources. The major weakness of this configuration lies on the extensive communication needs, which requires to cover extended geographic areas, big data treatment and analysis, and high computation needs in case of extended microgrid with more than hundreds of components. Moreover, an in-depth understanding of the system, which implies a low level of privacy for the users and also an extensive knowledge of component models, are additional conditions to implement

centralized management of microgrids. Furthermore, these characteristics make the system not easily extensible.

On the other side, a decentralized configuration is suitable in case of several dominant decision makers with different or competitive objectives to satisfy. In fact, decentralized means every participants in the system is a decision maker. Hence, each participant makes a decision by following its own behaviours and needs. At the end, the resulting system behaviour is the aggregated response of all the single responses, in the same manner of human's groups where each one makes constrained decisions, while these decisions influence everyone around. In this configuration each unit is controlled by its local controller, which only receives local information and is neither fully aware of system-wide variables nor other controllers' actions [34]. This approach benefits of lower (or null) knowledge needs and it is suitable for microgrids heterogeneous in components and with users' profiles and constraints difficult to predict. For example, it is extremely complicated to model both the comfort requirements in a complex of apartments and available flexible appliances, such as washing-machines, and include all their constraints (time-of-use, interval of flexibilities, etc.) in a single optimization problem. Also, this solution requires lower computational capacities and communication requirements by locally solving complex constraints or sub-problems. On the other hand, it is not possible to find a global optimal functioning point but only many local optimums.

A hybrid or distributed configuration is a compromise between the two approaches analysed above whose characteristics depend on design choices. The main principle is that the process is shared between multiple elements with a well-known hierarchy of the system. Decisions can be taken in different levels and by different decision makers using part of the system knowledge.

II.3. Multi-Microgrid Systems

The massive implementation of active microgrids, will be a critical challenge for electrical grids that will require new management and control strategies. A new grid architecture based on multiple distributed microgrids is known as Multi-Microgrid System [23].

A multi-microgrids corresponds to a high-level structure, formed at MV level, whioch comprises a number of LV microgrids, DG and consumers connected to adjacent MV feeders, as in Fig. II.5 [15]. Each microgrid, MV DG and MV consumer constitute the active cells of

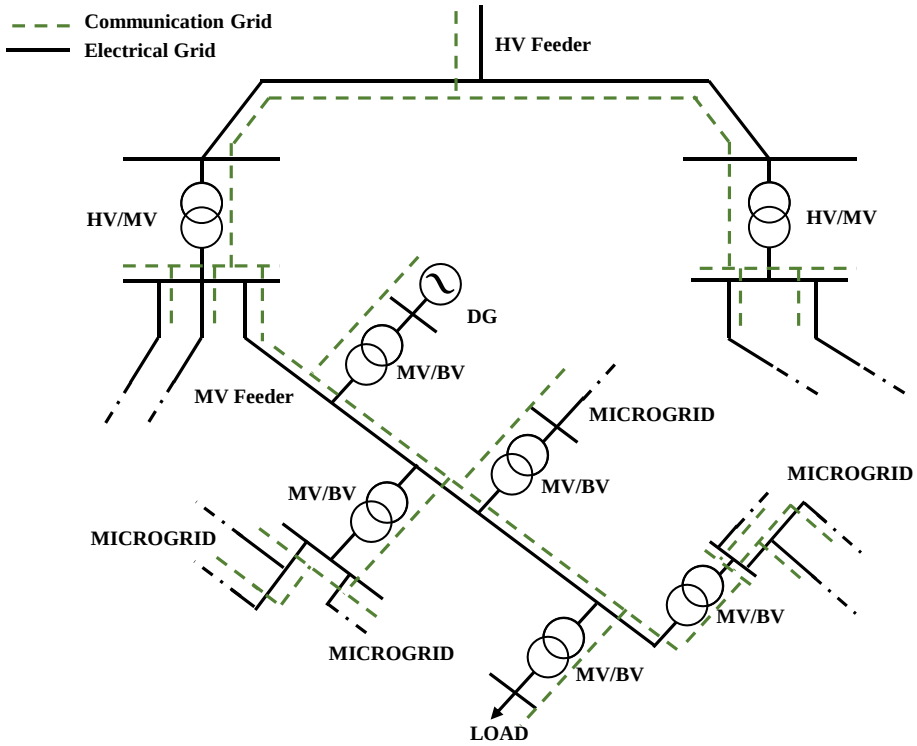

Fig. II.5 Multi-Microgrid System (inspired by figure in chapter 5 in [15])

new power systems in which each cell can supply flexibilities to the DSO in order to increase grid hosting capacity and hence RES integration in a cost-effective and energy efficient way. Thin new architecture of distribution grids based on cluster of microgrids, which share generation and storage system, is also applied in PARADISE project [35], reported in Fig. II.6.

The concept of flexibility is in-depth discussed in the literature. In general, a flexibility can be defined as a "modification of generation injection and/or consumption patterns in reaction to an external signal (price signal or activation) in order to provide a service", as proposed in [36] [37]. A flexibility can be offered by a single element, such as a PV system or an ESS, or an aggregated group of elements, such as a fleet of EVs. Flexibility providers can be industrial and commercial customers as well as household customers [36]. Each flexibility is characterized by basic parameters, such as the amount of power modulation, the duration, the location [36] [37]. The use of flexibilities for distribution grid applications and its feasibility is still under study in several projects. For example in the framework of SENSIBLE project, partner's societies are working on a Portuguese demonstrator in Évora which aims to demonstrate the benefits for both users and DSOs in exploiting LV customers' flexibility, in

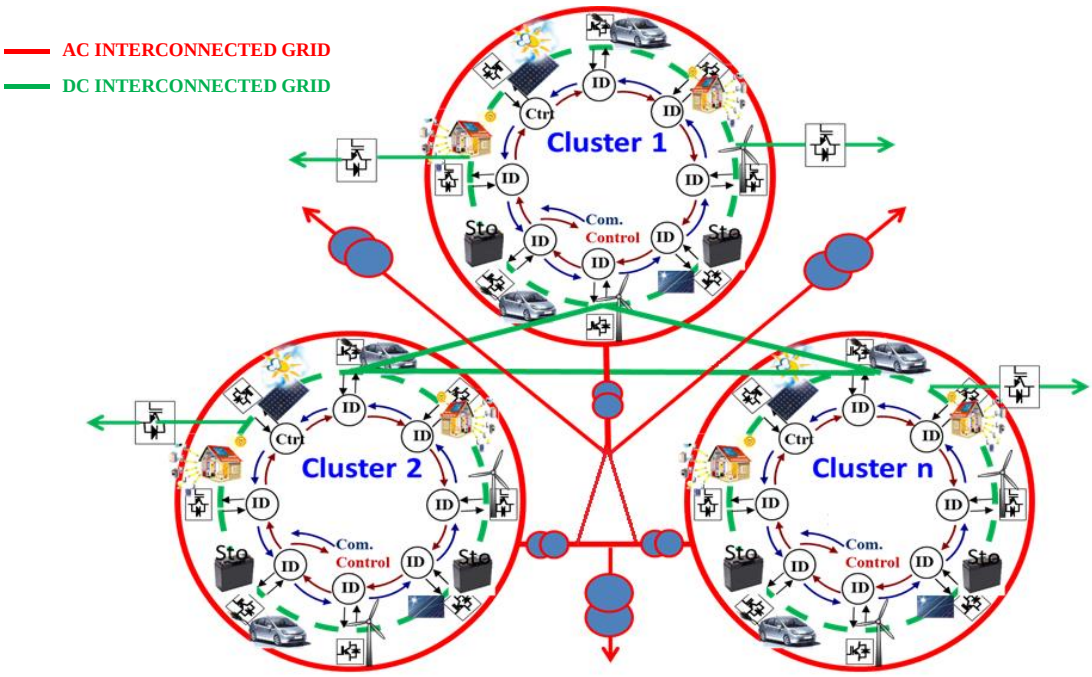

Fig. II.6 Cluster of Microgrids defined in PARADISE Project [35]

particular ESS, in both regulated and market environments [38]. A market participation of DER-based flexibilities to defer or avoid grid reinforcement on distribution networks is also discussed in [39] by underlying results obtained in three European projects eBADGE, IEA HPP Annex42 and hybridVPP4DSO.

Furthermore, such a system inherits most of characteristics and properties of the constitutive microgrids. One of these properties concerns its operation. In fact in [15], it is proposed that also multi-microgrid systems need to be able to work in two modes of operation:

- Normal operating mode - the multi-microgrid system is operated interconnected to the main grid in normal state of grids;
- Emergency operating mode - the multi-microgrid system is operated in an islanded mode in case of faults in the main grid or in case of blackouts to contribute to the restart procedure.

As for microgrid's components, a fully decentralized approach for the management of the cluster consists on an independent operation of each microgrid operate. That means that there is no interaction among microgrids, neither through an intermediary nor through a direct negotiation microgrid-to-microgrid. This strategy could increase costs and energy losses in certain situation. For example, if some neighbouring microgrids have available production

and others needs to satisfy their loads, a lack of interaction could let microgrid's consumer to buy energy from energy suppliers with higher costs. Moreover in this situation, renewable sources could be induced to reduce their production wasting free and green energy or reducing system efficiency by storing energy in batteries.

The other approach could consider to introduce a central energy management which knows and manages all resources simultaneously. Statements in section II.2.2 explain sufficiently the inefficiency of this second approach, because of the conflicts of interest, the impossibility of complete model knowledge, the privacy conflicts, the computational complexity and the expensive communication. Thus, the best way to manage and control this complex system with a large amount of decision makers, which need to accomplish different tasks with competitive behaviour, need to be built with a hierarchical architecture and with a distributed decision making. For centralized and distributed approaches, a coordinated operation needs to be implemented based on information exchange through communication networks. Hence, data gathered via smart metering and information and communication infrastructure will be fundamental pillars for the implementation of this kind of operation.

II.4. Aggregator position and needs

In section II.1, microgrids are proposed as a solution for the aggregation of small-sized resources, such as households or commercial facilities. In most cases, a single microgrid is composed of small-sized and variable systems, that can't be introduced in electricity markets and can't be used as flexibilities for network criticality resolutions. Hence, in order to fully integrate microgrids and medium-sized systems in the operation of power systems, they may be further aggregated in larger virtual systems through an intermediary entity placed between them and utility operators.

Since many years, the role of aggregator has been proposed as a solution for the integration of RES, DR and microgrids into both markets and grids. Several aggregator entities have been already created and are currently operating in energy markets. Representative examples that show roles and potentiality of aggregators are for example *EnergyPool* [40] and *Voltalis* [41] in French, or *Flextricity* in [42] United Kingdom.

The aggregator (often named as virtual power plant) is a new commercial entity, more

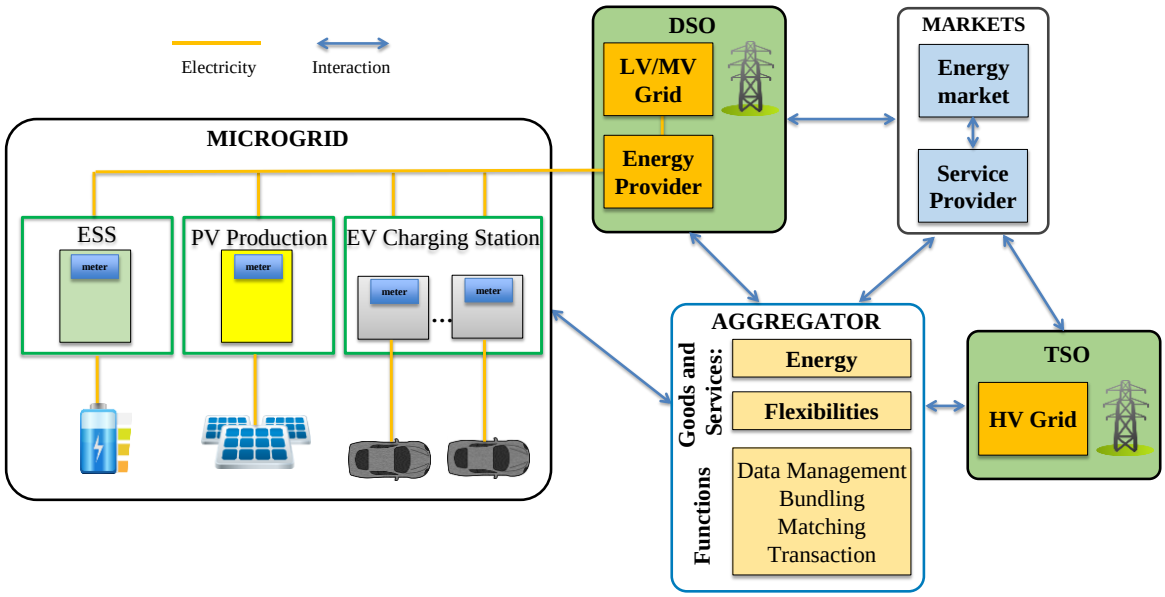

Fig. II.7 Interactions among microgrids, aggregators, markets and system operators

precisely a firm (as defined by authors in [43]), acting as an *intermediary*[5] and expected to aggregate small and medium size DGs, ESSs and consumers using their flexibilities. In general, the main task of an aggregator is to pack and optimize the use of its affiliated resources generating an appropriate aggregated proposal for selling (or buying) goods and services to other actors making a profit. It acts as a single entity when engaged in transactions. In the electricity sector, the electrical energy and power flexibilities are the good and services traded with different actors, such as wholesale and retail markets, DSOs or TSOs (as proposed in Fig. II.7).

Aggregators and microgrids, in a certain manner, may look similar because they were both introduced as aggregation element, which allows a coherent operation of a number of DERs, ESSs and flexible loads. In reality, there is a substantial difference between these two actors. In fact as explained in section II.2, microgrids perform the optimal management and control of resources placed on geographical contiguity. On the contrary, this characteristic is not required in aggregators and the affiliated resources can be delocalized through the territory.

The basic functions that characterize an *intermediary* are described by Spulberg in [44] and Codognet in [45]: data management, bundling, matching and transaction guarantee. These functions represent also the different phases of aggregator's process and interactions with

[5] In economics: An intermediary is an economic agent that purchases from suppliers for resale to buyers or that helps buyers and sellers meet and transact [195].

other energy actors. Moreover, these concepts have been applied for the first time by authors in [43] for the case of electricity sector.

A strong point of a decision maker such as an aggregator lies on the knowledge of its affiliated units (even if in part aggregated) and of energy and services market trends and needs. In fact, during data management, forecast of the energy demand and production of its customers can be obtained by using forecast algorithm. Also, it can compute statistic on market needs and estimates the size and the reliability of services that users will furnish. In this manner, aggregators can understand how influence customers' behaviour, for example with advantageous tariffs, and how give tradable value to users resources before to pass to the trading phase with customers, where they submit their needs and flexibilities. In the bundling phase, the intermediary aggregates many different tradable products, energy-based or capacity-based, using forecast data, medium-sized users or microgrids availabilities and technical characteristics required by electricity and services market. During matching phase, these products are bid to the entity of interest. For example, as energy-based products into day-ahead or intra-day markets or long-term forward contracts to energy provider, capacity-based product to TSOs, DSOs or service providers. The last required function of an aggregator represents a juridical and reliability condition. In fact, the aggregator has to manage the risk of delivery the product sold and it will be remunerated or penalized with an *ex-post* control.

Aggregators can create value and benefits for both users and the electricity system. In fact, in the first case it can create a growth in the economic wellbeing of one or more users. In the second one, an increase in the energy and/or economic efficiency of the power system as a whole. The aggregator signs different contracts with users according to user's characteristics, needs and wills. The design of management and the pricing model of aggregators are an important subject that can impact not only the income of customers, but also the revenue of the aggregator itself. The design of stipulated contracts among aggregators and microgrids must represent a compromise that converges to an equilibrium among the needs of both. This equilibrium is strictly correlated to the wills of microgrids to exploit their available resources at minimum cost, maximize their income and protect some private information. Essentially, three approaches can be used for contract design based on the amount of information exchanged and the degree of cooperation between resources agreed by microgrids:

centralized, decentralized and hybrid [46] [47]. The main principles behind these approaches can be deduced by the descriptions of microgrids' control and management, given in section II.2.2. Also in this case, the primary difference between centralized and decentralized approaches lies in the decision maker. In fact, in the second approach the aggregator is not a profit-maximizer for all the users, but only an intermediary between microgrids and the system operator and costumers' information about costs and constraints are not shared.

II.5. Agents and Multi Agent System

II.5.1. Agent and intelligent agent concept

Agent technology has been the subject of several discussions within scientific community for several years and recently there has been a significant exploitation progress. The term agent is utilized to describe several technologies in different applications, such as in artificial intelligence, operating systems, telecommunications, e-healthy, e-commerce, etc.. The widely use of the term agent in different areas has led to several difficulties in the creation of a single and universally accepted definition. In fact, the computer science community produced a myriad of definitions on what an agent is, which differ on terminological details or on the level of details [48]. Anyway, they all share a basic set of concepts, as agreed in the review study on the multi-agent systems for power engineering applications carried out by the IEEE Power Engineering Society's Multi-Agent Systems (MAS) Working Group, where an agent is defined like *"a software (or hardware) entity that is situated in some environment and is able to autonomously react to changes in that environment* [48]*".*

An interesting and elementary definition of agents come from two renowned scholars in computer science, Stuart J. Russell and Peter Norvig, on their book on artificial intelligence:

"An agent is anything that can be viewed as perceiving its environment through sensors and acting upon that environment through actuators [49] *".*

Regarding to these definitions, it can be deduced that everything could be considered as an agent, both physical and a virtual entities, and everything external to the agent can be named with the term of environment. Also the environment may be constituted of physical or virtual entities, which can be fully or partially observed by the agents [49]. In the first case, the environment can be easily perceived through sensors. Otherwise, in the second one, through messages or program invocation. Also humans can be seen as the smartest agents in the

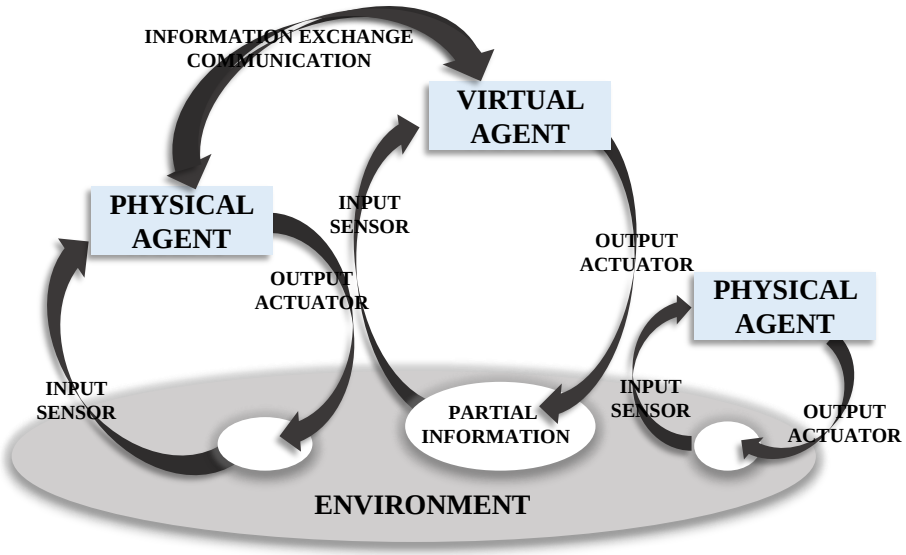

Fig. II.8 Intelligent Agents in their Environment

world. In fact, they use the sensory nervous system to receive all external stimuli thorough its five receptors (visual, auditory, olfactory, somatosensory and gustatory cortices). These information are then transduced and probably transformed in actions which are applied via one of our actuators (limbs, hands, legs) to modify or interact with the external environment. In electrical systems, a physical agent may represent each hardware component, such as a PV, an ESS or an EV, and a virtual agent may be each entity, such as aggregators, network operators or market operators. In this case the same power system will represent the environment.

In the publication on the theory and practice of the intelligent Agent (1995), Wooldridge and Jennings extended the concept of agent with the definition of intelligent agent, asserting:

"Perhaps the most general way in which the term agent is used is to denote a hardware or (more usually) software-based computer system that enjoys the following properties [50]*:*

- *autonomy: agents operate without the direct intervention of humans or others, and have some kind of control over their actions and internal state;*
- *social ability: agents interact with other agents (and possibly humans) via some kind of agent-communication language;*
- *reactivity: agents perceive their environment, (which may be the physical world, a user via a graphical user interface, a collection of other agents, the*

INTERNET, or perhaps all of these combined), and respond in a timely fashion to changes that occur in it;

- *pro-activeness: agents do not simply act in response to their environment, they are able to exhibit goal-directed behaviour by taking the initiative."*

Important and fundamental properties of agents could be discovered with these definitions allowing readers to deduce all potentials of agents. For example, a typical agent-agent and agent-environment process is resumed in Fig. II.8.

The autonomy property is defined as the ability of "exercise control over its own actions [51]". Agents having this feature are able to make autonomous decisions based on input information, and consequently act or schedule actions. In fact, each agent has some particular tasks (named as functions), which specifies the action taken by the agent in response to any percept sequence. Agent capabilities are defined in its program that has a well-defined skeleton. Each agent program implements the agent functions and maps agent's perceptions to agent's actions. In practice, the agent program takes in input and elaborates the perceptions captured by sensors and returns an action to the actuators [49]. Changing environment, the functionalities of an agent and their objectives are not impacted. Nevertheless, their reply changes in response of different inputs. The type of environment defines the appropriate agent design and implementation.

The pro-activeness is the property of agents to be goal-oriented. Proactive agents are capable to dynamically adapt their behaviours, act in anticipation or reply to unpredictable events, in order to achieve as well as possible their fixed purposes. In the true meaning of the term proactive, this property is the most hard to implement. However, this property is fundamental in case of fault management, in order to guarantee a reliable and robust system, and also for implementation of flexibilities and extensibility of complex systems, in order to be able to manage different components.

Social ability is an innovative property that permits to agents to acquire plenty of other capabilities that alone couldn't have. For example, communication helps agents to increase their ability to be aware of their environment. Social ability also leads to delocalize agents' activities and allows reducing the amount of information that each agent needs to acquire in order to accomplish its tasks. In fact, an agent can see other agents in the system as integral part of the surroundings environment. In agents' social societies, agents communicate through

messages exchanged in telecommunication infrastructures, such as computer networks. In these agents network, each agent must be able to deliver and receive messages. Hence first of all, the messages exchange requires the implementation and the use of a physical communication infrastructure. Secondly, agents need to be able to correctly decode the received messages, which require to parse the content using a shared syntax among agents and to understand the parsed symbols using a common shared semantic.

A system constituted of more than one agent, which interact among them, is named in the literature: multi-agent system (MAS). In general a MAS, agents can either work to reach different goals or interact with their activities in order to solve a common goal [52].

II.5.2. Multi-Agent System benefits for Smart Grids

The use of intelligent agents has great potentialities, in management, control, modelling and simulation fields for power systems. Let consider a network operator (NO) example. In general, it exchange partial or aggregated information with connected producers and consumers. Production and consumption systems can be considered as agent in the network operator environment. For a certain feeder, the agent representing the NO is able to estimate voltage violations by gathering voltage measures and by running state estimator programs in its skeleton. Hence, the NO agent has implemented in its software, the Distributed Management System (DMS), smart functionalities which leads to autonomous and pro-active properties implementation. As response of these smart properties, it can act on its actuators, such as the on load tap changers in order to modify voltage transformation ratios, or can interact with other agents (representing the users) through a communication infrastructure activating their flexibilities and avoid critical conditions in the grid.

In general, as discussed in sections II.2 and II.3, the advent of numerous small-sized DG and elastic consumption in power grids, managed in the aggregated form of microgrids, is making power systems more and more complex. The use of multi-agent systems to provide distributed control capabilities to microgrid applications offers various advantages. A MAS in power grid can be used either as a way of building robust and flexible hardware/software systems to monitor and control microgrid or as a modelling approach to manage it. In the literature, different structure of MAS are proposed to distributed control, modelling and simulation (e.g. energy markets), protection, monitoring and diagnosis. In complex systems

management and modelling, the communication capability made available by MAS is probably one of the most important property. In fact as introduced in section II.5.1, this property permits to share tasks between agents. Firstly, the delocalization of tasks gives to systems the possibility to be more easily scaled and extended. Secondly, the distribution of tasks allows to manage resolution of problems, which need interaction between system components due to a lack in the individual capabilities of the agent or in its knowledge.

Hence, MAS could be a useful and powerful tool for analysis, management and control of Multi-Microgrid Systems compared to traditional approaches. Some of the most important benefits are clearly underlined by Logenthiran in [53] and can be resumed in:

- Unit autonomy, which is a basic characteristic of an intelligent agent. It allows to users in power system to act autonomously with collaborative or competitive strategies as function of the implemented architecture;
- Knowledge manipulation and local data management, which are based on social ability of agents. It allows to manipulate locally information and exchange knowledge through messages.
- Extensibility, flexibility and openness of the system. New micro-sources and loads can join the system, independently by their model and manufactory house, without requiring modification of the existing system. In fact, agents can be added, removed, replaced or reconfigured during runtime at any time.
- Increased reliability and robustness. Agents with autonomy and proactive properties are able to proceed and adapt their work in order to guarantee the system reliability, also in case of failures and shortages.

During last years, the amount of MAS application is rapidly increased due to all these advantages. Therefore, the effectiveness of MAS for smart power systems is already demonstrated in several publications for different kind of applications, such as for the control of a distributed smart grid based on microgrids [54], for the scheduling of distributed energy resources (DER) of islanded or grid-connected microgrid [55] [56], for microgrids reconfiguration [57], for secondary voltage control implement [58], for protection operation [59], and so on.

II.5.3. MAS implementation

The technical elements to realize and implement a MAS have been developed by researchers and industrials and continue to be subject of research work. Many challenges remain and numerous improvements are expected, e.g. standards for interoperability and more performing platforms.

In the first part of the work of the IEEE Power Engineering Society's MAS Working Group [48] authors introduce these key elements:

- Platforms and Toolkits,
- Intelligent Agent Design,
- Agent Communication Languages and Ontologies,
- Data Standards,
- Security,
- Mobility.

II.5.3.1. Platforms and Toolkits

MAS platform and toolkits allows to model, implement and simulate phenomena, simultaneous operations, link and interactions of multiple components in real complex systems. The choice of platforms is very important in order to successfully implement all the desired characteristics in each agent, such as system openness to new functionalities' development or system extension facility.

The Foundation for Intelligent Physical Agents society (FIPA)[6] [60] developed a fundamental specification which defines based elements required in any agent-based system. FIPA standard SC00023K [61] provides the Agent Management Reference Model which defines the framework in which FIPA compliant agents exist and operates. Fig. II.9 resumes this reference model by showing its basic components and interactions. In fact, in this standard two fundamental component of an agent platform are defined: the Agent Management Service (AMS), which is a mandatory component, and the Directory Facilitator (DF), which on the contrary is optional. The AMS manages the agent platform and acts as a supervisor. It makes available a white pages services where agents must register receiving a unique Agent Identifier (AID). One or more DF could exist in one agent platform and they

[6] FIPA is an IEEE Computer Society organization formed in Swiss in 1996 which promotes agent-based technology developing standards to increase interoperability among agents and agents with other technologies.

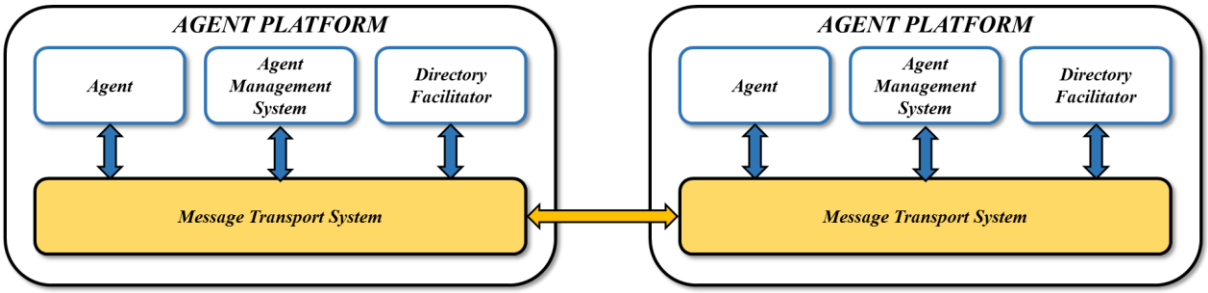

Fig. II.9 Agent Management Reference Model defined by FIPA standard SC00023K [61]

provide yellow pages services to agents. Agents may register their services in the DF or query DFs to find out services provided by other agents.

Nowadays, a large number of platforms and toolkits for the implementation, modelling and simulation of MASs have been developed. In fact, over than 100 software products [62]) are available with different quality and maturity level. Those available platforms have been extensively studied in many previous publications. Therefore, it is need to define fundamental parameters and criteria to consider in order to compare and find the adequate tool to use. MAS platforms choice needs to be guided by an attentive and accurate analysis of platform properties, operating abilities and practical characteristics.

They can be evaluated considering criteria suggested by authors in [62] and [63]. When developing MAS, properties and abilities that will encourage developers' choices are certainly the organization, used programming language, robustness, latest release and stability of the platform. Moreover, platform simplicity and learnability could also influence developers' choice in order to reduce the consumption of time and the efforts during the development phase [63].

Standard compatibilities and scalability are also requirements that need to be considered. In fact, standards compliant platforms and toolkits are an indicator of the platform's flexibility [63] and permit to guarantee an easy interoperability between agents, system openness, reliability, efficiency and interchangeability. Indeed, a scalable platform allows to handle with issues related with size increment and then system extensibility. A scalable platform is in fact able to manage increased response time and message transport behaviour when the number of agent raises rapidly.

Furthermore, practical factors to be considered are software licencing model and costs, which could encourage massive use and promotes collaboration among different stakeholders.

Detailed documentation and availability, e.g. books and practical example, are a typical practical factor which may support new and non-expert users. Communication capability which considers the capacity of inter-platform communication need to be considered as well. Inter-platform communication allows to perform and increase interoperability by supporting communication between agents living in different platforms. In certain kind of applications, the agent ability to migrate or also to generate a clone of itself from its original location to another one maintaining at the same tome its abilities and continuing its tasks may be evaluated. This property is known as mobility. At the end, also security policies into the same platform and among platforms are suggested as fundamental parameters in [62].

In order to individuate the most appropriate platform for power system applications, the characteristics of four of the most used platforms in the literature, which are JADE, Zeus, Madkit and JACK, are compared. In the following tables (Tab. II.1, Tab. II.2, Tab. II.3, Tab. II.4) are highlighted platform properties, usability, pragmatics and security characteristics of each platform.

JADE

Jade is a software framework distributed by *TILab* (Telecom Italia Labs) to implement multi-agent systems; it the most used platform for academic and industrial applications in several field of application and also in power system applications, e.g. in [64] [65] [66] [53]. In Tab. II.1 the main characteristics of JADE are summarized [67] [62] [54].

Platform Properties			***Pragmatics***
Licence	***Programming Language***	***Operating System***	***User Support***
Free software under **LGPL**[7] **Open source** software	**JAVA**	All	FAQ; Mailing list; Defect list; Examples; Tutorials; API; Documentation and Book
Usability			***Security***
Standards	***Communication***	***GUI***	***Security policy***
FIPA, work with CORBA (Orbacus)	**ACL**[8], support for inter-platform messaging with plug-in MTPs, ACL and XML codec for messages	Good	Connection authentication, user validation and RPC message encryption through JADE Object Manager

Tab. II.1 JADE platform main characteristics [62]

[7] LGPL: Lesser General Public License Version 2.
[8] ACL: Agent Communication Language (see section II.5.3.2).

JADE's characteristics and advantages are already shown in numerous practical application from universities and companies, such as the field test Kythnos Microgrid in Gaidouromandra (Greece) for power systems [15], the production of travel packages for customers for the e-commerce [68], for memory management frameworks in the framework of CoMMA European project [69], for online medical diagnosis system and for e-health functionalities [70], etc.

Zeus

Zeus is another widely used platform, e.g. in [54]. The main characteristics of Zeus are resumed in Tab. II.2 [62] [54] [71].Zeus platform is also used in several applications for power systems, such as in [54] where it is chosen for its user-friendly features useful to implement intelligent distributed autonomous power system, and for e-commerce applications, such as in [72] to build an electronic marketplaces, etc.

Platform Properties			***Pragmatics***
Licence	***Programming Language***	***Operating System***	***User Support***
Open source **Free software**	**JAVA**	Windows 95; Windows 98; Windows NT; Windows 2000; Windows XP; Linux; BSD; UNIX-like OSes; Solaris	Documentation; Author contact
Usability			***Security***
Standards	***Communication***	***GUI***	***Security policy***
FIPA	**KQML** and **ACL**[9]	Excellent	ASCII-encoded, Safe-Tcl scripts or MIME-compatible e-mail messages for transportation; using public-key and private-key digital signature technology for authentication, cash and secrecy

Tab. II.2 Zeus platform main characteristics [62]

Madkit

Madkit is another platform proposed in the literature to model and simulate MAS, e.g. in [73]. In Tab. II.3, the main characteristics of Madkit are shown [73] [71].

[9] KQML: Knowledge Query and Manipulation Language (see section II.5.3.2).

Platform Properties			***Pragmatics***
Licence	***Programming Language***	***Operating System***	***User Support***
Free software under **LGPL** for **basic libraries** Under **GPL**[10] for **Development and non-commercial applications**	**JAVA**	All	FAQ; Documentation; Online forum; Examples; Defect list

Tab. II.3 Madkit platform main characteristics [62]

JACK

JACK is another agent oriented development environment supplied by AOS Group, found in literature [74] [75]. The main characteristics of JACK are reported in Tab. II.4 [62] [76].

Platform Properties			***Pragmatics***
Licence	***Programming Language***	***Operating System***	***User Support***
Free for 1 testing month	**JAVA**	Windows; Macintosh; Unix; Linux; Android; Web	Documentation; Online forum; FAQ; Examples; Defect list
Usability			***Security***
Standards	***Communication***	***GUI***	***Security policy***
FIPA	DCI[11] network for communication; similar to TCP/IP it needs one process running as a name-server	Good	Internal security provided by JDK

Tab. II.4 JACK platform main characteristics [62]

II.5.3.2. Agent Communication Languages, Ontologies and Data Standards

Communication is a fundamental property of agents that allows to exchange information and share knowledge. Agent communication and cooperation need to be guaranteed independently by agents' developers and platform usage. Therefore, languages, ontologies and interfaces are crucial points when developing a flexible and open MAS. The transmission of messages can be accomplished via any traditional communication system, such as IP communications, wired or wireless channels [15]. However in order to ensure agent interoperability, appropriate communication languages needs to be adopted, and in addition ontologies and universal standards need to be stated. The agent languages most used in the

[10] GPL : General Public License
[11] DCI: Data Center Interconnect.

Parameter	*Description*
performative	The communication act of the message
sender	Identity of the sender of the message
receiver	Identity of receivers of the message
reply-to	Identify the receivers of subsequent messages in this conversation
content	The content of the message
ontology	The ontology used in the content
language	The language used in the content
protocol	The interaction protocol that the sender is employing
encoding	The specific encoding of the content language expression
conversation-id	An expression to identify the ongoing conversation
reply-with	An expression used by receiver to identify this message
in-reply-to	An expression to reference an earlier action to which this message is a reply.
reply-by	Time and/or date expression to indicate the latest time by which the sender would like to receive a reply

Tab. II.5 FIPA-ACL Message Parameters [77]

literature are Knowledge Query Manipulation Language (KQML) and the FIPA's Agent Communication Language (FIPA-ACL) developed by FIPA group.

The FIPA-ACL has currently a high degree of acceptance in the agent developer community and different platforms already comply with this standard (e.g. JADE). ACL conversations rely on speech acts which define a set of performatives called communicative acts. A basic FIPA-ACL message contains a structure based on one or more parameters define in standard SC00061G [77] listed in Tab. II.5.

In this standard, the performative parameter is the unique mandatory parameter. Otherwise in each message, the used parameters vary according to the information to exchange.

The content of a message comprises two parts: content language and ontology [78]. The content language defines syntax, or grammar, of messages content. The ontology represents the semantic or lexicon of message content which means the terms that compose agents' vocabulary and the shared meaning of each word. FIPA has proposed standards for four different content languages [78]: FIPA-Semantic Language (FIPA-SL); Knowledge Interchange Format; Resource Definition Framework; and Constraint Choice Language. At present, FIPA-SL, defined in standard SC00008I [79], is the only standard which reached a stable level and concrete applications [78]. The use of JADE platform is also benefit for

ontology development because of a class hierarchy of concepts, predicates, and agent actions [67].

Nowadays, there is no a well-defined standard for ontology in power systems applications [78]. Some example of existent standards which may be used as base to develop a unique standard for power systems are the Common Information Model (CIM) for data exchange between Energy Management Systems and related applications and the IEC 61850 Communication Networks and Systems in Substations standard for data exchange between intelligent electronic devices. Considering the importance of this subject, the industrial and scientific community working on power system interoperability are putting several efforts in this task, e.g. SEAS Project [80] and AMES Research Centre for NASA ontology [81].

II.5.3.3. Intelligent Agent and MAS Design

The design task is a crucial part when using agents. In fact, agent design requires specific techniques to develop a reliable and extensible system with re-usable agents and easy to comprehend. In general, design a MAS requires a deepened knowledge of the system to represent which demands a detailed analysis of all its aspects and particularities. When a MAS architecture and agents are designed, there is a need to answer to questions such as:

- How should the environmental state be perceived?
- How should the agent's reasoning be affected by the environmental inputs?
- How should agent reasoning impact on the environment?
- What processing can provide this particular relation between input and output?
- Which information we need to receive from the environment?
- …

When designing agents, it is important to define how sophisticated the agents' reasoning has to be, the key role of each part and their relationships, and then it is possible to define the architecture (agent class hierarchy). The model of decision making of an agent is known as practical reasoning [52]. We can outline two typical type of agent reasoning: reactive and deliberative agents. Reactive agents are the simplest type because they simply act under the impulse of automatic reflexes. They implements pre-set actions using current environment perception, without maintaining any historic precepts (internal state), as in Fig. II.10 (a). Reactive architectures implement decision-making as a direct mapping of situation to action

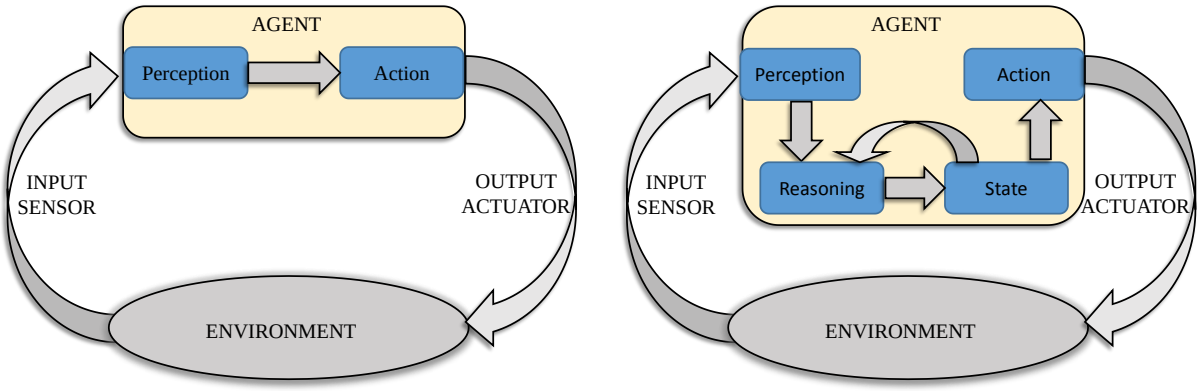

(a) Reactive Agent (b) Deliberative Agents

Fig. II.10 Decision-making process of reactive and deliberative agents [82]

and are based on a stimulus–response mechanism triggered by sensor data [83]. Otherwise, deliberative agents have more developed thinking way. When they receive inputs from the environment, they invoke a reasoning process taking into account historical precepts of the environment, creating and maintaining an internal state, learning, planning and re-planning to decide about current or future actions, as in Fig. II.10 (b). Reactive agents are simple, economic and they have easy computational tractability, but limited decision quality [82]. Otherwise, deliberative agents have higher decision quality, but are more complex. An internal structures of an agent has to include data structures, data flow between structures and agent operation and functionalities [82].

In the literature are proposed several style of architecture for MAS. A MAS may be organized on the basis of one of four main categories or a hybrids of them [84] [85]: hierarchical, flat, subsumption and modular.

In hierarchical MASs, agents communicate according to a hierarchical structure allowing a significant reduction of communication exchanges. On the other side, this organization is based on a strict structure where some level (partially or fully) control or influence other levels preventing the total autonomy of agents. This organization does not permit agents to dynamically organize themselves to best fit the needs of a specific task [85]. Otherwise flat organizations are flexible and each agent may contact any other agents dynamically organizing the communication exchange to best perform tasks. These structure requires high efforts for communication. A subsumption MAS is a system in which agents are themselves made up of other agents [84]. Agents are arranged in a number of layers in which agents in lower layers represent simpler behaviours with high priority, and agents in higher layers

represent more abstract behaviours and have lower priority [86]. A subsumption architecture is in such a way an extremized hierarchical organization in which subsumed agents completely surrender to the container agent [85], e.g. objects within a larger object in object-oriented programming language. Then, this structure is strict and doesn't allow dynamic organization guaranteeing efficient tasks execution and low communication efforts. The modular MAS are constituted of a number of modules where each module can be seen as a virtually stand-alone MAS [85]. Each module may employ different structure, but it is often a preferred to increase module flexibilities with flat structures. The partition of the system into modules may be done based on geographical vicinity or intensity of interaction among agents within the same module [85].This structure is useful for build growing systems that need to extend their functionalities and characteristics. Such in subsumption MAS, this architecture increases efficiency of task execution and reduces communications.

II.5.4. MAS development with JADE for Smart Grid

II.5.4.1. JADE Platform Advantage for Smart Grid

JADE is based on the Agent Management Reference Model defined by FIPA standard SC00023K [61] described in II.5.3.1. JADE platform is a completely distributed middleware in which agents live in one or more containers which can be distributed over a communication network as in Fig. II.11. Each container represents a JAVA process which provides the JADE run-time and the services needed for hosting and executing agents [83]. In each JADE-based platform a main container comprising AMS and DF need to be initialized when creating a new platform. Then, other agents' containers can be created on client computers connected to the through the same communication network. Each agent in the platform runs in separate threads, in one or more machines, and communicates among them through a unique communication network, such as a TCP/IP data network (Transmission Control Protocol/ Internet Protocol).

Agents running a separate thread can control its life-cycle and its actions. Moreover, JADE is a peer-to-peer platform where each agent is identified by a unique AID (as described in section II.5.3.1) and they can join and leave a host platform when and whenever they desire and need [83]. Peer-to-peer model and separated threads make JADE agents completely

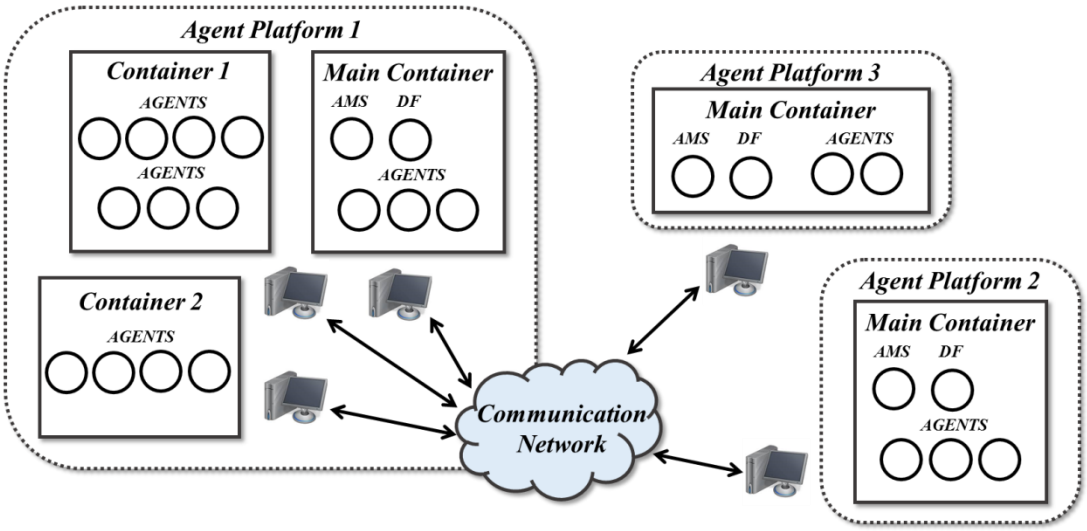

Fig. II.11 JADE Architecture

autonomous and proactive. In JADE, agent tasks are carried out through behaviours and several behaviours can be executed behaviours (see *jade.core.behaviours* in [83] [87]).

JADE platform is chosen for smart grid applications because its architecture and characteristics (described in II.5.3.1) provides a flexible structure easy to extend and scale without radical code modification, where agent run in separate threads, in one or more machines, and communicates among them. This architecture supports plug-and-play capabilities essential for smart grid development [88]. Moreover, it is fully compliant with FIPA specifications and allows efficient transport for asynchronous messages [83]. MAS with JADE are easy and fast to design and implement since to numerous APIs, accurate documentation and support for ontologies and content languages. JADE implements white pages and yellow pages and provides a simple life-cycle management for agents, assigning to each agent a unique identifier and a transport address [83].

II.5.4.2. Adopted Methodology for MAS Developing

There are several methodologies to develop MAS. We will focus on a methodology proposed by Nikraz *et al*. in [89] designed for JADE platform. This methodology consists of four main phases:

I. Planning,
II. Analysis,
III. Design,
IV. Implementation and Testing.

However, descriptions covers essentially the two central phases of the methodology which are the most important in MAS developing process, the analysis and the design. In fact, the initial and final phases are common to all development processes. The planning phase consists in development preparation, in which developers analyse the most appropriate approach to use. In this particular case, the fitness of agent-based solutions is verified for the studied system. Whereas, implementation and testing phase concerns the practical realization of the MAS (writing, debugging, etc.) and the analysis of test cases results, its robustness and performances. An overview of the methodology steps is described in Fig. II.12.

The analysis phase goal is to clarify system needs and goals by focusing on both single agent and overall system point of view. This stage is completely independent to the platform or toolkit chosen to implement the MAS. During this phase, the tasks related to each agent and the knowledge it needs to accomplish them are analysed and defined. This stage starts with the identification of use cases (step 2.1). In fact, the use of representative case studies is a mean diffusely applied to capture all characteristics of each agents, and to identify all interactions between agents and between agents and other elements, such as users or other kind of technologies.

According to *Nikraz et al*., the identification of these representing parameters through use cases support requires some sub-stages of the global analysis phase. In each sub-stage will be identified:

- Types of agent to add in the system based on actors or devices to represent (step 2.2), such as a PV, an ESS or an Energy Management System (EMS);
- Main responsibilities of each agent (step 2.3), such as day-ahead electricity scheduling of *n* components or PV monitoring and control;
- Acquaintances of agents (step 2.4), to underline all needed interactions and relations between agents.

After this general analysis of tasks and interactions a refinement stage (2.5) is applied based on more detailed considerations related to agents' knowledge, e.g. additional data to stock and when acquire information, interactions, e.g. agents discover agents to contact, and practical management, e.g. who monitor living agents. These kind of considerations are divided by authors in three classes: support, discovery and monitor and management, respectively.

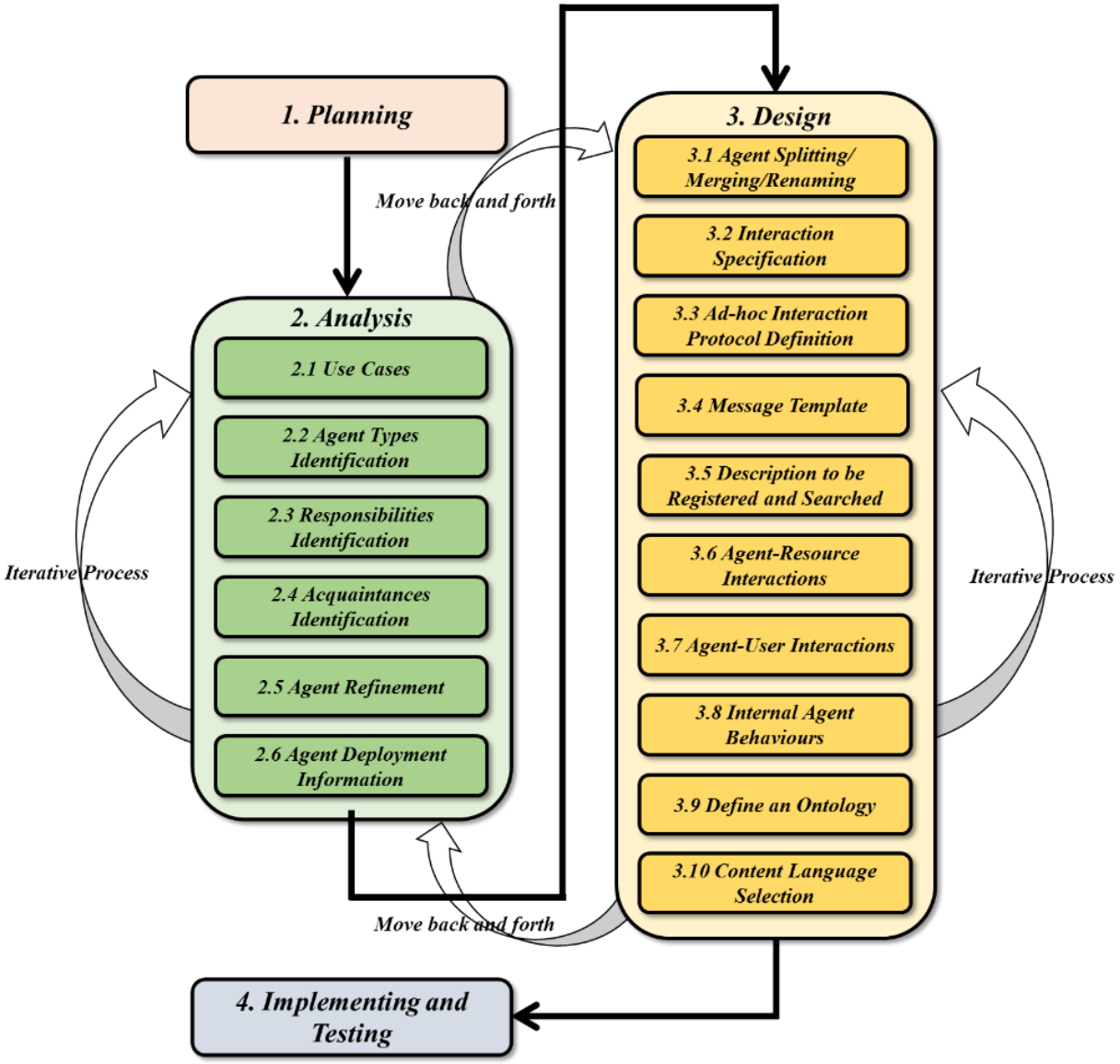

Fig. II.12 Overview of Methodology for MAS Development using JADE Proposed in [89]

When a suitable level of detail is reached, it is possible to move to the design phase which aims to detail all concerning the practical implementation. Contrary to the analysis phase, these one is related to the chosen platform, and in our particular case refers to classes and concepts characterizing JADE. As in analysis phase, various sub-stages can be identified in the design stage. This stage starts with an analysis of previous phase outcomes, which permits to find and then remove the existence of alterations, redundancies and similarities (step 3.1). An example furnished by *Nikraz* consider the case of two different type of agents defined in 2.2 which could be merged because they use same information. Next, interaction defined in 2.4 are detailed in steps 3.2 and 3.3 adding practical information for their implementation, such as interaction protocol to use (standard or *ad-hoc*), agent name and role in the

communication (sender/receiver), and so on. In JADE, agent interactions are implemented in the form of behaviours using *jade.core.behaviours*. In step 3.4, messages template are defined to differentiate messages based on some representative parameter, such as a conversation identifier, e.g. "*Trade-Electricity*", or a performative act "*Request*". In JADE, an easy and flexible way to generate templates is provided using *jade.lang.acl.MessageTemplate* class [83]. Step 3.5 is an important sub-stages of the design phase. In fact, information about agents naming convention and services to be registered in the DF are defined. JADE provides a specific class, the *jade.domain.DFService,* to publish and search for agent services [83]. Agent-Resource and Agent-User Interaction steps (3.6 and 3.7) focus on how agents may obtain information from external resources identified in 2.1, 2.2 and 2.5, such as databases, software, files or humans. Agent-resource interactions could be implemented using both basic JAVA classes, such as java.io to read .txt files, and more sophisticated classes, such as establishing a connection to a server program using the *java.net.Socket* class or to a Matlab function using a proxy through *matlabcontrol* class. Agent-user interactions could be implemented in several ways such as a developing an agent interface or a GUI. Nikraz proposes to develop or a local GUI, using for example Swing, or a web GUI, using for example JavaServerPages [89]. Step 3.8 defines how to build and implement agent tasks outlined in 2.1 and 2.3. As introduced in II.5.4.1, in JADE behaviours are implemented using *jade.core.behaviours* which provides the skeleton to model agents' responsibilities and actions including different type of behaviours as function of task's complexity, such as *OneShotBehaviour* class, *CyclicBehaviour* class, *TickerBehaviour* class, *CompositeBehaviour* class (see [87]). The last parameter to define are the ontology and the language to use which are decided in steps 3.9 and 3.10. *jade.content* contains classes to support in creating and manipulating complex content expressions providing schemas which define the types of predicates, agent actions and concepts relevant to the addressed domain and codecs for two content languages (SL and LEAP languages) [83]. At the end of the iterative process between analysis and design, the MAS could be implemented and tested.

For highly complex systems, these two phases need to be repeated several times within an iterative process in order to capture the real nature of the system and all peculiarity, and to avoid possible redundancies.

II.6. Conclusions

This chapter proposed an overview of issues and potentialities of a multiple microgrid environment, considering i.e. physical building blocks and management strategies. In fact, microgrid concept as fundamental building blocks of Smart Grid is introduced, their physical characteristics are discussed and management strategies are evaluated. The considerations in sections II.2 and II.5.2 constitute the basic elements used to develop the management architecture and strategies for smart and cost-efficient microgrids developed in chapters III and V using multi-agent system.

Moreover, multi-microgrids and aggregator concepts and goals in addition to discussions and evaluation of management strategies are widely discussed. These elements introduce in sections II.3 and II.4 in addition to II.5.2 are the basics used to develop the agent-based strategies developed for multiple microgrids integration and support of distribution grids and electricity markets.

The implementation of MAS for all agent-based applications hang on platforms comparison, standards and methodology disused in sections II.5.3 and II.5.4.

III. DEVELOPMENT OF MICROGRID STRATEGIES FOR DAY-AHEAD SCHEDULING BASED ON MULTI-AGENT SYSTEMS

III.1. Introduction

During last decade, the rapid diffusion of renewable-based generators has shown that LV and MV distribution grids can no longer be considered as a passive member of the electrical system. Therefore, the development of new management and control strategies based on a decentralized architecture has become a necessity to ensure power reliability, quality and low operational costs. In the literature, microgrids, advanced control strategies, integrated information and communication technologies, as well as smart meters are considered as key elements for the smart grid paradigm shift. Microgrids are seen as the tool to implement an organized structure for large integration of distributed generators and demand response.

Optimal scheduling of all energy resources connected to a microgrid can induce several benefits for both users and distribution system operators. Hence, the main goal of this chapter is to discuss the management architecture and the energy management algorithms developed for microgrids. In particular, section III.2 discusses the requirements for a new management architecture. This architecture has to improve certain limits of the current system, such as the scarce flexibility and extensibility, by trying to sufficiently distribute tasks among users. Whereas, sections III.3 and III.4 discuss the implemented smart algorithms, which on one side permits to efficiently use energy resources in microgrids by respecting users' needs, and on the other side allows to generate an aggregated profile with a certain degree of freedom to be submitted to aggregators or grid operators. In general, the contextualization of this architecture in a multi-microgrid environment combined with the development of the energy management algorithm for microgrids can be seen as the main contribution of this chapter.

III.2. Energy Management of Microgrids

III.2.1. Objectives and Phases

The task of energy management (EM) includes all coordination actions to handle production and consumption resources in a system. The purposes of EM can be the most varied and it normally depends on many factors including user's needs, such as energy or cost

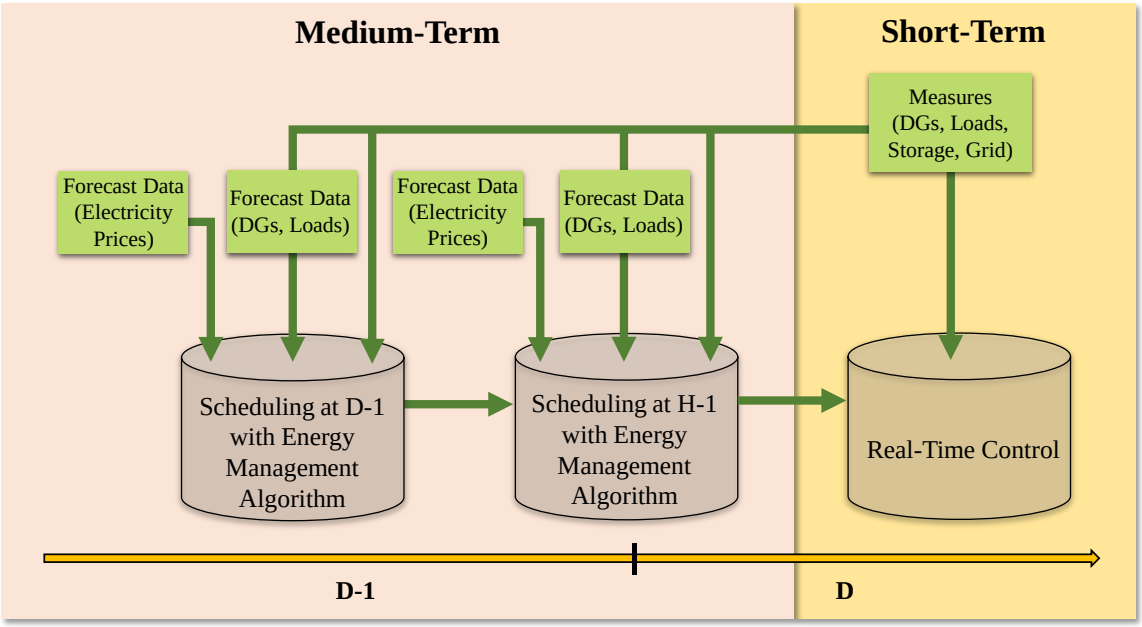

Fig. III.1 Microgrid management timescale for EM (figure inspired by [90])

saving, and operation constraints, which change for islanded or grid-connected systems.

An energy management system (EMS) includes both planning and real-time operation phases. In general, the planning stage comprises both the installation phase (sizing) of sources and the resources scheduling in various timeframes. In fact, the design of a system and its energy scheduling go hand in hand in order to find an optimal comprise between investiment costs and optimal use of the installed systems [91].

In this thesis, the sizing stage of microgrids is not taken into account. Whereas, the focus is on the scheduling and real-time operation of all energy systems in a microgrid (production, storage and consumption units). As suggested by authors in [92], the EM timescale of microgrids can be subdivided as resumed in Fig. III.1.

The medium-term EM includes the day-ahead and hour-ahead phases as suggested by the electricity market organization. The implementation of medium-term scheduling phases is becoming more and more important in order to guarantee a cost-efficient and reliable system, able to manage the scarce predictability of RES by approaching the scheduling time with the operation time. The first step of medium-term phase is covered by the day-ahead phase. It aims to efficiently schedule the operation of all energy resources at daily scale by means of rule-based or optimization algorithms [90]. This can be done by using information obtained through forecast algorithms. The granularity of these information, such as hourly, fifteen or

ten minutes, can be chosen and can increase the accuracy of the schedule by representing more in detail the behaviour of variable production and consumption. A typical example could be a photovoltaic system which power injected increases rapidly during an operating hour. However, day-ahead forecast is a hard task and it is not possible to reach a high degree of detail, such as minutes scale profiles. Hence often, a fifteen-minute data granularity is chosen to model energy profiles of production and consumption.

The second step of medium-term phase is concerning the hour-ahead scheduling. Its goal is to correct and refine the day-ahead planning results induced by forecast errors or unplanned events by applying a correction to the scheduled operation. In general, as the day-ahead, the hour-ahead energy scheduling can be seen as a tool to reduce money expense and rationally use installed resources. As for the day-ahed phase, this phase can also support the integration of DGs by increasing the hosting capacity of the distribution grids and supporting short-term electricity markets. For example, distribution companies can schedule and monitor their operation by knowing the users' behaviour and avoid power and voltage congestions.

The last phase of EM is called short-term power management. It comprises minutes, seconds and milliseconds scales [90]. This stage includes all actions related to real-time power dispatching of resources. In islanded microgrids, it has to support voltage and frequency control as well.

III.2.2. Management Architecture Description

In the vision of power grids introduced in chapter II, a large amount of small and medium size components will inhabit the electricity system of the future. Considering the principles of centralized management discussed in section II.2.2, it is possible to conclude that this new fragmented system will be hard to manage in a centralized way due to the number, ubiquity and heterogeneity of these systems. Summarizing what previously discussed, the complexity of this system is enormously increasing by requiring first of all an enormous amount of data exchange. In addition, a great number of users will coexist in this new power system giving rise in some case to a competitive environment where users' objectives can be in conflict and data privacy need to be respected. Furthermore, the management architecture of this multi-component system need to guarantee interoperability capability to power systems. New components have to be able to join the grid without imposing any modification of the system. The different technology used, manufactory houses, software and hardware components, and

internal standards applied do not have to represent an obstacle. Hence, extensibility, flexibility and openness have to be fundamental requirements when thinking and developing this new management architecture.

Therefore, a modular and distributed structure should be the solution to implement an interoperable, flexible and robust system. In this architecture, each module can be constituted by a microgrid. In general, from an external point of view, each microgrid can be seen as a single entity which provides power and/or services by using its flexibilities [93]. On the contrary internally, each microgrid can implement local decision and control capabilities.

In the literature, the distributed approach is the most discussed and recognised for the management of smart grids. However, several questions are still open, such as tasks distribution, responsibilities of different actors, relationships between them, etc.. The implementation of the management and control strategies is one of these questions as well. Hence in this thesis, a management architecture for a multi-microgrid system is discussed and developed in order to implement a system with all described characteristics.

In the literature, the most discussed and applied architecture for Microgrid is the hierarchical one (see section II.2.2). In fact, this solution represents an interesting compromise between the two extreme management architectures: centralized and distributed. A totally decentralized architecture may not be satisfying due to the small size of microgrid constitutive users. First of all, this solution would need a massive installation of smart EMS, e.g. in each single house or apartment. Consequently, this would require a high initial expense, which could not be frowned upon by users. Secondly, the forecast error, in particular for day-ahead scheduling, would be high due the variable nature of small consumption profiles. Hence, it would be hard to implement a robust EMS making less affordable all initial expenses for implementing the smart EMS.

In the hierarchical architecture, tasks are subdivided among components, or group of components, which communicate and work in a collaborative way to reach common goals. In distributed structures, also the information exchange among components is made according to a hierarchical order [94]. In this context, as introduced in section II.5, multi-agent systems are a useful tool for the implementation and simulation of distributed microgrids. Several hierarchical structures are discussed in the literature. One of the earliest conceptualization of distributed control is described by *Dimeas* in [95]. In this paper, a three level architecture is

discussed and the role of Microgrid Central Controller (MGCC) is introduced. The MGCC is the actor responsible for Microgrid optimization and coordination of lower level controllers (e.g. DGs and ESSs controller) [95]. *Pipattanasomporn* presented a four-agents structure constituted of Control, DER, User and Database Agents [54]. DER and User Agents are responsible to store information, as well as to monitor and control the associated DER and consumption [54]. Moreover, *Nagata* implemented a seven-agent multi-agent system in [96]. Each agent represents a different kind of components that is possible to find in microgrids: load, generator, photovoltaic, wind-turbine, battery, grid and microgrid controller. A multi-agent model, which discusses roles and strategies of Virtual Power Plant Agent and Wholesale Market Agent, is discussed by *Vale* and *Santos* in [97] [98].

In this thesis, the developed MAS-based architecture takes into account these advancements. Hence, a hierarchical option for control and management is considered based on four main classes of agents:

- Electricity Sector Operators Agents (ESOA). In this level all current electricity system actors and new actors as well are parts:
  - Transmission System Operator Agent (TSOA)
  - Distribution System Operator Agent (DSOA)
  - Wholesale Electricity Market Agent (WEMA)
  - Retail Electricity Market Agent (REMA)
  - Flexibility Services Market Agent (FSMA)[12]
  - …
- Aggregators Agents (AGGA)
- Microgrid Management, Monitoring and Control Agent (MMCA)
- System Agents (SA):
  - Distributed Generators Agent (DGA)
  - Energy Storage System Agent (ESSA)
  - Load Agent (LA)
  - …

[12] The Flexibility Services Market is a new entity proposed in this thesis and discussed in section IV.4.2.

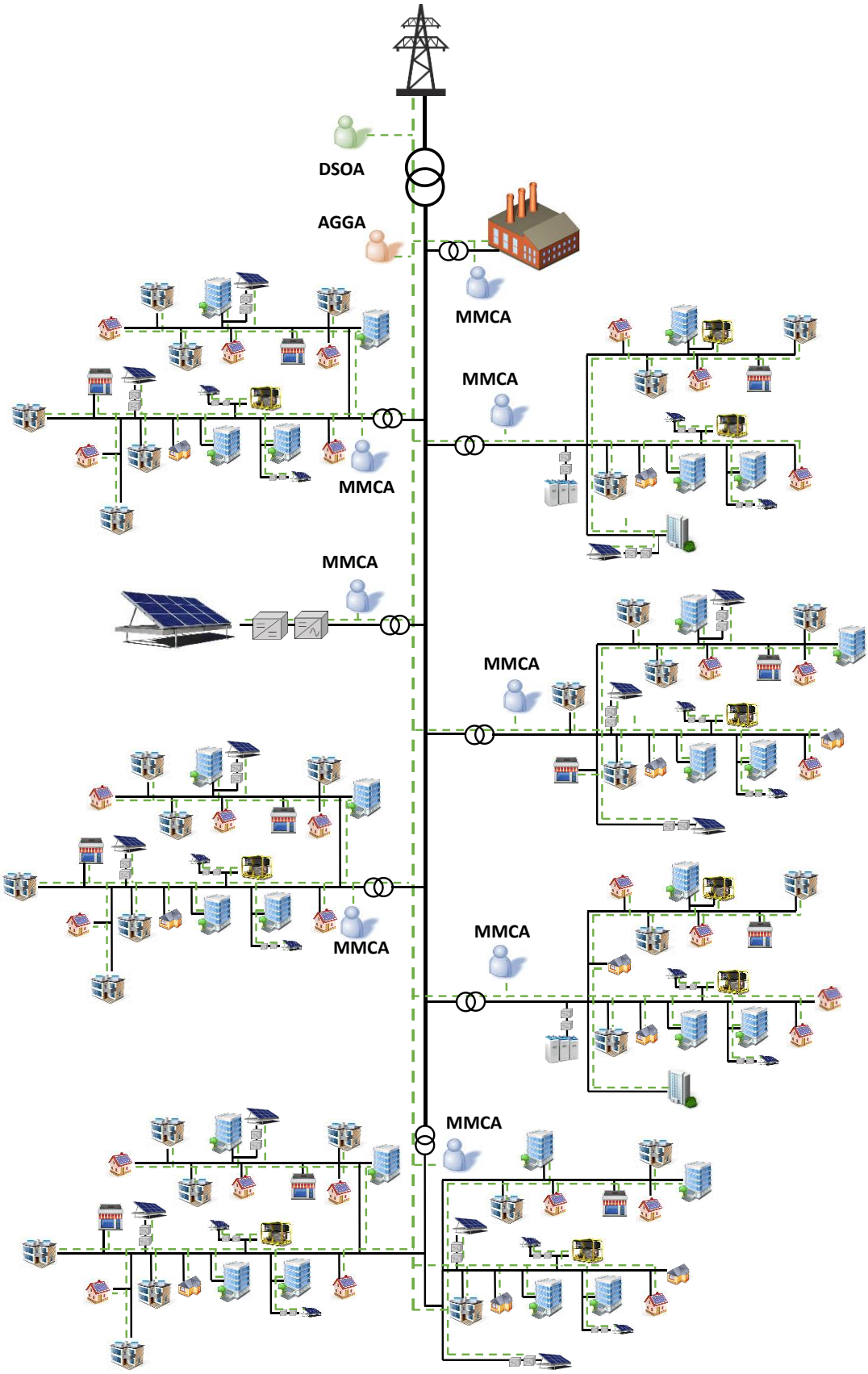

Fig. III.2 MAS-based hierarchical architecture

In this thesis only the role and actions of certain agents are discussed. In particular, the DSOA, the MMCA, the AGGA and the various SAs are addressed in order to discuss the implemented strategy for the energy scheduling of microgrid and multi-microgrid systems. The size of a single microgrids is considered to correspond to a LV/MV substation, such as a small community of residential and commercial users. The strategies used for the energy management impact the agent actions and their information exchange. In this thesis, the strategies implemented take into account only the needs and issues related to grid-connected microgrids. An example of distribution grid composed of connected clusters of microgrid with a MAS-based management architecture is shown in Fig. III.2, which is in part described in this chapter, and will be detailed in chapter IV.

In the following, a general framework and the main goals of each studied agent are discussed. Next sections and next chapter will detail for each agent: the tasks, the distribution of knowledge, the needed information to accomplish their goals and the time in which each action is made. In this chapter, discussions are more focused on the role and model of the MMCA and the SA as well as on their interactions. Whereas, chapter IV will focus on the model of the AGGA and DSOA, interactions among them and their interaction with the MMCA. It is difficult to build a general model for each agent, due to the fact that each model is strictly dependent to the applied strategy for EM and to the represented technologies. However, once defined an EM strategy, the exchanged information among agents have to remain the same without impacting the quality of management. This condition will guarantee the microgrids interoperability and flexibility by allowing the integration of different technologies.

Distribution System Operator Agent

The DSOA manages the distribution networks on MV and LV voltages. If dynamic tariffs are activated, it communicates with the REMA (or the WEMA, in case of medium-sized users) to obtain information about the forecast prices and send it to the MMCA or the AGGA. Otherwise, it communicates the type of daily tariffs for simpler options, e.g. the “Tarif Tempo” of EDF [99]. After that, it receives the results of the day-ahead and hour-ahead scheduled energy profile of each microgrids [90]. It uses this information to check if there are technical violations and sends them a final response (accept or reject).

Aggregators Agents

Generally, the AGGA control level is not required in all kinds of applications. It is needed in applications in which a more high level of responsibility and aggregation of active and/or passive resources is required, such as electricity or ancillary services markets. Details about the AGGA are unveiled in chapter IV.

Microgrid Management, Monitoring and Control Agent

The MMCA is the microgrid coordinator. Its main role is to guarantee the optimal EM of the microgrid in all timescales. Hence, it needs to exchange information with uppermost and lower control levels in order to accomplish its tasks. It communicates with the DSOA (or the AGGA if inserted) to take information about electricity prices and to negotiate the energy to sell or buy [90]. Meanwhile, it also gathers data from the LAs, DGs and ESSs connected to the microgrid. After the information gathering stage, it runs an EM algorithm and sends its results, which consist on day-ahead, hours-ahead and real-time dispatching orders for each SAs. For microgrids sized to work in islanded mode, the MMCA has also to monitor the voltage and frequency. In this manner it is able to detect contingency situations or grid failures and it can decide when work in islanded mode (as proposed by authors in [31]). In this case, it have also to communicate to the SAs when a change in the microgrid state occurs (grid-connected or islanded mode of operation).

System Agents

User's system agents are in the lower level of the control architecture. Each SAs could represent a single equipment, such as a PV systems, or an aggregation of components, such as all inflexible loads of a house or a building. Each DGA, ESSA and LA exchanges information with the MMCA through a bidirectional communication. Each DGA gathers information such as nominal data, type and measures of the generation system and stores them. From a general point of view, each user in the microgrid has to be free to decide if and when enter in the system and participate in the EM program. For example, also if an EV is plugged to the grid, its owner have to be able to decide when use its own car. Moreover, the DGA can decide if enter in the microgrid, based on electricity price, and its production and operational costs. It is responsible for adjusting active and reactive power of generators to regulate the voltage and in case of islanded mode operation to regulate frequency. Each DGA and LA runs forecast algorithms in order to predict production and consumption for aggregated components, which have the same characteristics.

In general, each agent has to represent a well-defined behaviour, which is identified by standard information exchanged, with respect to other level components, e.g. each SAs to the MMCA. However, depending on microgrid architecture, size and strategy, an agent could also has the possibility to change its nature from the point of view of the MMCA. This functionality can be implemented in agents that represent different systems. For example an agent that is representing an entire building, it can enter in the system as a DGA during certain hours and as LA during others.

III.3. Rule-Based Approach for Day-Ahead Scheduling

III.3.1. Logic Rules for Rule-Based Microgrid Scheduling

As stated in III.2.1, one of the most crucial objectives of implementing a distributed management lies on the distribution of knowledge and tasks among agents. In this strategy, the distribution of tasks was applied by giving to each SAs the ability to estimates and evaluate its own parameters, such as the state of charge for an ESS or the injected power for a PVS. This distribution of assignments will allow reducing the MMCA's workload.

This hypothesis influences all future development in this thesis starting by component models. In the literature, a wide variety of energy model for type of component are used for microgrid modelling. Hence, contributions focus more on global architecture and MMCA models, then DGA, LA and ESSA models, which are strictly related to the applied technology.

In this section, the day-ahead collaborative scheduling process is implemented by trying to reduce the amount of exchanged information among agents and trying to extremely distribute tasks and knowledge. This strategy is based on freedom choice concept, which aims to give the greatest possible freedom to each user. Hence, the process is implemented hourly and a Rule-Based Algorithm (RBA) is used. An hourly process can give a higher flexibility to users. In fact, if the MMCA's decision impacts on some user planning, the user has nevertheless the possibility to adapt itself by using its own flexibilities. For example, in a building with a PV system and an ESS system, a DGA representing a generation source, such as a PVS, can also manage an ESS and decide to store the energy, which is not shared in the microgrid. In this chapter, the MAS structure is composed of a DSOA, a MMCA and several DGAs, LAs and ESSAs.

Distributed Generators Agent

As discussed, each DGA manage and control one or more generators. The EM tasks requires a detailed knowledge of generators under its supervision, which means the type, its behaviour, its reaction to external solicitations and also the willingness of the DG's owner. Hence, a characteristic model has to be implemented in the DG agents in order to predict the DG behaviour. The aggregated behaviour of the generators is then sent to the MMCA.

In the literature, there are several models to represent generation systems for energy management applications. For PV systems, the climatic factors, which more influence their production, are the temperature and the irradiance. As is known, an increase in the irradiance induces a large increase in the injected current, which implies an increase in the injected power [100] [101]. On the contrary, an increase in the ambient temperature causes a decrease in the voltage, which means a reduction of the injected power [100] [101]. In most classical applications, PV systems are modelled by means of a linear power source which value varies according to the forecasted or measured ambient temperature and irradiance, as discussed in [102] [103] [100]. For day-ahead applications, the temperature and irradiance values are forecasted data in the PVS location or in a close site. These data can be directly forecasted by the DGA or by another agent called Weather Agent. Whereas in real-time applications, the temperature and irradiance used are the measured-valued.

An exhaustive and validated model for PV systems is discussed in [101]. The maximal producible power at the Maximum Power Point Tracker can be computed by using Eq. III.1:

$$P_{PV} = \eta_{INV} \cdot N^{mod} \cdot P_{STC} \cdot \frac{I}{I_{STC}} \cdot \left[1 - \frac{\gamma}{100} \cdot \left[T^{cell} - T_{STC}^{cell}\right]\right] \qquad \text{Eq. III.1}$$

where η_{INV} is the conversion stage efficiency, P_{STC} is the maximal power provided by PV system at standard condition [101], I and I_{STC} are the average forecasted solar irradiation incident on the PV and the irradiation at standard condition, T^{cell} is the cell temperature estimated and T_{STC}^{cell} is cell temperature at standard condition, γ is a coefficient defines as in [101]. The conversion stage efficiency depends on the used technologies and is function of the injected power and the working voltage. The tendency of this parameter is normally known and given by manufacturers, e.g. in [104].

On the contrary, diesel generators are not a variable source function of climatic parameters and they can work at their rated power at any time. Hence, it can be modelled by using a linear power source. However, it is needed to consider that their efficiency strictly depends on the operating power. The generator's performance decreases enormously when working at operating powers much smaller than the rated power, by inducing a high fuel consumption. Hence, it is more economical to operate this system with more than 30% - 50% of the rated power [105], depending on the size and the manufacturing house. In scheduling applications literature, other phenomena, which are not needed for inverted-based system with quasi-zero inertia, are sometimes taken into account. In fact, starting, ramp-up and ramp-down times have to be considered when modelling an engine-driven generator. These parameters are strictly related to the size of the system and the manufacturer. Consequently, it is interesting to locally use this information. Hence, in a distributed vision of *D-1* applications these considerations can be applied *a posteriori* directly by the DGA. For example, if in a certain time frame *h* the diesel generator has to be operated, the DGA knows that have to start the generator in advance.

In conclusion, taking into account these considerations, each generation system in the microgrid is modelled in the EM algorithm by using linear controllable power sources between a maximal and minimal power ($P^{g}_{\max_h}$ and $P^{g}_{\min_h}$) with an associated selling price (C^{g}_{t}). In case of PV technology, $P^{g}_{\max_h}$ can take as maximal value the average *D-1* forecasted power which can be computed by using the model implemented in the DGA (such as in Eq. III.1). For diesels, this value can be represented by their rated power. However at the end, DGAs decides if the associated generators have to participate in the trading process as a function of the hourly electricity price and generation costs

Energy Storage Agent

ESSs are complex bi-directional non-linear systems. Today, hundreds of different technologies are available. Hence, several kind of model depending on the used technologies and the phenomenon to simulate are available in the literature. In fact, each model aims to represent the behaviour of various parameters that identify the ESS. Following discussions are more focused on electrochemical systems, which convert chemical energy into electrical energy and *vice versa*.

The choice and the detail of the model strictly depend on the aspect that we need to highlight. However for EM applications energy models are needed. An ESS can be modelled by using a deterministic ideal model, as also proposed by *Haessig* in [106]. An ideal model allows to consider an ESS as a stock of energy without energy losses. Hence from the MMCA point of view, it can be seen as a linear power source between its maximal charging and discharging powers ($P^b_{ch_{max}}$ and $P^b_{disch_{max}}$) with limited charging and discharging capacities ($E^b_{ch_{max}}$and $E^b_{disch_{max}}$).

The model in the ESSA is hence a single-input/single-output dynamic model in which the capacity at timeframe *h+1* depends on the power order (P^b_h) computed by the MMCA at timeframe *h*, according to Eq. III.2. The stored energy allows to computes the maximal charging and discharging capacities available at *h+1*, by using Eq. III.3 and Eq. III.4, respectively.

$$E^b_{sto_{h+1}} = E^b_{sto_h} + P^b_h \cdot \Delta t \qquad \text{Eq. III.2}$$

where $P^b_h > 0$ for charging and $P^b_h < 0$ for discharging

$$E^b_{ch_{max}} = E_n - E^b_{sto_{h+1}} \qquad \text{Eq. III.3}$$

$$E^b_{disch_{max}} = E^b_{sto_{h+1}} \qquad \text{Eq. III.4}$$

Energy models are able to represent the energetic capacity of the ESS, but they are not able to represent the healthy state of the system. The state of health of the battery is fundamental because it has a strictly impact the performance of the battery. Moreover, a correct use of the battery can preserve the battery performances. In the literature, the State-of-Health (SOH) parameter is used to model the battery ageing. The SOH is defined as a "*measure that reflects the general condition of a battery and its ability to deliver the specified performance in comparison with a fresh battery* [107]". This parameter is often included in energy management algorithm in order to operate the ESS in the best possible performative-way. This practice is easily implementable in centralized EM, such as in [102]. However, it is not possible to apply same ageing models in distributed EM. In fact, the tasks of SOH estimation and implementation of strategy to reduce the ageing of an ESS have to be included in the ESSA. Hence, the ESSA needs to take into account the battery health when estimating the values of $P^b_{ch_{max}}$, $P^b_{disch_{max}}$, $E^b_{ch_{max}}$and $E^b_{disch_{max}}$ to send to the MMCA.

The ageing of the battery depends on several factors, such as the used technology, and the working temperature and current. Moreover, how deeply the battery is discharged impacts the total lifespan of batteries. The ageing of the battery is often expressed as function of the Depth of Discharge (DOD), which is defined as "*the amount of withdrawn capacity from a battery expressed as a percentage of its maximum capacity* [107]". Several efforts are made to characterize different battery technologies. For example, Fig. III.3 shows the lifespan variation as function of the DOD for four types of batteries widely used in industrial and research applications [101]. Based on these results, a good practice could be to limit the values the depth of discharging. Hence in the ESSA, this consideration is modelled by limiting the available $E^{b}_{ch_{max}}$ considering a lower rated capacity. Strategy to extend the ESS lifespan strictly depends on the system and has to be applied locally. Hence, the framework of ESSA can be easily extended with future considerations.

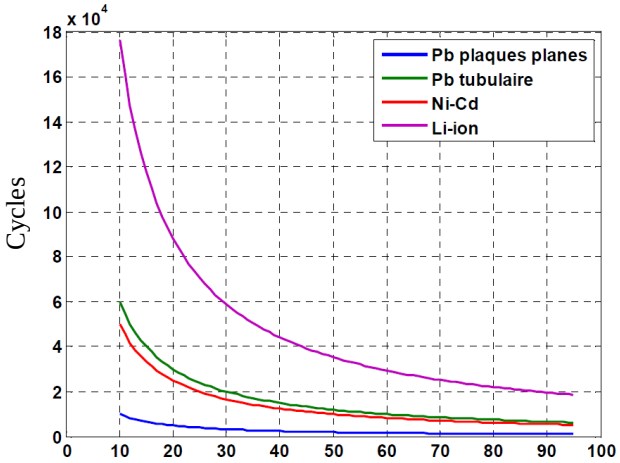

Fig. III.3 Number of cycle to decrease of 30% the ESS capacity as function of the DOD [101]

Load Agent

In this strategy, the consumption is considered inflexible and can be modelled with an hourly forecasted power profile (P^{l}_{t}), which have to be supplied by the MMCA through DGA or the DSOA. In hourly process, it is hard to add time-shiftable loads, such as appliances, which requires a more global vision to find the optimal operating timeframes. However, elastic load in power, such as HVAC, could be introduced in the LA programs.

Microgrid Management, Monitoring and Control Agent

As already introduced, the main goal of the MMCA is to implement a strategy for an energy-efficient and cost-efficient use of all resources connected in the microgrid. Hence, the core of this agent resides in the EM model. The MMCA is subject to numerous bidirectional exchange of information, due to its central position in the hierarchical structure. In fact at the same time, it works as distributor and aggregator of information for other levels. The description of the MMCA tasks requires the analysis of all the information exchanged among

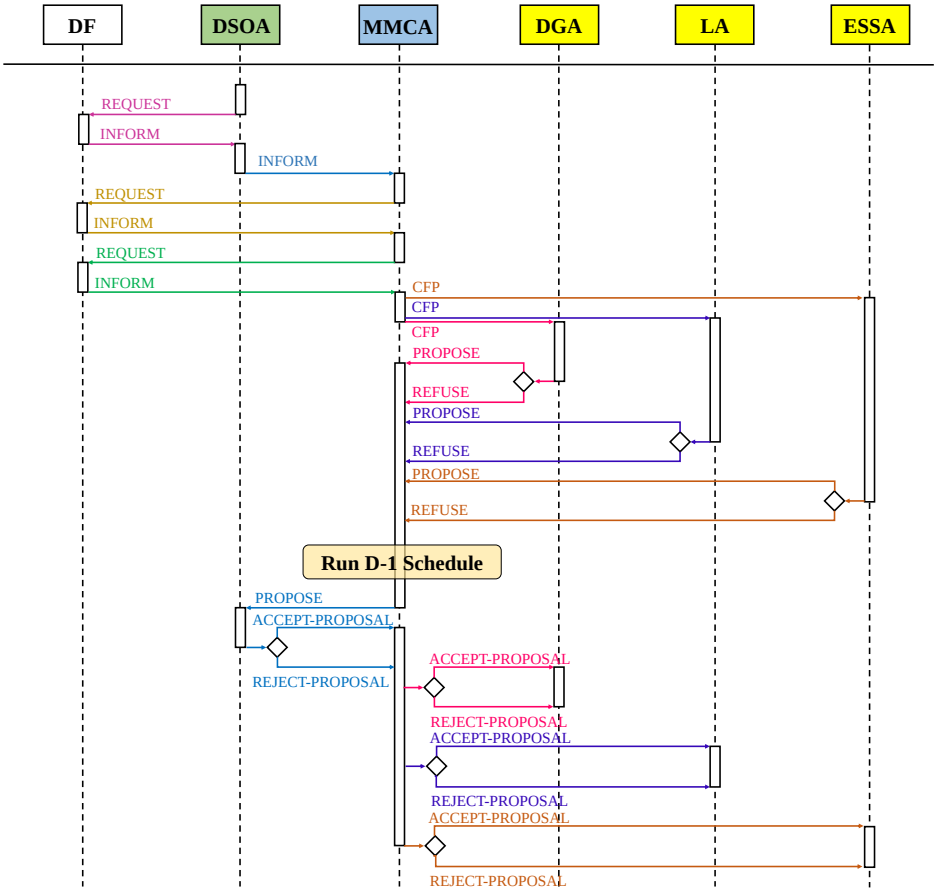

Fig. III.4 Sequence Diagram for Microgrid Day-Ahead Energy Management for each time frame

agents. Hence, all the needed interaction to implement the distributed EM are shown in the sequence diagram in Fig. III.4.

For the purpose of flexibility, the MMCA does not know *a priori* the number and the type of SAs which are working in the system. At any scheduling timeframe *h* of the day *D*, it checks available agents in the systems. These components can vary during the Agents' life based on equipment's failures or users desires. Hence, when the process starts, the DSOA search all working MMCA in the yellow pages service by using a *request* performative act. In JADE platform, the yellow pages service is implemented in the DF Agent [83] (as in Fig. III.4). In this manner, the hourly scheduling process starts. The same action is carried out by the MMCA in order to find all the SAs in the DF. The MMCA receive a *call-for-proposal* (CFP) by the DSOA and it is informed about forecasted electricity prices. Consequently, the MMCA call all available SAs by sending a *call-for-proposal* and by informing all LAs and DGAs about the hourly forecasted buying and selling price, respectively. Each SAs can positively or negatively responds to the MMCA based on their management software answer.

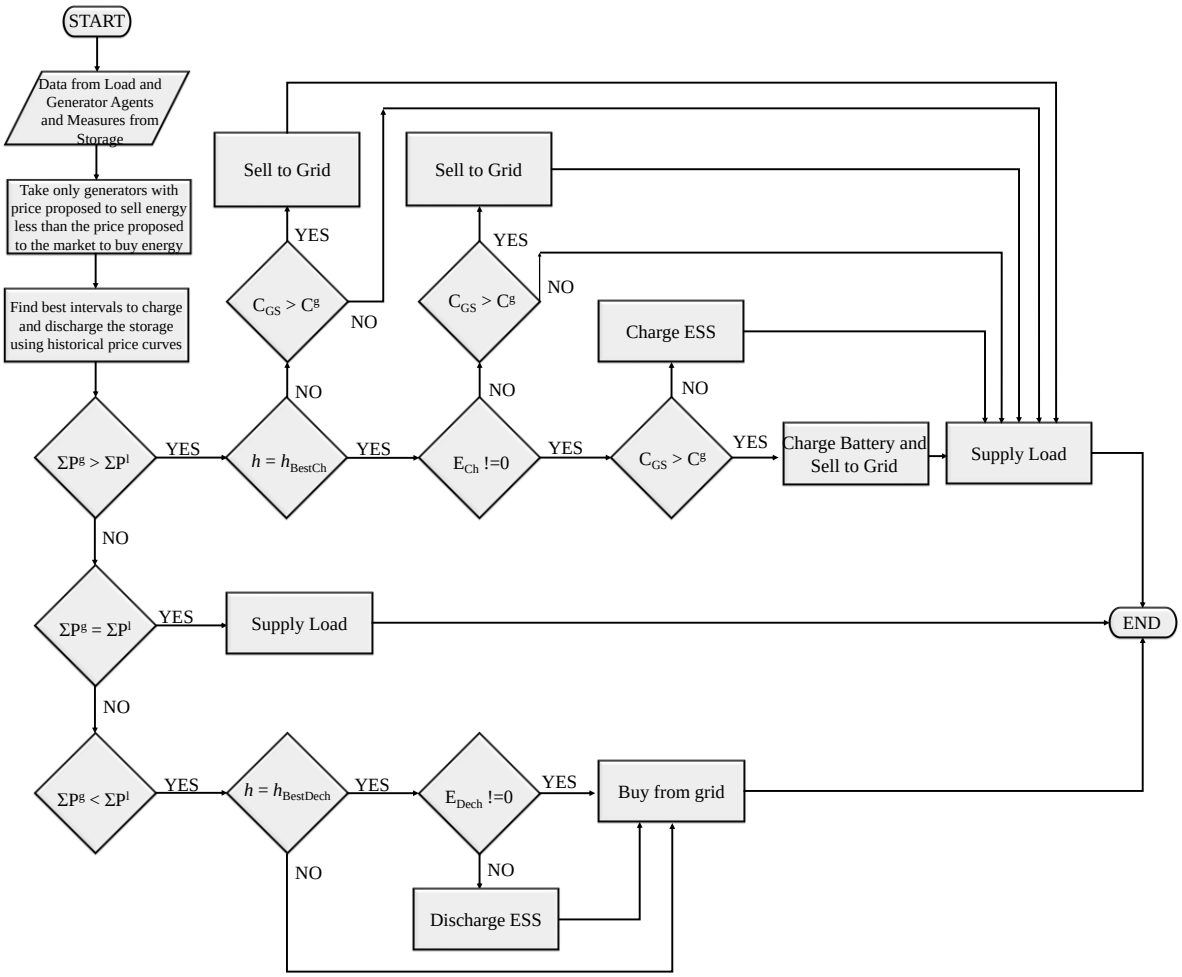

Fig. III.5 Rule-based flow chart for the day-ahead scheduling of microgrids in the MMC Agent

It can build its answer by using two opposite performative acts, *propose* or *refuse*, and put in the content the forecasted data of its production or consumption. In the same manner, the ESSA sends the computed charging and discharging powers, and maximal energy obtained by the battery management system. After computing the dispatch point of each resource, the MMCA submits the scheduled profile to the DSOA with a *proposal* performative act and waits its answer. As for SAs, the response is built by using the same performative acts: *accept-proposal* or *refuse-proposal*. At the end of the hourly scheduling, the MMCA inform each lower level agent of the concerned result and the process start again for the timeframe *h+1*.

The hourly operating point of the microgrid is computed by using the rule-based EM integrated in the MMCA. Rule-based approaches manage the controlled systems according to prefixed rules. The logic rules implemented in the MMCA resumed in the flow chart depicted

in Fig. III.5. At the beginning of the resources planning process, the day-ahead EM algorithm finds the best interval to charge and discharge the storage devices as a function of the historical data of market buying price and the historical data of the power exchange.

After that, it starts to analyse the forecast data for day *D+1* received by respective agents. The D-1 hourly price signals received by the DSOA provide an indication about next day prices. These prices are not the real prices payed to/from users. In fact, the actual prices are announced at the end of the scheduling process [108]. As explained in the DGA section, a first selection of the generators is locally made by each DGA, which previously received the forecasted selling price. Hence, each DGA selects participant generators as a function of the hourly electricity price and generation costs. For each timeframe, the energy sold or bought from the grid, the charge or discharge of the storage system and the accepted production of each generator are calculated based on inflexible load to satisfy and available production in the microgrid. The operating variable limits for each kind of technology are resumed in Eq. III.5-Eq. III.9. At the end of the scheduling, the MMCA stores the aggregated data of the total generation and consumption at the PCC (excluding the storage devices).

$$P^{g}_{\min_h} \leq P^{g}_{h} \leq P^{g}_{\max_h} \quad \text{Eq. III.5}$$

$$-P^{b}_{disch_{max}} \leq P^{b}_{h} \leq P^{b}_{ch_{max}} \quad \text{Eq. III.6}$$

$$0 \leq E^{b}_{ch_h} \leq E^{b}_{ch_{max}} \quad \text{Eq. III.7}$$

$$0 \leq E^{b}_{disch_h} \leq E^{b}_{dishch_{max}} \quad \text{Eq. III.8}$$

III.3.2. Case Study

As discussed in section II.5.3, the MAS was developed in JADE [67] according to the methodology described in II.5.4.2 and suggested by authors in [89]. Information exchange is based on speech act theory following standards proposed by the Foundation for Intelligent Physical Agents specifications [61] [77] [79]. For simplicity and continuity with JADE libraries, the rule-based EM algorithm in the MMCA was implemented by using JAVA.

The microgrid in analysis this case study represents a community of small-scale residential and commercial users. It comprises 4 main groups of users. Tab. III.1 resumes main characteristics of these groups, such as the number of connected households, the type,

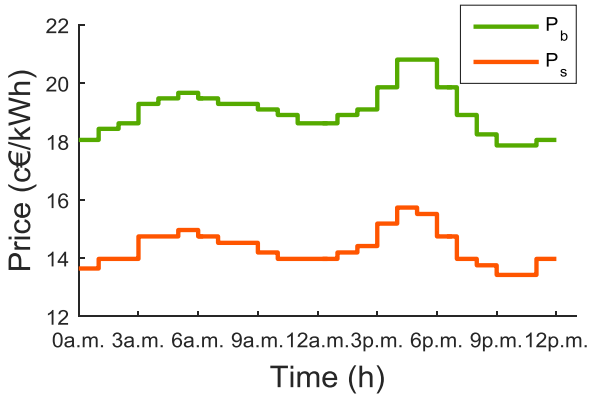

Fig. III.6 Daily dynamic prices for selling and buying electricity to/from the DSO used in the case study 1

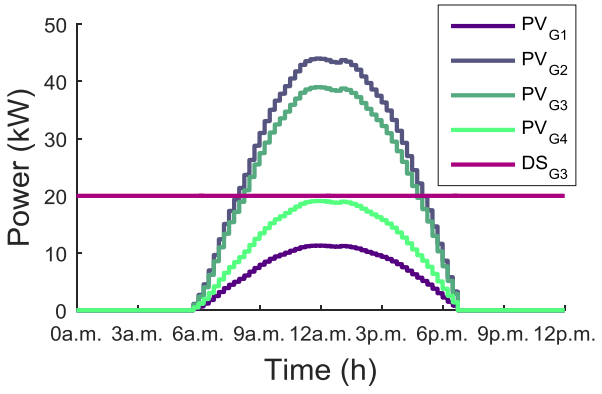

Fig. III.7 Daily PV and DS forecasted or available power profiles for group of users

Group	n° Users	Type	Nominal Data	IC	MC	LCOE	Num.
1	25	PV	Pn=45 kW	114.2 k€	0.02 % IC	13 c€/kWh	1
2	25	PV	Pn=39 kW	99.4 k€	0.02 % IC	13 c€/kWh	1
3	20	PV	Pn=20 kW	52.0 k€	0.02 % IC	13 c€/kWh	1
		Bio-fuel	Pn=20 kW	40 k€	200 €/kW	19 c€/kWh	1
4	15	PV	Pn=3 kW	8.3 k€	0.02 % IC	14 c€/kWh	3
		PV	Pn=6 kW	16.2 k€	0.02 % IC	14 c€/kWh	1

Tab. III.1 Nominal data, number and costs (LCOE, IC and MC) of generators in the Microgrid

the number and the rated power of connected DG. Both photovoltaic and bio-diesel technologies are discussed in order to consider a general case study. The group 3 has four small rooftop systems. Otherwise, other three groups installed on their building a unique medium-sized rooftop system. The PV day-ahead forecasted profiles and the bio-diesel available power (called DS) are shown aggregated for users' groups in Fig. III.7. The total consumption of the day in analysis is equal to 2050.1 kWh. Furthermore, a storage system is considered installed by the community. The storage system used is a Li-ion battery of 30 kW capacity and 45 kWh energy content. The state of charge of the battery is set to be between 10% and 90% and the initial SOC is set equals to 30%. All the agents participate in all the 24 time frame. However, it is possible to increase or decrease the number of participant agents because of the hourly process. This fact makes more flexible the system.

Moreover, the price to buy electricity and the contractual price are considered the same also if the contractual power of users is different. However this hypothesis is not restrictive and it will be reasonable to imagine a unique price for collaborative communities. The use of dynamic prices with two different prices for buying and selling electricity is considered a

possible and performing solution, which, *inter alia*, may induce a more efficient use of grid infrastructures. The use of this tariff strategy can overcome some of the issues associated with self-consumption strategies, by inducing users to remunerate their real exploitation of grid infrastructure, both when they absorb and inject electricity. The chosen shape of electricity price profile simulates the daily tendency of electricity price in the market with two daily peaks during morning and late afternoon hours, as in in many European countries. The used profiles for this case study are shown in Fig. III.6. The average buying and selling price for the day in analysis are 19c€/kWh and 14.3c€/kWh, respectively. The buying price is considered to contain both electricity price and grid tariff and it was chosen by considering current trends in the European electricity price for small and medium sized household consumers[13] (see Fig. I.2 [6]).

The price of the electricity produced through DG is important parameter in this distributed vision, in which DG's owners can propose a production cost to other microgrid's users. In addition, this parameter influences the entire daily electricity cost of the microgrid.

In this thesis, this price is computed by using the Levelized Cost of Energy (LCOE) [90]. The LCOE includes total costs of installing and operating a plant. The formulation of the LCOE is based on discounted cash flow approach in Eq. III.9:

$$LCOE = \frac{IC + \sum_{i=0}^{N-1} MC_i (1+r)^{-1} + \sum_{i=0}^{N-1} OC_i (1+r)^{-1} - SV(1+r)^{-(N-1)}}{\sum_{i=0}^{N-1} E_i (1+r)^{-1}} \quad \text{Eq. III.9}$$

The terms *IC*, *MC* and *OC* in this equation are respectively the investment cost, the maintenance cost and the operating costs. Furthermore, *SV* states the salvage value of the system at the end of its useful life, *N* is the system operational lifespan and *r* is the discount rate.

The investment cost of a PV system is composed of the modules, electric components (wiring and inverter) and other costs, such as racks, installation costs, project and permits. The *IC* of the different PV systems is evaluated as a function of the installed power as proposed in [109]. The applied formula could be found in Eq. III.10:

[13] Annual consumption lower than 5000 kWh.

$$IC_{PV} = P_n \frac{a}{P_n^{\,b}} \qquad \text{Eq. III.10}$$

where P_n is the installed power. a and b are positive and constant parameters computed through statistical analysis [109].

As far diesel and bio-fuel technologies, the installation costs mainly includes the costs of the diesel generator, electric components and others, such as effluent storage tanks, installation, project and permits as well. The operational lifespan of solar systems does not depend on its utilization and it is given by manufacturers. On the contrary, it depends on the operating time for diesels. However, the operational lifespan *N* is considered fixed for both and equals to 25 years for PV systems [109] [110] and 15 years for diesel or bio-fuel systems [111].

The *MC* of PV systems mainly takes into account the cleaning cost of panels and the supervision costs of electronic components. In the literature, it is estimated as percentage of the annualized investment cost [109]. As the *IC*, also the *MC* and the *OC* of diesel-based DGs depends on three factors: the annual operating time, the fuel consumption and the fuel purchase price. The diesel and bio-fuel annual operating time are respectively estimated to be 5.000 h/year and 7.000 h/year [111]. Furthermore, also if the diesel and the bio-fuel (e.g. palm oil) prices vary, they are supposed fixed and equal to 0.58 €/l [110] and 0.6 €/kg [111].

For both technologies, the computed *IC* and the applied *MC* values are listed in Tab. III.3. Hence by applying all these hipotesis, it is possible to compute the *LCOE* for both technologies, which are 19 c€/kWh for the bio-fuel systeme and, 14 c€/kWh and 13 c€/kWh for PVs.

An analogous analysis can be done for the proposed price of the battery in the microgrid. The installation cost of an electrochemical storage system comprises the purchase price of several components, the installation costs and transportation costs. The purchase cost mainly includes the battery packs, the conversion stage and the battery management system prices. As for DGs, the calculation of the LCOE can be used to represent the cost of the ESS. The installation costs are taken equal to 400 €/kWh for the battery pack and 250 €/kW the conversion stage. Also in this case maintenance and labour costs need to be added. The maintenance cost is assumed to be the 0.5% of the IC. Furthermore, the system is considered

to be replaced after 10 years of operation [112], after a life cycle (charge/discharge) of 5.000 cycles. Hence, the ESS battery costs are estimated to be 10 c€/kWh/day.

The efficiency of the implemented models is evaluated by analysing some important parameters that give indications about the microgrid's daily revenues/expense and the amount of locally produced energy. In particular, the used parameters are:

- the daily average kWh cost payed by µgrid's consumers, stated as $\mathrm{CB_{\mu G}} = \frac{\sum_{t=1}^{T} P_t^{grid\_buy} \cdot C_t^{grid\_buy} \cdot \Delta t + \sum_{t=1}^{T} \sum_{g=1}^{DG} P_{loc_t}{}^{g} \cdot C_t^{g} \cdot \Delta t}{\sum_{t=1}^{T} \sum_{l=1}^{L} P_t^{l} \cdot \Delta t}$, where the first part denotes the expense for buying energy from the main grid and the second the expense for buying energy from DGs ($\sum_{g=1}^{DG} P_{loc_t}{}^{g} \cdot \Delta t \leq \sum_{g=1}^{DG} P_t^{g} \cdot \Delta t$).
- the daily total expenses or revenues of the microgrid, which takes into account the money flow with the DSOA/AGGA and the generation and storage costs $DC = \sum_{t=1}^{T} P_t^{grid\_buy} \cdot C_t^{grid\_buy} \cdot \Delta t - \sum_{t=1}^{T} P_t^{grid\_sell} \cdot C_t^{grid\_sell} \cdot \Delta t + \sum_{t=1}^{T} \sum_{g=1}^{DG} P_t^{g} \cdot C_t^{g} \cdot \Delta t + \sum_{t=1}^{T} \sum_{g=1}^{B} Pch_t^{b} \cdot C_t^{b} \cdot \Delta t$
- the daily money flow between the microgrid and DSO, stated as $MF = \sum_{t=1}^{T} P_t^{grid\_buy} \cdot C_t^{grid\_buy} \cdot \Delta t - \sum_{t=1}^{T} P_t^{grid\_sell} \cdot C_t^{grid\_sell} \cdot \Delta t$
- the percentage ratio between the exploited and the available/forecasted power in the microgrid for the overall production, defined as $DG_{acc} = 100 * \frac{\sum_{t=1}^{T} \sum_{g=1}^{DG} P_{used_t}{}^{g}}{\sum_{t=1}^{T} \sum_{g=1}^{DG} P_{av_t}{}^{g}}$, and for each source stated with the same formulation and called $\mathrm{PV_{acc}}$ and $\mathrm{DS_{acc}}$, respectively.
- the self-consumption ratio defined as the ratio between the part of the consumption satisfied with electricity produced in the microgrid and the total daily energy generated in the microgrid, $\mathrm{SCR} = 100 * \frac{E_{loc}^{DG}}{E_{tot}^{DG}}$, as in [113].
- the self-production ratio defined as the ratio between the part of the consumption satisfied with electricity produced in the microgrid and the total daily consumption of the microgrid, $\mathrm{SPR} = 100 * \frac{E_{loc}^{DG}}{E_{tot}^{L}}$, as in [113].

$\mathrm{CB_{\mu G}}$, DC and MF give an indication on the economic benefits related to the applied energy management strategy and the possible benefits of distributed generation usage, as well. The percentage ratios give a practical idea on the strategy operation by showing its advantages and disadvantages. It can also be used to judge the sizing of systems to install in

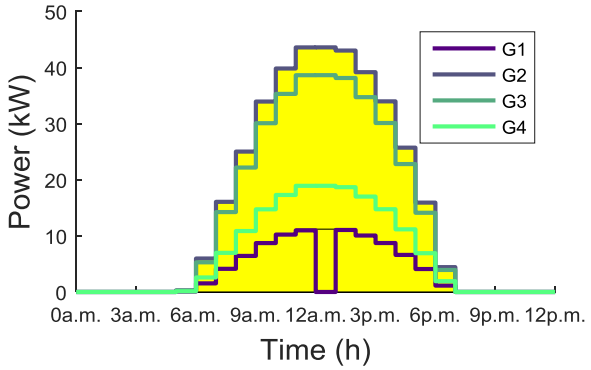

Fig. III.8 PV input and output for each group of users

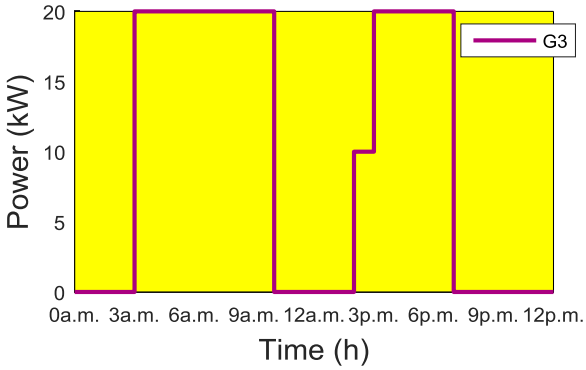

Fig. III.9 DS input and output of group 3

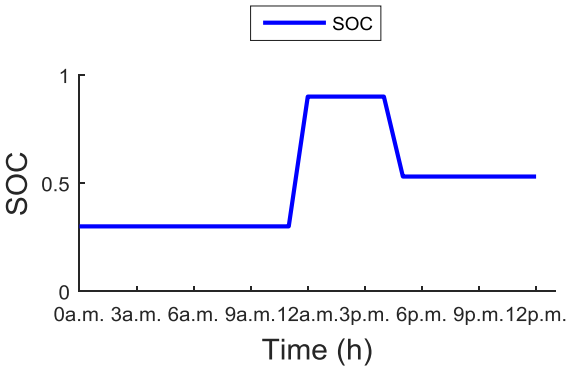

Fig. III.10 ESS SOC

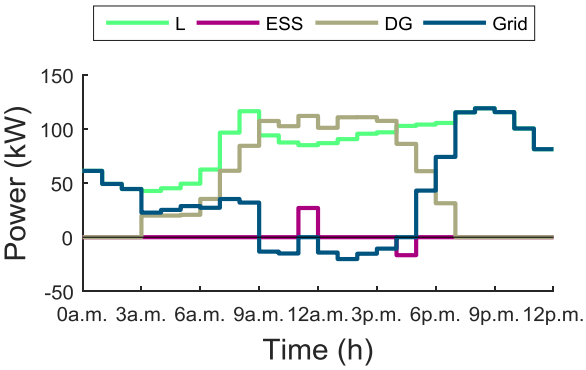

Fig. III.11 Microgrid aggregated daily profiles (grid exchange, consumption, generation and storage)

$CB_{\mu G}$ *	DC *	MF *	SCR	SPR	$CBref_{\mu G}$ *	DCref *
16.3 c€/kWh	364.8 €	194.9 €	91.6 %	52.4 %	19.0 c€/kWh	390.5 €
PV *	**DIES** *	**DG**	PV_{acc} *	DS_{acc} *	DG_{acc} *	**Load** *
954.8 kWh	480 kWh	1434.8 kWh	98.8 %	47.9 %	81.8 %	2050.1 kWh

*__Legend__: *MF* : Daily money flow between the µgrid and DSO (expenses and revenues); * *DC* : Daily expense or revenue of the µgrid considering the money flow with the DSOA/AGGA, the DG costs and the ESS costs; * *Load* : Daily consumption of each µgrid;* $CB_{\mu G}$: Daily average kWh cost payed by µgrid's consumers; DG_{acc} : Percentage of used energy on available/forecasted DG; * $CBref_{\mu G}$: Daily average kWh cost payed by µgrid's consumers buying all electricity needed by the DSOA; *DCref* : Daily µgrid expense buying all electricity needed by the DSOA.

Tab. III.2 Results of case study 1

the microgrid. The SFR is an important parameter for microgrid and DSO point of view. In fact, it allows to understand the overall behaviour of the microgrid and the exploitation of distribution networks by considering the exchanged energy in the PCC.

The results of the simulation are listed in Tab. III.2. Furthermore, the efficiency of the prosed scheduling algorithm is compared with a reference case. The reference case considers the same consumption and electricity prices, but without distributed generation and storage systems. In other words in the reference case, the electricity is directly bought from the retailer. DC is equal to 364.8 € in the case in analysis, which means a cost reduction of 6.6 %

compared to reference case. Moreover, about the 53.4 % of this expense is used to remunerate the installation of DG in the microgrid, by incentivizing in particular the diffusion of photovoltaic systems. The economic benefit can also be seen by the radical reduction in the average microgrid's daily kWh cost to 13.3 c€/kWh. Fig. III.8 compares the available PV production forecasted at D-1 and the accepted one, respectively as input and output to energy management algorithm. The same comparison is reported for the bio-diesel generator in Fig. III.9. As it is possible to see, the operation of this generator is scheduled between load peak-hours with high price of electricity and lack of PV production.

In general, the local production is highly exploited to satisfy the microgrid load and almost all the surplus is stored or injected in the distribution grid. In fact, the PV_{acc} accepted in the day-ahead scheduling phase, before being proposed to the AGGA/DSOA, is equal to 98.8 %. Otherwise, the DS_{acc} reaches simply the 47.9 % due essentially to high PV production. As in Fig. III.10, the storage system in charged during a low price time-frame and discharged during higher price time-frame, by considering historical buying price of electricity. The use of both PV, bio-diesel and storage technologies increase a lot the SCR, which reaches the value of 91.6 %. Furthermore, the SPR reveals that more than 50 % of the consumption is directly satisfied with on-site produced electricity.

On the whole, it is possible to conclude that the installation of PV systems in smart communities can on one side strongly reduce the kWh cost for consumers and on the other side can be a source of revenues for PV owners. This statement can be strengthened by considering the current downward trend in PV installation costs.

On the contrary, the installation of bio-diesel generators requires further investigation in order to conclude an economic benefit related to their installation. Statistical studies, which take into account the seasonality of production and consumption profiles, are needed in sizing stage. In particular, it is needed to analyse the exploitation of diesels in wintertime when PV production is strongly reduced. However, DS could be considered necessaries in other applications, such as islanding functionality in the microgrid, cogeneration and especially in case of incentives for high self-consumption or self-production rates.

III.4. Optimization-based Approach for Day-Ahead Scheduling of Microgrids

III.4.1. Single-Objective Optimization Problems

In section III.3.1, a basic algorithm based on logic rules was presented in order to schedule the operation point of all available resources in the microgrid. However, also if this kind of algorithm allows to find an efficient operation point, it is quite hard to reach the best possible allocation of resources, in particular for complex system with a large amount of freedom degrees. Hence, it is needed to introduce a branch of mathematics which studies the scientific approach for efficient decision making. This branch is called management science, or more commonly operational research. Mathematical programming or optimization is the area of operational research which studies how to reach the optimal allocation of available resources by taking into account the competitiveness of all activities under analysis and by considering the real nature of the problem.

Mathematical programming can be used to solve several kind of real-life problems with a completely different nature, such as financial, industrial and organizational, by reducing costs and improving activities. A typical example of mathematical programming application is the schedule process of aircraft, crews and tariffs. The use of optimization enormously decreased the costs of flight companies by positively impacting the people way of travel.

The optimal allocation of resources consists essentially of finding the most-efficient solution for the problem under study. Hence, a quantitative measure able to indicate the performance of the system or process in analysis is required [114]. This quantitative measure is completely problem-oriented and could be a cost, revenue or losses function, and so on. In optimization science, this quantitative measure is called objective function, which is strictly related to the system nature. From a mathematical point of view, this quantitative measure can be expressed by using a function. The value assigned to the variables of this function represent the operation point of each element in the system.

Moreover the real nature of the system or process in analysis needs to be represented by giving a mathematical formulation to all lows and limitations that identify the phenomenon under study. The system characteristics can be expressed by developing equations and/or inequalities, which put in relation and limit the variable of the problem. The set of equations and inequalities that identify the problem are called constraints.

Solving an optimization problem means to find the best combination of the single element operation points, that are the value to assign to each variable, in order to reach the optimal

value of quantitative measure. As known in mathematics, find the optimal value of a generic function means to find its minimal/maximal point on its variables.

The standard formulation of a generic optimization problem can be expressed as a minimization problem, without loss of generality, by Eq. III.11-Eq. III.12:

$$\min_{x \in S} f(x) \qquad \text{Eq. III.11}$$

$$S = \left\{ x \in \mathbb{R}^m : \; h_i(x) = 0 \;\; i \in I \, , g_j(x) \leq 0 \;\; j \in J \right\} \qquad \text{Eq. III.12}$$

where x is the vector of problem variables, $f(x)$ is the objective function and S is the set of constraints of I+J size that the solution of x have to satisfy. f, h and h are real-valued functions on a subset of $\mathbb{R}^m$ [114]. The best combination of operation points x is called the solution of the optimization problem, or better the global minimizer of $f(x)$. Formally, the optimal solution can be stated as the point x^* such that $f(x^*) \leq f(x)$ for all $x \in S$.

A problem with I and J equal to zero are called *unconstrained optimization problem*. On the contrary, all other problems are called *constrained problems*. This distinction is an important element in order to classify optimization problems. Real applications are often subject to limits, which requires the development of a constrained model. However, constrained problem can be reformulated as unconstrained by replacing constraint with penalty terms in the objective function [114]. This manipulation allows to give more flexibility to the model by discouraging constraint violations. This practice can also be applied to some particular constraints by maintaining a constrained problem.

Moreover, other classification are made in the literature according to the nature of the objective function and constraints, in particular linearity or nonlinearity, and the type, size or uncertainty of variables, e.g. continuous or integer variables, stochastic or deterministic, and so on [114]. Problem with linear functions for both objective and constraints are widely used for a variety of applications. They are known with the name of *linear programming* (LP) problems. However, nonlinear relationships are quite common in physics and engineering applications. Typical examples are the real and reactive power balance equations in AC circuits. Problems with at least one nonlinear relationship in constraints or in the objective function are then classified with the name of *nonlinear programming* problems. Moreover in practical applications, some variable have the necessity to assume integer values in order to make sense. For example in crew organization on a flight, we can't take in consideration a

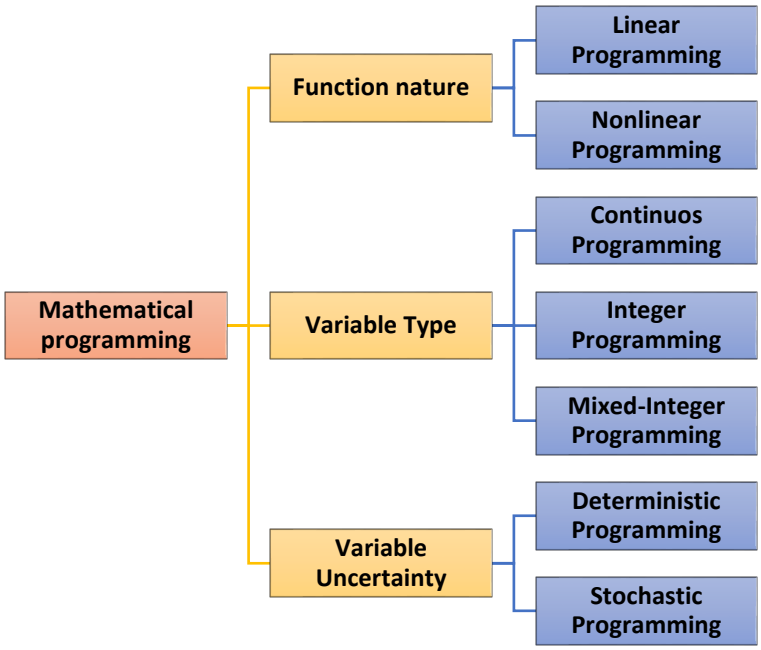

Fig. III.12 Mathematical programming classification

fraction of person. Problem with integer or continuous variables are classified with the name of *integer programming* (IP) and *continuous programming*, respectively. These two classes of problems are pure if all decision variables in the problem are of the same type. However, a hybrid of both kind of variable is possible and is widely used in real-life problems. This hybrid class of problems is known as *mixed integer programming* (MILP). An important special case of MILP problems is the binary case, also called *0-1 mixed integer programming*, which is used to model black and white decisions. A classification of mathematical programming problems based on discussed factors is resumed in Fig. III.12.

In most applications, optimization problem can't be solved analytically. Hence, the characteristics of the problem are fundamental in order to detect the best way to numerically solve the problem and the more appropriate algorithm to apply.

In general, linear problems are easier to solve and the convergence of their solution algorithms is more rapid than for nonlinear problems. Moreover nowadays, a large choice of solution algorithm to solve linear problems is available in the literature and a wide range of efficient toolbox was developed. The more ancient algorithm, which also made the rapid fortune of operational research, is the simplex algorithm. Simplex algorithm is based on iterative movements on the edge of the polytope, which represents the feasible region of the problem. All different variants of this method are still used in practice. In fact, it remains

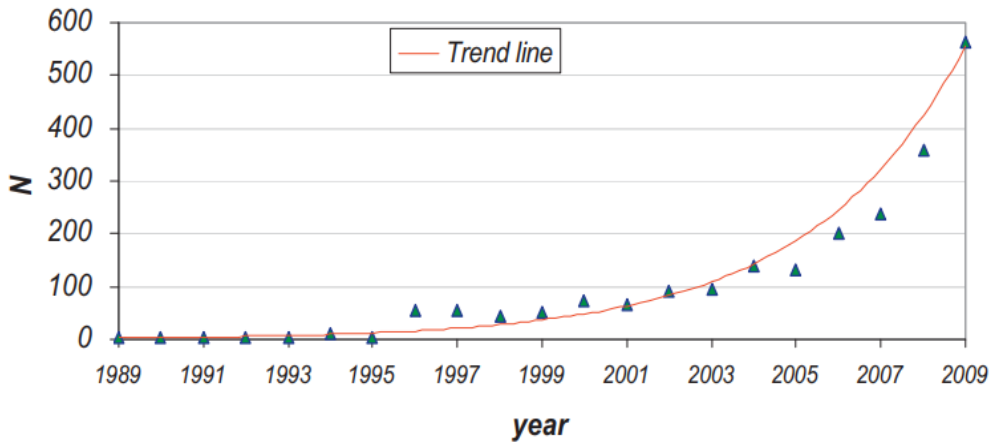

Fig. III.13 Review on articles using optimization to renewable systems applications [118]

fairly efficient and in most cases run sufficiently quickly [115]. However in worst cases, it does not run in polynomial time [115]. Hence, other classes of solver algorithm, which run in polynomial time, were developed, such as ellipsoid [116] and interior-point [117] methods. On the contrary of the simplex method, interior-point algorithms iteratively move the interiorly of the feasible region [115].

As in practice in a number of applications, in case of nonlinear programming, it is good practice to linearize nonlinear constraints. In fact, a nonlinear constraints can be replace by a set of linear inequalities by applying one of the technique proposed in the literature, such as in [119]. The reformulated problem can consequently solved in an easy and more efficient way as a MILP. Also MILP or IP are harder to solve than linear programming problems [95]. In fact, integer or binary variables make the problem non-convex, by increasing memory and solution time. Branch and bound algorithm is considered to be one of the most successful ways to solve practical IP [117]. Branch and bound (B&B) algorithms starts by solving a linear program in which all the variables are real, which is the "relaxation" of the original MILP. If in the solution of the relaxed problem, one or more integer variables have fractional solution, the B&B algorithm starts to branch the overall problem. It starts an iterative process in which some variable, that is supposed to be integer, is chosen and two new MILP sub-problems are generated. These two problem are the relaxed and solved, and so on. However, the integrity gap between the LP relaxed problem and the original problem are frequently too large by requiring an extensive branching process [120]. Hence, new technique was implemented and combined, such as cutting planes method with B&B, and several efforts

have been made in algorithm science in order to make MILP an efficient toolbox for real-life applications. Several stable and robust commercial and non-commercial solvers are available to solve MILP problem, such as GLPK [121], CBC [122] and SCIP [123].

Thanks to all improvements in solution techniques and available toolbox in last decades, mathematical programming has become an indispensable framework for solving complex problems in the field of RES-based systems. The growing use of these techniques for renewable systems applications is largely discussed in reviews on optimization methods and applications proposed by authors in [118], where they graphically shows the large increase of studied applications (Fig. III.13). To give just some example about the existing applications of mathematical programming in power systems, it is possible to consider: the economic dispatch of generation units for a small-sized isolated power system discussed in [124], the optimization approach to support the participation in the day-ahead and secondary reserve markets of an EV fleet reported in [125] and the building scheduling in order to reduce global costs of electricity and natural gas proposed in [126]. The effectiveness of MILP approach for microgrid optimal scheduling is also confirmed by comparative studies based on economic results and computational duration parameters, such as in [127].

III.4.2. Mathematical Formulation for Optimization-Based Microgrid Scheduling

III.4.2.1. Mathematical Formulation

Nomenclature

Sets:

T	Optimization problem timeframe
DG	Set of distributed generation
B	Set of energy storage system
L	Set of inflexible loads
FL	Set of Flexible Loads (FL)
D	Set of flexible load usage interval set by users

Parameters:

t_{start}, t_{end}	Initial and final time frames of set *T*
$t_{bid}^{fl} t_{start}^{fl}$	User desired start, end time for flexible load *f*
t_{bid}	Intervals in a bid proposal (h)
C_{GB_t}, C_{GS_t}	Price to buy/sell electricity from/to the main grid in time frame *t* (c€/kWh)

C_t^g	Distributed generation selling cost in time frame *t* (c€/kWh)
C_t^b	Battery cost in time frame *t* (c€/kWh)
$E_{nom}{}^b$	Battery capacity (kWh)
$\eta_{ch}^b, \eta_{disch}^b$	Battery and conversion stage efficiency during charging/discharging
SOC_{max}^b, SOC_{min}^b	Maximal and minimal State of Charge (SOC) of battery *b*
$SOC_{start}^b, SOC_{end}^b$	Battery initial and final SOC of battery *b*
$OM_{t,d}^{fl}$	Operating cycle matrix of flexible load *f* (kW)
$P_{max_t}^{\ g}, P_{min_t}^{\ g}$	Maximal and minimal power of distributed generation *g* in time frame *t* (kW)
$P_{\max\_ch_t}^b P_{\max\_disch_t}^b$	Maximal charging and discharging power of battery *b* (kW)
P_t^l	Power of inflexible load *l* in time frame *t* (kW)
Variables:	
P_{B_t}, P_{S_t}	Electricity bought/sold from/to the main grid in time frame *t* (kW)
P_t^g	Electricity produced by distributed generation in time frame *t* (kW)
$P_{ch_t}^b, P_{disch_t}^b$	Battery *b* charging and discharging power in time frame *t* (kW)
SOC_t^b	State of Charge of Battery *b* in time frame *t*
P_t^{fl}	Power of flexible load *lf* in time *t* (kW)
x_t^g	Binary variable (1 if g is operating in time frame *t*, else 0)
x_t^b	Binary variables (1 if *b* is charging/discharging in time frame *t*, else 0)
x_d^{fl}	Binary variable (1 if *f* is operating, else 0)
x_t	Binary variable (1 if *f* is microgrid is selling energy, else 0)

Mathematical Formulation Description

As for the RBA in III.3.1, the deterministic optimization-based approach for the EM of microgrids aims to find a global satisfactory operating point. As in previous section, one of the most crucial objective is the implementation of tasks distribution through the information distribution and parameter estimation among agents. Each SA has to estimates and evaluate its own parameters, and send it to the MMCA.

The optimal operating point of the entire microgrid is constituted by the optimal combination of the operating point of each unit in the microgrid:

- injected energy of each generation system,
- injected/absorbed energy of each storage system,
- absorbed energy of each inflexible and flexible load,
- absorbed/injected energy from/to the host grid,

all defined as a power set point (injected/absorber) for a certain time-frame of the day. The quantitative measure which defines the optimal operating point for the microgrid is defined by users and imposed by the objective function of the optimization problem. The objective function for the day-ahead scheduling problem aims from one side to minimize users' expense and on the other side to maximize their revenues by selling the surplus electricity [128].

As in the RBA, this model receives the day-ahead forecasted hourly price signals. However, this time the information are directly gathered for the entire day *D+1* and the optimization is run for the 24-hours profile. The trading process between the DSO and the MMCA is still implemented hour-by-hour (e.g. 0.00 a.m.-1.00 a.m., 1.00 a.m.-2.00 a.m., etc.) and with a bid duration of 1 h. At the end of the hourly scheduling, the final hourly profile of the microgrid is submitted to the DSOA and the microgrid is re-optimized for next hours of the day. The mathematical formulation of the problem implemented in the MMCA is expressed in equations Eq. III.13-Eq. III.25 [128].

The medium-term scheduling of a grid-connected microgrid can be mathematically formulated as a MILP. The objective function is expressed in Eq. III.13:

$$\min\ \Delta t \cdot \sum_{t \in T} \sum_{g \in DG} C_t^g \cdot P_t^g + C_{GB_t} \cdot P_{B_t} - C_{GS_t} \cdot P_{S_t} + \sum_{b \in B} C_t^b \cdot P_{ch_t}^{\ b} \qquad \text{Eq. III.13}$$

As in previous algorithm C_t^g and C_t^{batt} are fixed parameters proposed by the DG owner and contain costs related to the installation, maintenance and replacement. Moreover in this formulation, it is possible to integrate a cost associated to usage of the ESSs.

The formulation of the optimization problem incorporates simplified model of single or aggregated components through its constraints. The constraints applied in the implemented formulation are described from Eq. III.23 to Eq. III.25.

Distributed Generation

The desired or available power of each distributed generator is computed as described in DGA section in III.3.1. Hence in the MMCA for a certain time step *t*, DG systems are modelled through two power limits ($P^g_{\max_t}$ and $P^g_{\min_t}$), as in Eq. III.14. These bounds limit the value of the problem variable P_t^g, which corresponds to the operating point of g in a certain time step *t*. In this model, it is not applied the selection of DG groups to insert in the process as in RBA, due to the daily characteristic of the optimization horizon.

DG production upper and lower limits:

$$x_t^g \cdot P_{min_t}^g \leq P_t^g \leq x_t^g \cdot P_{max_t}^g \quad \forall t \in T \quad \forall g \in DG \qquad \text{Eq. III.14}$$

Energy Storage System

In section III.3.1, the behaviour of ESS was represent by using an ideal model. The same considerations made are valid. However, this model risks to be too approximate for daily optimization. Hence, a model which is able to deeply pick up the behaviour of the ESS by introducing power losses is needed. A dynamic linear energy model of battery can be introduced [129] [130] [131].

This model considers the ESS as a single input and single output system where the state variable is the stored energy. In general, the energy stored can be replaced by another parameter intrinsically related to energy, called State-of-Charge (SOC). The SOC is defined as "*the percentage of the maximum possible charge that is present inside a rechargeable battery*" [107]. The used model for the ESSs is represented by Eq. III.15- Eq. III.20. However, the optimization-based approach allows to detail the ESS implemented model with respect to the applied model in III.3.1. In the literature, several efforts concern studies related to the approaches used to estimate the state of the ESS (capacity, state of charge, etc.). Many of these methods today have achieved a great level of reliability [129] permitting this decentralization of tasks. The first two inequalities limit the charging and discharging power to $P_{\max\_ch_t}^b$ and $P_{\max\_disch_t}^b$, respectively. These values are subject to the maximal current which can be tolerate by the battery and the conversion stage in steady state for security reason. These currents can be considered with good approximation constant. However, power limits depends also to the battery open-circuit voltage. This value is not constant and is strictly related to the SOC. However in the literature, it is common practice to consider it as a static value for applications such as medium-term scheduling [129] [130] [132] of microgrids and virtual power plants. Constraint Eq. III.17 denotes the dynamic relation between the energy in the battery at time *t* and *t-1* by means of average values of charging and discharging energy efficiency [103]. The SOC can be bounded among SOC_{max}^b and SOC_{max}^b to slow down the battery degradation and ageing [102]. Finally, constraints in Eq. III.19 and Eq. III.20 impose the initial and final daily SOC.

ESS modelling:

$$0 \leq P^b_{\mathrm{ch}_t} \leq x^b_t \cdot P^b_{\mathrm{max\_ch}_t} \quad \forall t \in T \quad \forall b \in B \qquad \text{Eq. III.15}$$

$$0 \leq P^b_{\mathrm{disch}_t} \leq (1 - x^b_t) \cdot P^b_{\mathrm{max\_disch}_t} \quad \forall t \in T \quad \forall b \in B \qquad \text{Eq. III.16}$$

$$SOC^b_t = SOC^b_{t-1} + \frac{\eta^b_{ch} \cdot P^b_{\mathrm{ch}_t} \cdot \Delta t}{E^b_{nom}} - \frac{P^b_{\mathrm{disch}_t} \cdot \Delta t}{E^b_{nom} \cdot \eta^b_{disch}} \quad \forall t \in T \quad \forall b \in B \qquad \text{Eq. III.17}$$

$$SOC^b_{min} \leq SOC^b_t \leq SOC^b_{max} \quad \forall t \in T \quad \forall b \in B \qquad \text{Eq. III.18}$$

$$SOC^b_{t_{start}} = SOC_{start} \quad \forall b \in B \qquad \text{Eq. III.19}$$

$$SOC^b_{t_{end}} = SOC_{end} \quad \forall b \in B \qquad \text{Eq. III.20}$$

Flexible and Inflexible Loads

Consumption can be constituted by inflexible load, such as refrigerators, and flexible loads, such as washing machines and heating systems. The inflexible load is modelled by using forecasted power profile (P^l_t), as in previous profile.

On the contrary, flexible loads require the characterization of their consumption. In this model only time-shiftable appliances are introduced. This kind of flexible loads can be shifted in time, but their power shape is not flexible. Hence, it can be modelled by using an operating cycle matrices built by using the load profile and represents all the possible combination of working between t^l_{start} and t^l_{end}. Hence, constraints in Eq. 11 imposes that the power of an appliance *f* in a certain period *t* of operation is related with its operating cycle described by matrix $OM^f_{t,d}$.

Respect FL profiles:

$$P^{fl}_t = \sum_{d \in D} x^{fl}_d \cdot OM^{fl}_{t,d} \quad \forall t \in \{t^{fl}_{start}; t^{fl}_{end}\} \quad \forall fl \in FL \qquad \text{Eq. III.21}$$

$$\sum_{d \in D} x^{fl}_d = 1 \quad \forall fl \in FL \qquad \text{Eq. III.22}$$

Microgrid Overall Profile

Power balance:

$$P_{B_t} - P_{S_t} + \sum_{g \in DG} P^g_t - \sum_{l \in L} P^l_t - \sum_{fl \in FL} P^{fl}_t - \sum_{b \in B} P^b_{\mathrm{ch}_t} + \sum_{b \in B} P^b_{\mathrm{disch}_t} \quad \forall t \in T \qquad \text{Eq. III.23}$$

The power balance equation in Eq. III.23 allows to satisfy flexible and inflexible loads in each timeframe by using both electricity produced in the microgrid or bought from the DSO. This equation defines the final exchange with the host grid as well.

Grid exchange block bids:

$$P_{S_t} = P_{S_{t+1}} \quad \forall t \in \left\{(h-1)\cdot t^{bid}; h\cdot t^{bid}\right\} \quad \forall h \in \left\{t_{start}; \frac{t_{end}}{t^{bid}}\right\} \qquad \text{Eq. III.24}$$

$$P_{B_t} = P_{B_{t+1}} \quad \forall t \in \left\{(h-1)\cdot t^{bid}; h\cdot t^{bid}\right\} \quad \forall h \in \left\{t_{start}; \frac{t_{end}}{t^{bid}}\right\} \qquad \text{Eq. III.25}$$

Grid exchange buy or sell:

$$0 \leq P_{S_t} \leq x_t \cdot M \text{ with } M \gg P_{S_t} \qquad \text{Eq. III.26}$$

$$0 \leq P_{B_t} \leq (1-x_t) \cdot M \text{ with } M \gg P_{B_t} \qquad \text{Eq. III.27}$$

Constraints in Eq. 12 and 13 enable to generate an hourly proposal in energy and power for the aggregator. Whereas, Eq. III.26 and Eq. III.27 avoid that P_{B_t} and P_{S_t} are contemporary higher than zero, which impedes that the microgrid sells and buy electricity at the same time.

III.4.2.2. Flexibilities Definition

The importance of flexibilities is introduced in II.5.2 and their application for collaborative strategies among microgrids and active management of distribution grids are discussed in IV.4.2 and IV.4.3. In this section, an easy way to find and aggregate flexible elements in microgrid is presented. Flexibility can be classified into two categories [128]:

- downward flexibilities include all devices which can induce a power reduction: reduction of the produced power, increase in the absorbed load or increase the charging power of a storage system;
- upward flexibilities consist in devices able to induce a power increase: increase in the generation, reduction of consumption or increase the discharge power of a storage system.

Electric vehicles and Heating, Ventilating and Air Conditioning (HVAC) are examples of flexible loads, which can provide power flexibility. The load reduction/increase depends on the nature of the flexible device. It can be in power and time, such as in HVAC systems, or only in time, such as in washing machines and dishwashers. In fact in [133], *Aduda* proved that the power of HVAC system can be increased/reduced for a certain period, without

impacting the user's comfort. In the second case, the entire pattern of the appliance can be shift in the most useful period [108]. Each flexibility can be modelled through two types of bids [128]:

- Type A: pair of two elements Quantity-Price (kWh-c€/kWh), that corresponds to a binary response accepted/not accepted.
- Type B: a triple of elements Maximal Quantity-Minimal Quantity-Price (kWh-kWh-c€/kWh). The accepted amount can be chosen in continuous manner between the minimal and maximal proposed quantity.

Each proposal is referred to a well-known time lapse (e.g. 0.00 a.m.-1.00 a.m., 1.00 a.m.-2.00 a.m., etc.) and with a bid duration of 1 h, as proposed in section II.A for the aggregated exchange profile. The first type of proposal is suitable to represent each kind of flexibilities (DGs, appliances, HVAC, etc.). It allows more flexibility to the aggregator, but requires to exchange less information.

III.4.3. Case Study

The optimization-based EM algorithm is tested using the small-sized community of residential and commercial users described in III.3.2. Some important details are also highlighted in this section. However, for the detailed description of the microgrid's components refer to this section. It comprises 4 groups of residential and small-commercial users, and 25 single houses. The amount of components and the nominal data of installed generation are resumed in Tab. III.3.

The DG's costs are calculated by using the LCOE as described in III.3.2. The DG aggregated profiles used as input for the case study are represented with the yellows areas in Fig. III.16. These areas represent the forecasted energy for PV systems and the nominal power for the bio-diesel generator. A Li-ion battery is also installed in the microgrid. This ESS has a nominal power of 30 kW and a capacity of 45 kWh. However, the optimization-based model allows to easily introduce a more accurate battery's model. The state of charge of the battery is set to be between 10% and 90%, and the SOC_{start} and the SOC_{final} are set to 30%. η_{ch}^{b} and η_{disch}^{b} are set to 0.96 and 0.97 respectively. The ESS battery cost is estimated to be 10c€/kWh.

G1	25 Users; P_{PVn}: 45 kW C_{PV}=13cent€/kWh
G2	20 Users; P_{PVn}: 40 kW C_{PV} =13cent€/kWh
G3	20 Users; P_{PVn}: 20 kW C_{PV} =13cent€/kWh $P_{Dieseln}$: 20 kW C_{Diesel}=19cent€/kWh
G4	15 Users; P_{PVn}: 15 kW C_{PV} =14cent€/kWh

Tab. III.3 Microgrid components number and nominal data

Moreover, 18 flexible appliances are considered in this case study, 10 washing machines and 8 dishwashers respectively. The consumption profiles are taken from studies in papers [108] [134]. For the sake of simplicity, the appliances usage-times are chosen equals to 8.00a.m.-8.00p.m. and 7.00a.m.-1.30p.m. for the washing-machines and for the dishwashers, respectively. The total daily load is equal to 2050.1 kWh and the total daily PV available 954.8 kWh, as resumed in Tab. III.4.

Two case study are considered to evaluate the behaviour of the model. In the first one, the selling and buying prices received by the MMCA are considered to be dynamic and vary according to the wholesale electricity market prices with an average daily selling price of 14.3c€/kWh and buying price of 19c€/kWh, as described in III.3.2. The shape of the daily prices is the same used in this section. However for simplicity, it is plotted again in Fig. III.14. In the second one, constant daily prices equal to the average values of the previously case are considered (Fig. III.20). It is considered that the energy surplus is sold by the DSO at the defined price. Results of both case studies are then compared with a case without DG installed, called basic case, in which the electricity to satisfy the consumption is completely bought from the host grid.

The optimization problem uses Mixed Integer Linear Programming (MILP). It was implemented using Matlab and the free toolbox OPTI TOOLBOX [135] that allows to build and solve linear, nonlinear, continuous and discrete optimization problems, supplying a wide range of solvers.

Fig. III.15 depicts the aggregated microgrid day-ahead profile composed of inflexible and flexible loads, DGs and the ESS. The scheduled operating point of each aggregation of DGs, which is obtained with the optimization-based approach, overlaps the available generation in Fig. III.16. Fig. III.19 shows the operation time scheduled of each flexible appliance. As the figure shows, they are scheduled in the low-cost timeframes of the microgrid that coincide with the photovoltaic production's peak.

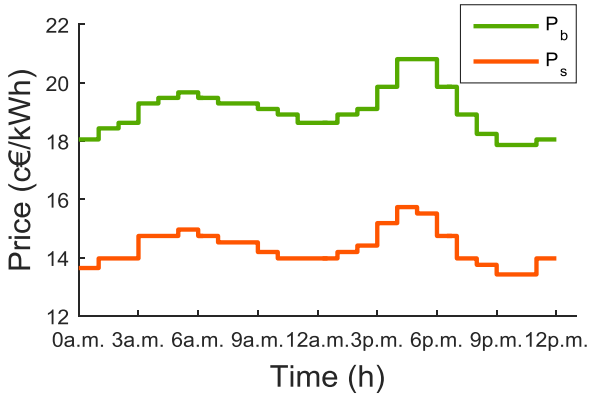

Fig. III.14 Daily dynamic prices for selling and buying electricity to/from the DSO used in the case study 1

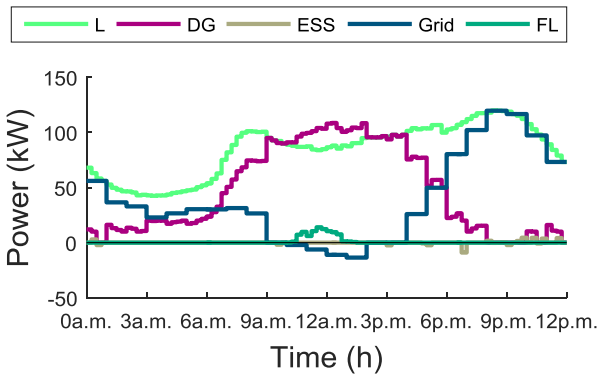

Fig. III.15 Microgrid aggregated daily profiles (grid exchange, consumption, generation and storage) for case study 1

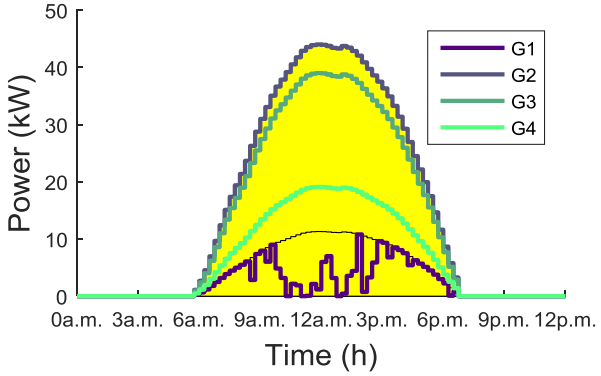

Fig. III.16 PV input and output for each group of users for case study 1

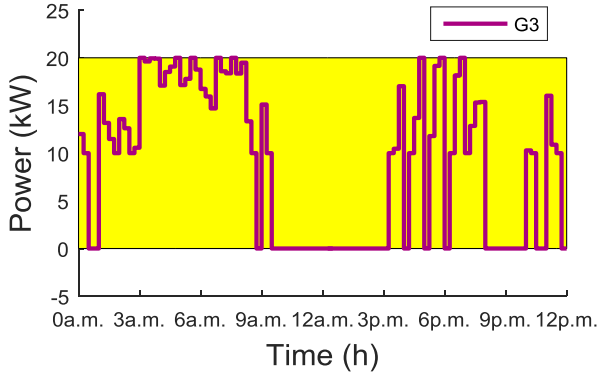

Fig. III.17 DS input and output of group 3 for case study 1

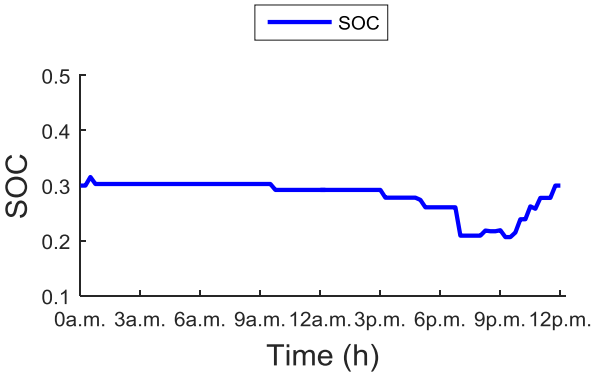

Fig. III.18 ESS SOC for case study 1

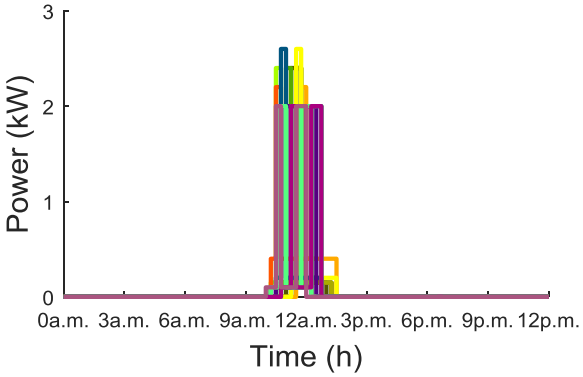

Fig. III.19 Appliances's activation for case study 1

The parameters used to evaluate the implemented model are resumed in Tab. III.4. The total PV accepted in the day-ahead plan, before being proposed to the AGGA/DSOA, is equal to 94.6% of the available energy. This result is essentially due to the higher cost of small rooftop PV systems and to the assumption of sending daily constant DG prices. Instead, for

$CB_{\mu G}$ *	DC *	MF *	SCR	RSP	$CBref_{\mu G}$ *	DCref *
16.2 c€/kWh	335.3 €	175.1 €	97.0 %	53.3 %	19.0 c€/kWh	390.5 €
PV *	DS *	DG	PV_{acc} *	$DIES_{acc}$ *	DG_{acc} *	Load *
954.8 kWh	480 kWh	1434.8 kWh	95.7 %	44.2 %	78.5 %	2050.1 kWh

Tab. III.4 Results of case study 1

$CB_{\mu G}$ *	DC *	MF *	SCR	RSP	$CBref_{\mu G}$ *	DCref *
16.3 c€/kWh	337.1 €	161.3 €	95.1 %	56.4 %	19.0 c€/kWh	390.5 €
PV *	DS *	DG	PV_{acc} *	DS_{acc} *	DG_{acc} *	Load *
954.8 kWh	480 kWh	1434.8 kWh	98.4 %	57.7 %	84.8 %	2050.1 kWh

***Legend**: $CB_{\mu G}$: Daily average kWh cost payed by µgrid's consumers; *MF*: Daily money flow between the µgrid and DSO (expenses and revenues); *DC*: Daily expense or revenue of the µgrid considering the money flow with the DSOA/AGGA, the DG costs and the ESS costs; *SCR*: Self-consumption ratio; *RSP*: Self-production ratio; $CBref_{\mu G}$: Daily average kWh cost payed by µgrid's consumers buying all electricity needed by the DSOA; *DCref* : Daily µgrid expense buying all electricity needed by the DSOA; *PV – DS- DG* : Available/Forecasted PV/DS/DG energy; PV_{acc} - DS_{acc},- DG_{acc}: Percentage of used PV/DS/GS energy on available/forecasted; *Load* : Daily consumption of each µgrid;

Tab. III.5 Results of case study 2

the Diesel system this amount is equals to 47.2%. As results show, because of the low price of PV systems, the energy produced by PV is almost completely used and flexible appliances are activated between 10.00 a.m. and 1.30 p.m. which correspond to the PV peak hours.

The daily expense obtained for the microgrid is 335.3 € and the average kWh cost is 16.2 c€/kWh. The daily self-production ratio is equal to 53.3%, which means that only the 46.7 % of the electricity is absorbed from the main grid. Moreover, the daily self-consumption ratio is very high, which allows to reduce electricity bills. In fact, the microgrid economizes the 14.1 % compared to the basic case for the day in analysis. The average value of $CB_{\mu G}$ is reduced of 2.7 c€/kWh, which corresponds to a reduction of 14.7 %. It possible to see an increase in the locally generated energy for both technologies. In case 1, the electricity price was lower during PV peak-hours, which induced the reduction of the locally-produced energy. In this case, the static nature of the price with a value inferior to the PV cost allows to increase of 2.7 % the energy injected (see Tab. III.5). However, the value of PV_{acc} does not reach 100% because of the hourly proposal constraint. Also the use of the bio-fuel generator is increase of 13.5 % due to the higher buying price in night-time bands, such as 8.00 p.m. – 10.00 p.m. in Fig. III.23. Also in this case, the flexible appliances are activated in the hours of PV peak, but this time between 10.00 a.m. and 2.45 p.m., as in Fig. III.19. As clearly shown in Fig. III.24, the use of the storage system is limited to satisfy hourly proposal constraints and it is not used

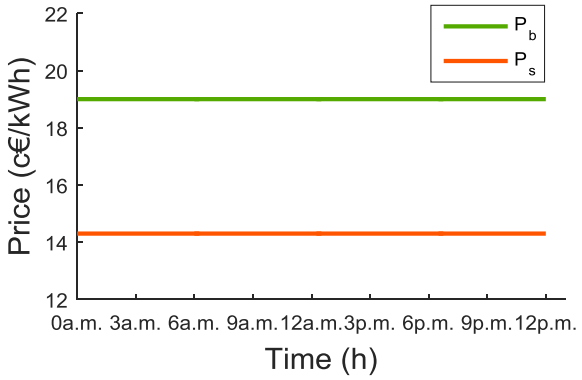

Fig. III.20 Daily static prices for selling and buying electricity to/from the DSO used in the case study 2

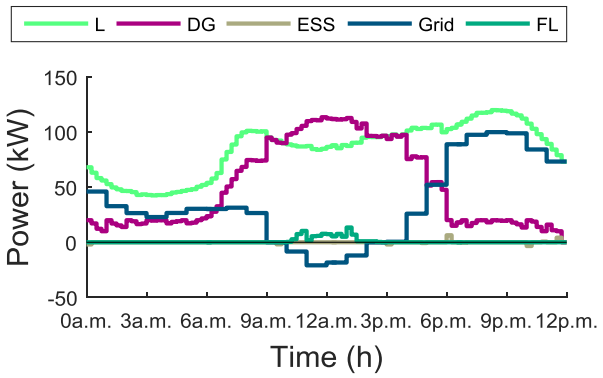

Fig. III.21 Microgrid aggregated daily profiles (grid exchange, consumption, generation and storage) for case study 2

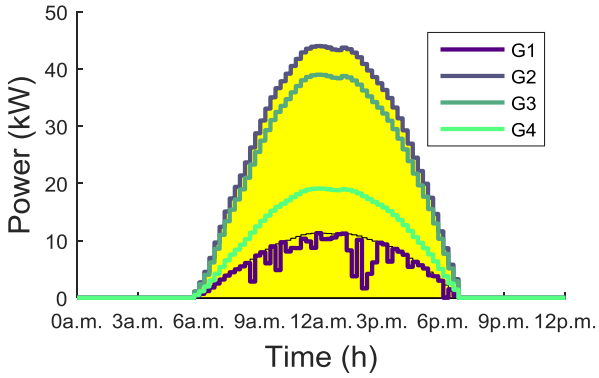

Fig. III.22 PV input and output for each group of users for case study 2

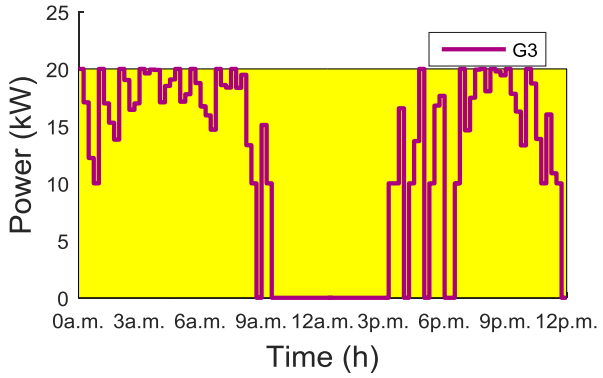

Fig. III.23 DS input and output of group 3 for case study 2

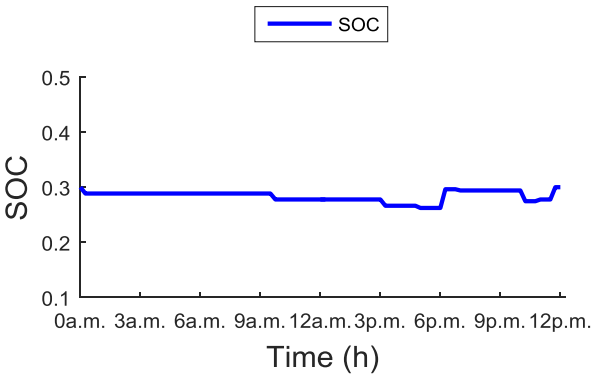

Fig. III.24 ESS SOC for case study 2

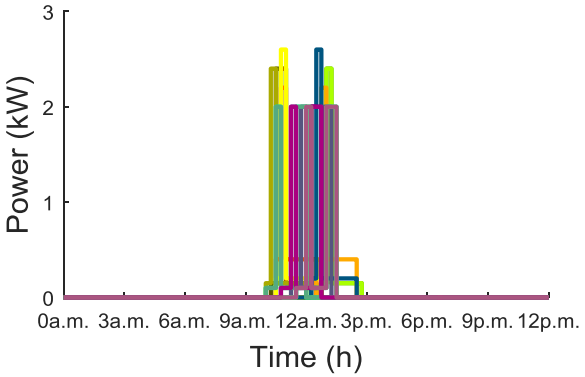

Fig. III.25 Appliance activation for case study 1

to increase self-consumption. Moreover, also with a flat shape of electricity prices, the microgrid decreases the value of *DC* and $CB_{\mu G}$ in respect of the reference case of 13.7 % and 14.2 %, respectively. Furthermore, the daily self-production and self-consumption ratios are subject to a light increase taking respectively the values of 56.4% and 95.1 %. However, a

sensitivity analysis on these parameters will be needed in order to understand the real impact of the price shape and draw general conclusions (see III.4.4).

III.4.4. Sensitivity Analysis

In this section, the results of a sensitivity analysis on fundamental parameters characterizing the model discussed in section III.4.2.1 are presented in order to confirm the performance of the proposed strategy. In addition, these evaluations are fundamental for the sizing stage of microgrids. The method used to carry out this sensitivity analysis is one of simplest one used in the literature. It consists on repeatedly vary the parameter under analysis while leaving the other parameters fixed. The sensitivity ranking was obtained by moving the maximal daily PV power (PPV_{max}), the DG and ESS values of the LCOE (C_{PV} and C_{ESS}, respectively) and the initial and final SOC of the ESS, at a time. The output variables quantified to evaluate the impact of the sensible parameters are:

- the daily average electricity cost in each microgrid ($CB_{\mu G}$),
- the daily expense or revenue of the µgrid (DC),
- the percentage ratio between the exploited power and the available/forecasted power for each type of source (DG_{acc}, PV_{acc}, DS_{acc}).

The first campaign of simulations concerned the variation of the maximal PV power in the aggregated groups 2 and 3. It was increased in both with a step of 2.5 kW between 0 kW and 80 kW. This corresponded to a variation of the total PPV_{max} from 30.4 kW to 190.4 kW, which represent a PV rate[14] of 12.5 % and 78.2 %. This campaign aims to evaluate the stability of the microgrid electricity costs subject to variations of locally produced generation by PV systems.

The influence of this parameter on the three reference variables is resumed in Fig. III.26 and Fig. III.27. Furthermore, the final aggregated power profile of the microgrid and battery SOC are shown in Fig. III.28 and Fig. III.29 to better understand the behaviour of the microgrid components exposed to PPV_{max} variation. As we can see, the daily microgrid expense and the daily average electricity are impacted with a maximal percent variation of

[14] The PV rate is defined as the ratio between the daily PV available and the daily consumption of flexible and inflexible loads, computed by using the formula: $PV\ Rate = \frac{\sum_{i=1}^{NPV} P_{daily}^{i}}{\sum_{i=1}^{L} P_{daily}^{i}} * 100\%$, where NPV is the total number of PV systems and L is the total number of loads.

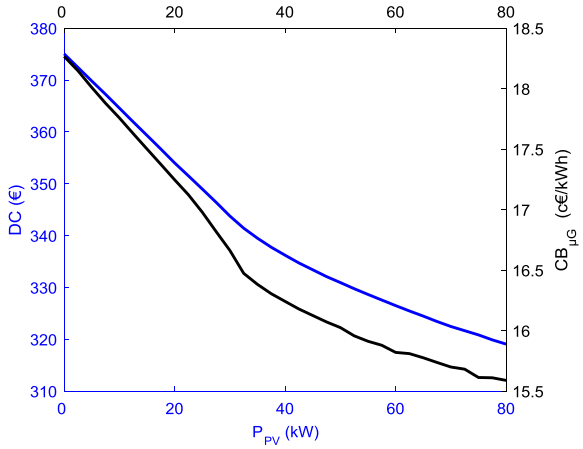

Fig. III.26 Influence of PPV_{max} variation on DC and $CB_{\mu G}$

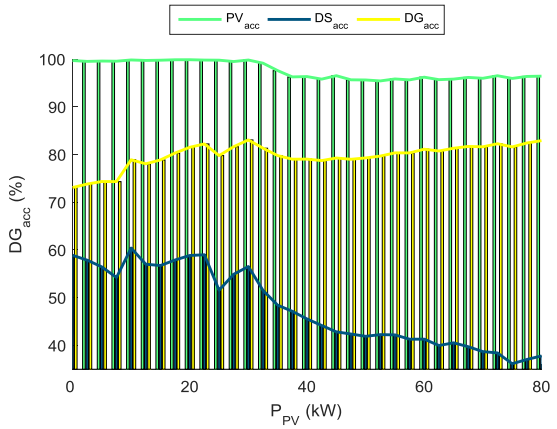

Fig. III.27 Influence of PPV_{max} variation on DG_{acc}, PV_{acc}, DS_{acc}

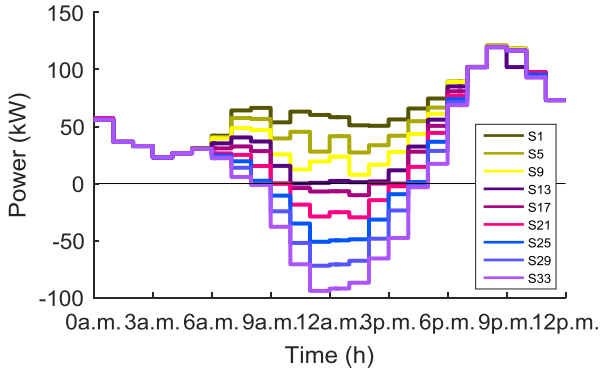

Fig. III.28 Influence of PPV_{max} variation on aggregated final profile of microgrid

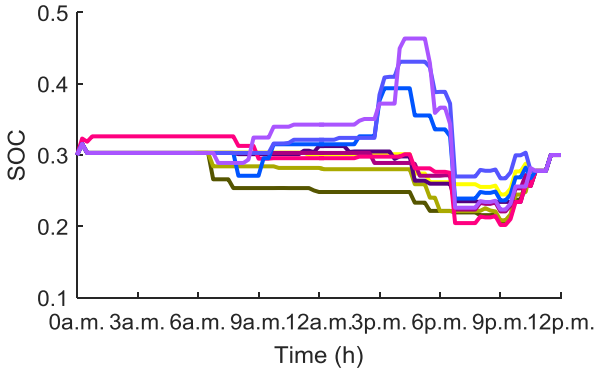

Fig. III.29 Influence of PPV_{max} variation on battery SOC

17.5% and 17.2%. Both curves have the same tendency with a rather steadily decreasing slope. In case of DG lack, both technologies, the electricity price will collapse to 19.0 c€/kWh (Tab. III.4). In general, it is possible to deduce that the increase of locally produced generation is beneficial for microgrid users. In fact, the increase of renewable-based generation will decrease the kWh cost by both the decrease of expenses due to the increase of self-consumption and the increase of revenues from the sale of electricity in power peak hours. Hence, the installation of a PV system for an aggregated group of users will be more advantageous. The DG_{acc} and the PV_{acc} are slightly impacted by this variation maximal variation of 10.0 % and 4.4 %, respectively. This is due to the fact that the chosen LCOE is 13 c€/kWh lower than the selling electricity price. Whereas, DS_{acc} is more impacted and suffers a decrease of 24.3 %. The variable slope of the DS_{acc} (in Fig. III.27) is produced by the minimal power of 10.0 kW imposed by constraint in Eq. III.14.

However, these considerations are strictly related to the LCOE of PV. Hence, the second analysis was made on the input parameter C_{PV}. This analysis takes a great importance. In fact,

the LCOE of PVs is not yet a stable parameter. In the basic case studies, the value of C_{PV} was computed considering real costs in 2013-2014, by obtaining 13 c€/kWh and 14 c€/kWh for small-sized and medium-sized rooftop solar systems, respectively. These values are completely in line with current literature (see [110]). However, they will be subjected to decrease during next years. This will be induced by the several efforts, which are made on technology improvements (installation costs reduced and increase in the efficiency), but also by the well know effect of scale economies. In 2030, the LCOE of small and medium size solar system in Germany is expected to decrease until 9 c€/kWh [110]. Hence, even small rooftop PV systems will be competitive on both conventional technologies, such as hard coal plants, and new technologies, such as onshore wind power plants [110]. Moreover, costs of a renewable-based power system are highly site specific. Hence, these studies will also allow to understand the operating behaviour of the connected microgrid in a certain location.

In simulations, C_{PV} was varied from 6 c€/kWh to 17 c€/kWh with an increase of 1 c€/kWh for PV systems of group 2, 3 and 4, and from 7 c€/kWh to 18 c€/kWh for group 1. The results of these simulations are drawn in Fig. III.30 and Fig. III.31. As can be seen, the C_{PV} variation strongly influences the values of DC and $CB_{\mu G}$ with a maximal percent variation of 38.0 % and 35.7 %. The tendency of both curves is linear with a constant slope of approximately 0.43 c€/kWh/c€/kWh and 9.3 €/c€/kWh. Otherwise, the percentage ratio between the exploited power and the available/forecasted power are slightly impacted, with maximal percent values of 5.6 %, 8.6 % and 1.5 % for DG_{acc}, PV_{acc} and DS_{acc}, respectively. Fig. III.31 and Fig. III.32 shows that high values of the C_{PV} for small and medium size solar systems, in combination with a high value of C_{ESS}, limits the self-consumption. The optimal size of the system have to limit or completely avoid the case in which the available energy is in surplus with respect to the local consumption power in production peak-hours. In fact, the surplus energy is not accepted by the DSO and it is not even advantageous to store it in the ESS (see S10-S12 curves in blue and sea water). In S10-S12 curves the ESS supplies in part consumption due to the high price of electricity and will recharges immediately afterwards. Hence, the oversizing of PV systems

have to be avoided. On the contrary, the decrease of the LCOE will allow rapid integration of small size systems, which will be able to compete in an aggregated way in electricity markets. In addition, Fig. III.31 and Fig. III.32 suggests that low values of C_{PV} drives the increase of

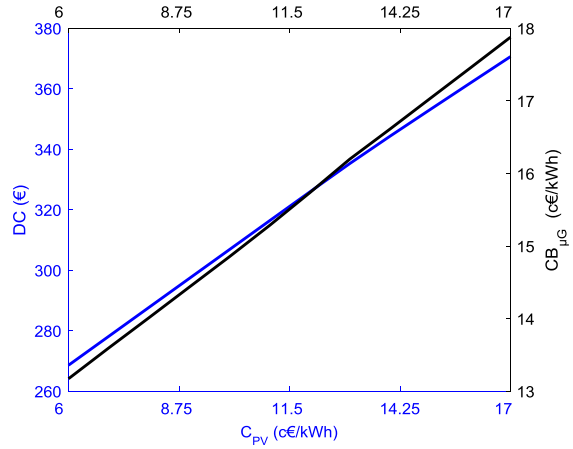

Fig. III.30 Influence of CPV variation on DC and $CB_{\mu G}$

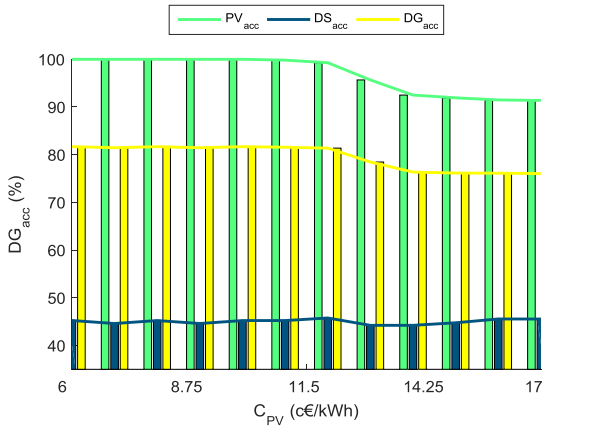

Fig. III.31 Influence of CPV variation on DG_{acc}, PV_{acc}, DS_{acc}

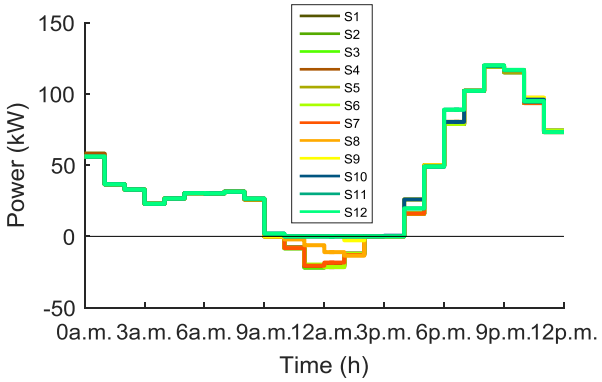

Fig. III.32 Influence of CPV variation on aggregated final profile of microgrid

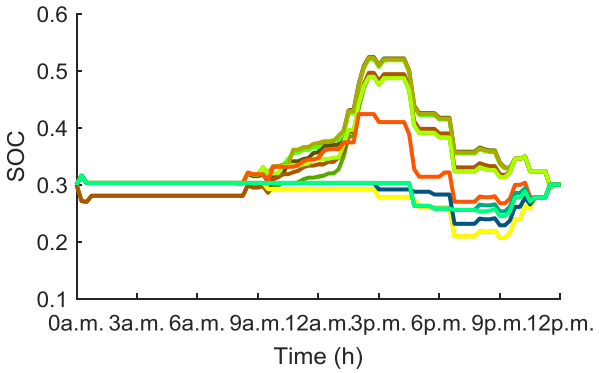

Fig. III.33 Influence of CPV variation on battery SOC

self-consumption. In fact, energy is in part stored during low-peaks hours of grid prices also with a C_{ESS} of 10 c€/kWh (see S1-S3 curves in green).

Another parameter which impacts were needed to be analysed was the battery initial and final SOC. Hence, the initial and final state of charge, defined as SOC_{start} and SOC_{end}, were varied from 20% to 80 % with a step of 5 %. Fig. III.34-Fig. III.37 show that with the hypothesis made a change in the SOC_{start} does not impact the results. In fact, the kWh cost and daily cost of the microgrid has a constant tendency. Also, the percentage ratios of used energy are almost completely not affected: 1.2%, 0.7 % and 0.8 %, for the PV, the DS and the DG in general, respectively. Hence the choice of this parameter will be guided by the real-time needs, discussed in section V.4. Moreover, it will be needed to investigate more in-depth the variation of this parameter in case of islanded applications and in case of lower value of levelized cost of storage in which will be rentable the storing of locally-produced renewable energy.

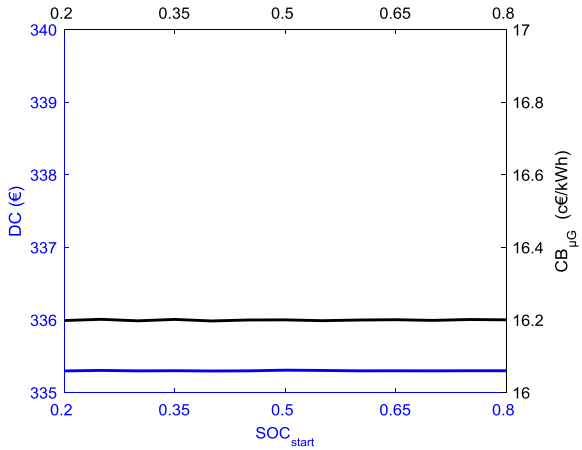

Fig. III.34 Influence of SOC_{start}/SOC_{end} variation on DC and $CB_{\mu G}$

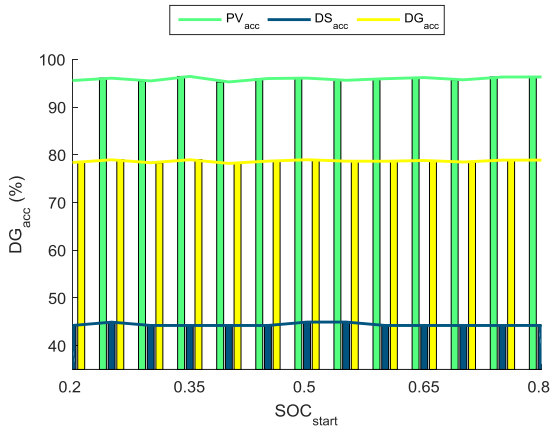

Fig. III.35 Influence of SOC_{start}/SOC_{end} variation on DG_{acc}, PV_{acc}, DS_{acc}

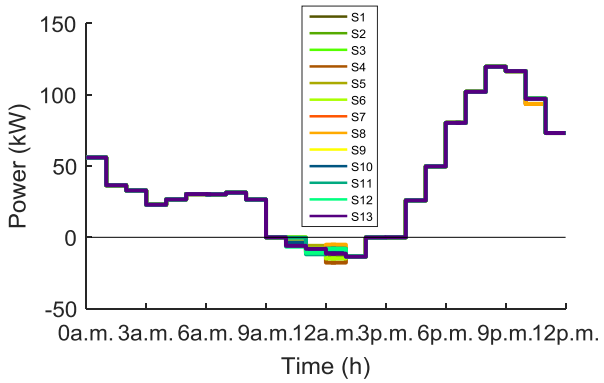

Fig. III.36 Influence of SOC_{start}/SOC_{end} variation on aggregated final profile of microgrid

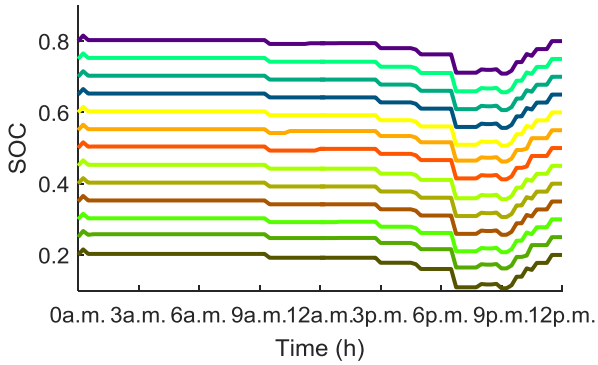

Fig. III.37 Influence of SOC_{start}/SOC_{end} variation on battery SOC

As suggested in the previous analysis, changes in the value of C_{ESS} may severely impact the operating scheduling of the microgrid. Renewables use is radically growing all around the word. In consequence, this is driving emphasis on ESS applications in grid-scale applications for frequency regulation, congestions resolution, avoiding renewable cutting, etc.. Hence, the perspective of ESS are promising due to improvements in manufacturing process and in technology enhancement by introducing new materials and increasing the batteries lifetime [112].

All these factors, combined with the scale economy, suggest a rapidly fall in batteries price during next years. For example, authors in [19] reviewed the current purchase cost of Li-ion battery for EV application and traced it tendency with confidence intervals for coming years. In 2025 according to authors, this cost will be decline between 300 $/kWh and 150 $/kWh. In the sensitivity analysis, the C_{ESS} was varied from 0 c€/kWh to 20 c€/kWh with an

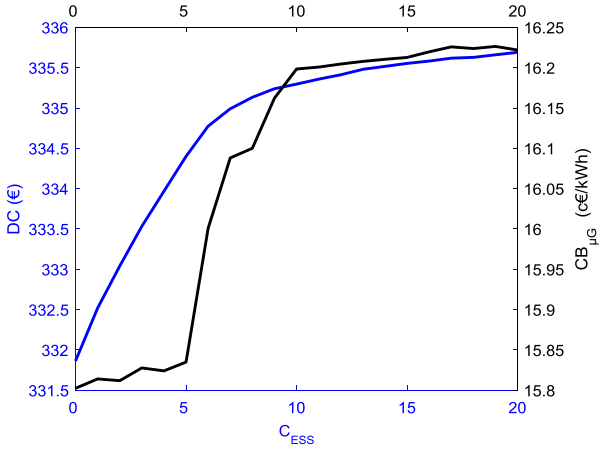

Fig. III.38 Influence of C_{ESS} variation on DC and $CB_{\mu G}$

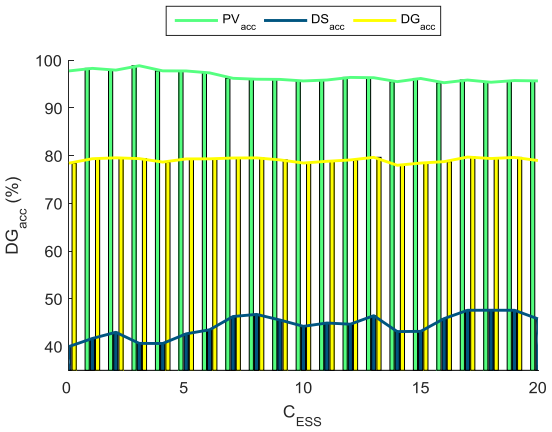

Fig. III.39 Influence of C_{ESS} variation on DG_{acc}, PV_{acc}, DS_{acc}

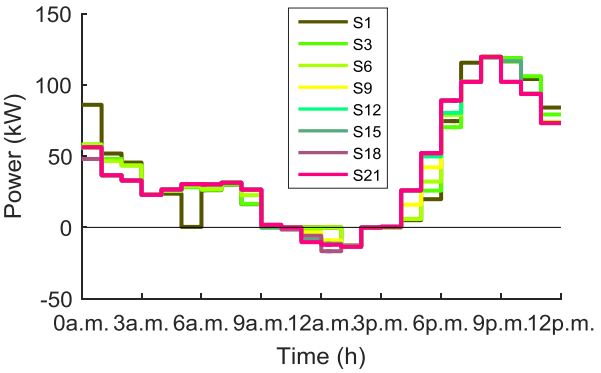

Fig. III.40 Influence of C_{ESS} variation on aggregated final profile of microgrid

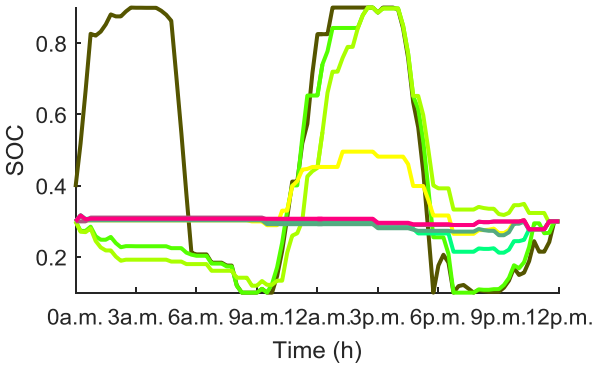

Fig. III.41 Influence of C_{ESS} variation on battery SOC

increasing step of 1 c€/kWh. It is evident that the C_{ESS} value will not be close to 0 c€/kWh neither in less restrictive tendency.

However, the battery cost is not taken into account in some daily model, for example in centralized applications in which the self-consumption want to be maximized or in case of arbitrage. The parameter DC and $CB_{\mu G}$ are slightly impacted by the variation of C_{ESS}. In fact, the maximal distance between the minimal and maximal value are 1.2% for the DC and 2.7 % for C_{ESS}.

The main difference can be found between 0 c€/kWh and 10 c€/kWh. Thereafter, the tendency of both curves is almost constant with a slope close to zero. Also PV_{acc}, DS_{acc} and DG_{acc} are lightly influenced with maximal distances of: 3.6%, 1.6% and 1.7%, respectively.

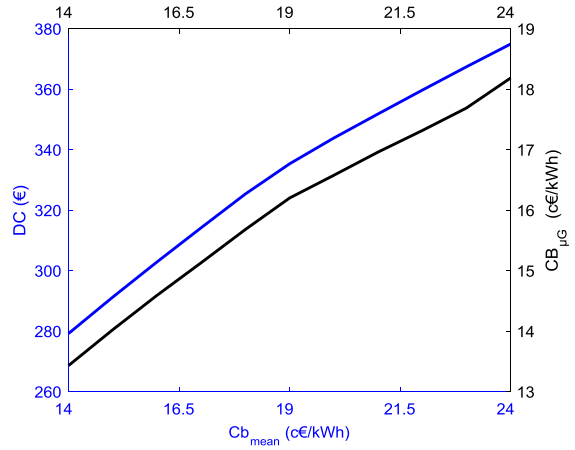

Fig. III.42 Influence of dynamic C_s/C_b variation on DC and $CB_{\mu G}$

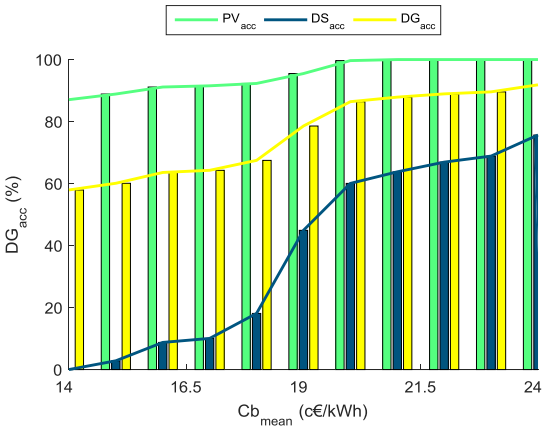

Fig. III.43 Influence of dynamic C_s/C_b variation on DG_{acc}, PV_{acc}, DS_{acc}

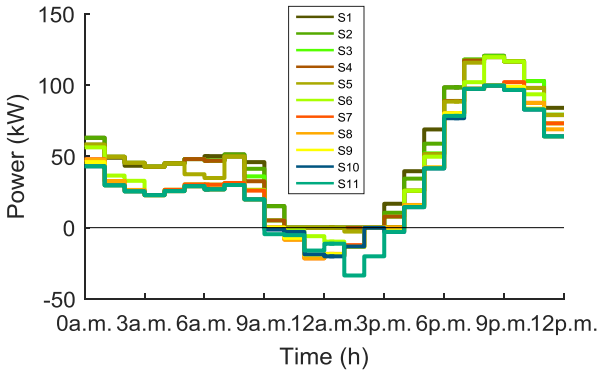

Fig. III.44 Influence of dynamic C_s/C_b variation on aggregated final profile of microgrid

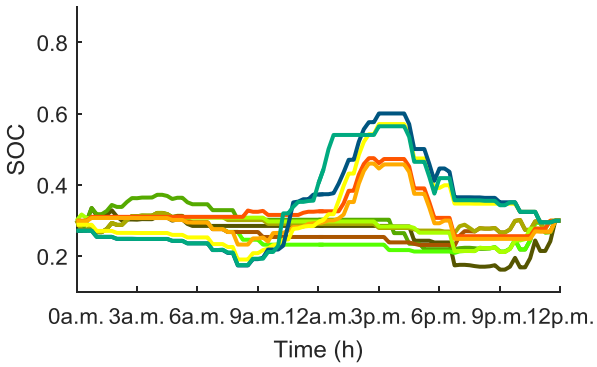

Fig. III.45 Influence of dynamic C_s/C_b variation on battery SOC

Fig. III.40 and Fig. III.41 show the occurrence of three different situations based on the battery price variation:

- 0 c€/kWh - 6 c€/kWh (S1-S7): in case of low C_{ESS} the energy is stored in the battery by using both locally-produced electricity and grid electricity. In this case, the electricity produced with small rooftop PV is almost completely used (~99%) and the use of the bio-fuel system is reduced to its minimal value.
- 7 c€/kWh - 9 c€/kWh (S8-S9): in case of medium low C_{ESS} the energy is stored in the battery by using only locally-produced electricity.
- 10 c€/kWh - 20 c€/kWh (S10-S20): in case of high C_{ESS} the energy stored in the battery is negligible.

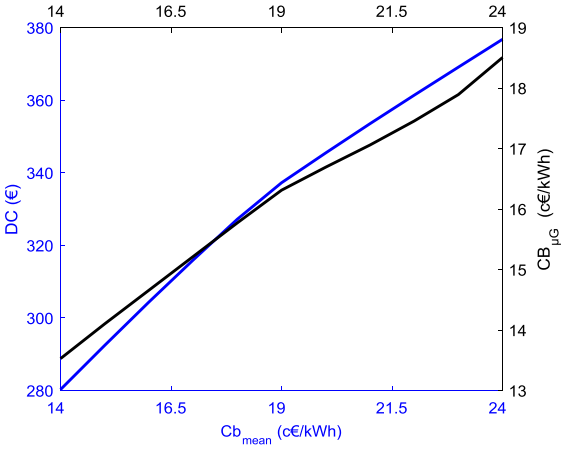

Fig. III.46 Influence of static C_s/C_b variation on DC and $CB_{\mu G}$

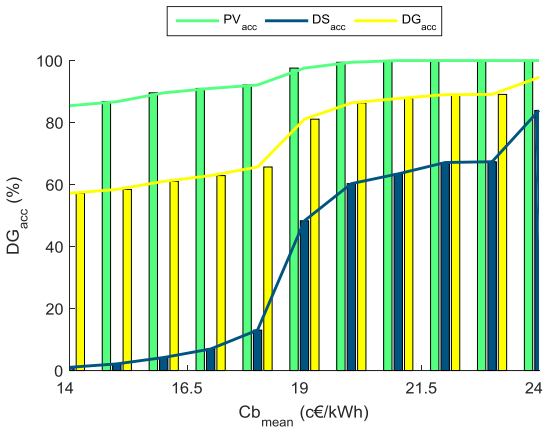

Fig. III.47 Influence of static C_s/C_b variation on DG_{acc}, PV_{acc}, DS_{acc}

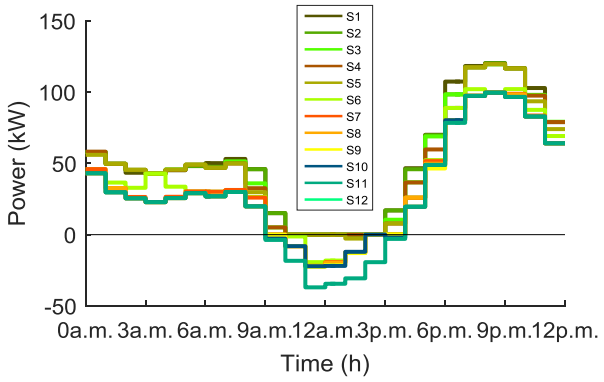

Fig. III.48 Influence of static C_s/C_b variation on aggregated final profile of microgrid

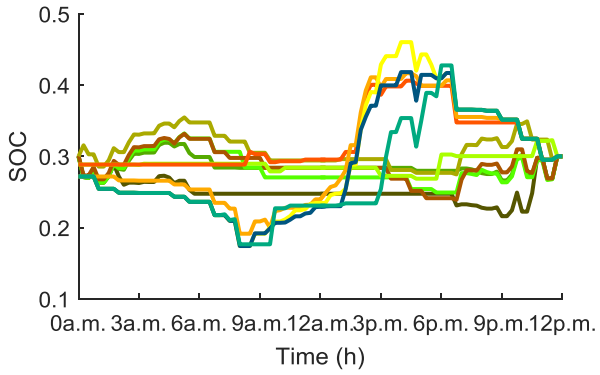

Fig. III.49 Influence of static C_s/C_b variation on battery SOC

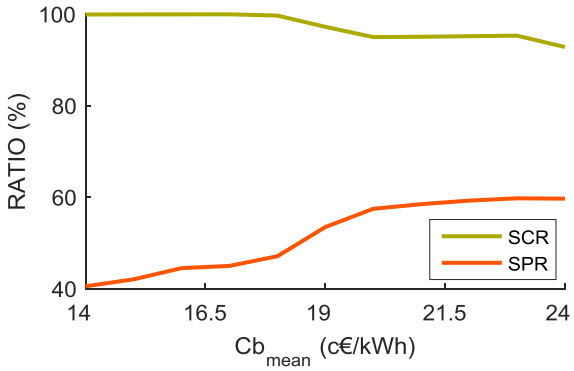

Fig. III.50 Influence of dynamic C_s/C_b variation on self-consumption and self-production ratios

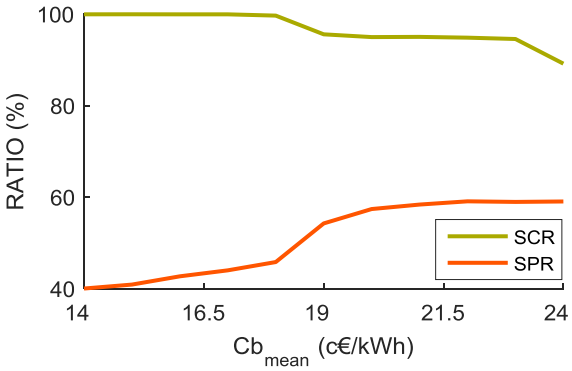

Fig. III.51 Influence of static C_s/C_b variation on self-consumption and self-production ratios

The last campaigns of sensitivity focused on electricity price variation. Both cases analysed in the previous section (dynamic and static prices) are taken into account. In both cases, the C_b and Cs curves were varied of 1 c€/kWh by keeping the same shape of curves in Fig. III.14 and Fig. III.20. Their mean and fixed values were increased from 13 c€/kWh to 24

c€/kWh and 8.3 c€/kWh to 19.3 c€/kWh, respectively. As expected, simulations showed a linear and growing variation of DC and $CB_{\mu G}$ with the increase of the buying and selling prices, in both cases (Fig. III.42 and Fig. III.46).

The grid price has a strong impact on these parameters. In fact, DC is subject to an increase of 34.3 % in case of dynamic prices and of 34.5 % in case of static prices. $CB_{\mu G}$ is more or less subject to the same variations, which are equals to 35.6 % and 36.8 %, respectively. The same impact can be observed in the usage of local generation.

A low price of the electricity will induce to buy higher amount of electricity from the host grid, to reduce the energy sold and also the energy stored in the ESS. This behaviour is particularly visible in green curves (S1-S2) in Fig. III.44 and Fig. III.45 for the first case, and Fig. III.48 and Fig. III.49 for the second case.

On the contrary, the self-consumption by storing energy in the ESS and the injection of energy in the host grid are increased for higher values of C_s and C_b (e.g. S8 in Fig. III.48 and Fig. III.49 and S11 in Fig. III.44 and Fig. III.45). Furthermore, it is not convenient to install bio-fuel generators in case of low electricity prices, as shown in blue lines in Fig. III.43 and Fig. III.47. The distance between the lower and higher percentage of the used generation on the available generation are listed in source order (PV, DS, DG): 12.9 %, 77.9 % and 34.7 % for the dynamic case, and 14.6 %, 82.9 % and 37.4 % for the static case.

Furthermore, an analysis of self-consumption and self-production ratios is made in order to compare flat and variable shape of electricity price influence. Fig. III.50 and Fig. III.51 reports the tendency of both ratios for both sensitivity analyses. The tendency of both S*PR* is growing. In both cases, *SPR* assumes constant tendency starting from 19 c€/kWh. In the first case, the *SPR* is increasing from 40.5 % to 59.6 %. Instead in the second, from 40.0 % to 59.0 %. The dynamic curve leads to a slightly increase of self-production, due in particular to the increase of PV. For example, PV_{acc} is 87.1 % and 85.4 % in the sensitivity analysis with average/fixed values of C_b equal to 13 c€/kWh, respectively.

Globally, it is possible to see that the introduction of daily variable C_{PV} will be a solution to increase the amount of "free" energy produced by small PV systems. The future decrease of C_{ESS} and C_{PV} will surely push self-production. Moreover, the tendency of analysis parameter is the same in case of dynamic and static prices.

III.5. Comparison between Rule-Based and Optimization-based Approaches

Sections III.3 and III.4 discussed the properties and the outcomes of the rule-based approach (RBA) and the optimization-based approach (OBA) both implemented in the MAS.

The RBA is run hourly by using hourly information. This strategy guarantees more flexibility to user, which can change their following proposal. However, it makes harder the scheduling of components, such as batteries and time-shiftable appliances, which requires a more global vision in order to be scheduled in the more fitting time intervals.

On the contrary, the OBA runs one for the *D-1* scheduling by using 15 or 10 minutes forecasted information. It allows to model more in detail the behaviour of components and to engage the microgrid in an hourly proposal in energy and in power. Furthermore, the use of 15 or 10 minutes interval in the optimization-based model allows to better model the variability of consumption and renewable systems. For example in a general scheduling hour, the power injected by a PV system can be subject to a high variation between the starting and the ending time-frame.

Both strategies are compared to the reference case (electricity bought from the retailer) and to each other, in order to grasp their benefits and potentiality. Tab. III.6 summarizes the most important parameters for both strategies. As it is shown, the daily cost and the average kWh cost are decreased by applying both smart strategies with renewable-based generation. In fact, DC is decreased of 6.6 % with the RBA and of 14.1 % with the OBA. Moreover, the daily cost is halved by using the OBA with an additional gain of 6.6 % compared to the RBA. However, the different scheduling time frame and the use of grid exchange block bids to prepare a coherent hourly proposal, induce a reduction in the accepted DG power of 3.1% and 7.7 % for PV and DS systems, respectively.

Furthermore, the run-time of both strategies was analysed taking into account also other case studies not discussed in this thesis with lower and higher number of components (10 to 50). The OBA takes around 7 to 20 seconds according to the global number of components, but as well as to the amount of each component's type. For example, the increase of the number of time-shifting load induces a higher run-time compared to the same increase in number of distributed generators. This is due to the amount of variable and constraints used to

RBA				*REF*		*RBA-REF*	
$CB_{\mu G}$	*DC*	PV_{acc}	DS_{acc}	$CB_{\mu G}$	*DC*	CB_g=14.2%	DC_g=6.6%
16.3c€/kWh	*364.8 €*	*98.8 %*	*47.9 %*	*19.0c€/kWh*	*390.5 €*		
OBA				*OBA-REF*		*OBA-RBA*	
$CB_{\mu G}$	*DC*	PV_{acc}	DS_{acc}	CB_g=14.7%	DC_g=14.1%	CB_g=0.8%	DC_g=8.1%
16.2c€/kWh	*335.3 €*	*95.7 %*	*44.2 %*			PV_g= -3.1%	DS_g= -7.7%

Tab. III.6 Results summary and comparison among strategies

model each type of components in the microgrid. On the contrary for the RBA, the run-time for each time that the logic-rules are applied vary between 0.1 and 0.8 milliseconds, which corresponds to 2.4 and 19.2 milliseconds for the 24 times.

III.6. Conclusions

This chapter focused on distributed strategies for the economic scheduling of microgrids. These strategies aim to massively integrate active components, such as PV and ESS, by building a flexible system with a multi-level framework for sharing knowledge and distributing tasks. Hence, a multi-agent architecture was discussed and implemented. The tasks, the communication and tasks sequences and the information exchange of each agent were analysed. Moreover, two management strategies were developed based on logic rules and optimization techniques, respectively.

Simulation results of both implemented strategies show that a smart use of microgrid sources can reduce users' costs and incentive future investments on renewable technologies. However, the optimization-based algorithm has higher performances, which is essential for scheduling applications in which are required lower performance in run-time compared to real-time applications. In fact, it allows to have a daily vision of the electricity prices and available resources by finding the global optimal operating point of the microgrid. Moreover, the use of 10 or 15 minutes intervals as timeframes for the optimization permits to represent also small-sized component with variable profile during one hours, such as appliances but as well the photovoltaic systems. However, the principle described in the rule-based algorithm strategy can be applied for the management of large-sized microgrid with several competitive decision makers. In fact, an hourly process allows to reschedule next hour profile by taking into account the results of the scheduling in the last hour.

Furthermore, simulation results for the optimization-based model show that both dynamic and static prices incentive self-production. However, results of dynamic shape simulations are more promising for both microgrid's owners and for DSO prospective. In fact on one side, consumers can economize money and producers/prosumers can increase revenues. On the other side, DSOs can drive microgrids behaviour by adapting distribution network tariffs. In fact, the total electricity price is composed of three main components: the electricity purchasing cost, the network tariff and taxes. The purchasing cost for microgrids can be fix or dynamic based on future retail market design. However, the DSO can play on network tariffs, by increasing network tariffs during PV peak-hours and reducing it during off-peak time-slots.

However in future works, it will be needed to consider that the diesel's lifespan depends on the usage. On one side, an intermittent usage with several switching on and off will decrease the lifespan and increase maintenance costs. On the other side, a frequent no-load operation will increase operating costs. Hence, the diesel model can be extended by adding the hourly block operating constraint. Moreover, a variable price for both the ESS and the DG can be included in the model in order to use more rationally and increase revenues for component's owner. For example, a daily variable cost function can be introduced for DGs and a stepwise cost functions, which vary as function of the battery's solicitations, can be used for ESSs.

IV. DEVELOPMENT OF MULTI-MICROGRID STRATEGIES FOR DAY-AHEAD SCHEDULING BASED ON MULTI-AGENT SYSTEM

IV.1. Introduction

In Chapter III, we focused on the concept of microgrid and we discussed their capability to create a coherent structure that can guarantee an efficient way to manage and control multiple distributed resources. The control and management of microgrids are carried out by means of smart algorithms and ICT frameworks. Besides, microgrids are only the first stage of a complex system called "Smart Grid". In fact, in most cases, the size of a single microgrid and the nature of its resources are not apt to participate in electricity and services markets. A solution to achieve these goals could be the development of collaborative strategies between microgrids. In addition, collaborative strategies can also lead to cost reduction for consumers and revenue increase for producers, by incentivizing a more local and efficient use of energy.

Moreover, today in Europe, more than 90% of solar and wind plants are connected to distribution grids [14]. In 2016 in France, for example, this percentage reaches about 93.3% [136]. The massive integration of DGs into distribution grids modifies its scope and changes its nature from a passive downstream distribution of power to a hub of bidirectional power flows. This change poses technical and operational issues, including voltage stability on the one hand, and grid congestions on the other hand. These issues may induce an increase in network tariffs for consumers to finance necessary grid reinforcements. This reinforcement of distribution infrastructure may not be the most cost-efficient solution. Excessive costs may justify to take alternative solutions to use existing networks efficiently. The investments in new smart and adaptive strategies that use available users' flexibilities are necessary, as well. Short-term markets (day-ahead and real-time) and forward contract which exploit single or grouped flexible resources also need to be developed.

The overall goal of this chapter is to analyse how microgrids can collaborate to use efficiently their resources in order to support an active management of distribution grids, while at the same time optimizing the economic benefits of using distributed resources. A collaborative hierarchical process and the microgrids' way of interacting are discussed in section IV.3. Furthermore, two different strategies to support active management of grids and

sell/buy energy to the market are introduced and developed in section IV.4. The developed solutions and the several studies presented in the remainder of this chapter mainly differ to other approaches in the literature in two respects:

- The decentralization of the decision-making process through the development of a distributed multi-level sliding process
- The detailed conceptualization and implementation through comparative case studies of two management strategies for active management of distribution grids: flexibility services market and capacity limit allocation.

IV.2. Multi-Objective and Multi-Level Programming

In chapter III.4.1, a general constrained optimization problem is described with single-objective problem and for the reader's convenience reported in Eq. IV.1 and Eq. IV.2:

$$\min_{x \in S} f(x) \qquad \text{Eq. IV.1}$$

$$S = \left\{ x \in \mathbb{R}^m : \; h_i(x) = 0 \;\; i \in I \, , g_j(x) \leq 0 \;\; j \in J \right\} \qquad \text{Eq. IV.2}$$

The class of Multi-Objective Optimization Problems (MOOP) is discussed in [137] with a recall of some of the most relevant research papers related to this topic. From the mathematical point of view, this class of problem can be stated as following:

$$\min_{x \in S} [f_1(x), f_2(x), \dots, f_n(x)] \text{ with } n > 1 \qquad \text{Eq. IV.3}$$

$$S = \left\{ x \in \mathbb{R}^m : \; h_i(x) = 0 \;\; i \in I \, , g_j(x) \leq 0 \;\; j \in J \right\} \qquad \text{Eq. IV.4}$$

For this kind of problem, a single global optimal solution, defined as “Complete Optimal Solution” in notion in Def. IV-1 [138], that simultaneously minimizes (or maximizes) all objective functions does not always exist. In this class of problems, the scalar concept of optimality can’t be directly applied (see [137]). A trade-off must be created, when two or more objectives are in conflict. Hence, a set of points which correspond to a predetermined definition or better to a predetermined condition of optimum have to be determined. This condition is described by the concept of “Pareto optimality”, also known as “Pareto efficiency”. Mathematically, a Pareto optimal solution is expressed by Def. IV-2 [139]:

Def. IV-1: Complete Optimal Solution. *$x_0 \in R^m$ is said to be a complete optimal solution, if and only if there exists a x_0 such that $f_i(x_0) \leq f_i(x)$ for all i=1,2,…,n and for all $x \in S$.*

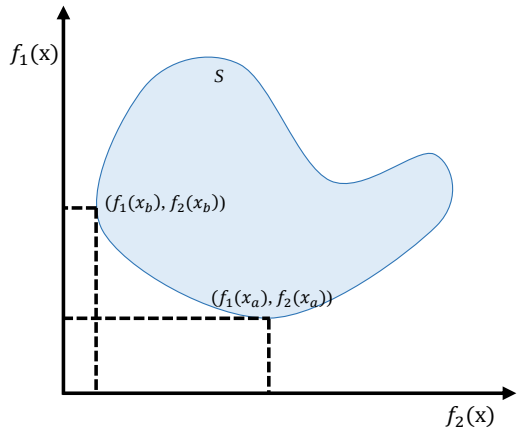

Fig. IV.1 Example of Pareto front between points A and B for two-objective minimization problem

Def. IV-2: Pareto Optimal Solution. *A point* $x_0 \in R^m$ *is called Pareto optimal for the problem in Eq. IV.*4 *and Eq. IV.*9 *if there does not exist another* $x \in S$ *such that* $f_i(x) \leq f_i(x_0)$ *for all* $i = 1,2,\dots,n$ *and* $f_j(x) \leq f_j(x_0)$ *for at least one* $j\epsilon\{1,2,\dots,n\}$.

The Pareto optimal condition defines the solution for which there are no other alternative allocations of x which obtains a gain for every objective. In other words, there is no another x that improves at least one objective function without the detriment of another function. In Fig. IV.1, an example of the set of all Pareto-efficient solutions (called Pareto Front) for a two-objective optimization problem is illustrated. The Pareto Front is fundamental for this class of mathematical problem and indicates the nature of the trade-off among the different objective functions. In the literature, methods for determining whether x is a Pareto optimal solution or not are extensively discussed. For details in [140], authors reports a simple test conceived by Benson and commonly used in engineering applications.

However, for users who are not interested in a trade-off among the objective, a Multi-Level Optimization Programming (MLOP) may be a useful approach [137]. In fact, a MLOP can be seen as another approach to MOOP problems, in which the n objectives are ordered with a certain hierarchy and the objective is to find one optimal point in the entire Pareto Surface. In real applications, a typical example is given by problems which involve multiple decision-makers with conflicting goals but coupled actions.

Among hierarchical optimization problems, Bi-Level Programming (BLP) is widely used for different applications, such as in market economies, chemical reactions and waste minimization [141]. BLPs consists of two nested optimization problem in two different

hierarchical levels which involve two different decision makers. In this kind of problems, the feasible region of the upper-level problem is constrained by the decisions of the lower-level problem. The general form of a BLP can be formulated as in Eq. IV.5 and Eq. IV.6:

$$\min_{x_1 \in S_1} f_1(x_1, x_2)$$

$$S_1 = \{x_1 \in R^m \; x_2 \in R^n : h(x_1, x_2) = 0 \, , g(x_1, x_2) \leq 0\} \qquad \text{Eq. IV.5}$$

$$\text{subject to: } \min_{x_2 \in S_1} f_2(x_2, x_3)$$

$$S_2 = \{x_2 \in R^n \; x_3 \in R^p : h(x_2, x_3) = 0 \, , g(x_2, x_3) \leq 0\} \qquad \text{Eq. IV.6}$$

Where Eq. IV.5 represents the upper-level problem and Eq. IV.6 the lower-level. In general, this problem can be seen as a two-player hierarchical game, where the player who makes a choice first is called leader and the second one who reacts on the leader's selection is called follower [142].

IV.3. Architecture and Sliding Multi-Level Optimization for Multi-Microgrid Scheduling

IV.3.1. Sliding Multi-Level Optimization using MAS

The goal of this chapter is to describe the developed process and system architecture for the integration of Multi-Microgrids Systems into distribution grids. These strategies need to deal with a large number of decision-makers, who interact among themselves, with the DSO and with the market through an aggregator. This kind of system becomes complex and requires a model which accurately represents all the particularities and the needs of each actor.

In this aspect, the distribution of tasks among actors/components can be seen as a fundamental aspect able to reduce the complexity of the system. In fact, the distribution of a certain degree of intelligence through components working in different levels of the system allows to reduce the need to create a complete and huge model of the system, the amount of information exchanged between top and bottom hierarchical entities and guarantees users' privacy. In other words, the idea is to distribute simpler tasks and knowledge among different actors/components in various levels in order to overcame the disadvantages of a centralized approach, mentioned in chapter II.

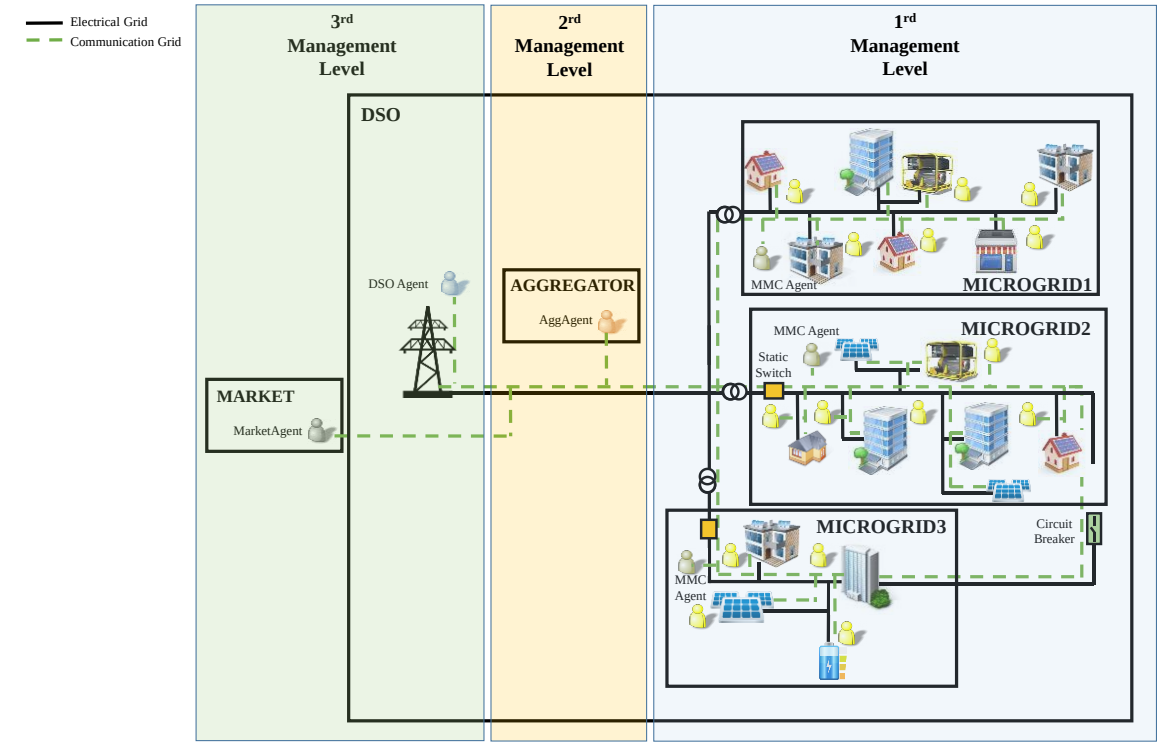

Fig. IV.2 Hierarchical architecture for multi-microgrid systems (inspired by [128])

This system is then composed of three levels of intelligence with different goals and responsibilities according to Fig. IV.2:

- The first level is composed of microgrids managed by the microgrid manager who calculates the optimal operation mode for single or aggregated users and generates a first assembly of available flexibilities (this level is described in depth in chapter III);
- The second level is composed of aggregators, who manage the collaborative strategies among microgrids and interfaces microgrids with the DSO and the electricity market applying by defined rules defined in the chosen strategy;
- The third level is constituted by the Distribution Management System (DMS) and the Electricity Market (EM).

This work is based on resources shared among microgrids through flexibilities proposal. However, microgrids are considered to interact in line with their own self-interest and the construction of shared flexibilities are built prioritizing their needs. The hierarchical structure allows to implement this behaviour. In fact, first, each microgrid manages its resources autonomously, reducing its costs and guaranteeing its users the required privacy. Only after

these objectives are achieved, microgrids share generation or demand-response as available flexibilities and each aggregator reaches its goals using these flexibilities. All planning, monitoring and control tools are considered implemented by DSOs in the third management layer in order to efficiently manage the distribution network. EM platform is considered to be in this third management level as well. The various management strategies developed to increase RES hosting capacity while avoiding grid tariffs increase and guaranteeing the required technical performances defined in grid codes (service continuity, power quality, etc.) are implemented in the level.

Based on the explanations in IV.2, the scheduling and control problem of multi-microgrids and distribution grids can be seen and solved by means of a hierarchical MLOP. In fact, our decision-makers are microgrids, aggregators, DSOs and EMs. On the one hand, each decision-maker tries to implement best decisions from its point of view, e.g. minimizing total costs of microgrids or respecting technical performances requirements for DSOs. However on the other hand, they also influence the decision made by others. In the formulation of this hierarchical multi-level problem, aggregators occupy the medium-level and microgrids the upper-level. In fact, microgrids can dictate energy profiles and amount/prices of flexibilities to the aggregators. From the mathematical point of view, this can be modelled by putting the optimal solution of the microgrids problems as the constraints of the aggregator mathematical problem. However, microgrids incomes/expenses strictly depends on aggregator decisions and the mix of affiliated microgrids. Hence, microgrids should anticipate the possible reactions of the aggregator. The goal of this thesis is to build the interaction framework and to propose the implementation methodologies. For this purpose, deterministic models are studied, also if they are not able to forecast aggregator reactions and forecast errors in microgrids' production and consumption profiles.

The multi-level optimization process with microgrid cooperation requires a well-structured architecture with a well-known information exchange. Multi-agent systems can comply with these requirements represent and they are used in different analysis where a unique objective function is assigned to each agent [142].

The lower level comprises both physical and software elements of microgrids and it is extensively described in sections III.2.2 and III.3.1. The interface between microgrids and the upper level is achieved through the MMCA (Microgrid Manager and Controller Agent) which aims to control each controllable source or an aggregation of different sources in its operating

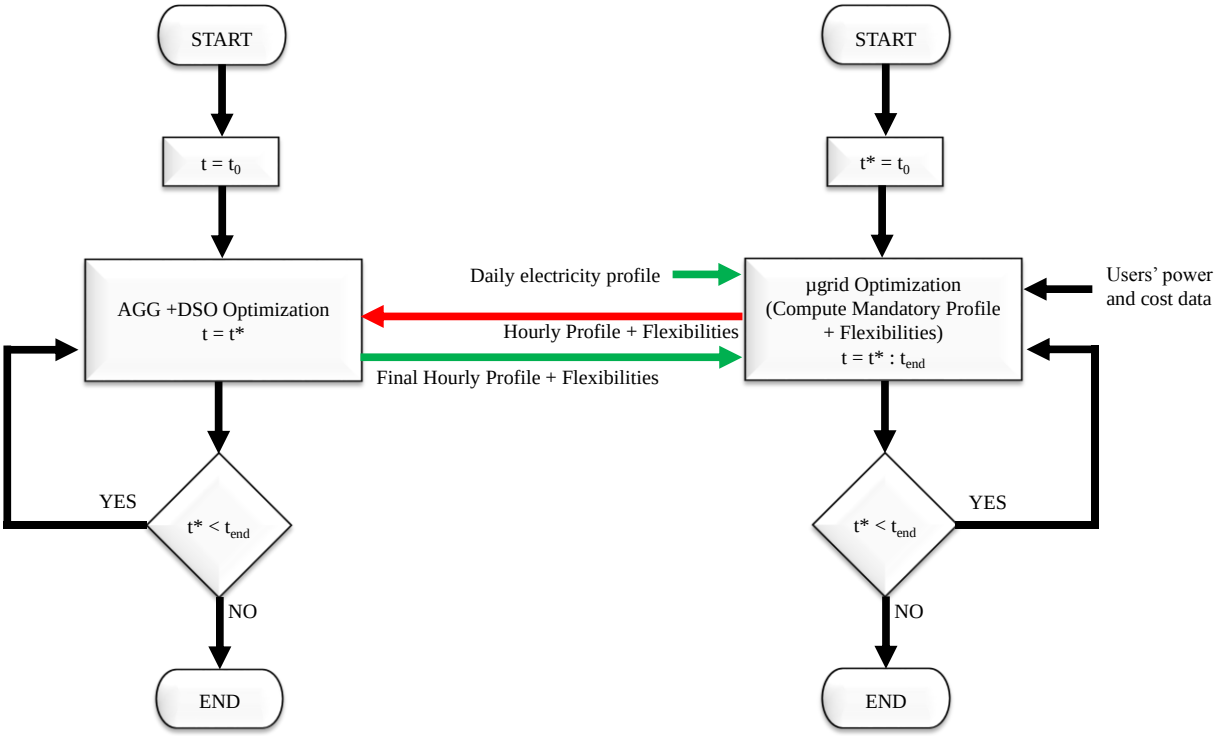

*__Legend__: Black Line: Process; Green Line: Communication exchange from AGGA to MMCA; Red Line: Communication exchange from MMCA to AGGA

Fig. IV.3 Flow-chart representing the Proposed Sliding Two-Level Optimization for Planning Problem

area. All tasks and characteristics of an MMCA have been already defined in section III.2.2

In the upper level, the aggregator takes the responsibility of these microgrids and acts as a mediator between the lower level, the utilities, the market and the DSOs. The aggregator is the Multi-Microgrid manager and it is represented by the Aggregator Agent (AGGA). It communicates with the Market Agent (MA) and the DSO Agent (DSOA) in the upper level. From the MA, it receives the 24-h day-ahead hourly forecasted prices and transfers this information to all the MMCAs within its zone. Each microgrid runs a first daily scheduling. Afterwards, an hourly process is started between each MMCA and the AGGA, as illustrated in the flowchart in Fig. IV.3. This process needs to be adapted to the applied strategy for active management of distribution grids. This is due to the specific characteristics of the model that requires a modification of the exchanged information and of the implemented algorithm in the DSOA and AGGA as well. Hence, for each developed model the process will be further discussed and examined in-depth (see sections IV.4.2.1 and IV.4.3.1). The AGGA runs its optimization algorithm using the information gathered from the microgrids and build aggregated bids/offers for the market and aggregated flexibilities for the DSOs. The

negotiation process between each MMCA and the AGGA takes place hour-by-hour. The outcome of the optimization performed by the AGGA will be the daily proposal for the MA.

IV.3.2. Aggregator model: Cost and Revenues Allocation

The solution of the algorithm inserted in the AGGA and described in following sections aim to optimize the total costs to supply loads and the revenues of microgrids by satisfy the possible constraints imposed by the DSO using customers' flexibilities. However, it is necessary to allocate costs and revenues among different microgrids in the aggregator. Different models for costs/revenues allocation can be proposed, based on the contract stipulated with users and based on the primary objectives fixed by the aggregators. Furthermore, in the same aggregator as well can be considered different models.

However in these analyses, a common model to compute pricing and remuneration for microgrid is considered. The model proposed is based on the idea that the primary task of the aggregator is to satisfy the consumption. This means that the energy produced locally is first used to satisfy consumption and then, the remaining energy is sold to retailers or into markets. Moreover, considering the size of aggregator under analysis, it cannot substantially influence market prices. Therefore, it is considered a price-taker, which means that it will accept prevailing prices to sell/buying energy in the market.

The procedure used to calculate costs and revenues is based on the computation of local[15] prices to sell/buy energy for each h=1…24 using Eq. IV.7 and Eq. IV.8.

Aggregator buying price

$$C_{lb} = \frac{E_{pl} \cdot C_{pl} + (E_{pl} - E_l) \cdot C_{bm}}{\max(E_{pl}\ ,\ E_l)} \qquad \text{Eq. IV.7}$$

Aggregator selling price

$$C_{ls} = \frac{E_l \cdot C_{pl} + (E_{pl} - E_l) \cdot C_{bs}}{\max(E_{pl}\ ,\ E_l)} \qquad \text{Eq. IV.8}$$

Where E_l is the total energy consumption required by microgrids under the aggregator subscription in timeframe h, E_{pl} is the part of E_l satisfied by microgrids' generation, C_{pl} is the

[15] The term local in this context is not used to indicate geographical proximity, but to indicate the membership of microgrids in the aggregator.

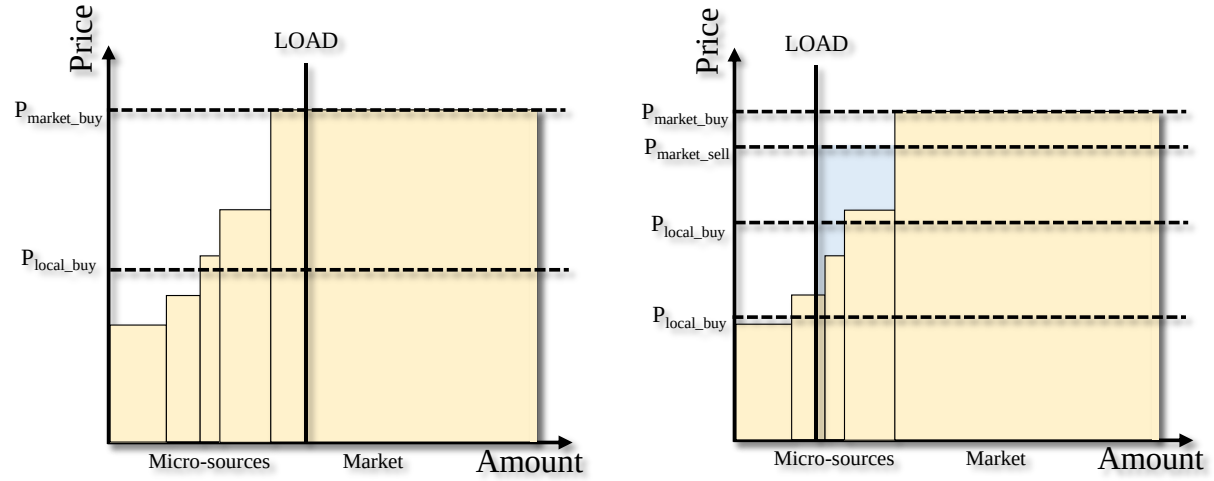

(a) Higher load case *(b) Higher generation case*

Fig. IV.4 Aggregator Local Price Calculation

average cost of electricity produced by microgrids' generation, C_{bm} and C_{bs} are the buying and selling prices to buy/sell electricity from/to the retail or wholesale market.

In general, two different cases could be identified in the aggregator considering the balance between generation and demand: demand request lower than requested generation injection and vice versa. In the first case, the situation looks like example in Fig. IV.4 (a) in which energy put up for sale by the microgrids and its flexibilities for production increase are lower than load demand for a certain period *h*. The energy purchasable from the market is considered to be unlimited. All the flexibilities with price greater than the market price are automatically excluded.

In the aggregator, the mechanism considered to remunerate used generation by microgrids is the pay-as-bid. In this manner the local cost of electricity for consumers will decrease respect to the market price or take the same value. Effectively, microgrid are aware about market forecasted prices to sell energy and they could propose the same price.

In case of aggregators with a large pool of medium-sized producers and/or microgrids, which products will be traded on the day-ahead market, a competitive price for the bid need to be computed if its size is sufficiently large to influence the market price. Howevwer in this thesis, the aggregator is considered as a price-taker also in case studies in which energy is traded in the elecricty market. Hence, the electricity is always sold at the market clearing price also when proposed with a lower competitive price.

IV.4. Multi-Microgrid Scheduling for Active Congestion Management and Market Participation

IV.4.1. Active Congestion Management Methods

At planning stage, before connecting new active or passive users, DSOs undertake studies on possible scenarios of network connections (location and rate of power increase). Today, most distribution networks are mainly not controlled in real-time. The real-time control is in fact limited to fault restoration in medium voltage networks through grid reconfiguration technique. Control action in general did not involve the active control of generation and demand. This passive operation requires planning and design of grids, which guarantee that the network can cope with two extreme scenarios: maximum consumption without local production and maximal peak production with minimum level of consumption.

Historically, the regulatory framework imposed to DSOs to plan their network expansion based on the principle of "fit-and-forget" using these two worst-case scenarios in order to accommodate up the last kWh injected by producers (e.g. article 10 of law on modernization and development of public electricity service [143]). However, the worst-case analysis based on these two scenarios may not be the best solution to size the electrical networks of the future. In fact, a worst-case analysis would lead to a disproportionately oversized infrastructure and new regulatory framework needs to be evolved considering following considerations. First and foremost, RES variability makes production peaks infrequent and it is limited only to a few hours per year. Furthermore, the diffusion of tariff-based energy management strategy will lead flexible consumers, such as EVs, to shift to minimum-price intervals and producers to sell during maximum price intervals. This situation will lead to hourly load peak or injection peak, which will cause an inefficient operation of the grid infrastructure. Hence, regulation needs to be modified from both network planning and operation point of view according to a conscious use of the grid by costumers and DSOs.

In 2016, the German law in the sector of energy, the *Energiewirtschaftsgesetz* (EnWG) [144], adopted, in clause 2 of article 11, the possibility to curtail up to 3% of the annual production of wind or photovoltaic systems for DSOs. According to [145], the value of 3% will be an optimal compromise between savings due to reduced grid reinforcements and costs associated with the installation of ICT infrastructure and to remunerate this service to producers.

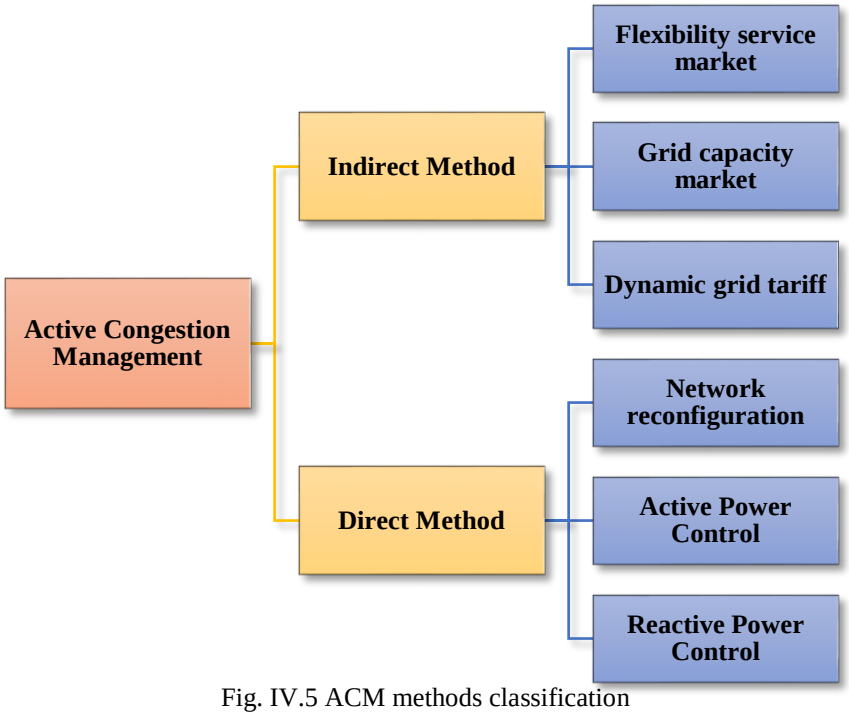

Fig. IV.5 ACM methods classification

This study estimates also a net saving of 15% (network investment savings minus ICT and remuneration costs).

All these considerations facilitate the understanding that a cost-efficient way to increase RES hosting capacity, keeping a high level of security and supply quality, can be found in the development of operation strategies which will utilize lines and transformers capacities more efficiently by using generation and consumption flexibilities.

Active Congestion Management (ACM) refers to a class of active strategies used to solve power or voltage congestion in some location in the electrical network. In general, ACM methods can be organized into two main classes based on the capability of a DSO to take direct or indirect actions on users or grid components. The class of methods called indirect takes into account all practices in which end users take the final decisions on their systems. Basically, the DSO can simply influence users' behaviour through price signals or purchase users' flexibilities on market platforms and remunerate them for the services they provided. On the contrary in direct methods, DSO can directly act on network infrastructure, e.g. by reconfiguring network structure, or on units connected to the network by varying active or reactive power profile of those users with whom stipulated an agreement contract. In Fig.

IV.5, a more detailed overview of methods falling into both categories is given, inspired by existing approaches proposed in the literature.

Huang et al. [146] discussed different congestion management methods and their mathematical models based also on direct and indirect approach classification. *Andersen et al.* [147] investigated three different strategies for distribution grid congestion management based on operations and interactions of two particular actors, the fleet operators and DSOs: "*Distribution grid capacity market*", "*Advance capacity allocation*" and "*Dynamic grid tariff*". Naturally, the use of these strategies could be extended to other actors, such as microgrid and virtual power plants operators. More extensively, the concept of "*Flexibility service market*" (FSM) for DSO is promoted and formalized by *Zhang et al.* [148] to actively manage the participation of small and medium-sized DERs (up to 5 MW) in flexibility trading. Furthermore, good advancements have been made by these authors by giving an advanced contribution in FSM architecture and then firstly discussing two different trading models, and the possible types of services to be traded. An interesting contribution to this topic comes from *Verzijlbergh et al.* [149], who investigated possible congestion management mechanisms using EVs based on IT requirements and uncertainty. This contribution provided and discussed a mathematical formalization of "*Dynamic Grid Tariff", "Distribution Capacity Market"* and "*Optimal Tariff*" approaches taking into account an empirical case study. An important outcome of this study was the analysis of "*Optimal Tariff*" strategy as a substitute to the more difficult-to-implementation bi-level "*Dynamic Grid Tariff"* approach.

However, results proposed in the literature are not complete and all these strategies need to be further conceptualized, investigated and tested. Hence, following sections aims to examine in depth the main characteristics and actors' interactions for two indirect methods: "*Flexibility service market" and "Capacity Limit Allocation"*, using a distributed approach and guaranteeing privacy and full autonomy to make decisions to microgrids. Mathematical formulations are developed, implemented using MAS and tested with case studies to prove the advantages and disadvantages of each method.

Moreover, in "*Capacity Limit Allocation"* strategy, market rules are introduced to test the simultaneous participation and engagement of microgrids to ACM and EM. These approaches are tested for power congestion issues, but the use of these strategies can be easily extended to other issues, which require the acquisition of flexibilities from DSOs, such as voltage congestions.

IV.4.2. Flexibility Service Market

IV.4.2.1. Overview and assumptions for services market model

The "Flexibility Service Market (FSM)" strategy aims to propose and analyse a framework for trading services for ACM of distribution networks [150]. In fact, as introduced in IV.4.2.1, the development of a FSM is a crucial question to face operational challenges due to the large diffusion of DER. Among ACM strategies, FSM may be one of the most efficient and economical methods for congestions resolution.

This new market may have to be developed in the form of a parallel market beside the already existing markets, i.e. the electricity and the ancillary services markets. It can be managed by DSOs or by new authorities, such as a local services market operator, according to the rules defined in each country. The main goal of this new market is to allow DSOs to purchase user's flexibilities to solve network congestion in a competitive environment, instead of an expensive and inefficient grid reinforcement. Microgrids, virtual power plants and medium-sized users will participate in this market as service providers proposing their aggregated flexibility products in the market platform.

The organization of these services' procurement can be organized on three main phases:

- year-ahead planning,
- short-term planning, which comprises day and hour ahead phases,
- real-time operation.

The real trading process requires a year-ahead planning and scenario analysis in which the DSO can identify all requirements of flexibility services to purchase in day and hour ahead planning phases (service category, area, location, quantity, etc.) [148]. During this phase, the DSO forecasts the availability of services and plans network reinforcement actions based on services unavailability or economic analysis. They could also stipulate forward contracts with users or aggregators to buy flexibility.

Hence, after this initial step of preparation, the trading process takes place. It can be organized in different sessions. The ahead-markets are crucial parts of the entire process. In fact during these phases, the DSO can adjust the users' energy program buying their flexibilities, before it will be submitted to a local energy market or to the wholesale market.

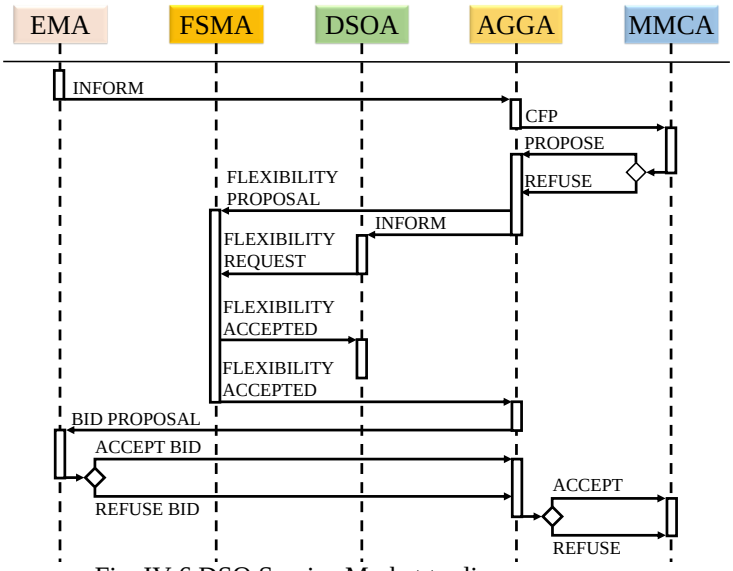

Fig. IV.6 DSO Service Market trading process

Within a framework for achieving efficient ahead markets, there are several options for organizing a services market.

Each market model has its own advantages and disadvantages, and has different impacts and implications. Economists have debated advantages and disadvantages in several contexts, such as in [151]. There are many methods for auctioning energy services, of which the most common is the sealed-bid auction mechanism [151]. According to this mechanism, in the day-ahead market, as well in the intra-day, participants submit simultaneously their power and energy flexibilities associated with the minimum price at which they are willing to sell their flexibility for each traded block. The FSM is cleared before the closure of the energy market based on economic criteria considering the characteristics of the proposed flexibilities (e.g. capacity, minimal and maximal power to be activated, etc.).

When designing a new market, one of the hardest topics is the proper pricing system. According to the analysis in [151] there are three important pricing rules for electricity auctions: uniform pricing, pay-as-bid pricing and *Vickrey* pricing. Although the analysis and comparison of different market designs are fundamental, they are out of the scope of this work.

Therefore, the model construction is based on hypotheses developed from recent studies in the literature. In FSMs, the nature of bids and offers are complex and non-homogeneous; this creates a high degree of product fragmentation. This suggests that a pay-as-bid pricing may be promising, as mentioned by authors in [152]. A merit-order pricing could only consider the

energy/power bid based on its marginal price and could not consider the real nature of the offers. In fact, under pay-as-bid pricing, all accepted offers are paid at the offered prices.

During market design, another important question is about the market participants and the rules that they need to respect for participating. In this model, aggregators, microgrids and single users with enough installed capacity are considered suitable to submit offers in the FSM. Some analyses about this concept are presented in section III.4.

Trading interactions between actors are shown in Fig. IV.6 and are repeated for each hour of the day. The duration of traded products may be an hour, as in the electricity market, or a smaller time-step, such as 15 or 30 min, or a mix of products as well. As introduced in section IV.3, each microgrid runs a local optimization of its production and consumption profiles as well as available flexibilities. For each time-step, the flexibilities are then sent to the FSM and the resulting energy profiles to the DSO. In the FSM, pay-as-bid mechanism is used to clear the bids. Thereafter, microgrids are informed about the corresponding accepted flexibilities. The accepted flexibilities are also transmitted to the DSO.

Depending on the FSM results rescheduling is then carried out in each microgrid depending on its needs. This procedure will increase microgrids' efficiency and system flexibility, allowing for example to store energy in an ESS or activate demand response in case of a flexibility demand to decrease production. The real-time market represents the real-time actions applied by DSOs to solve grid criticalities not expected during ahead-phases (e.g. caused by DSO or users forecast errors). This process begins when DSOs detects the possibility of criticalities in the network after the cloture of ahead markets. During this phase, DSO could continue to negotiate flexibilities in the same manner as in ahead markets, and if it fails because of a lack of offers, it could takes over the control of some DERs, controllable loads or ESSs. In this case, DSO will incur a penalty payment [153].

All these hypothesis are used to elaborate all the interaction in the MAS and build the algorithm in the core of the DSOA. The implemented day-ahead and hour-ahead active management of distribution grids with "FSM" is based on process described in the flow chart shown in Fig. IV.7, which is an extension of Fig. IV.3 for this strategy.

In following studies, the DSOA and the FSM are implemented in one agent. In this flow chart, the main tasks of each agent are resumed by describing the information exchanged

among the DSOA, the AGGAs and the MMCAs and the algorithms implemented in each of them. The developed mathematical model of the optimization algorithms implemented in the DSOA and the ACCA are described in sections IV.4.2.2 and IV.4.2.3, respectively.

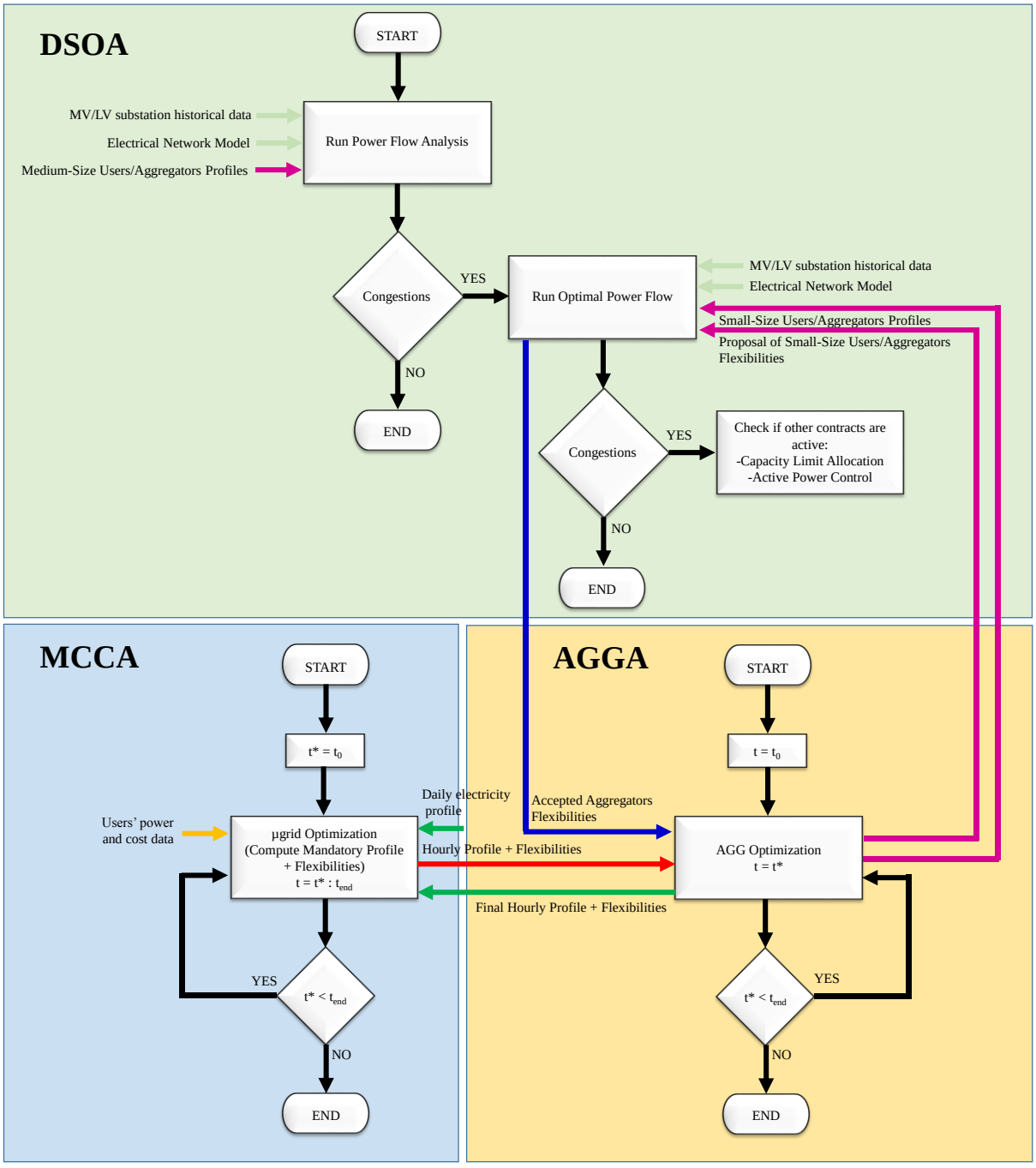

*__Legend__: Black Line: Process; Green Line: Communication exchange from AGGA to MMCA; Red Line: Communication exchange from MMCA to AGGA; Blue Line: Communication exchange from DSOA to AGGA; Fuchsia Line: Communication exchange from AGGA to DSOA; Yellow Line: Communication exchange between UA (e.g. DGA, EESA, LA) and MMCA and DSOA; Light-green Line: Communication exchange between DSOA and SCADA

Fig. IV.7 Flow chart for day-ahead and hour-ahead active management of distribution grids through "FSM"

IV.4.2.2. Mathematical Formulation for DSO Optimization Problem

Nomenclature

Sets:

H	Optimization problem timeframe
F	Set of generation power flexibilities
G	Set of distributed generators
N	Number of buses
M	Line number

Parameters:

$\boldsymbol{P_{D_i}}$	Absorbed active power by load in bus *i*
$\boldsymbol{P_{G_i}}$	Injected active power by generator in bus *i*
$\boldsymbol{P_{f_i}^{max}}, \boldsymbol{P_{f_i}^{min}}$	Max and min active power of flexibility bids *f*
$\boldsymbol{Q_{D_i}}$	Absorbed reactive power by load in bus *i*
$\boldsymbol{Q_{G_i}}$	Injected/absorbed reactive power by generator in bus *i*
$\boldsymbol{G_{ij}}$	Real part of series admittance $\boldsymbol{Y_{ij}}$ for line *ij*
$\boldsymbol{B_{ij}}$	Imaginary part of series admittance $\boldsymbol{Y_{ij}}$ for line *ij*
$\boldsymbol{V_i^{max}}, \boldsymbol{V_i^{min}}$	Max and min voltage magnitude in bus *i*
$\boldsymbol{\vartheta_i^{max}}, \boldsymbol{\vartheta_i^{min}}$	Max and min voltage angle in bus *i*
$\boldsymbol{S_{max_{ij}}}$	Max apparent power flow in line *ij*

Control Variables:

$\boldsymbol{V_{m_i}}$	Voltage magnitude in bus *i*
$\boldsymbol{\vartheta_i}$	Voltage angle in bus *i*
$\boldsymbol{S_{f_{ij}}}, \boldsymbol{S_{f_{ij}}}$	Apparent power flow from and to line *ij*
$\boldsymbol{P_{g_i}}$	Final injected power in bus *i*
$\boldsymbol{P_{f_i}}$	Accepted active power of flexibility bids *f*

Mathematical Formulation Description

The optimization problem posed by the acceptance of bids in the services market for DSO can be solved using optimal power flow problems (OPF). The OPF has a long history since 1960s and is still subject of research and algorithmic improvements [154]. The most important formulations in the literature are described in detail in [154].

The objective of this kind of problem is to find the optimal value of a fixed objective, such as costs for producing electricity or losses mitigation, including voltage and other operating constraints. The formulation is based on the classical power flow problem, which consists of solving a set of static nonlinear equations in terms of active and reactive power injections and voltages at each node in the system.

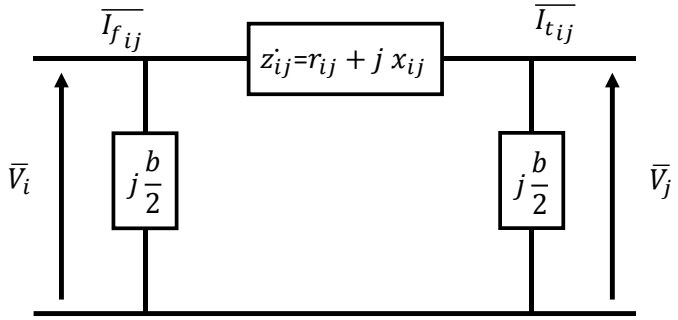

Fig. IV.8 π line model

In this thesis, the FSM is considered to be managed by the DSO, i.e. the FSM and the DSO are considered to be one entity. The objective function described by Eq. IV.9 has the goal of minimizing the cost for buying flexibilities from different kind of actors, such as aggregators or retailers. The control variables for the OPF include the accepted power for each flexibility bid. The model is based on discrete time equations $\forall h \epsilon H$ and uses a timeframe of 1 hour.

Minimization of congestion resolution cost:

$$\min \sum_{f \in F} F(P_f) \qquad \text{Eq. IV.9}$$

Constraints in the problem take into account both physical constraints of power systems through power flow equations as well as users' type of flexibilities bids. The equality and inequality constraints, used in this formulation, are described by Eq. IV.11-Eq. IV.18.

As usual in electrical engineering, all lines and transformers are modelled using the standard representation of lines in the π model. Hence, a generic line *ij* connecting bus *i* with bus *j* is represented by a circuit with series impedance z_{ij} and two parallel susceptances as in Fig. IV.8.

In the following formulation, the real and imaginary terms of the admittance matrix in the *ith* row and the *jth* column (Y_{ij}) are indicated with G_{ij} and B_{ij}, respectively. The injected/absorbed complex power in the generic bus *ith* is defined as the difference between generation and consumption as in Eq. IV.10, where $\overline{V_i}$ is the voltage in bus *i* and $\overline{I_i}^*$ is the complex conjugate of current in bus *i*. For numerical applications, it is necessary to reformulate this equation obtaining two real-valued equations. Hence, addition formulas of trigonometry are applied as shown in Eq. IV.10. Thereafter, it is easy to obtain active and

reactive power equations extracting the real and imaginary parts of the complex power, which are used in balance constraints in Eq. IV.11 and Eq. IV.12.

$$S_i = P_i + jQ_i = \overline{V_i} \cdot \overline{I_i}^* = \overline{V_i} \cdot \sum_{j=1}^{N} \dot{Y}_{ij}^* \cdot \overline{V_j}^* =$$

$$V_i(\cos\varphi_i + j\sin\varphi_i) \cdot \sum_{j=1}^{N} V_j\big(\cos\varphi_j - j\sin\varphi_j\big) \cdot \big(G_{ij} - jB_{ij}\big) =$$

$$\sum_{j=1}^{N} V_i V_j\big(G_{ij} - jB_{ij}\big)(\cos\varphi_i + j\sin\varphi_i)\big(\cos\varphi_j - j\sin\varphi_j\big) =$$

$$\sum_{j=1}^{N} V_i V_j\big(G_{ij} - jB_{ij}\big)\big[cos\,\varphi_i\,cos\,\varphi_j - j\,cos\,\varphi_i\,sin\,\varphi_j + j\,sin\,\varphi_i\,cos\,\varphi_j + sin\,\varphi_i\,sin\,\varphi_j\big]$$

$$= \sum_{j=1}^{N} V_j V_j \cdot \big(G_{ij} - jB_{ij}\big)\Big[\frac{1}{2} \cdot \big(\cos(\varphi_i - \varphi_j) + \cos(\varphi_i + \varphi_j)\big) - j\frac{1}{2} \cdot \big(\sin(\varphi_j - \varphi_i) + \sin(\varphi_j + \varphi_i)\big) + j\frac{1}{2} \cdot \big(\sin(\varphi_i - \varphi_j) + \sin(\varphi_i + \varphi_j)\big) + \frac{1}{2} \cdot \big(\cos(\varphi_i - \varphi_j) - \cos(\varphi_i + \varphi_j)\big)\Big]$$

$$= \sum_{j=1}^{N} V_j V_j \cdot \big(G_{ij} - jB_{ij}\big)\big(\cos(\varphi_i - \varphi_j) + j\sin(\varphi_j - \varphi_i)\big) \qquad \text{Eq. IV.10}$$

Active power balance in bus i:

$$P_{g_i} - P_{D_i} = Re(S_i) = \sum_{j=1}^{N} V_i V_j \cdot \big(G_{ij} \cdot \cos\big(\varphi_i - \varphi_j\big) + B_{ij} \cdot \sin(\varphi_i - \varphi_j)\big) \qquad \text{Eq. IV.11}$$

Reactive power balance in bus i:

$$Q_{G_i} - Q_{D_i} = Im(S_i) = \sum_{j=1}^{N} V_i V_j \cdot \big(G_{ij} \cdot \sin\big(\varphi_i - \varphi_j\big) - B_{ij} \cdot \cos\big(\varphi_i - \varphi_j\big)\big) \qquad \text{Eq. IV.12}$$

Eq. IV.11 and Eq. IV.12 are two sets of N non-linear equations, which connect active and reactive power balance to voltage magnitude and angle in each bus *i*. Each microgrid in each bus is characterized by a hourly aggregated energy consumption or production P_{D_i} and P_{G_i}.

Line Flow Limit Constraints (from the line ij)

$$\left|S_{f_{ij}}\right| \leq S_{max_{ij}} \;\forall\; ij \in M \text{ with } S_{f_{ij}} = \overline{V_i} \cdot \overline{I_{ij}}^* \qquad \text{Eq. IV.13}$$

Line Flow Limit Constraints (to the line ij)

$$\left|S_{t_{ij}}\right| \leq S_{max_{ij}} \forall\, ij \in M \text{ with } S_{t_{ij}} = \overline{V_j} \cdot \overline{I_{ij}}^{*} \quad \text{Eq. IV.14}$$

Operating limit of each cable is imposed using two sets of M inequality constraints in Eq. IV.13 and Eq. IV.14. This are two sets of M non-linear equations of bus voltage magnitudes and angles, which model line thermal limits.

Bus Voltage Magnitude Limit Constraints:

$$V_i^{min} \leq V_i \leq V_i^{max} \forall\, i \in N \quad \text{Eq. IV.15}$$

Bus Voltage Angle Limit Constraints:

$$\varphi_i^{min} \leq \varphi_i \leq \varphi_i^{max} \forall\, i \in N \quad \text{Eq. IV.16}$$

Constraints in Eq. IV.15 and Eq. IV.16 enable to limit magnitude and phase difference of voltage in each bus taking into account magnitude limits defined in the European standard EN 50160 [155].

Active Power Constraints for all Flexibility

$$P_{f_i}^{min} \leq P_{f_i} \leq P_{f_i}^{max} \forall\, i \in F \quad \text{Eq. IV.17}$$

Active Power Balance for Flexible Proposal

$$P_{f_i} + P_{g_i} = P_{G_i} \forall\, i \in F \quad \text{Eq. IV.18}$$

In this formulation, only DGs are taken into account for flexibilities, which are considered adjustable between the maximal and minimal value proposed in the bids. Hence, P_{G_i} consists of an uncontrollable part and a controllable part between $P_{f_i}^{min}$ and $P_{f_i}^{max}$. Upper and lower bounds of each active power flexibility are imposed in constraint Eq. IV.18.

Other types of flexibilities, which use active and reactive power, could be easily added to this formulation for further applications.

IV.4.2.3. Mathematical Formulation for Aggregator Optimization Problem

<u>*Nomenclature*</u>

Sets:

T	Optimization problem timeframe
F	Set of flexibilities

Parameters:

$\boldsymbol{C_{s_t}}$, $\boldsymbol{C_{b_t}}$	Price to buy/sell electricity from/to the main grid in time frame t
$\boldsymbol{P_{ub_t}}$, $\boldsymbol{P_{lb_t}}$	Upper and lower power bounds imposed by DSO in timeframe t
$\boldsymbol{P_{F_{min}}^{f}}$, $\boldsymbol{P_{F_{max}}^{f}}$	Max and min active power of flexibility bids f

Control Variables:

$\boldsymbol{P_{b_t}}$, $\boldsymbol{P_{s_t}}$	Power to buy and to sell in time interval t at aggregator level
$\boldsymbol{P_{F_t}^{f}}$	Power of flexibility f activated in time frame t
$\boldsymbol{x_F^f}$	Binary variable (1 if f is activated in time frame t, else 0)

Mathematical Formulation Description

The objective of this day-ahead optimization is to establish collaboration among microgrids and generate a cost-efficient resources planning to be submitted to a retail market for selling/buying energy. The optimization model uses as input users' hourly flexibilities to decrease overall cost for buying electricity or increase revenues for selling electricity.

The model further uses as input the 24-h day-ahead (forecasted) hourly price signal several hours before market closure. This means that the signal used is not the actual price that the microgrid will pay/receive, but it provides an indication about the expected prices of the next day. The actual prices are announced in real time. In order to safeguards small-sized microgrids, the actual prices can be imposed to vary within a certain known bounds.

The objective of this problem is to find the final aggregated profile minimizing costs to satisfy consumption and maximizing revenues for selling production.

Cost minimization and revenues maximization:

$$min \sum_{f \in F} C_t^f \cdot P_{F_t}^f \cdot \Delta t - C_{s_t} \cdot P_{s_t} \cdot \Delta t + C_{b_t} \cdot P_{b_t} \cdot \Delta t \quad \text{Eq. IV.19}$$

Power Balance:

$$\sum_{m \epsilon M} P_{b_t}^m - \sum_{m \epsilon M} P_{s_t}^m = -\sum_{gn \epsilon F} P_t^{gn} - \sum_{ln \epsilon F} P_t^{ln} + \sum_{gp \epsilon F} P_t^{gp} + \sum_{lp \epsilon F} P_t^{lp} - P_{s_t} \quad \text{Eq. IV.20}$$

Flexibilities upper and lower bounds

$$x_F^f \cdot P_{F_{min}}^{\ f} \leq P_{F_t}^f \leq x_F^f \cdot P_{F_{max}}^{\ f} \quad \text{Eq. IV.21}$$

The balance constraint in Eq. III.20 allows to supply the flexible and inflexible loads using electricity produced locally by DGs or bought from the main grid; it also permits to define the final exchange with the main grid. The constraint in Eq. III.21 limits the minimal

and maximal power of each flexibility *f* in time step *t*, according to the users' desired or available limits.

IV.4.2.4. Case Studies

a) Hypothesis and Development Information

In this chapter an illustrative examples is proposed with the purpose of analysing the interactions between the different actors and to test the business model proposed for the FSM. The simulation framework is developed using MAS and it was coded using Java and JADE libraries [67] with the methodology described in section II.5.4.2.

The implementation of the OPF was done extending the code supplied by MATPOWER version 6.0b2 using default solver, based on a primal-dual interior point method [156]. The MILP problem to optimize microgrids and aggregators profiles was implemented using Matlab and OPTI TOOLBOX version 2.16 [157] [135].

Moreover, the interface between the object agents developed in Java and the part of software developed in Matlab is realized using the free MatlabControl class [158]. The implemented pseudo-code in the DSOA is resumed in Tab. IV.1. Some details about the structure and the ontology used in the agents' messages are reported in Appendix C.

The selected case study takes into account an application on a 74-bus MV grid with flexibilities supplied by micro-sources, in which the proposed "Flexibility Service Market" strategy is tested by introducing upward and downward flexibilities bids by distributed generators.

Two different simulations are carried out in order to compare advantages and disadvantages from technical and economic point of view of the implemented collaborative strategy for all involved actors:

- collaborative strategy with aggregator,
- individual strategy without aggregator.

Algorithm Detect and Solve Congestion

```
1: Function detect congestion(grid_structure, microgrids_information)
2:     → run power flow
3:     → check congestion(power_flow_results, grid_limits)
4:     if congestion exist
5:         → run optimal power flow(grid_structure, microgrids_information, grid_limits)
6:     end
7: end
```

Tab. IV.1 Pseudo-code for ACM using FSM

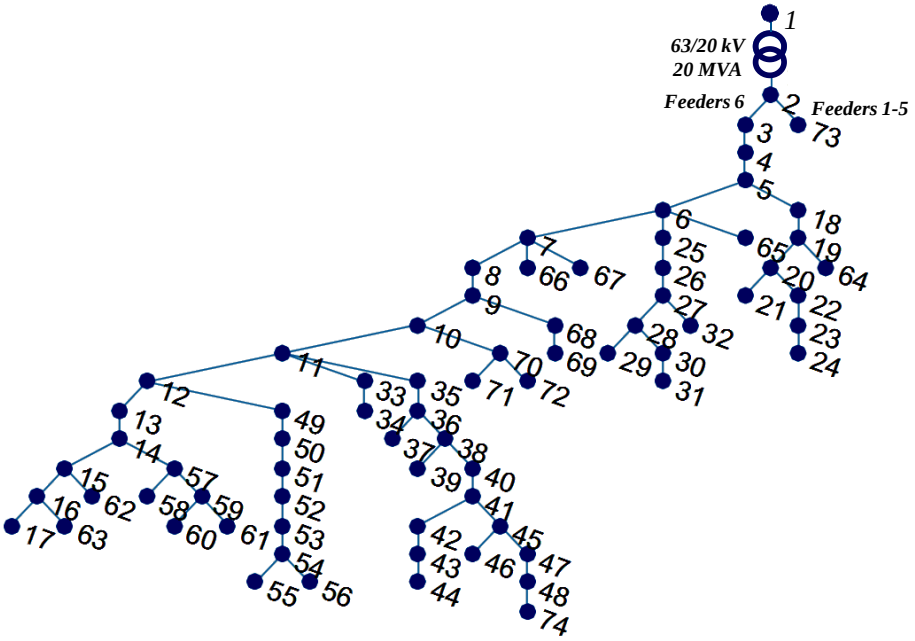

Fig. IV.9 74-Bus MV Grid

b) Application on 74-bus MV grid without and with aggregator

Description and Input/Output Data

The proposed methodology is applied on a real 74-bus MV grid displayed in Fig. IV.9. The grid is composed of approximately 100 km of 20 kV radial grid of 73 lines. The characteristics of the distribution grid are provided in Tab. VII.2 in Appendix B.

In this network, six MV feeders are connected to the HV/MV substation transformer which has a nominal power of 20 MVA. For simplicity the six MV feeders are simulated as two feeders. One feeder represents the MV feeder in analysis and the other represents the aggregated sum of the other five feeders (bus 73 in Fig. IV.9). This hypothesis however does not affect the validity of the results.

The maintenance, development and operation of the entire network, included microgrid 1, 3 and 4, is considered entrusted to the DSO, as it occurs in many European country, such as France. Users use to install a smart EMS with the objective of saving money and rationalizing the resource and energy usage by sharing locally produced electricity. In each installation is installed a smart meter and the information could be exploited by both users and the DSO. The used algorithms for microgrid optimization is described in section III.4.2.

Four microgrids type with inflexible loads, flexible loads, DERs and ESSs are connected

Microgrid 1			
Inflexible Load			
	n.		***P_c***
	30		*6 kW*
	15		*3 kW*
Distributed Generation			
n.	***Technology***	***P_n***	***LCOE***
12	*PV*	*3 kW*	*14 c€/kWh*
Energy Storage Systems			
n.	***Technology***	***P_n***	***E_n***
	Li-ion Battery	*50 kW*	*100 kWh*
	η_{ch}	***η_{dec}***	***SOC_{start}***
1	*0,96*	*0,97*	*0,2*
	SOC_{final}	***SOC_{max}***	***SOC_{min}***
	0,2	*0,8*	*0,2*

Tab. IV.2 Type and Nominal Data of Components in Microgrid 1

Microgrid 2			
Inflexible Load			
	n.		***P_c***
	-		*-*
Distributed Generation			
n.	***Technology***	***P_n***	***LCOE***
1	*PV*	*1.000 kW*	*10 c€/kWh*
1	*PV*	*1.500 kW*	*10 c€/kWh*
Energy Storage Systems			
n.	***Technology***	***P_n***	***E_n***
	Li-ion Battery	*200 kW*	*500 kWh*
	η_{ch}	***η_{dec}***	***SOC_{start}***
1	*0,98*	*0,98*	*0,2*
	SOC_{final}	***SOC_{max}***	***SOC_{min}***
	0,2	*0,9*	*0,1*

Tab. IV.3 Type and Nominal Data of Components in Microgrid 2

Microgrid 3			
Inflexible Load			
	n.		***P_c***
	30		*6 kW*
	5		*9 kW*
Distributed Generation			
n.	***Technology***	***P_n***	***LCOE***
1	*PV*	*7 kW*	*13 c€/kWh*
1	*PV*	*9 kW*	*13 c€/kWh*
1	*PV*	*15 kW*	*13 c€/kWh*
1	*PV*	*20 kW*	*12 c€/kWh*
1	*PV*	*40 kW*	*12 c€/kWh*
1	*Diesel*	*35 kW*	*19 c€/kWh*
1	*Bio-Diesel*	*80 kW*	*8.5 c€/kWh*
Energy Storage Systems			
n.	***Technology***	***P_n***	***E_n***
	Li-ion Battery	*100 kW*	*150 kWh*
	η_{ch}	***η_{dec}***	***SOC_{start}***
1	*0,97*	*0,98*	*0,4*
	SOC_{final}	***SOC_{max}***	***SOC_{min}***
	0,4	*0,9*	*0,1*

Tab. IV.4 *Type and Nominal Data of Components in Microgrid* 3

Microgrid 4			
Inflexible Load			
	n.		***P_c***
	40		*6kW*
Demand Response			
n.	***Technology***	***P_n***	***Usage-time***
10	*Washing Machine*	*3 kW*	*8.00 a.m.-10.00 p.m*
8	*Dish Washer*	*3 kW*	*0.00 a.m.-1.30 p.m.*
Energy Storage Systems			
n.	***Technology***	***P_n***	***E_n***
	Li-ion Battery	*100 kW*	*250 kWh*
	η_{ch}	***η_{dec}***	***SOC_{start}***
1	*0,97*	*0,98*	*0,5*
	SOC_{final}	***SOC_{max}***	***SOC_{min}***
	0,5	*0,8*	*0,2*

Tab. IV.5 *Type and Nominal Data of Components in Microgrid 4*

in this grid with the purpose of study the interactions between microgrids and the DSO:

- Microgrid 1, 3 and 4 represents communities of users composed of small-sized residential and commercial activities with DGs installed directly by users, in particular PV systems. Microgrids are connected via a MV/BT transformer of 250 kVA in bus 48, 40 and 47, respectively. Each user is represented by an agent and each microgrid interfaces through the MMCA with the DSOA or the AGGA.
- Microgrid 2 represents a medium-sized producer with two PV systems and ESS. It is connected via two MV/BT transformer of 1.500 kVA in bus 74.

	h=12			*h=14*		
Bus	P_{flex_min} ***(MW)***	P_{flex_max} ***(MW)***	C_{flex} ***(c€/kWh)***	P_{flex_min} ***(MW)***	P_{flex_max} ***(MW)***	C_{flex} ***(c€/kWh)***
16	*0*	*0,100*	*13*	*0*	*0,100*	*13*
33	*0*	*0,250*	*8,5*	*0*	*0,250*	*8,5*
35	*0*	*0,012*	*13*	*0*	*0,012*	*13*
37	*0*	*0,809*	*12*	*0*	*0,809*	*12*
38	*0*	*0,350*	*13*	*0*	*0,350*	*13*
40	*0*	*0,031*	*12*	*0*	*0,018*	*12*
42	*0*	*0,034*	*13*	*0*	*0,034*	*13*
43	*0*	*0,126*	*13*	*0*	*0,126*	*13*
44	*0*	*0,475*	*13*	*0*	*0,475*	*13*
46	*0*	*1,609*	*8,5*	*0*	*1,609*	*8,5*
55	*0*	*0,150*	*10*	*0*	*0,150*	*10*
70	*0*	*0,105*	*9*	*0*	*0,105*	*9*
74	*0*	*0,100*	*7*	*0*	*0.100*	*7*

Tab. IV.6 Negative Flexibilities proposed by microgrids in timeframe 12 and 14 for congestion management

As mentioned, the collaboration between users in each Microgrid 1, 3 and 4 is controlled by the intelligent MMCA which has the tasks to receive all information about its users, stock and manipulate this information, forecast users' behaviours and profiles, and run the smart optimization algorithm described in section III.2.1. Type and nominal data of related to the installed components in each Microgrid are listed in Tab. IV.2-Tab. IV.5.

The dynamic selling and buying prices are considered to vary according to the wholesale electricity market prices with an average daily selling price of 14.3 c€/kWh and buying price of 19 c€/kWh (see Fig. IV.20). These prices comprise both the electricity price and the grid tariff. Market constraints are not taken into account in this formulation and the surplus energy produced by microgrids is considered to be completely bought by the DSO.

Data used for PV production corresponds to day-ahead forecasted data obtained by forecast algorithm developed at CEA-INES and consumption data represent aggregation of a weekday type. Production and consumption data used for the month of June are used. Filled curves in Fig. IV.12, Fig. IV.13 and Fig. IV.14 show the day-ahead forecasted production of PVs, which is the input for the scheduling algorithm.

The data chosen for the simulation represent a critical situation, which might occur in a summer day with high production of PV systems. The selected time-window for microgrids optimization is chosen equals to 15 min. The energy schedule is constructed based on individual forecast signals sent by the users. In this simulation the aggregator profit is considered to be a monthly fee with contracted microgrids, as in [159].

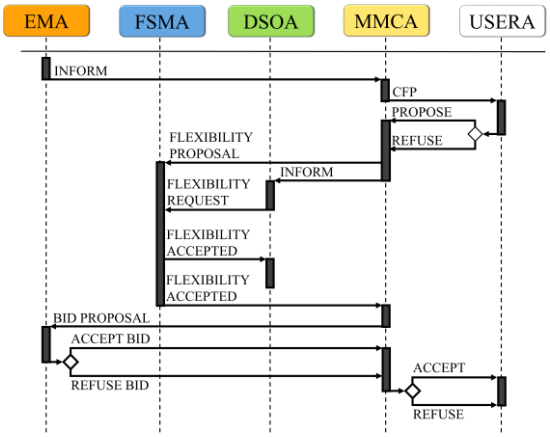

Fig. IV.10 Day-ahead trading interactions for FSM without aggregator

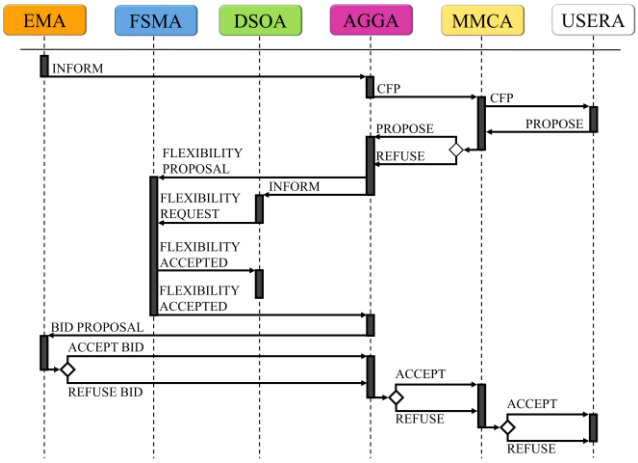

Fig. IV.11 Day-ahead trading interactions for FSM with aggregator

Flexibilities are generated only considering available generation, but not the demand-response capacities. DGs are used for providing both upward and downward flexibilities. Downward flexibilities consist on generation reduction in the microgrid. The bid price is fixed equal to the DG selling price. Upward flexibilities are composed of DGs that are not accepted in the bidding interval and the price is taken equal to price proposed by the user. Both upward and downward flexibilities are modelled as Type A bid, in section III.4.2.2.

Two critical situation, due to power congestion, are detected during the power flow (PF) in timeframes h=12 and in h=14. For this reason, only negative flexibilities related data are reported in Tab. IV.6.

Simulation Results

According to the descriptions in section IV.3, during the day-ahead operational planning the MMCA defines an initial energy schedule for each resource which can be represented by a piecewise function having a finite value for each settlement period, t=1 …96, of 15 min duration. The aggregated energy schedule ($P_{sch}(h)$) for each microgrid obtained with the initial optimization by using the model described in section III.4.2.1 is depicted in Fig. IV.12-Fig. IV.15 and is the same with and without aggregator. In these figures, light-blue curves represents the total load to satisfy in each microgrid and yellow lines are the hourly exchange in the PCC with the main grid. Furthermore, orange curves show the aggregated accepted generation, which can be compared with the total available generation drawn with filled curves. Finally, violet

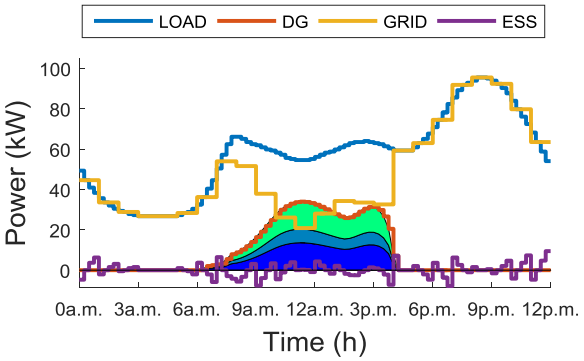

Fig. IV.12 Aggregated plan of Microgrid 1

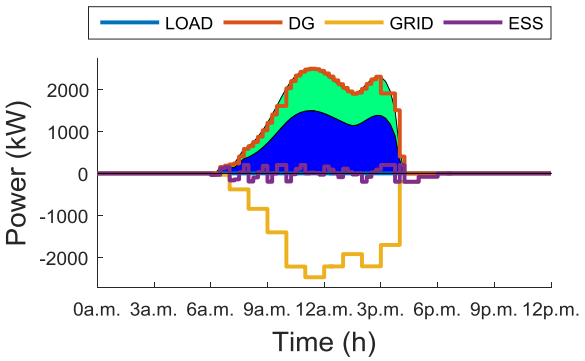

Fig. IV.13 Aggregated plan of Microgrid 2

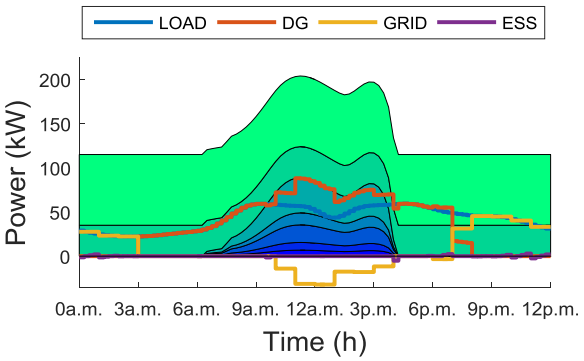

Fig. IV.14 Aggregated plan of Microgrid 3

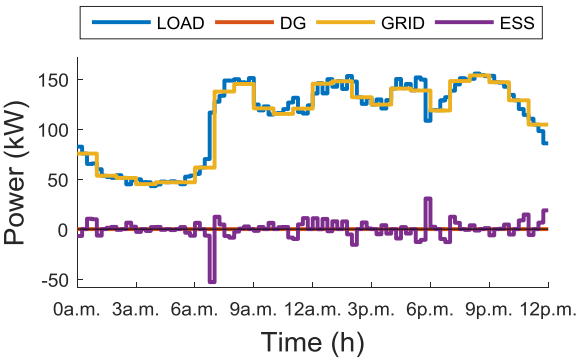

Fig. IV.15 Aggregated plan of Microgrid 4

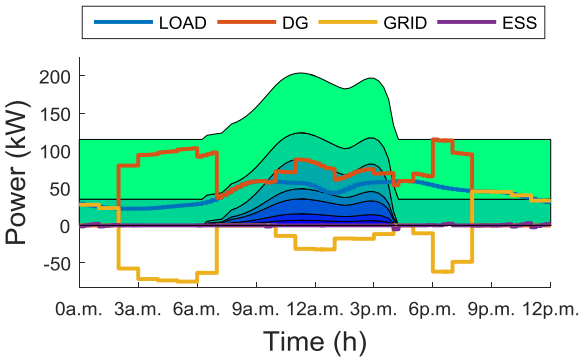

Fig. IV.16 Aggregated energy schedule of Microgrid 3 with aggregator

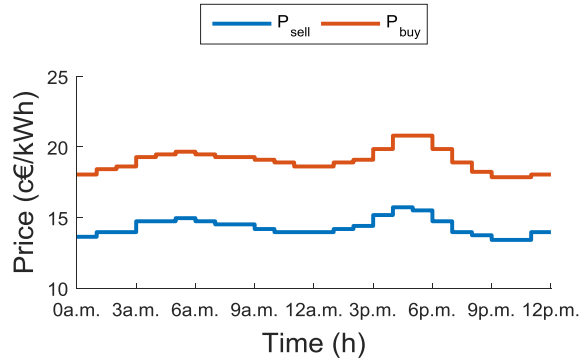

Fig. IV.17 Day-ahead forecasted dynamic market prices

lines represent the charged or discharged power in each battery[16]. For efficiency and flexibility reasons as discussed in section IV.4.2, the DSOA receives hourly aggregated profiles $P_{sch}(h)$ (yellow lines in previous figures) and available flexibilities $P_{\text{flexy}}(h)$ for each h=1…24 for each bus. These data are sent directly from each MMCA in the case of aggregator absence or from the AGGA, as illustrated in Fig. IV.10 and Fig. IV.11, respectively.

[16] Positive values of power indicate that the ESS is charging, otherwise that is discharging.

Bus	P_{sch} (MW)	P_{flex} (MW)	P_{new_sch} (MW)	C_{flex} (c€/kW)
46	1.609	0.105	1.504	8.5
74	2.473	0.100	2.373	7

(a) Interval 12

Bus	P_{sch} (MW)	P_{flex} (MW)	P_{new_sch} (MW)	C_{flex} (c€/kW)
74	1.922	0.081	1.865	7

(b) Interval 14

Tab. IV.7 Flexibilities purchased by the DSO for solving congestions in lines 47 and 48 using extended OPF: (a) in interval 12 (b) in interval 14

	µgrid 1	µgrid 2	µgrid 3	µgrid 4	µgrid 1	µgrid 2	µgrid 3	µgrid 4
MF (€)*	220.9	-2249.1	30.6	504.4	177.5	-2164.6	-64.5	365.7
CI (€)*	253.6	-664.2	163.8	510.8	210.2	-579.7	163.8	372.1
Load (kWh)*	1380.4	-	1033.8	2668.3	1380.4	-	1033.8	2668.3
CB (c€/kWh)*	18.2	-	16.0	19.0	15.1	-	16.0	13.8
CS (c€/kWh)*	14.0	14.3	14.2	-	14.0	13.6	16.3	-
DG_{acc} (%)	100	98.1	26.9	-	100	98.1	42.3	-
PVacc (%)	100	98.1	95.1	-	100	98.1	95.1	-
DIESacc (%)	-	-	12.8	-	-	-	31.4	-

(a) Without Aggregator *(a) With Aggregator*

***Legend**: *MF* : Daily money flow between each µgrid and DSO+AGG (expenses and revenues); * *DC* : Daily expense or revenue of each µgrid considering DG and ESS costs; * *Load* : Daily consumption of each µgrid;* *CB:* Daily average kWh cost payed by µgrid's consumers;* *CS:* Daily average kWh cost gained by µgrid's producers; DG_{acc} : Percentage of used energy on available/forecasted DG energy; PV_{acc} : Percentage of used energy on forecasted PV energy; DS_{acc} : Percentage of used energy on available DS energy.

Tab. IV.8 Comparison between expenses and revenues of microgrids and kWh_{cost} with and without aggregator based on business model described in IV.3.2

The DSOA uses $P_{sch}(h)$ as input for the power flow. In case a congestion is detected, it runs the OPF using $P_{\text{flexy}}(h)$ and $P_{sch}(h)$. In this case study, it detects a first criticality in h=12. It detects a power congestion of 194 kVA in line 47 and 191 kVA in line 48, which is approximately equal to 4.5% and 4.4% of S_{max} on each line. A second congestion of 47 kVA and 55 kVA, 1.1% and 1.3% respectively, is detected in the same lines in h=14. The detailed results of OPF for these timeframes are enclosed in Tab. VII.3 and Tab. VII.4 in Appendix B. In Tab. IV.7, the flexibilities purchased by the DSO for solving congestions are shown for both timeframes. In the first timeframe, Microgrids in bus 74 and 46 proposed the more competitive negative flexibilities with a price proposed of 7 c€/kW and 8.5 c€/kW, respectively, as shown in Tab. IV.6. Moreover, Microgrid 2 in bus 74 proposed a maximal flexibility of 100 kW as in Tab. IV.7, which causes the acceptance of the second most economic flexibility in bus 46.

Given that the resource used by Microgrid 2 is available and "free", it runs a re-optimization to reschedule its energy planning. The following calculations are based on the hypothesis that the total energy proposed to the energy market is accepted. For Microgrid 2,

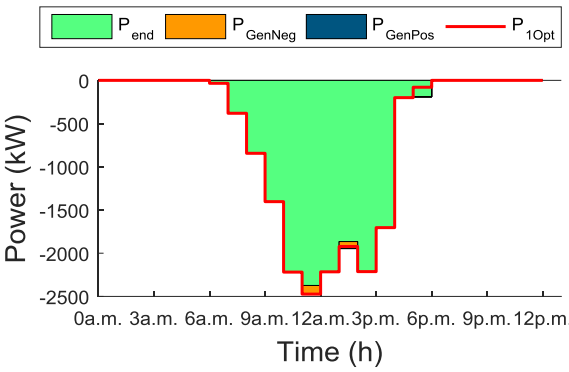

Fig. IV.18 Zoom on accepted flexibilities by aggregator for Microgrid 2 and comparison with initial scheduled exchange

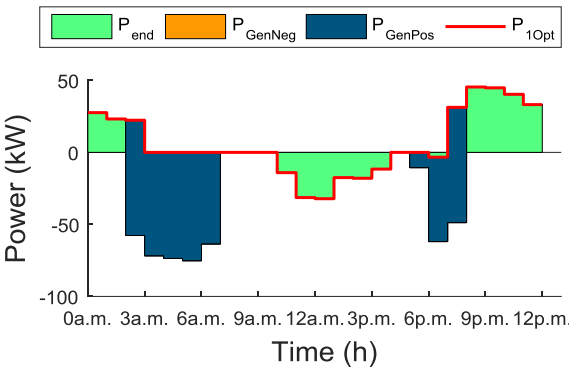

Fig. IV.19 Zoom on accepted flexibilities by aggregator for Microgrid 3 and comparison with initial scheduled exchange

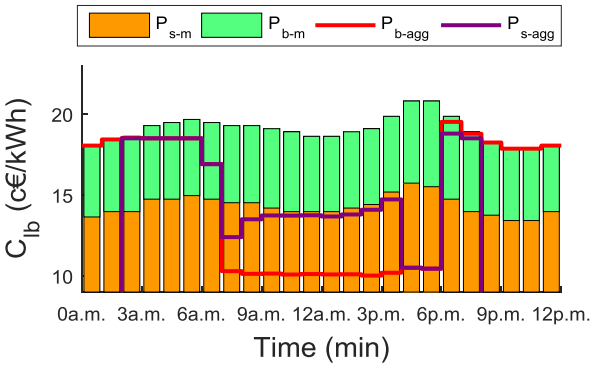

Fig. IV.20 Day-ahead forecasted dynamic market prices and aggregator local buying price

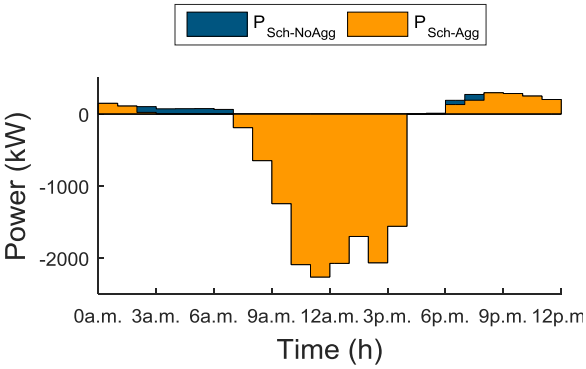

Fig. IV.21 Comparison between Aggregated profile obtained with and without Aggregator

the expected income from the sale of $P_{sch}(t)$, obtained with the first optimization by selling electricity at the market prices is equals to 2241.2 €. If the sale of services is considered, the total expected income is 2249.1 €, of which 12.7 € are the income for selling 181 kW as flexibility and 2236.4 € are the expected income for selling the rescheduled energy $P_{new\_sch}(t)$. Moreover, analysis of results showed that the re-optimization produces an increase of 0.6% of incomes and permits to increase of 0.7 % the usage of solar energy using the ESS.

In presence of the aggregator, the economic model proposed in section IV.3.2 produces a cost reduction for microgrids, which are mostly passive and an income reduction for totally active microgrids, as resumed in Tab. IV.8. The total expected income for Microgrid 2 has a reduction of 3.8% by selling both electricity and services. In fact, the total gain is 2164.6 €, of which 12.7 € are the income from services and 2151.9 € are the income from energy.

Otherwise, there is an expense reduction of 19.7% and 27.5% for Microgrid 1 and 4, respectively. The locally produced energy in Microgrid 3 increased by 15.4% inducing a rise in revenues. In fact, in the first case the daily revenues were 18.2 € due only to the net solar energy sold. In the second case, the revenues increased to 113.2 €.

This solution is proposed as alternative for grid reinforcement to use more efficiently the current electric infrastructure. If we consider 25.000 €/km for grid reinforcement to avoid congestion issues and corresponding power curtailment/shift, the DSO will pay approximatively 125.860 € for line 47 and 48 which are respectively 1.748 m and 3.286 m length. The DSO expense for the day in analysis is 20.0 €. Assuming a congestion occurrence of 30 days per year in this lines with a maximal power congestion of 5% in each line that corresponds to 13.000 kWh/year with an average service cost of 10 c€/kWh, the estimated expense will be 1.300 €/year that means 13.000 € in 10 years equivalent to 10.3% of the reinforcement cost.

IV.4.2.5. Conclusions

A "Flexibility Service Market" may be an interesting alternative to avoid additional investments in physical grid reinforcement. The effectiveness of this solution needs to be assessed *ex ante* by the DSO. This evaluation will be carried out by considering the necessary infrastructure costs to organize this new market (communication systems, control and automation systems, etc.). During the year-ahead phase, the amount and the location of necessary services compared to the reinforcement expenditure needs to be evaluated as well.

Moreover, the development of this strategy requires a new regulatory contractual framework. Hence, this method is the most complex strategy from both the implementation and technical point of view.

In contrast, simulation results show how this solution could represent an additional source of incomes for microgrids. Furthermore, this strategy offers less risk for the DSO if compared with other active management strategies, such as dynamic tariffs method. Also, this strategy guarantees a more efficient use of energy resources, compared for example with limit allocation strategy. This is because the DSO knows energy profile of microgrids and aggregators within a certain margin of error and doesn't need to excessively overestimate necessary services. This strategy encourages competition between microgrids, which will lead to lower costs for services. However, the re-optimization is a necessary step to optimize both the revenues of microgrids and the usage of renewable sources.

The introduction of the aggregator is an interesting solution to encourage microgrid collaboration. This collaboration allows a more efficient use of energy resources because it is locally produced. Moreover, the aggregation of microgrids may lead to reduce the overall forecast error as well as enable economies of scale that lead to overall cost reduction and facilitate the participation in electricity and ancillary services markets.

From the implementation point of view, the mathematical model needs to be extended to other type of flexibilities, such as demand response, and with other trading intervals, e.g. 15 mins.

IV.4.3. Capacity Limit Allocation

IV.4.3.1. Overview and assumptions for Capacity Limit Allocation model

The "Capacity Limit Allocation" strategy for DSO congestion management is based on the idea that an efficient use of grid capacity could be achieved by pre-allocating the available feeder capacity among group of users. This pre-allocation may be applied for a certain time-frame by imposing a power limit to medium-sized or aggregated customers, such as microgrids or aggregators.

The key principle in the implementation of this strategy is in the development of suitable contracts between these users and DSOs. This kind of contracts will give the DSOs the capability to amend aggregated user's profiles, reducing or increasing production or consumption. At the same time, this strategy could also have benefits for users. Different approaches could be used by DSOs to encourage grid users to participate in this program. A first approach would be to remunerate this new service through a regulated national tariff or through a tariff stipulated in the contract between the user and the DSO. Alternatively, the DSO could decide to propose more advantageous grid tariffs to consumers, or connection costs to producers as well. In this study, the first option is chosen.

The implementation process of this strategy requires different phases as presented in Fig. IV.22:

- Long-term planning stage. This first phase requires a delicate planning process to define all contract agreements with aggregators or directly with medium-sized users. During periodic analysis of grid extension planning, DSOs could detect

possible congested areas and define the amount of flexibilities, which will be required in the coming years. With these analyses, DSOs can stipulate contracts with aggregators and users. The most fundamental parameters which have to be defined in this contract are: the maximal annual and monthly call that each party can receive; the maximal flexibility power and duration that the DSO can require.

These parameters will influence DSOs extension planning and users sizing, e.g. the size of the installed ESS may vary based on flexibility power and duration of the service.

- Short-term planning stage or activation stage. DSOs shall calculate capacity limit needs for day-ahead and intraday time-frames and procure the necessary flexibility. In scheduling phases, network analysis can be performed to detect probable grid congestions using historical data of loads and DGs gathered with smart meters, weather forecast data and/or users forecasted energy profiles. In day-ahead and intra-day scheduling, the DSO can activate the capacity limits sending signals to aggregators to limit their power exchange with the grid during different daily time intervals. Thereafter in real time, if the DSO detects additional, unexpected congestion, it can send a mandatory request to reduce/increase users' power incurring in penalty payment.

Capacity allocation strategy is a proposition that has already drawn interests from the power system industry and has been used in the scientific analysis of DSO congestion management. An interesting concept is described in [147] focusing on EV equipped-households that share a certain capacity with the fleet operator for DSO congestion management.

Contract clauses and pricing rules are crucial parameters for the implementation of this strategy. Currently, energy economists are analysing contract options that allow the DSOs to utilize users' flexibilities. Authors in [160] claims that DSOs have two types of contracts available for DGs power modulation, based on the leniency of contracts: non-firm and firm contracts. Firm contracts, which represent the traditional kind of contracts, allows the export of full generation capacity to the distribution network. Otherwise under non-firm contracts, the DSO does not guarantee the full export of the generated energy in case of grid constraints and reserves the right to reduce the generation output based on the terms and conditions set in the contract agreement. As such, the occurrence of low power demand and high RES

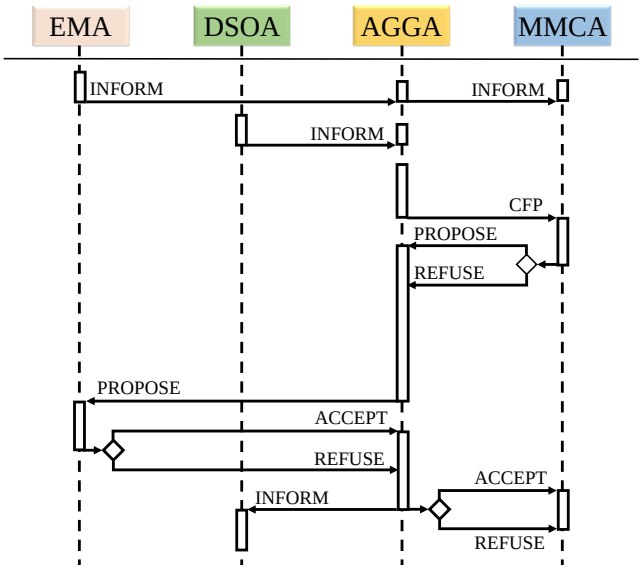

Fig. IV.22 Actors Interactions for "Capacity Limit Allocation"

generation at the same time will tend to occur for a relatively small fraction of time. Therefore, the option of firm connection is more reasonable for non-variable energy sources [161].

Different pricing policies may be proposed in the strategy model. If the user has some benefits from the contract agreements (e.g. connection cost reduction) they could agree to supply these services without an additional remuneration, otherwise they can opt for constant-tariff policy or for variable-tariff based for example on day-ahead zonal electricity prices.

Based on these considerations, the proposed strategy takes into account a multi-microgrid system that interacts with market and DSO through an aggregator. This work is only concerned with the development of an ahead strategy for "Capacity Limit Allocation" and does not analyse the long-term planning.

A general idea of interactions at *D-1* between various actors is depicted in Fig. IV.22. However the process is detailed in-depth in the following. In this process two general classes of aggregated users, based on their total size, can participate:

- Retail electricity market participant: these users sell/buy their electricity directly to an electricity retailer;
- Wholesale electricity market participants: these users sell/buy their electricity directly in the wholesale electricity market.

For the sake of completeness, a short overview of electricity market is provided in Appendix A. Developing strategies require a differentiation for the aforementioned categories in the mathematical formulation of the implemented algorithm in the AGGA. For the first category, the net energy of each microgrid or of an aggregation of microgrids is directly sold to/bought from a retailer. A competitive retail market gives to customers the possibility to choose the best supplier [162]. Hence, in a general vision, the retailer and the network operator could not be the same entity. This situation requires two contracts [162]. The first contract is with the distribution network operator for connection and electricity transportation. The second one with the supplier for the consumed energy. However, in this work the retail electricity supplier is assumed to also be the DSO.

In the second category, microgrid/aggregators sign electricity sale/purchase spot contracts directly with the EM. In the day-ahead auction market, hourly energy blocks are traded for the next day. Each participant submits its offers/bids. In each offer/bid the amount and the minimum/maximum price at which they are willing to sell/purchase are specified. Bids/offers are traded after the closure of the market based on the economic merit-order criterion and considering transmission capacity limits between zones. The intra-day market allows market participants to modify the schedules defined in the day-ahead auction by submitting additional offers/bids. The participation to short-term EM imposes a need to satisfy certain criteria and to respect rules summarized in Tab. VII.1 for Italy, Germany and France.

The sequential order of interactions at day *D-1* in the microgrid is the same as applied in the previous strategy and detailed in III.4. To briefly summarize, each microgrid performs an initial daily operational scheduling for $t=1 \dots T$ with a time step that can be lower or equal than *h*, using information from users as described in section III.4.2. At this point, each microgrid submits its hourly planning and a set of flexibilities for each time frame *h*. At day D-1, the DSOA pre-allocate needed capacity reduction (or increase) by defining conservative static limits for each MV feeder performing a statistical power flows analysis. The process and data exchange are detailed in the flow chart in Fig. IV.23. Also, in this case the process is implemented stepwise for each daily hour $h=1 \dots 24$. In these analyses, the DSOA uses historical data gathered through smart meters and forecasted day-ahead and hour-ahead energy profile at each PCC.

After identifying probable congestions, the DSOA forecasts aggregators (or medium-sized users) that can intervene according to contractual conditions. In this study, an aggregator is placed between microgrids and the DSOs (Fig. IV.22). This setup is suggested by results

obtained in section IV.4.2.4 and by the necessity to reduce information exchange with the DSOA. After that, the DSOA submits to each aggregator a proposal with the power limits of congested feeders in timeframe *h*.

Thereafter, the hourly definitive operational scheduling is performed by the aggregator by using flexibilities proposed by each microgrids with the objective of:

- maximizing the energy produced by active microgrids by exchanging energy with other microgrids;
- satisfying DSO requirements;
- preparing a proposal for the retail/overall market from fragmented users products.

The scheduling process in the AGGA consists of two phases. A preliminary phase in which the AGGA performs the *D-1* multi-microgrid profile for timeframe *h*, respecting users willingness and market rules if microgrids participate in the wholesale electricity market. Thereafter, if a congestion is detected, it computes a final energy profile including DSO limits.

The use of this sliding process allows to each microgrid to use efficiently their resources re-optimizing their planning for $t=h\cdot t^{*}\ldots T$ considering flexibilities used by the aggregator. At day *D*, the DSOA validates the final remuneration for each aggregator through the real computation of allocated capacity through whether and smart meters data. The same is done for the net electricity sold/bought respectively to the REM or the WEM.

The implemented day-ahead and hour-ahead active management of distribution grids with "CLM" is based on process described in the flow chart shown in Fig. IV.23. The main tasks of each MMCA, AGGA and DSOA are resumed and the information exchanged among them is shown. The developed mathematical model of the optimization algorithms implemented in the ACCA is described in section IV.4.2.3.

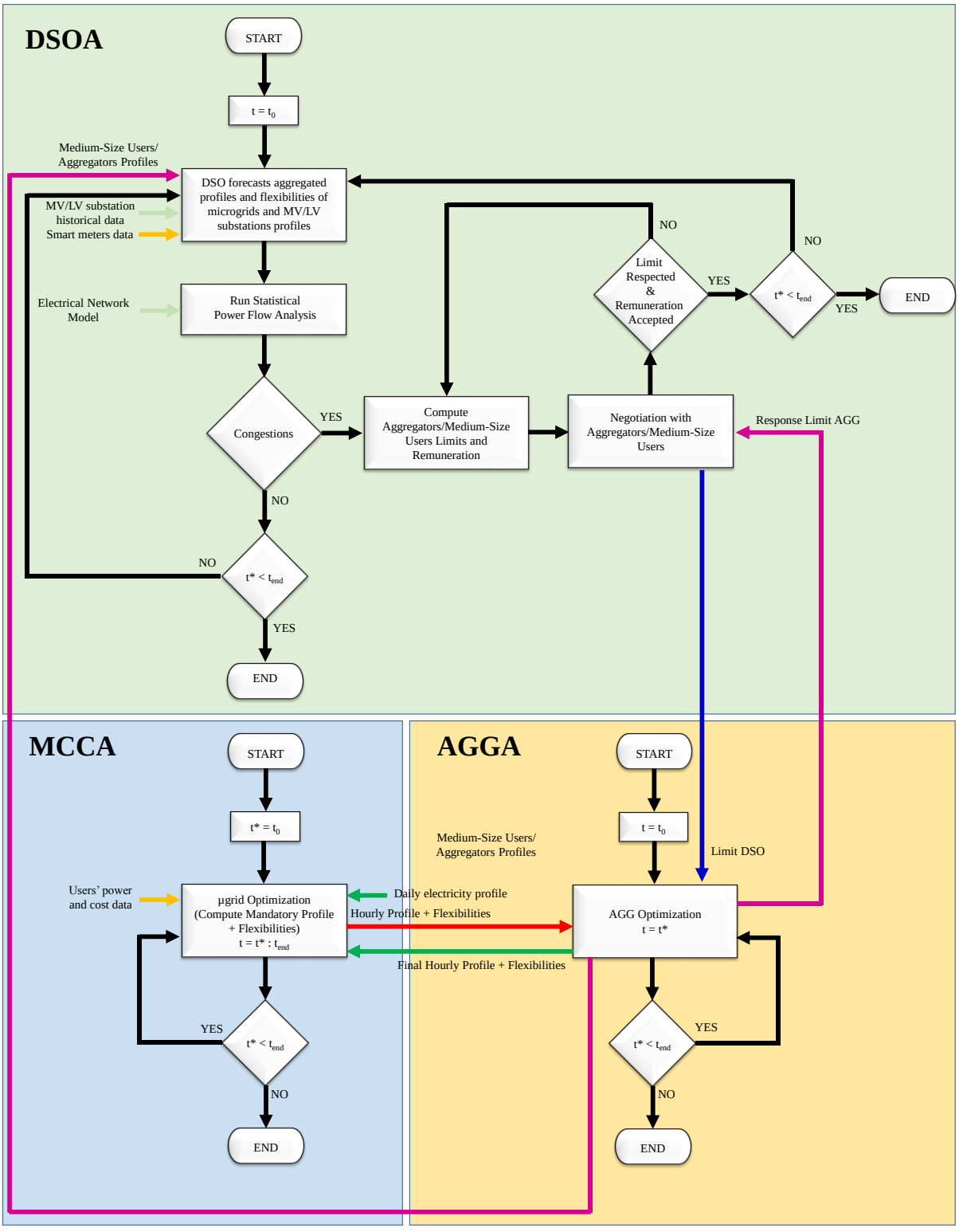

*__Legend__: Black Line: Process; Green Line: Communication exchange from AGGA to MMCA; Red Line: Communication exchange from MMCA to AGGA; Blue Line: Communication exchange from DSOA to AGGA; Fuchsia Line: Communication exchange from AGGA to DSOA; Yellow Line: Communication exchange between UA (e.g. DGA, EESA, LA) and MMCA and DSOA + DSOA and Network; Light-green Line: Communication exchange between DSOA and SCADA

Fig. IV.23 Flow chart for day-ahead and hour-ahead active management of distribution grids through "CLA"

IV.4.3.2. Mathematical Formulation for Aggregator Optimization

Nomenclature

Sets:

T	Optimization problem timeframe
F	Set of flexibilities

Parameters:

$\boldsymbol{C_{s_t}}$, $\boldsymbol{C_{b_t}}$	Price to buy/sell electricity from/to the main grid in time frame t
$\boldsymbol{P_{ub_t}}$, $\boldsymbol{P_{lb_t}}$	Upper and lower power bounds imposed by DSO in timeframe t
$\boldsymbol{P_{F}^{f}_{min}}$, $\boldsymbol{P_{F}^{f}_{max}}$	Max and min active power of flexibility bids f

Control Variables:

$\boldsymbol{P_{b_t}}$, $\boldsymbol{P_{s_t}}$	Power to buy and to sell in time interval t at aggregator level
$\boldsymbol{P_{F_t}^{f}}$	Power of flexibility f activated in time frame t
$\boldsymbol{x_F^f}$	Binary variable (1 if f is activated in time frame t, else 0)

Mathematical Formulation Description

The objective of this model is to compute a day-ahead cost-efficient resources planning to be submitted to retail market for selling/buying energy while respecting constrains imposed by the DSO. The model determines which flexibilities have to be activated in each timeframe *t* to guarantee the request from the DSO and respect the users' schedule. It was developed extending the mathematical model discussed in section IV.4.2.3.

The objective of this problem is to find the final aggregated profile minimizing costs to satisfy consumption and maximizing revenues for selling production.

Cost minimization and revenues maximization:

$$min \sum_{f \in F} C_t^f \cdot P_{F_t}^{\ f} \cdot \Delta t - C_{s_t} \cdot P_{s_t} \cdot \Delta t + C_{b_t} \cdot P_{b_t} \cdot \Delta t \quad \text{Eq. IV.22}$$

Power Balance:

$$\sum_{m \epsilon M} P_{b_t}^m - \sum_{m \epsilon M} P_{s_t}^m = -\sum_{gn \epsilon F} P_t^{gn} - \sum_{ln \epsilon F} P_t^{ln} + \sum_{gp \epsilon F} P_t^{gp} + \sum_{lp \epsilon F} P_t^{lp} - P_{s_t} \quad \text{Eq. IV.23}$$

Flexibilities upper and lower bounds

$$x_F^f \cdot P_{F_{min}}^{\ f} \leq P_{F_t}^{\ f} \leq x_F^f \cdot P_{F_{max}}^{\ f} \quad \text{Eq. IV.24}$$

DSO required bounds

$$P_{s_t} \leq P_{lb_t} \quad \text{Eq. IV.25}$$

$$P_{b_t} \leq P_{ub_t} \quad \text{Eq. IV.26}$$

Balance constraint in Eq. IV.23 allows to supply the flexible and inflexible loads by using electricity produced locally by DGs or bought from the main grid; it also allows to define the final exchange with the main grid. The constraint in Eq. IV.24 limits the minimal and maximal power of flexibility *f* in time step t, according to the users' desired or available limits. T constraints in Eq. IV.25 and Eq. IV.26 imposes the limits of exchanged power required by the DSO in time step *t*.

In case of WEM participation, the model could be extended adding market rules constraints described in Eq. IV.27 and Eq. IV.28. These constraints impose the minimal energy amounts and offer increments which can be traded in the spot market, following rules summarized in Tab. VII.1. In this model product block constraint is not introduced because the process is already based on hourly transactions.

Minimal Volume

$$b_S \cdot P^{spot-mv} \leq P_{s_t} \leq b_S \cdot M \quad \forall\, t \in \mathrm{T} \quad \text{with} \quad \mathrm{M} \gg P_{s_t} \quad \text{Eq. IV.27}$$

Minimal Increment

$$P_{s_t} = n_s \cdot P^{spot-incr} \quad \forall\, t \in \mathrm{T} \quad \text{Eq. IV.28}$$

IV.4.3.3. Case Studies

a) Hypothesis and Development Information

In this chapter, some illustrative example is proposed with the purpose of analysing the interactions between the different actors and to test the proposed CLA strategy. As in section IV.4.2.4, the MAS simulation framework was implemented trough Java and JADE libraries [67]. The Matlab-based free toolbox OPTI TOOLBOX version 2.16 [157] [135] is used to implement optimization problems. The interface between Java and Matlab is implemented using MatlabControl class [158]. In these case studies, the OPF is not implemented.

As explained in IV.4.3.1, the process is based on historical data gathered by the DSO; only the aggregator receives upper and lower limits for areas within its responsibility[17].

[17] Each aggregator could act on different areas in the overall network. In this case, it receives upper and lower limits for each area. Definition of area boundary depends on DSO network organization and are defined in the contract agreement between aggregators and DSOs.

Statistical analysis of the DSO's need for detecting critical situations and of the ting resources are out of the scope of this work. However, this limitation does not impact the validity of the study. A Network Analysis Toolbox is discussed in ADDRESS project and described in [163]. Two fundamental functionalities are added to the DMS through this toolbox: the contingencies calculation of critical situations in distribution networks at both MV and LV levels and determination of network areas which have a strong impact on critical situations in each zone.

In this section two case studies are proposed:

- Application on 74-bus MV grid with aggregator and flexibilities supplied by micro-sources, in which the proposed "Capacity Limit Allocation" strategy is tested by introducing upward and downward flexibilities bid by distributed generators. Three different simulations are proposed in order to compare the impact of grid limits and market rules on the aggregator strategy:
  - without grid limits and without market rules (REF)
  - with grid limits and without market rules (CLA)
  - with grid limits and with market rules (CLAM)
- Application on 74-bus MV grid with aggregator and flexibilities supplied by micro-sources and consumption, which aims to show the potentiality of demand response in active management of grids through "Capacity Limit Allocation" strategy. Results of two case studies are proposed:
  - without grid limits (REF)
  - with grid limits (CLA).

b) Application on 74-bus MV grid with aggregator and flexibilities supplied by micro-sources without and with market rules

Description and Input/Output Data

As mentioned before, in this analysis the CLA strategy is tested in order to understand all its advantages and disadvantages without taking into account market rules. Then, market rules are introduced to study their impact on microgrids and aggregator scheduling (hereafter called CLAM strategy). Results are compared with a reference case which does not implement

"Capacity limit allocation" strategy, while implement only the collaborative process to optimize the resource's usage between microgrids (hereafter called REF).

The EM algorithm for microgrid scheduling and the case study parameters are the same described in section IV.4.2.4 (b). Hence, the first optimization results before the negotiation process between microgrids and aggregator could be directly found in Fig. IV.12, Fig. IV.13, Fig. IV.14 and Fig. IV.15. As described in IV.4.3.1 the process takes place hour by hour. Then, upper and lower limits are sent for each zone hour by hour to each aggregator by the DSO. For the aggregator in the case studies, these asymmetrical limits are depicted in red in Fig. IV.34. For simplicity, only one zone is taken into account for the aggregator.

Simulation Results

Considering previous analysis, the congestions are forecasted in the same time frames than in power flow run in section IV.4.2.4 (i.e. h=12 and h=14 between 11.00-12.00 a.m. and 1.00-2.00 p.m., respectively).

Since Microgrid 1 and 4 are passive, their profiles are not taken into account in this profile adjustment process. Otherwise, aggregator can play on Microgrid 2 and 3 flexibilities as in FSM strategy presented in IV.4.2.4. Flexibilities used are plotted in Fig. IV.24 and Fig. IV.25 for CLA strategy. The light green area is the final energy exchange at the PCC obtained after the hourly trading process with the AGGA. Furthermore, orange and blue areas are respectively the negative and positive flexibilities accepted by the aggregator. In these figures, the final energy profile is also compared with the energy profile computed by the MMCA before the sliding optimization with the AGGA (red line). In Fig. IV.28, the re-scheduled usage of the ESS connected to Microgrid 2 after the two re-optimizations for CLA case study is illustrated.

As we can see, negative flexibilities of Microgrid 2 are used also in this case study to solve congestion situations (orange areas) and additional production of bio-diesels in Microgrid 3 is used to satisfy a part of Microgrid 1 and 3 consumption in PV off-peak time frames, precisely in h=3 p.m. …7 p.m. and 6 p.m. …20 p.m. (blue areas in Fig. IV.25).

Main results for all three cases under analysis are resumed in Tab. IV.9. The expected income from the sale of $P_{sch}(t)$ for Microgrid 2, computed with the first optimization, and obtained

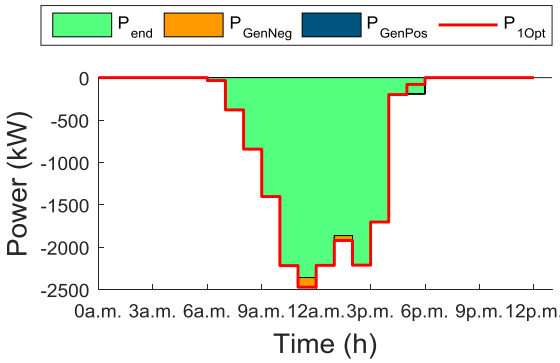

Fig. IV.24 Zoom on accepted flexibilities by aggregator for Microgrid 2 and comparison with initial scheduled exchange for CLA

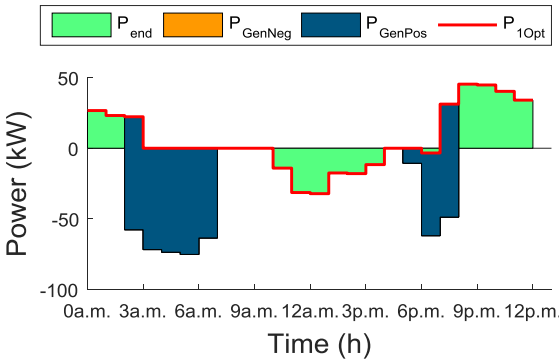

Fig. IV.25 Zoom on accepted flexibilities by aggregator for Microgrid 3 and comparison with initial scheduled exchange for CLA

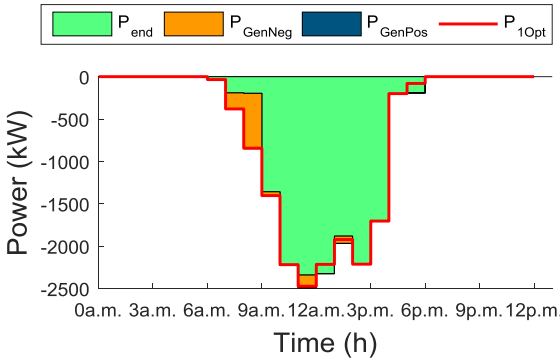

Fig. IV.26 Zoom on accepted flexibilities by aggregator for Microgrid 2 and comparison with initial scheduled exchange for CLAM

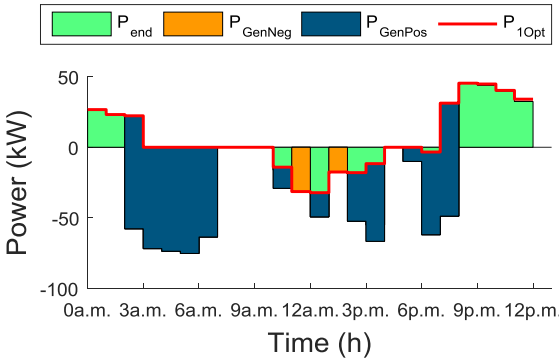

Fig. IV.27 Zoom on accepted flexibilities by aggregator for Microgrid 3 and comparison with initial scheduled exchange for CLAM

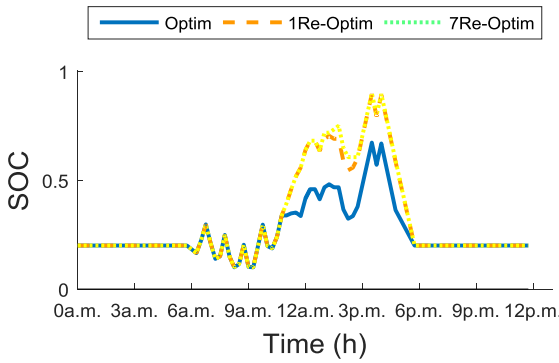

Fig. IV.28 SOC of ESS in Microgrid 2 for CLA

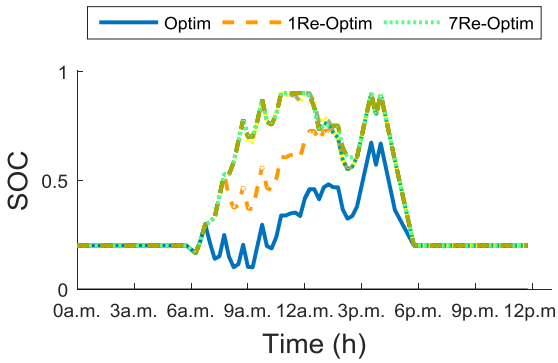

Fig. IV.29 SOC of ESS in Microgrid 2 for CLAM

when selling the entire available energy to the electricity market is 2.241.2 €. However by implementing the collaborative process, the income without imposing any grid strategy is reduced to 2162.7 €, because of the share of a part of the available energy in Microgrid 2 with other microgrids.

When the limits imposed by the DSO are applied, the total expected income is slightly in

	μG1	μG2	μG3	μG4	μG1	μG2	μG3	μG4	μG1	μG2	μG3	μG4
MF (€)*	*180.9*	*-2162.7*	*-73.2*	*373.3*	*177.5*	*-2167.0*	*-64.5*	*365.7*	*178.8*	*-2096.3*	*-95.4*	*369.3*
DC (€)*	*213.6*	*-577.3*	*163.7*	*379.6*	*210.2*	*-585.2*	*163.8*	*372.1*	*211.5*	*-595.0*	*163.8*	*375.7*
Load (kWh)*	*1380.4*	*-*	*1033.8*	*2668.3*	*1380.4*	*-*	*1033.8*	*2668.3*	*1380.4*	*-*	*1033.8*	*2668.3*
CB (c€/kWh)*	*15.4*	*-*	*16.0*	*14.0*	*15.1*	*-*	*16.0*	*13.8*	*15.2*	*-*	*16.0*	*13.9*
CS (c€/kWh)*	*14.0*	*13.7*	*16.4*	*-*	*14.0*	*13.6*	*16.3*	*-*	*14.0*	*13.8*	*16.6*	*-*
DG_{acc} (%)	*100*	*98.3*	*43.6*	*-*	*100*	*98.0*	*42.3*	*-*	*100*	*93.0*	*47.1*	*-*
PV_{acc} (%)	*100*	*98.3*	*95.1*	*-*	*100*	*98.0*	*95.1*	*-*	*100*	*93.0*	*92.8*	*-*
DS_{acc} (%)	*-*	*-*	*33.0*	*-*	*-*	*-*	*31.3*	*-*	*-*	*-*	*37.7*	*-*
	(a) REF				*(b) CLA*				*(c) CLAM*			

**Legend*: *MF*: Daily money flow between each µgrid and DSO+AGG (expenses and revenues); * *DC*: Daily expense or revenue of each µgrid considering DG and ESS costs; * *Load*: Daily consumption of each µgrid;* *CB:* Daily average kWh cost payed by µgrid's consumers;* *CS:* Daily average kWh cost gained by µgrid's producers; DG_{acc}: Percentage of used energy on available/forecasted DG energy; PV_{acc}: Percentage of used energy on forecasted PV energy; DS_{acc}: Percentage of used energy on available DS energy.

Tab. IV.9 Comparison between expenses and revenues of microgrids, kWh_{cost} and used DG in nCLA CLAM strategies

113.3 kW in h=12 and 57.6 kW in h=14 is around 17 €, while the expected income for selling the rescheduled energy $P_{new\_sch}(t)$ is 2150.0 € is. Also in this case, part, but not all, of this energy is stored in the battery as shown in Fig. IV.28, because of the small size in power and energy of the ESS. Hence, the service's remuneration is a source of revenues, which allows to compensate for both the loss due to the lack of energy sales in the desired timeframes and the loss for storing part of this energy in the ESS, while slightly increasing the revenues. Moreover, the energy stored in the ESS is sold in late afternoon hours (5.00 p.m. - 6.00 p.m.). In REF case study, the electricity is produce by the bio-diesel generator in this timeframe. Hence, the increase of the injected energy by Microgrid 2 induces a reduction of 1.3 percentage points of DS_{acc} in CLA respect to REF, which in turn induces the reduction of MF and DC in Microgrid 1 and 3 (see comparison in Tab. IV.9).

The introduction of market constraints makes an efficient scheduling of resources more important and requires an accurate sizing and contract stage for the aggregator. The flexibilities used are plotted in Fig. IV.26 and Fig. IV.27 for the CLAM strategy with the same colour legend applied in figures in CLA case study. As already explained, these strategies are based on complete freedom for microgrids in the decision-making process and collaborative process based on proposed flexibilities. However, this may induce inefficiency from the energetic and economic point of view such as in h=11 for Microgrid 3 (see orange and blue areas in Fig. IV.27). In fact, in this case positive and negative flexibilities are accepted in the same time. In this case, this is caused by the lower bound on the output power of the bio-diesel generator.

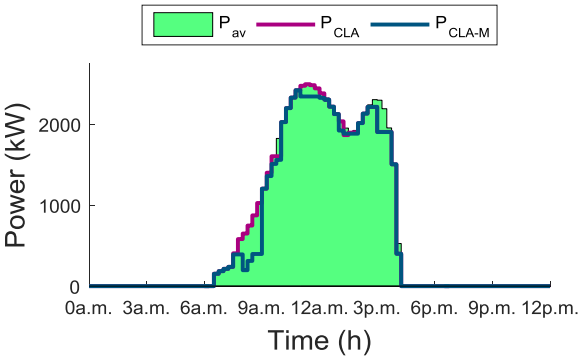

Fig. IV.30 Comparison between forecasted/available power profile, final power profile for CLA strategy and CLAM for Microgrid 2

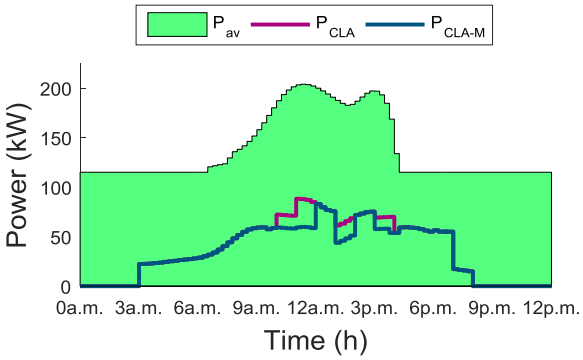

Fig. IV.31 Comparison between forecasted/available power profile, final power profile for CLA strategy and CLAM for Microgrid 3

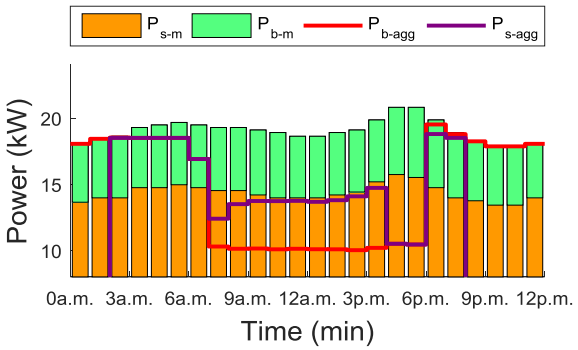

Fig. IV.32 Forecasted Electricity Prices and Local Aggregator Buying Price for CLA strategy

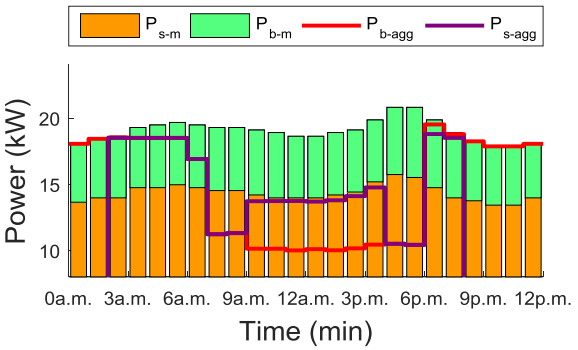

Fig. IV.33 Forecasted Electricity Prices and Local Aggregator Buying Price for CLAM strategy

Moreover in this strategy, unlike CLA, users may not be completely free in their decision-making process. In fact, the user cannot choose the prices for the flexibilities offered with complete freedom. This condition is fundamental to guarantee to the aggregator a degree of freedom on some flexibility to pack and optimize the use of its affiliated microgrids generating the appropriate aggregated proposal to be traded on the market platform.

For this purpose, the aggregator can contract with each microgrid the amount of free flexibilities that it has to guarantee to the aggregator based on microgrid characteristics and aggregator set of users. In this case study, the expected income for Microgrid 2 is 2096.3 € of which 30.0 € are the congestion income. There is then a reduction in the total income. This is essentially produced by the minimal bidding amount and offer increments rules. In fact, these market constraints impose a reduction of 5% of the PV production used.

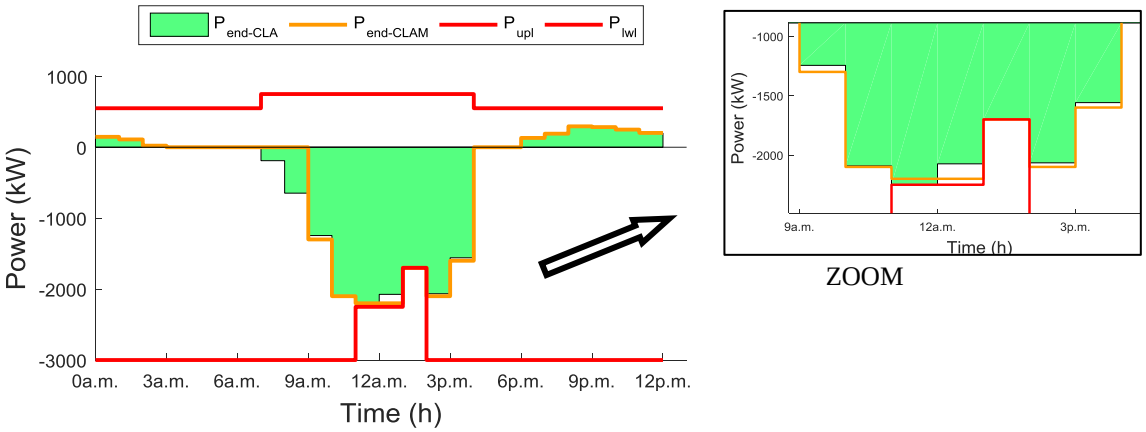

Fig. IV.34 Final D-1 Aggregator Scheduling with DSO Upper and Lower Limits for CLA and CLAM strategies

Conversely, the congestion income is subject to an increase. This increase is the consequence of the stepwise bidding pattern in the WEM, which requires to introduce a stepwise of 0.1 MW also for flexibilities. The flexibilities are 200 kW and 100 kW for h=12 and h=14, respectively.

In general, market constraints induce a less efficient use of solar energy which is particularly evident in early morning hours for Microgrid 2 (7.00 a.m. - 9.00 a.m. in Fig. IV.26) and in late morning hours for Microgrid 3 (11.00 a.m. - 12.00 a.m. and 1.00 p.m. - 2.00 p.m. in Fig. IV.27).

Aggregator final power profiles of both strategies are compared in Fig. IV.34. Moreover, DSO upper and lower limits (drawn in red) are respected in both cases.

Furthermore, it is important to consider that the use of solar energy depends on the size of the PV power. Hence, in the next sub-section a sensitivity analysis is made based on the maximal daily power of the PV system in Microgrid 2 while increasing its rated power.

Sensitivity analysis regarding PV maximum power and ESS installed capacity

The nominal power of PV systems composing the generation mix in the aggregator is one of the most influential parameter on CLAM model. Hence, in this section a sensitivity analysis on fundamental parameters characterizing Microgrid 2 is used for the management model validation. It can also guide the aggregator sizing in future research works. The method used to carry out this sensitivity analysis is a simple method commonly used in the literature. It consists of repeatedly varying the parameter under analysis while leaving the other parameters fixed, as done in section III.4.4 for microgrid optimization model. For the CLAM strategy, the sensitivity ranking was obtained by increasing the maximal PV power output

during the day in analysis (PPV_{max}) and the nominal power of the ESS ($PESS_n$) at a time, quantifying:

- the change in the percentage ratio between the power used and the available/forecasted power in each microgrid (denoted with P_{exp}),
- the daily average electricity cost in each microgrid (denoted with $CkWh_m$).

In simulations, the maximal PV power output was increased by 100 kW steps between 1.000 kW and 2.500 kW. The influence of this parameter on the two evaluated outputs are shown in Fig. IV.35 and Fig. IV.36, respectively. As it can be seen, the P_{exp} in Microgrid 1 is not affected due its passive nature and the power production in Microgrid 3 is only lightly influenced with a maximal variation of 5.3%. The maximal value for Microgrid 3 is 45.3 % and is obtained for a PPV_{max} equal to 1200 kW. Otherwise, PPV_{max} strongly influences the amount of energy injected by Microgrid 2 due to the low power consumption/power production ratio and the constrains imposed by the market rules. Actually, in this case there is a large variation between the maximal and minimal percentage of power production equals to 54.6%. The maximal value for Microgrid 2 is 97.4 % and is obtained for a PPV_{max} equal to 1.800 kW. As Fig. IV.35 shows, starting from this value of PPV_{max} this percentage (blue curve) is reduced with a maximal deviation from the initial value of 4.2 percentage points. Fig. IV.36 highlights that the influence of PPV_{max} on $CkWh_m$ for Microgrids 1, 3 and 4 is almost negligible with a maximal variation of 0.2 c€/kWh and 0.3 c€/kWh for Microgrid 1 and 3 respectively with minimal value for PPV_{max} equals to 1.800 kW.

The hourly accepted PV power in Microgrid 2 as function of PPV_{max} is illustrated in Fig. IV.37. The different bars represent results for each hour and for each PPV_{max} varing from lower values in blue to higher values in yellow. The impact on accepted power is almost negligible between 7.00 a.m. and 9.00 a.m., due to the fact that this amount of energy is shared among microgrids because it is lower or slightly higher than consumption of Microgrids 1 and 4. Otherwise, there is a strong impact between 9.00 a.m. and 11.00 a.m. due to the fact that the amount of energy is not enough to be sold in the electricity market and in this case study a demand response program is not activated. Between 11.00 a.m. and 1.00 p.m., the hourly power production is almost totally accepted, except for the case of 1 MW and 1.1 MW of peak production.

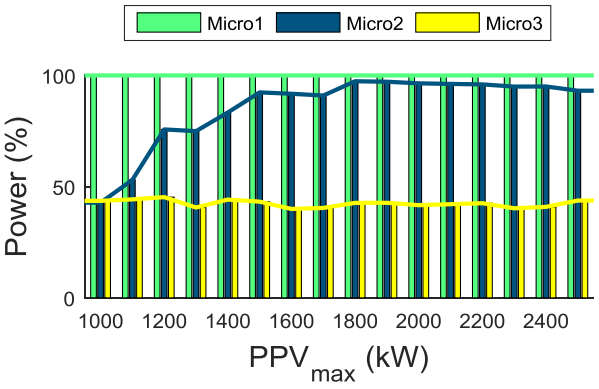

Fig. IV.35 Influence of PPV_{max} power in Microgrid 2 on power production in each microgrid

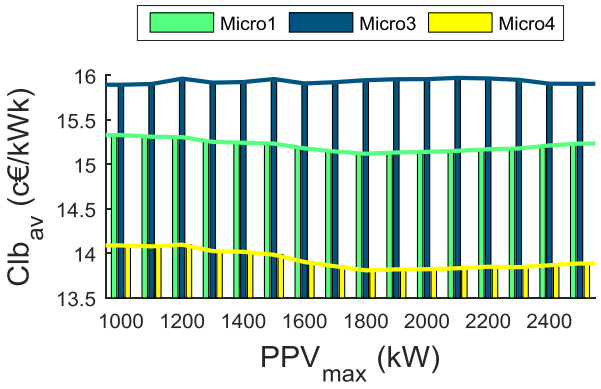

Fig. IV.36 Influence of PPV_{max} power in Microgrid 2 on the daily average kWh cost in each microgrid

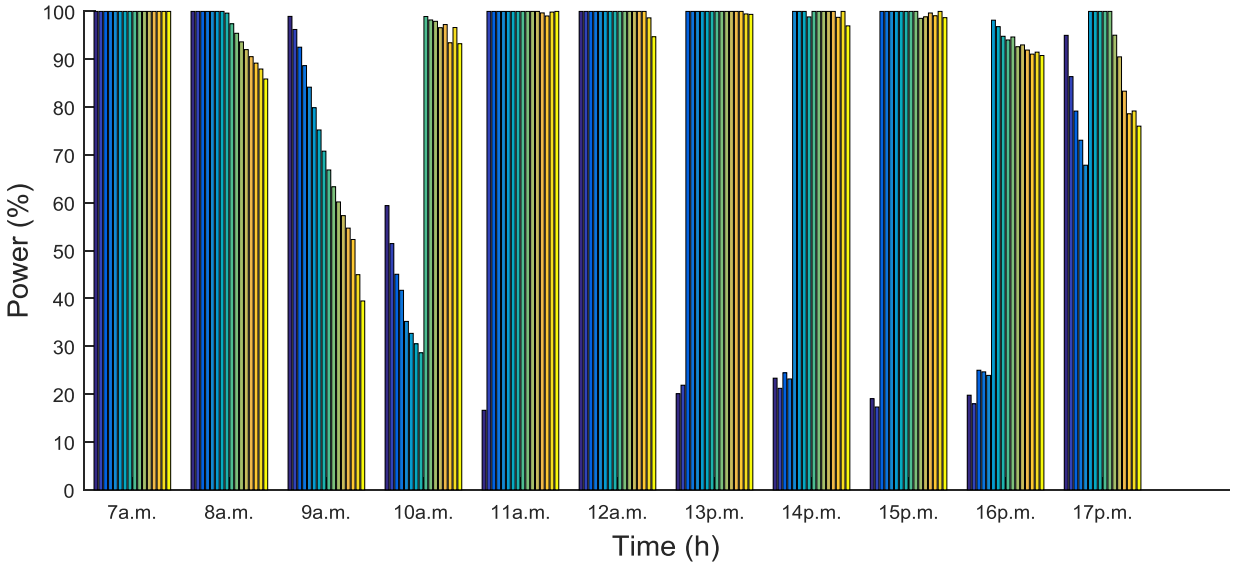

Fig. IV.37 Influence of PPV_{max} in the hourly power accepted for Microgrid 2

The second sensitivity analysis is obtained by varying the nominal power of the ESS by 100 kW steps between 200 kW and 900 kW. In each simulation, also the rated capacity is varied with a fixed capacity/power ratio of 2.5, which corresponds to a variation in energy capacity between 500 kWh and 2.250 kWh. The results of this analysis are presented in Fig. IV.38 and Fig. IV.39, respectively. The graphics show that the increase of the ESS size is needed in distributed strategies with high autonomy of microgrids in the decision-making process. In fact, Fig. IV.38 highlights that even a small increase in the $PESS_n$ induces an increase of the exploited PV production in Microgrid 2 slightly affecting Microgrid 3. This trend is typically due to the nature of the developed multi-level decision making process. The value of P_{exp} has a maximal variation of 6.9 % and 9.4 % for Microgrid 3 and 2, respectively.

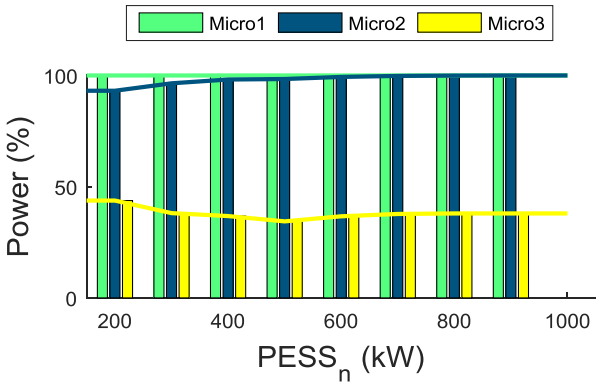

Fig. IV.38 Influence of PESSn power in Microgrid 2 on power production in each microgrid

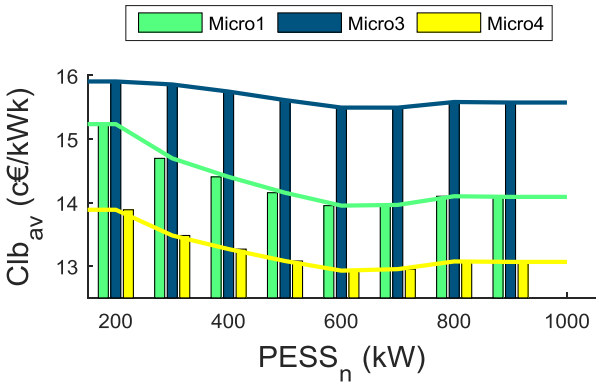

Fig. IV.39 Influence of PESSn power in Microgrid 2 on the daily average kWh cost in each microgrid

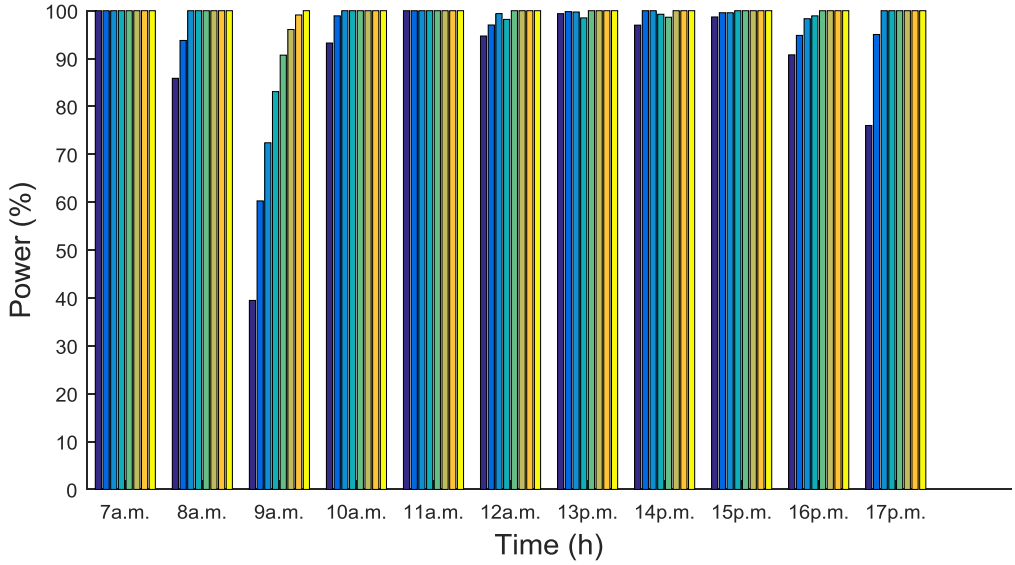

Fig. IV.40 Influence of PESSn in the hourly power accepted for Microgrid 2

The increase in size of the ESS has a modest but beneficial effect on CkWh values with a minimum peak for PESS$_n$ between 600 and 700 kWh. The maximal variation is 1.3 c€/kWh, 0.4 c€/kWh and 1 c€/kWh for Microgrid 1, 3 and 4. This trend is due to the fact that the increase in size of the ESS allows to stock energy during early morning off-peak time frames (8.00a.m.-10.00a.m.) and using it to satisfy aggregator consumption during early evening and night hours when electricity is more expensive (6.00p.m.-8.00p.m. and 11.00p.m.-12.00 p.m.) reducing both the imported electricity from the main grid and the electricity produced using the bio-diesel generator.

Fig. IV.40 shows the hourly accepted PV power in Microgrid 2 as function of PESS$_n$ using blue nuances for lower values and yellow nuances for higher values of PESS$_n$. Also in

this case, the results underline the positive impact of $PESS_n$ when the amount of available energy is not enough to be sold in the electricity market but too high to be consumed by other Microgrids (see time frames 8.00 a.m.-10.00 a.m.).

c) Application on 74-bus MV grid with aggregator and flexibilities supplied by micro-sources and consumption

Description and Input/Output Data

Also in this case study, the CLA methodology is tested using four microgrids installed through a MV/BT transformer. These microgrids consist on communities of users composed of small-sized residential and commercial activities with inflexible loads, flexible loads, DERs and ESSs.

The amount of users, the type of installed DGs and ESSs, and their nominal data are resumed in Tab. IV.10-Tab. IV.13. DSO upper and lower limits for the aggregator representing the four microgrids are taken as in red lines in Fig. IV.50. In this case study, market rules are not taken into account due to the small-sized of the aggregator.

The simulation was implemented using an agent for each user, a MMCA for each microgrid, an AGGA and a DSOA. The dynamic selling and buying prices are considered as in the previous case study (Fig. IV.17). Also in this case, 15 min is the time-window used for the microgrids optimization and data represent a critical situation which might occur in a summer or spring day. The energy schedule is constructed based on individual forecast signals that are sent from SA to the MMCA. The aggregator is considered non-profit entity.

DGs are used for providing downward flexibilities, which consist on generation reduction in the microgrid. The bid price is fixed equal to the DG selling price. In addition this time, demand response flexibilities are also taken into account in order to show the role of demand response in active management of grids. In particular, time-shiftable appliances, such as washing-machines and dish washers, are used for upward flexibility using Type A bid, described in section III.4.2.2.

The couple quantity-price for time step t is obtained aggregating all the appliances with $t_{start\text{-}optim}$ greater than t in one or more groups, creating one or more unique profile, using also the ESS. The price is computed according to the surplus cost faced by users for starting the appliance at time t instead of $t_{start\text{-}optim}$. In this case study, upward flexibilities are not taken into account.

Microgrid 1			
Inflexible Load			
	n.		***P_c***
	30		*6 kW*
	15		*3 kW*
Distributed Generation			
n.	***Technology***	***P_n***	***LCOE***
4	*PV*	*9 kW*	*13 c€/kWh*
Energy Storage Systems			
n.	***Technology***	***P_n***	***E_n***
	Li-ion Battery	*50 kW*	*100 kWh*
	η_{ch}	***η_{dec}***	***SOC_{start}***
1	*0,96*	*0,97*	*0,2*
	SOC_{final}	***SOC_{max}***	***SOC_{min}***
	0,2	*0,8*	*0,2*

Tab. IV.10 Type and Nominal Data of Components in Microgrid 1

Microgrid 2			
Inflexible Load			
	n.		***P_c***
	-		-
Distributed Generation			
n.	***Technology***	***P_n***	***LCOE***
2	*PV*	*300 kW*	*11 c€/kWh*
Energy Storage Systems			
n.	***Technology***	***P_n***	***E_n***
	Li-ion Battery	*100 kW*	*200 kWh*
	η_{ch}	***η_{dec}***	***SOC_{start}***
1	*0,98*	*0,98*	*0,2*
	SOC_{final}	***SOC_{max}***	***SOC_{min}***
	0,2	*0,9*	*0,1*

Tab. IV.11 Type and Nominal Data of Components in Microgrid 2

Microgrid 3			
Inflexible Load			
	n.		***P_c***
	30		*6 kW*
	5		*9 kW*
Distributed Generation			
n.	***Technology***	***P_n***	***LCOE***
4	*PV*	*15 kW*	*13 c€/kWh*
1	*PV*	*25 kW*	*12 c€/kWh*
Energy Storage Systems			
n.	***Technology***	***P_n***	***E_n***
	Li-ion Battery	*100 kW*	*200 kWh*
	η_{ch}	***η_{dec}***	***SOC_{start}***
1	*0,97*	*0,98*	*0,5*
	SOC_{final}	***SOC_{max}***	***SOC_{min}***
	0,4	*0,9*	*0,5*

Tab. IV.12 *Type and Nominal Data of Components in Microgrid* 3

Microgrid 4			
Inflexible Load			
	n.		***P_c***
	35		*6kW*
Demand Response			
n.	***Technology***	***P_n***	***LCOE***
1	*PV*	*25 kW*	*12 c€/kWh*
Demand Response			
n.	***Technology***	***P_n***	***Usage-time***
7	*Washing Machine*	*3 kW*	*6.00 a.m.-23.00 p.m*
5	*Dish Washer*	*3 kW*	*5.00 a.m.-1.00 p.m.*
Energy Storage Systems			
n.	***Technology***	***P_n***	***E_n***
	Li-ion Battery	*100 kW*	*250 kWh*
	η_{ch}	***η_{dec}***	***SOC_{start}***
1	*0,97*	*0,98*	*0,5*
	SOC_{final}	***SOC_{max}***	***SOC_{min}***
	0,5	*0,8*	*0,2*

Tab. IV.13 *Type and Nominal Data of Components in Microgrid 4*

Simulation Results

Microgrid 1 and 4 are passive from the DSO point of view. Their D-1 schedule at the PCC obtained with the first optimization is shown in yellow in Fig. IV.41 and Fig. IV.42. In the figures, the filled areas represent the forecasted production of various DGs, while the orange curve is the used generation. Microgrid 4 has twelve time-shiftable appliances described in Tab. IV.13. The initial operation of these appliances is scheduled as in green in Fig. IV.46, where the most economical use of dishwashers is scheduled before 12.00 a.m. due to the

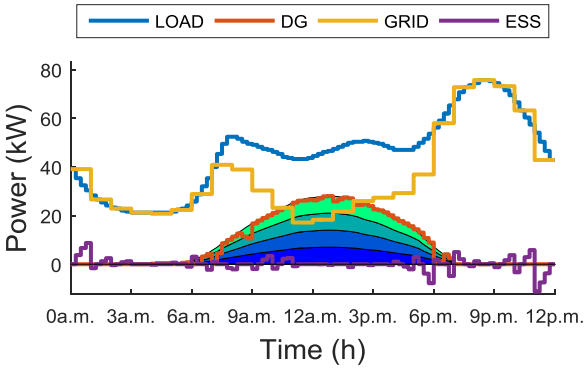

Fig. IV.41 Aggregated energy schedule of Microgrid1

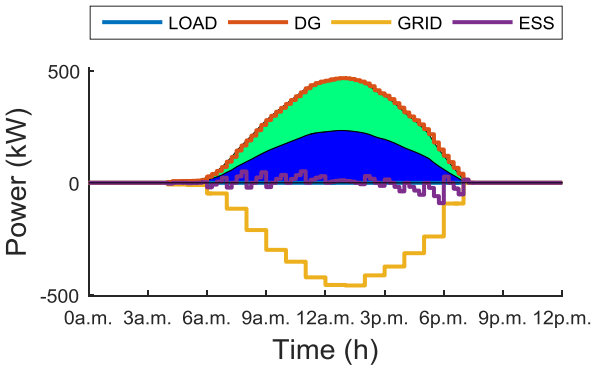

Fig. IV.42 Aggregated energy schedule of Microgrid2

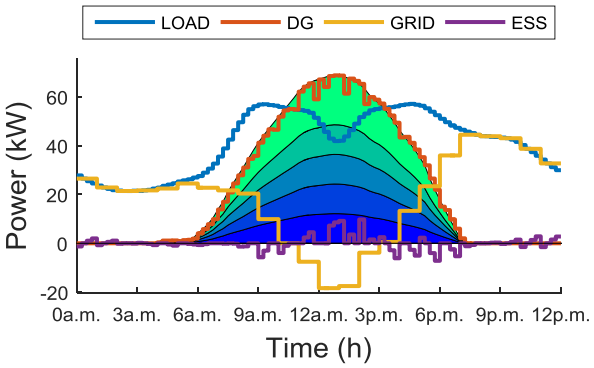

Fig. IV.43 Aggregated energy schedule of Microgrid3

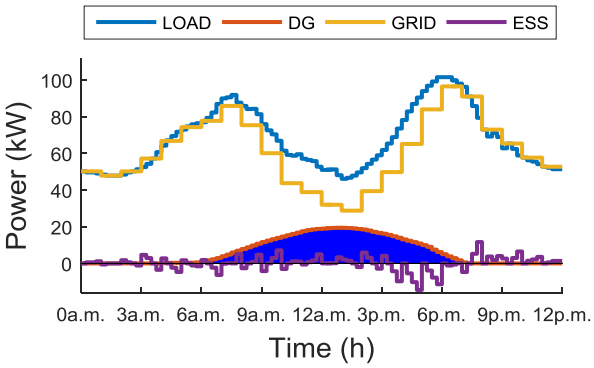

Fig. IV.44 Aggregated energy schedule of Microgrid4

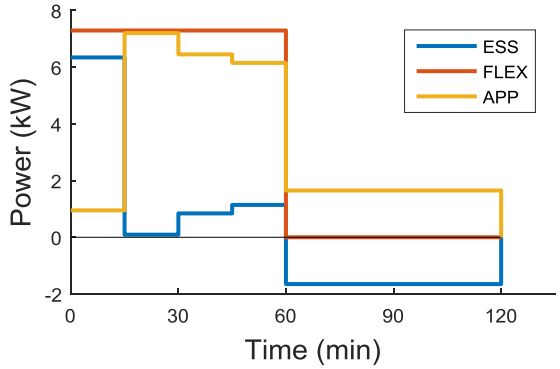

Fig. IV.45 Load flexibility computed in *t*=13 by Microgrid 4

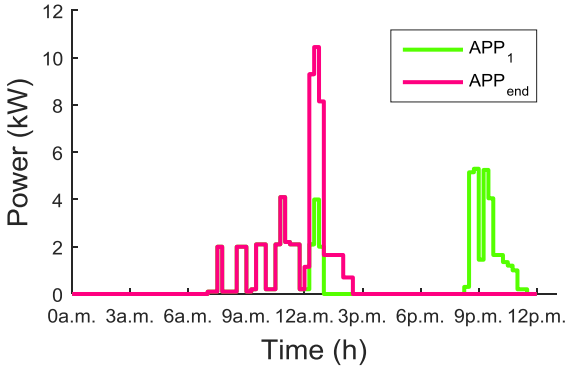

Fig. IV.46 Comparison between initial and final schedule for flexible appliances in Microgrid 4

usage-time imposed, while washing machines are scheduled around 12.00 a.m. and in late evening hours.

The flexible usage-time of these appliances scheduled for late evening hours can be seen as a source of flexibility in the microgrid. Hence, they can be combined with an ESS in order to compute a coherent hourly bid. In each timeframe between 5.00 a.m. and 13.00 a.m., different bid proposals are computed according to the available appliances. An example of load flexibility is depicted in Fig. IV.45. The combination of appliances and the storage system profiles are represented in yellow and blue respectively. In orange, the aggregated

flexibility consists of an on/off bid of 7.3 kW with price of 5.0 c€/kWh for timeframe 13. Naturally, if a load flexibility is accepted, the load profile has to be modified in the following time intervals according to the appliances operating cycle.

On the contrary, Microgrid 2 is completely active and Microgrid 3 plans to inject energy in the main grid between 11.00 a.m. and 3.00 p.m.. As shown in case I, the aggregator can play with the injected energy by Microgrid 2 and 3 by using the downward flexibilities proposed by users, which coincide with the proposed selling energy.

The aggregation of microgrids exceed DSO lower limit in timeframes 13 and 14. The used flexibilities to respect the imposed bounds are plotted in Fig. IV.47 and Fig. IV.48, where the light-green area is the final energy exchange at the PCC obtained after the hourly trading process with the AGGA. Whereas, orange and dark-green areas represent the negative flexibilities supplied respectively by generation and consumption and accepted by the aggregator. The final energy profile in black can be compared with the profile computed by each MMCA before the sliding optimization drawn in red.

Demand-response and generation are both used as flexibilities in timeframe 13, while only generation is available for timeframe 14. The reduction of the injected energy by Microgrid 2 corresponds to the 3.6 % and 5.1 % of the initial schedule (that are 16.4 kW and 23.4 kW), in timeframe 13 and 14, respectively. This energy is stored in the ESS and sold in part (due to the losses) between 3.00 p.m. and 5.00 p.m., as shown in Fig. IV.47 and Fig. IV.49. The appliances scheduled between 8.30 p.m. and 11.00 p.m. in Microgrid 4 are started at 12.00 a.m. as depicted in pink line in Fig. IV.46. The comparison of the initial and final scheduled profile of the aggregator is shown in blue and orange areas in Fig. IV.50.

Tab. IV.14 resumes the expenses or revenues, the average buying and selling kWh, and the used DG for each microgrid. The daily expense or revenue and the daily money flow between each µgrid and the aggregator are compared with the case without aggregator limits, in which the initial schedule proposed by each microgrid is accepted. The MF of Microgrid 2 is 505.0 € of which 4.0 € are the DSO's remuneration for the flexibility. The microgrid's revenue MF was increased of around 3.1 percentage points with respect to the value obtained without DSO limits. For microgrid 4, the costs remains almost equal with a slight decrease thanks to the DSO's compensation. Furthermore, Microgrid 1, 3 and 4 daily expense would be 25.2 %, 29.6 %, 33.1 % higher if the electricity would be entirely bought from the main grid.

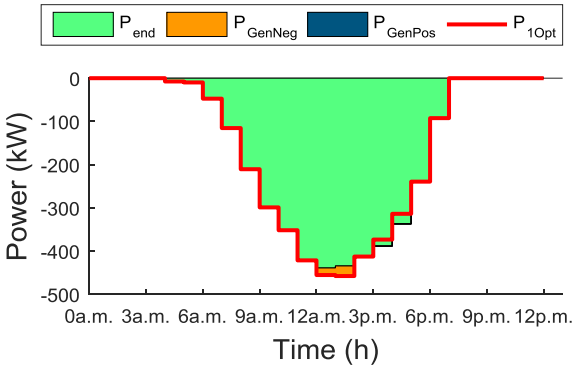

Fig. IV.47 Zoom on accepted flexibilities by aggregator for Microgrid 2 and comparison with initial scheduled exchange for CLA strategy

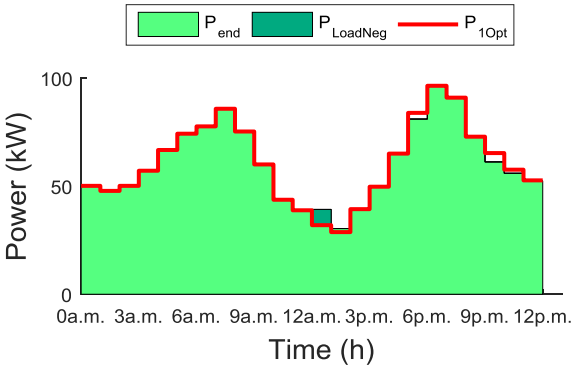

Fig. IV.48 Zoom on accepted flexibilities by aggregator for Microgrid 4 and comparison with initial scheduled exchange for CLA strategy

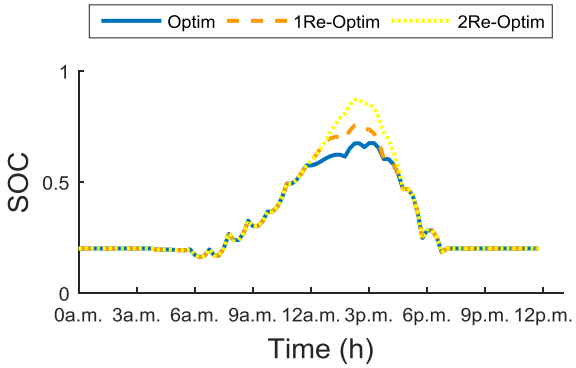

Fig. IV.49 SOC of ESS in Microgrid 2 for CLA strategy

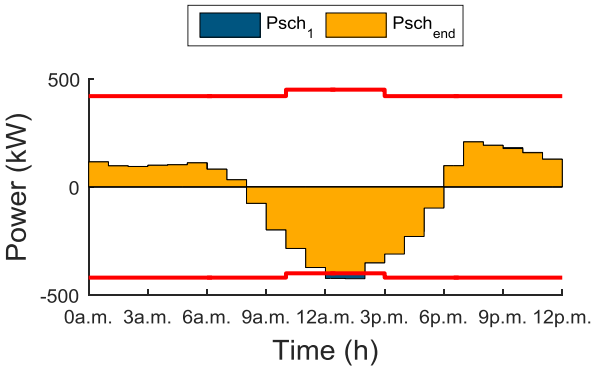

Fig. IV.50 Final D-1 Aggregator Scheduling with DSO Upper and Lower Limits for CLA

	µG1	***µG2***	***µG3***	***µG4***
MF (€)*	*133.7*	*-505.0*	*74.9*	*215.9*
DC (€)*	165.8	-120.2	146.5	235.6
Load (kWh)*	*1093.2*	-	*992.6*	*1620.4*
CB (c€/kWh)*	*15.1*	-	*14.7*	*14.6*
CS (c€/kWh)*	*14.0*	*13,1*	*12.8*	*12.0*
PV$_{acc}$ (%)	*95.1*	*100.0*	*98.0*	*100.0*
MFnolim (€)*	133.7	-500.8	74.9	216.7
DCnolim (€)*	165.8	-116.6	146.5	236.3
***DCref ** **	*207.6*	-	*189.8*	*313.7*

***Legend** *MF* : Daily money flow between each µgrid and DSO+AGG (expenses and revenues); * *DC* : Daily expense or revenue of each µgrid considering DG and ESS costs; * *Load* : Daily consumption of each µgrid;* *CB:* Daily average kWh cost payed by µgrid's consumers;* *CS:* Daily average kWh cost gained by µgrid's producers; *PV$_{acc}$* : Percentage of used energy on forecasted PV; *MFnolim :* MF obtained without DSO limits; *DCnolim : DC* obtained without DSO limits; *DCref* : Daily users' expense for buying all electricity needed by the DSOA.

Tab. IV.14 Expenses and revenues, kWhcost and used DG for each microgrid

IV.4.3.4. Conclusions

"Capacity Limit Allocation" strategy may be an interesting alternative to network reinforcement and needs to be evaluated as for the FSM strategy *ex ante* by the DSO. In general, this strategy requires a relatively simple mechanism compared to the "Flexible

Service Market" strategy. It needs nonetheless an important and delicate planning stage to define all agreements in bilateral contracts with aggregators or directly with microgrids. Whereas, a simpler day-ahead and intra-day scheduling phases have to be implemented. The communication exchanges and the amount of information to share are drastically reduced. Only a single way communication to inform aggregators or microgrids about hourly upper and lower limits have to be implemented between the DSOA and the AGGA/MMCA.

Moreover due to its simplicity, this strategy is also conceivable for small-sized microgrids and aggregators. However, the use of overestimates limits is needed in order to include all forecast error of such a small-sized aggregated systems. Hence probably, a less efficient use of connected systems can be induced due to the lower information gathered by the DSO.

At the end, the use of demand-response will have a key role for the active management of distribution grids and a more efficient use of the installed distributed generation.

IV.5. Centralized

The distributed management strategies described in sections IV.4.2 and IV.4.3, which use the sliding multi-level optimization-based process developed in this thesis, are compared with a centralized optimization-based process. The construction of a centralized model is discussed in-depth by several authors in the literature [164] [165] [166]. In a centralized optimization, all decisions concerning active and passive resources in microgrids are made in one central unit, the aggregator. The centralized process is implemented with a single *D-1* optimization stage. This means that all constraints are directly integrated in the first optimization. The architecture and the interactions among agents are shown in Fig. IV.51. The AGGA collects all the relevant information from each SA to determine the operation points which guarantee the global optimal.

The difference in performance, complexity and amount of information exchanged are tested using the case studies described in section IV.4.2.4 (b). Tab. IV.15 resumes the results obtained by simulations for three cases: no strategies applied, capacity limit allocation strategy and capacity limit allocation and market rules. In this context, the microgrid loses its main goal and nature due to the centralized management.

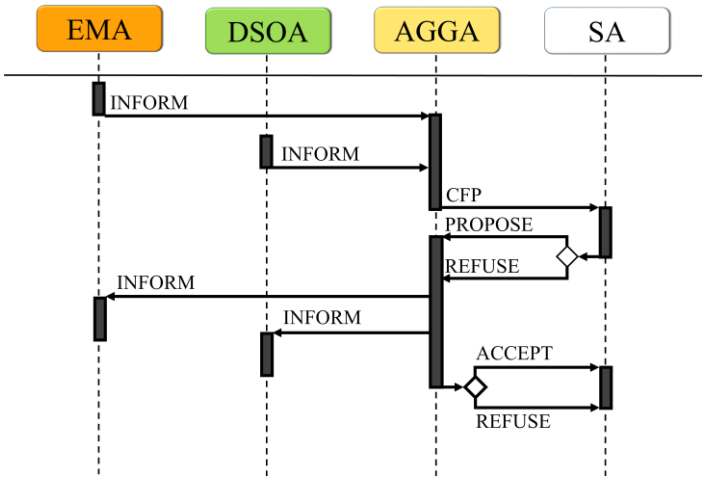

Fig. IV.51 Day-ahead trading interactions for aggregator centralized process

However, it is useful to compare the results of the centralized approach with the results obtained with the distributed approach in previous sections. The FSM strategy is not compared with the respectively centralized one, because it is not feasible in real applications. In fact, the role of the DSO is to assure a secure and high quality supply, which doesn't comprise the role of energy manager of users. Users have to be able to decide how and when to use their flexible resources to reduce their costs. Moreover, such a system would become prohibitively complex if implemented on a national scale.

The parameters used to compare and capture the main differences between the proposed approach and this classical approach are the percentage of:

- The daily money flow (MF) between each microgrid and the aggregator, defined as $100 \cdot (\mathrm{MF}_{SMLA} - \mathrm{MF}_{CA})/\mathrm{MF}_{CA}$;
- Daily average kWh cost ($CB_{\mu G}$) payed by microgrid's consumers, defined as $100 \cdot (CB_{\mu G_{SMLA}} - CB_{\mu G_{CA}})/CB_{\mu G_{CA}}$;
- Percentage of used energy on available/forecasted DG categorized for sources, defined as $100 \cdot (DG_{acc_{SMLA}} - DG_{acc_{CA}})/DG_{acc_{CA}}$;
- Data collection from the aggregator.

The values of these parameters are collected for the discussed strategy in Tab. IV.16. The main advantage of using the optimization-based centralized approach is that a globally optimal solution is guaranteed to be found. However, the global solution is contradictory with the way of microgrids to interact in line with their own self-interest, described in previous sections. This solution is efficient for more competitive users, such as microgrid 2, but not for small-sized users. In fact, the production of Microgrid 1 is subject to a great decrease. This is

	µG1	*µG3*	*µG4*	*µG2*	*µG1*	*µG3*	*µG4*	*µG2*	*µG1*	*µG3*	*µG4*	*µG2*
MF (€)*	*181.4*	*-91.9*	*368.5*	*-2184.1*	*183*	*-92.2*	*367.2*	*-2199.5*	*180*	*-86.1*	*366.8*	*-2146.5*
CB$_{agg}$ (c€/kWh)*		*13.8*		*-*		*13.8*		*-*		*13.8*		*-*
CB$_{µG}$ (c€/kWh)*	*14.3*	*13.6*	*13.7*	*-*	*14.3*	*13.6*	*13.7*	*-*	*14.2*	*13.6*	*13.7*	*-*
DG$_{acc}$ (%)	*37.1*	*40.9*	*-*	*100.0*	*26.5*	*41.2*	*-*	*100.0*	*31.9*	*37.7*	*-*	*98.0*
PV$_{acc}$ (%)	*37.1*	*90.0*	*-*	*100.0*	*26.5*	*91.4*	*-*	*100.0*	*31.9*	*64.1*	*-*	*98.0*
DS$_{acc}$ (%)	*-*	*30.9*	*-*	*-*	*-*	*30.8*	*-*	*-*	*-*	*32.2*	*-*	*-*
	(a) No Strategy				*(b) CLA*[18]				*(c) CLAM*			

Legend: *MF :* Daily money flow between each µgrid and DSO+AGG (expenses and revenues); *CBagg:* Daily average kWh cost in the aggregator; *CBµG:* Daily average kWh cost payed by µgrid's consumers; DG*acc* : Percentage of used energy on available/forecasted DG; *PVacc* : Percentage of used energy on forecasted PV; DS*acc* : Percentage of used energy on available DS

Tab. IV.15 Comparison between kWh_{cost} and used DG in different centralized strategies

	µG1	*µG2*	*µG3*	*µG4*	*µG1*	*µG2*	*µG3*	*µG4*	*µG1*	*µG2*	*µG3*	*µG4*
MF	*-0.2%*	*-0.8%*	*-29.8%*	*-0.8%*	*-3.0%*	*-1.5%*	*-30.0%*	*-0.4%*	*-0.7%*	*-2.3%*	*10.8%*	*0.7%*
CB$_{µG}$	*7.7%*	*-*	*17.6%*	*0.7%*	*5.6%*	*-*	*16.8%*	*0.7%*	*7.0%*	*-*	*17.6%*	*1.5%*
DG$_{acc}$	*62.9%*	*-2%*	*1.4%*	*-*	*73.5%*	*-2.0%*	*1.1%*	*-*	*68.1%*	*-5.0%*	*9.4%*	*-*
PV$_{acc}$	*62.9%*	*-2%*	*5.1%*	*-*	*73.5%*	*-2.0%*	*3.7%*	*-*	*68.1%*	*-5.0%*	*28.7%*	*-*
DIES$_{acc}$	*-*	*-*	*0.4%*	*-*	*-*	*-*	*0.5%*	*-*	*-*	*-*	*5.5%*	*-*
	(a) No Strategy				*(b) CLA*				*(c) CLAM*			

Tab. IV.16 Results comparison between sliding multi-level optimization and centralized

essentially due to the small-sized of PV systems which increases the installation costs. Hence, a centralized solution is more interesting for the management of various medium-sized microgrids with homogenous characteristics. The MF is almost unchanged for Microgrids 4, which does not have installed DG (Tab. IV.16). For microgrid 1, the MF is slightly decreased due to the increase of its own production in the distributed approach. Otherwise, the revenues for active microgrids are decreased. In general, results show that the impact on MF is small, except for microgrid 3.

Hence in general, the distributed approach complies with the self-interest of each microgrid by supporting the use of its own resources by slightly. From the economic point of view, revenues or expenses are only slightly impacted thanks to the economic model imposed in the aggregator. From the technical point of view, the amount of information gathered by the aggregator and the amount of components that it needs to monitor increase dramatically considering that the AGGA works directly with each SA (Fig. IV.51). Furthermore, the

[18] In the centralized approach, the services remuneration from the DSO is split among users by firstly compensating DG that reduced their power and the remaining income is redistributed among generators as function of the produced power.

optimization model requires to be extend when new components are introduced in the system and the behaviour of each components need to be integrated (for example for washing machine's profiles).

On the contrary in centralized approaches, results show a lower volatility of variable $CB_{\mu G}$ with respect to the applied strategy (e.g. CLA or CLAM). In fact, the average electricity cost CB_{agg} is equal to 13.8 c€/kWh independently from the applied strategy. This is essentially induced by the increase in size of the optimized system.

IV.6. Conclusions

The massive installation of distributed generation and storage systems combined to the increasing interest in demand-response are facing the electrical system to a prohibitively complex system to manage on a national scale. Furthermore, the huge integration of DGs into distribution grids modifies its scope and changes its nature from a passive system to a hub of bidirectional power flows, which requires new strategies for its planning and operation.

Hence in this chapter, a multi-level optimization framework is proposed to deal with by distributing tasks and knowledge among components. Microgrids are placed at the first stage of this smart distributed system and are considered to work in collaboration trough an aggregator. Furthermore, the conceptualization and implementation of a "Flexibility services market" and "Capacity limit allocation" strategies are debated for active management of distribution grids.

Simulation results show that the distributed approach is in line with the freedom in decision-making process of each microgrid. In fact from the economic point of view, expenses for passive microgrids and income for active microgrids obtained with the multi-level optimization framework slightly move away from results of the centralized framework, but optimizing the self-interest of microgrids. Furthermore, the collaborative strategy allows to reduce the average electricity cost of kWh for passive microgrids respect to an individual operation of microgrids. From the technical point of view, this hierarchical system meets the need of implementing a more flexible and extensible system and manageable on a national scale through a task and knowledge distribution, which will allows to integrated a large number of distributed systems into electrical and services market (for DSO and TSO).

Both implemented strategies for active grid management, "Flexibility Service Market" and "Capacity Limit Allocation", represent a high value solution for the massive integration

of distributed source into distribution networks. From the DSO point of view, results show that both strategies can increase grid hosting capacity of DGs by inducing a long-term secure, efficient and cost-efficient use of the infrastructure by reducing consumption and production peaks. Furthermore from the microgrid's point of view, they can also represents an additional source of incomes for owners. The development of these strategies requires nonetheless the development of a completely new regulatory framework. Furthermore, the large development of a reliable, scalable and interoperable information and communication infrastructure is required for the management of this complex multi-component and multi-actor system.

In future works, the aggregator's tasks can be extended, by adding for example algorithm to forecast the buying and selling prices in the aggregator, in order to make smarter the management strategy. Furthermore, the optimal sizing of the aggregator considering the described applications and the implemented distributed approach have to be studied in order to find the pool of microgrids which guarantee the best performance of the collaborative strategy.

V. REAL-TIME ASSESSMENT OF ENERGY MANAGEMENT STRATEGIES FOR GRID-CONNECTED MICROGRIDS

V.1. Introduction

In Chapter III, energy management strategies for the day-ahead scheduling of grid-connected microgrids have been discussed. Simulations showed the importance of these strategies in order to reduce users' costs, optimize the use of energy resources in microgrids and also support DSO's flexible operation. Nevertheless, theory and reality are often different. Real implementation can point out the real behaviour of components, the critical issues and the limits of the implemented and discussed strategies. The goal of this chapter is to contribute, at least in part, to answer to an easy but crucial question: " *Is really conceivable a flexible multi-microgrid system in which small-sized RES, ESS and flexible loads are actively used to support active management of distribution grids and to actively exchange energy with retail or overall markets?* "

Hence in this chapter, the microgrid energy management is experimentally validated in order to test the real performances of the implemented strategy under real conditions and to understand their real behaviour in a multi-microgrid vision. First of all, a hybrid optimization and rule-based approach for the intra-day and the real-time management of microgrids is presented in section V.2. These developments are followed by experimental tests in order to run the real-time simulations. The used test bench is discussed in section V.3. Thereafter, case studies representing different possible scenarios and the outcomes of the real-time implemented control strategy are analysed in V.4. At the end, section V.5 is concerning final discussions on performances and weaknesses of the overall implemented energy management strategy.

V.2. Rolling Optimization-based and Rule-based Approach for Intra-Day and Real-Time Control of Microgrids

As saw in section III.4, an offline algorithm for day-ahead scheduling of microgrids is implemented and tested. The development of this algorithm is based on perfect forecasting assumption for production and load profiles. In reality, the forecast errors may impact the reliable and economic operation of microgrids and distribution grids. Hence, an online control algorithm for energy management needs to be implemented in order to guarantee an efficient and economic operation of multi-microgrid systems.

In the literature, the importance of real-time control layer for the energy management process of microgrids is already discussed and tested by taking into account different applications. An example of a rule-based control algorithm is discussed and tested with simulations in [167] [168]. Furthermore, authors in [56] proposed a 5 minutes-ahead scheduling algorithm, based on MAS. This algorithm was tested for a 750 kW residential and grid-connected microgrid in a real-time digital simulator through a fixed simulation time step of 5 minutes. Moreover, other interesting results for a grid-connected microgrid operating under an import power constraint are obtained through a hardware-in-the-loop (HIL) real-time-digital simulator and resumed in [169]. In general, power hardware-in-the-loop (PHIL) platforms are widely used for the assessment of various energy management systems in order to increase their technology readiness level, such as [170]. The basic principle of the PHIL consists in associating power components with a HIL, such as in [171] [172].

In papers [56] [167], the main grid is assumed to supply power to satisfy consumption and to manage power quality at PCC in grid-connected mode. However, in the new vision of power system based on flexible multi-microgrid concept, microgrids may contribute to actively manage distribution grids. Hence, in this thesis, an algorithm for real-time control, which takes into account an intra-day re-scheduling process, is discussed. In any case, in order to guarantee a low cost system, the operation of microgrids needs to remain flexible by adapting itself to possible changes in both consumption due to human uncertain behaviour and production due to the variability of renewable sources. Then, these conditions incite the intra-day rescheduling process and in consequence the intra-day negotiation with markets and DSOs. Nevertheless, microgrids need to guarantee a certain degree of flexibility to DSOs to manage critical situations such as congestions and voltage stability, based on the day-ahead or forward engagement stipulated in contracts with the DSO.

The main goal of the real-time control algorithm (RTCA) implemented in the MMCA is to supply real-time consumption by activating local generation or absorbing electricity from the host grid. At the same time, the algorithm has to respect the profile engaged in the day-ahead negotiation, within a certain margin of error, also defined in contract terms. Moreover, periodically a check on the microgrid's state has to be applied. In case of high forecast error or low available flexibility, the microgrid can dynamically adjust the schedule based on real-time conditions through a re-optimization. After that, the MMCA submits the results of the new schedule to the DSOA/AGGA which will respond by accepting or rejecting the proposal.

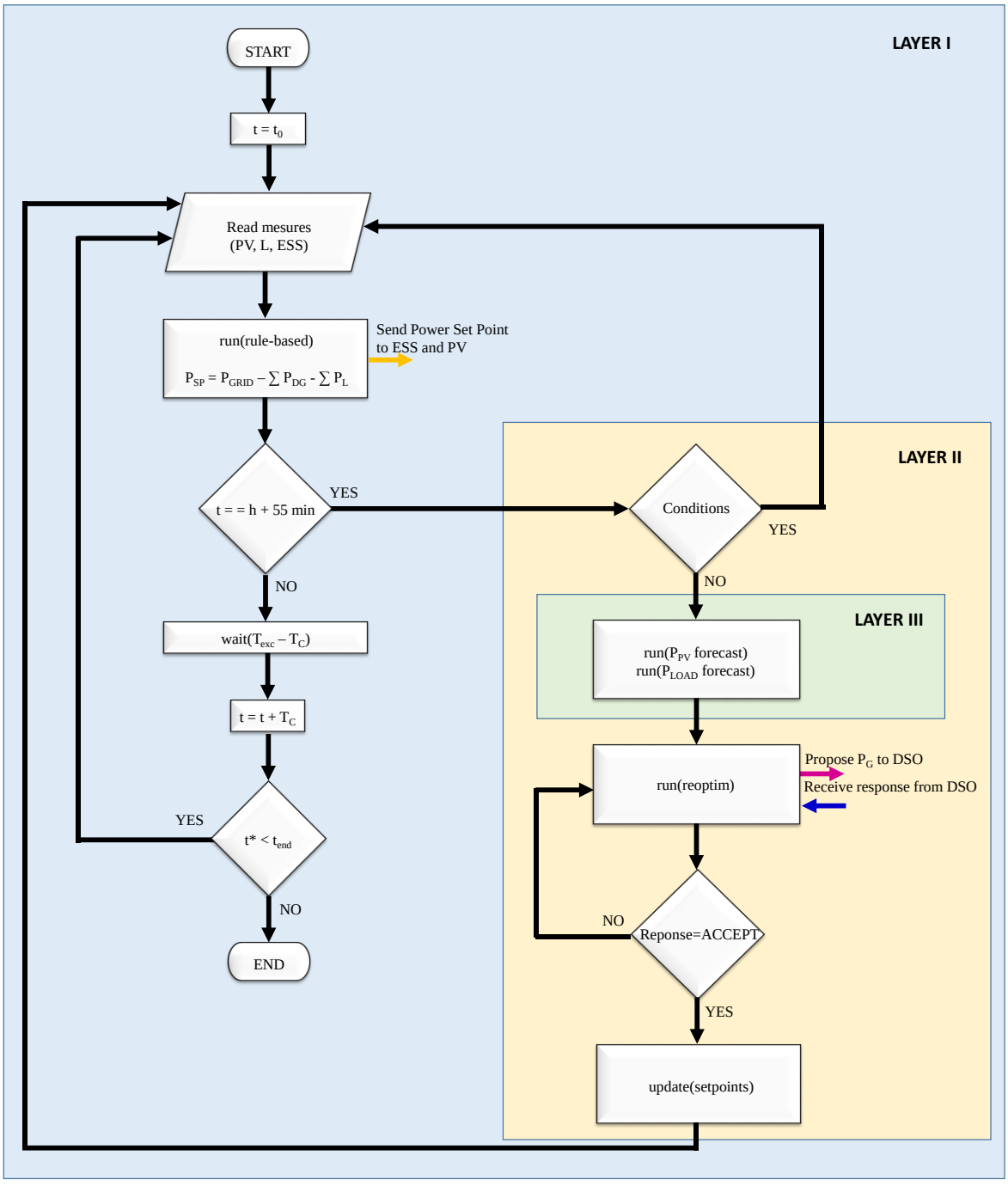

Fig. V.1 Flow Chart of Hybrid Optimization-based and Rule-based Algorithm for Microgrid Management

In the literature, this dynamic process is known as rolling optimization process.

The implemented process is resumed in the flow chart depicted in Fig. V.1 and consists of three main layers [173] [174]:

- Real-time control layer (I), which monitors and computes the operating point of each agent in real-time, e.g. each 10 seconds, by using a rule-based algorithm,

- Intra-day Optimization layer (II), which re-schedules the global operating point of the microgrid by using an optimization algorithm,
- Forecast layer (III), which forecast the intra-day power profiles of consumption and variable generation by using a Naïve Predictor method.

V.2.1. Real-Time Control Layer

As also disclosed in Fig. III.1, the RTCA takes as input both the day-ahead/intra-day scheduling results and also real-time measures. The feedback from the scheduling process is resumed in the form of one parameter: the aggregated power exchange at the PCC (P_{GRID} in Fig. V.1). Whereas, real-time measures needs to be gathered and analysed. Each physical quantity in the microgrid is monitored by the lower level agents ("Read Measures" function in the parallelogram in Fig. V.1). Nevertheless in line with the need of task distribution described in section III, the MMCA will receive only essential aggregated measures for running the hybrid process.

In this thesis, the use of PVS and ESS is discussed. However, the same concepts can be extended to other technologies. In Tab. V.1, a non-exhaustive list of collected measures is reported. As shown, each DGA gathers and stores all information about its reference resource based on the resource type and the system architecture. Usually for PV systems, it gathers all information related to each module and conversion stage, which are the solar irradiance, the direct currents and voltages of each module, the efficiency of each conversion stage, alternative currents and voltages of each inverter phase, the inverter active and reactive, and so on (see Tab. V.1).

For the ESS, the physical quantities to monitor increase proportionally to the number of battery packs, modules and conversion stages. Usually, the minimal data to collect for each battery module are: the state of charge, the maximal charging and discharging current, the available energy, the direct currents and voltages; which, in turn, allow to estimate other physical characteristics, such as the maximal charging and discharging power for each module and for each pack. From these considerations, the total amount of information gathered in real-time is huge even for a small-sized microgrids.

Information gathered by:					
DGA:			***ESSA:***		
-PV	-T (°C)	-I_v^m (W/m^2)	-*Li-ion*	-P_{INV}	-Q_{INV}
-I_{DC}^m	-V_{DC}^m	-P_{DC}^m	-η_{INV}	-P^b	-V^b
-η_{INV}	-P_{INV}	-P_{INV}	-I^b	-I_{MaxCh}^b	-$I_{MaxDech}^b$
-I_{ph1}^{INV}	-V_{ph1}^{INV}	-…	-E_{av}^b	-SOC^b	-…
Reassembled and manipulated information sent to *MMCA by*:					
DGA:			***ESSA:***		
-P^g	-P_{Max}^g		-P_{INV}	-SOC^p	-E_{av}^p
			-P_{MaxCh}^p	-$P_{MaxDisch}^p$	-SOC_{Max}^p
			- SOC_{Min}^p		

Tab. V.1 Example of infromation gathered by each DGA, ESSA and MMCA

Hence, information are aggregated and only needed data are selected and sent to the MMCA (as resumed in Tab. V.1), which are:

- injected power P^g and maximal injected power P_{Max}^g, if they do not coincide due to PV curtailment, control sensitivity s^g;
- state of charge SOC^p, maximal available energy E_{av}^p (which can coincide with the nominal power), maximal charging and discharging power, P_{MaxCh}^p and $P_{MaxDisch}^p$ respectively, state of charge limits SOC_{Max}^p and SOC_{Min}^p, control sensitivity s^p, each one for the entire battery pack;
- absorbed power P^L.

The value of SOC^p is computed in the ESSA by using a weighted average of each SOC^b computed by the BMS on the measured battery's contactor status (α^b) according to formula in Eq. IV.1:

$$SOC^p = \frac{\sum_{b=1}^{N} \alpha^b \cdot SOC^b}{N} \qquad \text{Eq. V.1}$$

The same technique is used to compute E_{av}^p, which is obtained by measuring each E_{av}^b, and the values of P_{MaxCh}^p and $P_{MaxDisch}^p$, which need to measure each P_n^b.

After receiving these aggregated measures, the MMCA can compute the control set-point for each flexible component. In the implemented rule-based control algorithm, the mainly

Algorithm rule-based control

```
1:  function rule_based_control
2:  P_C = −P_GRID − Σ_{g=1}^{DG} P_Max^g + Σ_{l=1}^{L} P^l
3:      if |P_C| > P_ins_syst
4:      if P_C < 0
5:          if |P_C| ≥ P_ins_b
6:                  if P_MaxDech^p ≥ |P_C|
7:                          P_bc = P_C
8:                  else
9:                          P_bc = P_MaxDech^p
10:                 End
11:         Else
12:                 P_bc = P_autoc
13:         End
14:     Else
15:                 if P^INV_PV > 0
16:                         if P_MaxCh^p ≥ P_C
17:                                 P_bc = P_C
18:                         else
19:                                 P_bc = P_MaxCh^p  &&  P_pvc = P^INV_PV − |P_C − P_bc|
20:                         end
21:                 else
22:                         if P_C ≥ P_ins_b
23:                                 if P_Maxch^p ≥ P_C
24:                                         P_bc = P_C
25:                                 else
26:                                         P_bc = P_MaxCh^p
27:                                 end
28:                         end
29:                 End
30:     End
31: End
```

Tab. V.2 Pseudo-code of Rule-based control algorithm

controlled components are the storage systems. The available flexibility of DGs is then used in case of lack or insufficient storage flexibility. The operating principle and the main applied rules of this algorithm are described in the pseudo-code in Tab. V.2. For simplicity, the pseudo-code describes the situation for a microgrid with a basic architecture: one controlled ESS and one controlled PVS. The global control value (P_C) is computed by using the scheduled exchange with the grid (P_{GRID}) and the real-time values of injected and absorbed powers by microgrid's components (P^g and P^L). The control algorithm is based on the structural limits of the system, including dynamic limitations, sampling time, control threshold of components. Real components are not able to respond to a continuous set of values between their minimal and maximal values. The control threshold of the microgrid

(P_{ins_syst}[19]) coincides with the lower control threshold of microgrid's controllable components. In our case the photovoltaic system. This means that no control is applied when the value of P_C is lower than P_{ins_syst}. Otherwise, the set-point of the battery and photovoltaic inverters (P_{bc} and P_{pvc}[20]) are computed following rules in Tab. V.2. The photovoltaic production, in case of production surplus with respect to forecasted value, is privileged. Hence first of all, a check of other available flexibilities is applied, in our case by analysing the value of P^p_{MaxCh}. If P^p_{MaxCh} is not enough, in general caused by a size limits or by a one or more fully charged batteries, the photovoltaic production is then cut off. This process is repeated each T_C, e.g. 10 sec or 30 sec, chosen by considering the algorithm execution time, the components' response time and the communication delay.

Furthermore, each hour, a check on microgrid state compared to the forecasted is applied (at the fifty-five minute of every hour as in the flow chart in Fig. V.1). In fact, a re-optimization can be needed in order to compensate consumption and/or generation forecast errors and to detect a change in the connected resources. The need of a re-scheduling can be related to different factors and can be adapted based on microgrid size and components. In this study the variation of the battery state of charge SOC^p and the real available PV power P^g_{real} are used. Hence, the activation of a re-optimization is triggered in the algorithm by the occurrence of one of the following conditions:

I. $SOC^p_{sch} - \beta < SOC^p < SOC^p_{sch} + \beta$

II. $mean\left(P^g_{real}\right) > (1+\gamma) \cdot \left|mean(P^g_{for})\right|$.

The first formula imposes a re-optimization in case of an increase or decrease in the forecasted state of charge of a minimal amount β. β is a fixed parameter with real value, e.g. 0.1 or 0.15 if the SOC is comprised between 0 and 1. It can be chosen based on flexibilities amount and can depend on clauses in the engaged profile with the DSOA or the AGGA. However in software design phase, it is needed to consider that small value of β, close to zero, would induce an instable process with frequent re-optimization sequences. On the

[19] The insensitivity threshold of the control coincide with the minimal increment power's value which induces a change in the microgrid's power.

[20] The set-point computed for the battery is than locally modified in order to compensate the power auto-consumption of the inverter. Hence, it is increased when the battery discharges and decreased when charges.

contrary, high value of β would lead to a deeper use of the battery, less frequent re-optimization sequences and sometimes less accuracy in the control.

The second formula imposes a re-optimization process when the average measured PV power in the last 30 minutes differs from the day-ahead or the intra-day forecasted power. γ is a fixed parameter as well, which can be fixed taking into account the same considerations made for the β value. However, a good practice could be to choose the coefficient β with a more strict value compared to γ, due to the fact that β takes into account both generation and consumption errors.

Afterward, when the control algorithm detects one of these two conditions, a re-optimization process starts. Firstly, new forecasted data of consumption and generation profiles are computed, by exploiting new real-time information (Fig. V.1). Forecasting data plays a fundamental role in the re-scheduling layer and can strongly affect re-optimization results. Hence, a brief description of the implemented algorithm is discussed in following sub-section V.2.2. The new forecasted data are then used as input of the optimization algorithm, discussed in sub-section V.2.3, which permits to compute new optimal operation set-point for each flexible component in the microgrid. The results of the aggregated power at the PCC are then sent for the next hour to the DSOA/AGGA. If the change in the schedule is accepted by the DSOA/AGGA, the control process goes on. Otherwise, in case of critical situation, a reschedule with the imposed power limit at the PCC have to be computed.

V.2.2. PV and Load Forecast Layer

As mentioned earlier, forecasting task plays an important role in the decision making process in both phases, day-ahead and intra-day. In fact, this task influences the choice of the optimal operating point of the microgrid. A bad forecast will influence the economical operation of both microgrids and distribution networks, in addition to a less reliable and efficient operation of the entire grid. The forecasting model depends on the forecasting time horizon (year-ahead, day-ahead, hour-ahead, etc.) [175] and also on the amount of gathered data.

Due to the importance of the topic, several papers propose reviews on current methods to solar irradiance forecast, and in consequence available power forecast [176] [175] [177] [178]. The energy consumption forecast is also an important subject. An interesting survey of the short-term forecast for consumption can be found in [179].

For PV forecast, these methods can be based on statistical, numerical or satellite images models. In general, one of the most easy-to-implement, but effective, statistical method is based on persistence concept. Persistent models are based on the assumption of "no change", which practically means that forecasted conditions can be assumed similar to current conditions [175]. Mathematically, this can be stated by asserting that the value of a generic physical quantity in a certain timeframe x_{t+1} depends on x_t. The persistence forecast, also known with the name of "Naïve Predictor" [176], is usually used as a benchmark model to assess other approaches. However, persistence method can be applied to compute PV power forecast for minutes to hours-ahead time scales [175]. In fact in [178], authors affirm that Naïve Predictor Method results even more accurate than other physical or statistical approaches for short-term horizons. In general, its accuracy decreases strongly with more than one-hour ahead forecast horizon and rapid changes in cloudiness conditions.

The Naïve Predictor Method is nonetheless also known for the simplicity of its implementation. Hence, it resulted convenient for both PV and consumption forecast in order to show the outcomes and the benefits of the implemented intra-day strategy. The description of the applied Naïve Predictor will focuses on PV forecast. The same concepts can be applied to the consumption forecast. The implemented intra-day forecast is based on the adjustment of the PV power profile $P_{t+1}^{PV} \dots P_T^{PV}$ by using the real-time energy injected between the timeframes *t-t** ... *t*. Authors in [180] have defined a daily weather-dependent coefficient for their predictive control strategy for PV plants, which can be used as adjustment factor. Based on this idea, the new shape of PV injection is regulated by using a time-varying factor computed taking into account the forecasted energy and the real energy in the chosen timeframes, such as the last hour or the last 30 minutes. The applied formulas are presented in Eq. V.2 and Eq. V.3:

$$k_t = \frac{\sum_{i=t-t^*}^{t} P_i^{PV-REAL} \cdot \Delta t}{\sum_{i=t-t^*}^{t} P_i^{PV_{FOR}} \cdot \Delta t} \qquad \text{Eq. V.2}$$

$$P_i^{PV} = k_t \cdot P_i^{PV_{FOR}} \qquad \forall i = t+1 \dots T \qquad \text{Eq. V.3}$$

In order to explain more deeply the advantages and disadvantage of the applied Naïve Predictor some simulation results are shown for both variable generation and consumption. For the PV system two different cases of bad forecast are analysed. The first case considers a

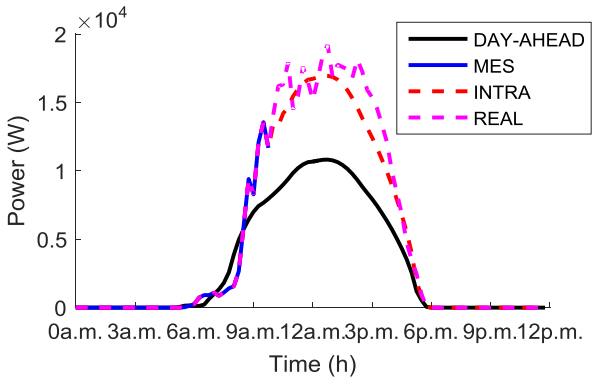

(a) At 10.00 a.m.

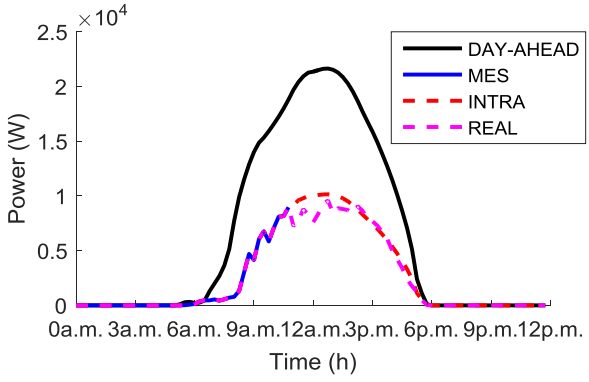

(b) At 11.00 a.m.

Fig. V.2 Example of intra-day PV forecast with the Naïve Predictor

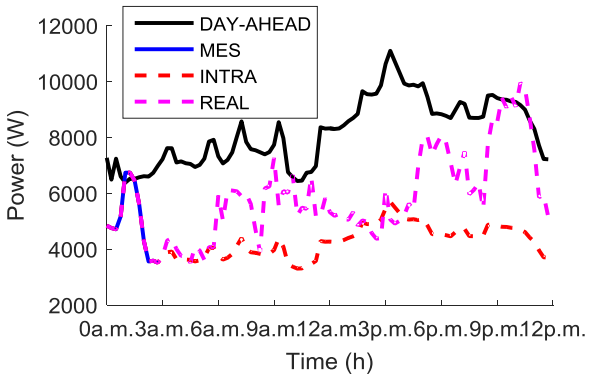

(a) At 3.00 a.m.

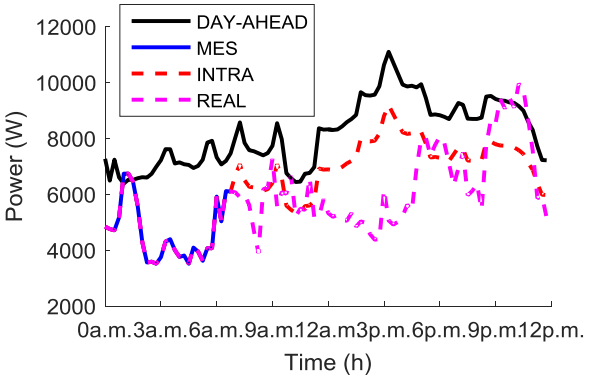

(b) At 7.00 a.m.

Fig. V.3 Example of intra-day consumption forecast with the Naïve Predictor

negative relative error of the power production, which means a higher power injection with respect to the forecasted one, such as in Fig. V.2 (a). In this case, the intra-day forecast is considered run after detecting the error at 9.00 a.m.. The black line shows the day-ahead forecasted profile and the red one the new forecasted profile between 10.00 a.m. and 11.00 p.m.. The blue line indicates the averaged value over fifteen minutes of the real measurements until the forecast instant. The second case analyses the re-forecast at 11.00 a.m. for positive errors, such as Fig. V.2 (b). The same scenarios with two different start-time are discussed for the load re-forecast. The first forecast is considered triggered at 3.00 a.m. and the second at 7.00 a.m., as reported in Fig. V.3 (a) and (b), respectively. In these figures, the same colour legend described above is applied.

Both examples clearly show the effectiveness of this method for very short-term forecast. Fig. V.3 (a) shows a good prediction between 3.00 a.m. and 6.00 a.m with an average error of -4.5 %. Moreover, in this timeframe the maximal and minimal errors are -13.0 % and -0.2 %, respectively. Instead, Fig. V.2 (a) shows a good daily prediction with an average error of -6.3

%. However, the prediction will have higher errors in case of sudden variation of direct irradiation due to high variability of the sky cloudiness, such as in consumption case.

V.2.3. Intra-Day Optimization Layer

Nomenclature

Sets:

T	Optimization problem timeframe
DG	Set of distributed generation
L	Set of inflexible loads

Parameters:

t_1, t_{end}	Initial, final time frame of set *T*
t^f_{bid}, t^f_{start}	User desired start, end time for flexible load *f*
t_{bid}	Intervals in a bid proposal (h)
$C^{grid\_buy}_t$	Price to buy/sell electricity from/to the main grid in time frame *t* (c€/kWh)
$C^{grid\_sell}_t$	
C^g_t	Distributed generation selling cost in time frame *t* (c€/kWh)
C^b_t	Battery cost in time frame *t* (c€/kWh)
$E_{nom}{}^b$	Battery capacity (kWh)
$\eta^b_{ch}, \eta^b_{disch}$	Battery and conversion stage efficiency during charging/discharging
SOC^b_{max}, SOC^b_{min}	Maximal and minimal State of Charge (SOC) of battery *b*
$SOC^b_{start}, SOC^b_{end}$	Battery initial and final SOC of battery *b*
$P_{max}{}^g_t, P_{min}{}^g_t$	Maximal and minimal power of distributed generation *g* in time frame *t* (kW)
$P^b_{\max\_ch_t}$ $P^b_{\max\_disch_t}$	Maximal charging and discharging power of battery *b* (kW)
P^l_t	Power of inflexible load *l* in time frame *t* (kW)
M , Q	Large constants

Variables:

P_{B_t} , P_{S_t}	Electricity bought/sold from/to the main grid in time frame *t* (kW)
P^g_t	Electricity produced by distributed generation in time frame *t* (kW)
$P^b_{ch_t}$, $P^b_{disch_t}$	Battery *b* charging and discharging power in time frame *t* (kW)
SOC^b_t	State of Charge of Battery *b* in time frame *t*
x^g_t	Binary variable (1 if g is operating in time frame *t*, else 0)
x^b_t	Binary variables (1 if *b* is charging/ discharging in time frame *t*, else 0)
x^{grid}_t	Binary variable (1 if the microgrid is injecting, else 0)
ε^b	Error between the computed and desired final SOC for battery *b*

Mathematical Formulation Description

As for the day-ahead scheduling in section III.4.2, a deterministic optimization approach formulated as a MILP is used to implement the intra-day re-optimization of microgrids. It aims to reschedule the global operating point of the microgrid by minimizing its global cost.

This algorithm receives the intra-day forecasted profiles between *t+1…t* of both generation and consumption, obtained as explained in section V.2.2. The mathematical formulation described by equations Eq.V.4-Eq. V.14 is similar to the one already described in III.4.2. However, it was needed to make the model more flexible. For reading simplicity, the equations described in III.4.2 are listed, but descriptions will focus on modified equations.

The objective function in Eq.V.4 aims to minimize the global costs of the microgrid. This time an additional term is added: the product $Q \cdot \varepsilon^b$, where ε^b is the error between the computed and desired SOC_{end}^b for battery b and Q is a constant parameter sufficiently large to impose a penalty on the variation of SOC_{end}^b.

This extension in combination with the added constraint shown in Eq. V.12 allows to make less strict the constraint in Eq. V.12. This inequality substitutes the strict equality (see Eq. III.21) in the previous model permitting to always find a feasible solution also in case of lack of flexibilities to restore the final state of charge of the batteries.

Objective function

$$\min \Delta t \cdot \sum_{t \in T} \sum_{g \in DG} C_t^g \cdot P_t^g + C_{GB_t} \cdot P_{B_t} - C_{GS_t} \cdot P_{S_t} + \sum_{b \in B} C_t^b \cdot P_{ch_t}^{\ b} + Q \cdot \varepsilon^b \qquad \text{Eq.V.4}$$

Power balance

$$P_{B_t} - P_{S_t} + \sum_{g \in DG} P_t^g - \sum_{l \in L} P_t^l - \sum_{b \in B} P_{\mathrm{ch}_t}^b + \sum_{b \in B} P_{\mathrm{disch}_t}^b \quad \forall t \in T \qquad \text{Eq. V.5}$$

DG production upper and lower limits

$$x_t^g \cdot P_{min_t}^g \leq P_t^g \leq x_t^g \cdot P_{max_t}^g \quad \forall t \in T \quad \forall g \in DG \qquad \text{Eq. V.6}$$

ESS modelling

$$0 \leq P_{\mathrm{ch}_t}^b \leq x_t^b \cdot P_{\mathrm{max\_ch}_t}^b \quad \forall t \in T \quad \forall b \in B \qquad \text{Eq. V.7}$$

$$0 \leq P_{\mathrm{disch}_t}^b \leq (1 - x_t^b) \cdot P_{\mathrm{max\_disch}_t}^b \quad \forall t \in T \quad \forall b \in B \qquad \text{Eq. V.8}$$

$$SOC_t^b = SOC_{t-1}^b + \frac{\eta_{ch}^b \cdot P_{\mathrm{ch}_t}^b \cdot \Delta t}{E_{nom}^b} - \frac{P_{\mathrm{disch}_t}^b \cdot \Delta t}{E_{nom}^b \cdot \eta_{disch}^b} \quad \forall t \in T \quad \forall b \in B \qquad \text{Eq. V.9}$$

$$SOC_{min}^{b} \leq SOC_{t}^{b} \leq SOC_{max}^{b} \quad \forall t \in T \quad \forall b \in B \qquad \text{Eq. V.10}$$

$$SOC_{t_{start}}^{b} = SOC_{start} \quad \forall b \in B \qquad \text{Eq. V.11}$$

$$SOC_{end}^{b} - \varepsilon^{b} \leq SOC_{t_{end}}^{b} \leq SOC_{end}^{b} + \varepsilon^{b} \quad \forall b \in B \qquad \text{Eq. V.12}$$

Grid exchange block bids

$$P_{S_t} = P_{S_{t+1}} \quad \forall t \in \left\{(h-1) \cdot t^{bid}; h \cdot t^{bid}\right\} \quad \forall h \in \left\{t_{start}; \frac{t_{end}}{t^{bid}}\right\} \qquad \text{Eq. V.13}$$

$$P_{B_t} = P_{B_{t+1}} \quad \forall t \in \left\{(h-1) \cdot t^{bid}; h \cdot t^{bid}\right\} \quad \forall h \in \left\{t_{start}; \frac{t_{end}}{t^{bid}}\right\} \qquad \text{Eq. V.14}$$

Grid exchange buy or sell:

$$0 \leq P_{S_t} \leq x_t \cdot M \text{ with } M \gg P_{S_t} \qquad \text{Eq. V.15}$$

$$0 \leq P_{B_t} \leq x_t \cdot M \text{ with } M \gg P_{B_t} \qquad \text{Eq. V.16}$$

V.3. Description of the Implemented Experimental Test Bench

The tested microgrid belong to an experimental platform called *PRISMES* [181] located at the *National Institute of Solar Energy* (INES) in Le-Bourget-Du-Lac (France). This platform is constituted of a real grid-connected microgrid, which interconnects different types of electrical systems: generators (including PV and diesel systems), storage systems (such as batteries and flywheels) and a fleet of EVs. Different load banks and a PV simulator are included as well.

In this thesis, the set up testbed is composed of a hybrid Hardware-in-the-loop (HIL) platform, shown in Fig. V.4, and composed of:

- two solar array I-V curve simulator of 12 kW rated power from *AIT - Austrian Institute Of Technology*
- a three-phase inverter of 27.6 kW nominal power from *ABB/DMSolar*
- a ZEBRA battery of 35 kW nominal power and 70.5 kWh capacity from *FIAMM/Sonick*
- a three-phase inverter of 60 kW from *Elettronica Santerno*.

The PV array simulator is supplied by an external DC source and works as a linear amplifier [182]. Emulators based on a controller and a power source are often used in test benches to emulate PV systems, in order to uncouple simulation needs from incontrollable

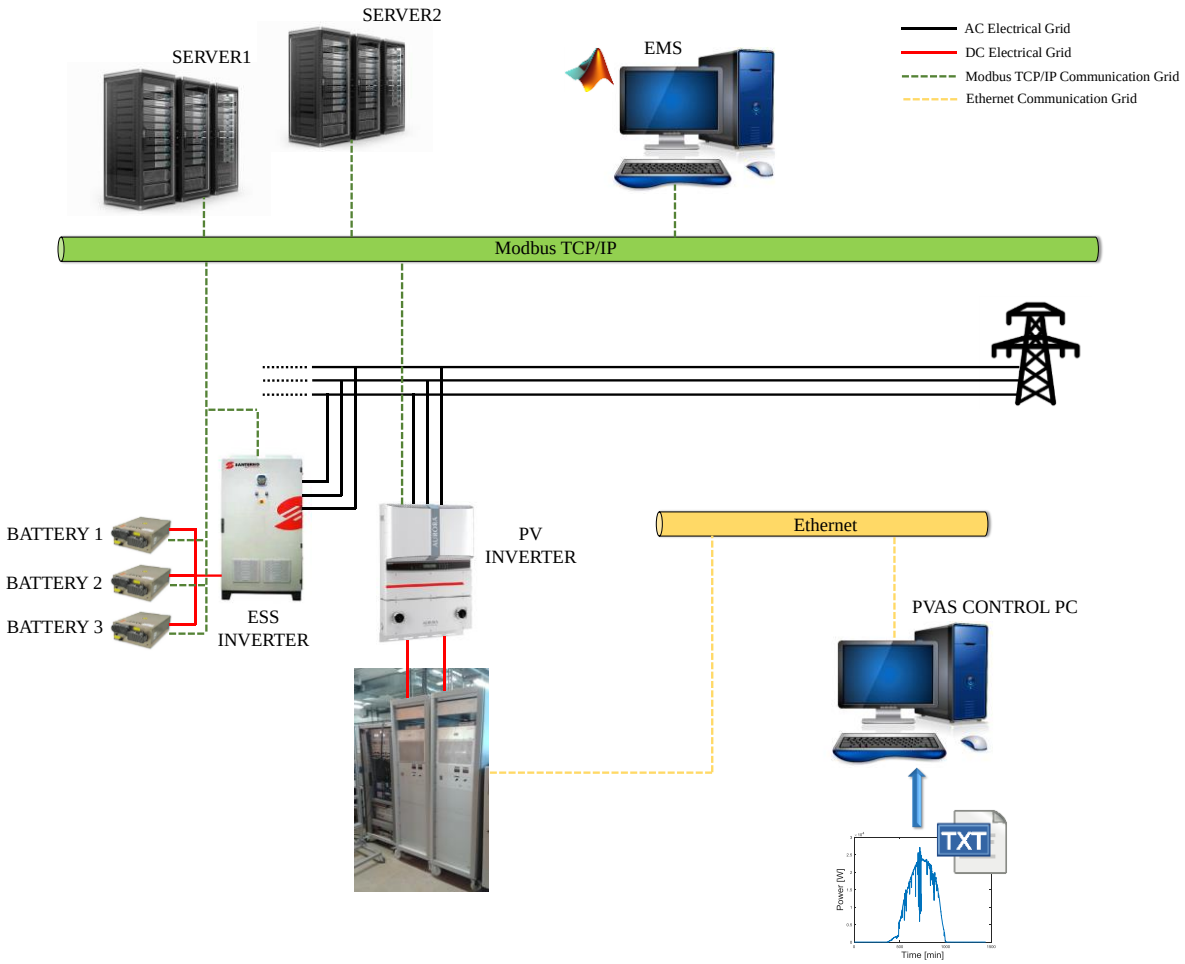

Fig. V.4 Experimental testbed configuration at INES

weather conditions [183] [184]. The PV array simulator takes as input a daily power production curve chosen by the user and received from an external PC. Hence, the current output of the simulator is controlled according to an I-V characteristic, defined by the PV implemented model. In these simulations, each simulator is set to represent a 33 cells PV system (3 parallel branch of 11 series cells each of 64 V and 8 A).

The data acquisition, management and equipment control are applied through a Supervisory Control and Data Acquisition called “INES SCADA”. The INES SCADA uses two redundant servers and the data acquisition is carried out using the Modbus TCP/IP protocol through different sub-networks. The INES SCADA allows to control each equipment manually or by machine. All shared variables in the SCADA can be read and write via Open Platform Communications Unified Architecture (OPC UA) protocol using these two servers. The OPC UA is a machine-to-machine communication protocol developed by the OPC Foundation in 2008 for industrial automation [185]. The OPC UA is completely independent

from the used platform and operating system. Moreover, it has a service-oriented architecture, which provides an extensible framework for all the OPC Classic functionality [185]. The algorithms for microgrid energy management are developed in Matlab. Hence, the OPC hierarchical object-oriented communication is implemented using the OPC Matlab Toolbox, which interfaces the two servers, identified by a unique server identifier (ID), and the client application in Matlab [186].

The instrumentation and data used as input to the real-time simulations are a crucial part in all experimentation fields. The selected data have a strong impact on both validity and success of the carried out simulations.

On one side, the validity and the relevance of test results require a reasonable imitation of the reality. The reproduction of reality requires to take into account sufficiently detailed and significant case studies, implement a suitable size of the banc test and make hypothesis which don't impact the phenomena under study.

On the other side, the simulations need to be adapted to the characteristics of the available equipment in the laboratory. Hence, the adaptation of collected data, obtained during measuring campaigns of real loads and PVS, to the characteristics of the available components were a hard tasks to guarantee the validity of results. The nominal size of the experimental microgrid could not exceed 25 kW due to the size of the 2 solar arrays.

The data used to simulate the consumption came from a measure campaign in the framework of "IPERD" project funded by ADEME [187]. The main goal of this project was the implementation of a real demonstrator to show the feasibility of RES and ESS integration into distribution grids to guarantee a reliable operation. These data are chosen essentially for the affinity of the project with the thesis' goals and also for the similarity in size between the microgrid in the project and the analysed microgrid in chapter III. The implemented microgrid in IPERD project is characterized by a MV/BT power transformer of 160 kVA, a Li-ion battery of 60 kVA of nominal power and 150 kWh of capacity and PV systems of 120 kW of nominal power. The consumption represents small-sized residential and commercial consumers. Details of used consumption profiles are given in section V.4. However, the consumption measures were available only for the last week of July and their size was adapted to the testbed size. This consisted of reducing the maximal amplitude to 10 kW by

maintaining the same variation level between all consumption points. This was realized by applying a common offset to each consumption point.

For the generation side, the simulated PV profile takes as input real measures obtained with a measure campaign on a PV system of 40 kW at INES. These data are then adapted to the size of the PV simulators. Otherwise, PV day-ahead forecast curves are computed with a forecasted algorithm developed by the laboratory of photovoltaic systems at INES and the start-up Steadysun [188], which is based on the same principles used for the solar thermal learning method described in [189]. The performance of this algorithm are tested on solar plants installed in Mayotte Island. Results tests and comparison with other forecast method can be found in [190].

V.4. Scenarios and Test Results

Generation and consumption sides are both subjected to prediction error. Microgrids have to be able to reschedule their operation in the most economical way and respond to DSO in case of services engagement. Hence, different case studies are considered to analyse how microgrid respond to forecast error by using the implemented hybrid process. In other words, the main goal of the implemented tests is to analyse the performance and weakness of the implemented optimization and control framework, with a particular regard to the role of the re-scheduling process and the engagement of microgrids in distribution grids operation.

The performance of the real-time control algorithm are evaluated considering the instantaneous and averaged behaviour of the microgrid by analysing the following parameters:

- P_m^{grid}, which is the measured profile of the final aggregated power exchanged at the PCC among the microgrid and the host grid in each instant t_m of measure with intra-day re-optimizations by imposing different production and consumption profiles;
- $\varepsilon_{a_m}^{grid}$, which is the absolute error[21] among the forecasted power exchange and the measured aggregated profile;
- P_{av}^{grid}, which is the mean profile taken over 30 seconds of P_m^{grid};

[21] Considering the classical definition known in the literature, the absolute error is obtained as the difference between the forecasted value of the considered system power for the instant *t* at D-1 and its actual value at time instant *t*, which is represented by the real measured power, given by $\varepsilon_a = P_{FOR} - P_{MES}$.

- $\varepsilon_{a_{av}}^{grid}$, which is the absolute error among the forecasted power exchange and the aggregated profile averaged over 30 seconds.

The usage of the flexible resources in the microgrids is evaluated by analysing the applied control to the ESS, namely $P_{BATT_{sp}}$, and to the PVS, namely $P_{PV_{sp}}$. While the behaviour of the battery packs in response to the microgrid's needs is studied by analysing its state of charge and the state of charge of each battery in the pack, called SOC^p and SOC^b as in Tab. V.1.

Different scenarios that consider different realistic profiles of consumption and production have to be performed in tests in order to validate the control framework. In any microgrid, there are dozens or even hundreds of different combinations of consumption and production as possible candidates to test. In fact, production and consumption profiles can vary in amplitude, shape and intermittence throughout the year. Additionally, also their forecast errors can hugely vary from day to day and they are the main cause for the RTCA implementation. However, in order to reduce the amount of needed tests, some interesting scenarios able to capture the behaviours of microgrid's components and the variability of forecast errors were chosen. Hence four different scenarios are taken into account:

- Scenario 1 – Good PV Forecast, which considers good PV forecast and high consumption forecast;
- Scenario 2 - High Forecasted PV Power, which analyses an extreme scenario with real-time PV profile inferior to the forecasted profile and at the same time higher consumption in respect of the forecast;
- Scenario 3 - Low Forecasted PV Power, which studies the opposite case of Scenario 2, that is real-time higher production and lower consumption with respect to the forecasted profiles;
- Scenario 4 - Low Forecasted PV Power with High Intermittence, which analyses the same extreme conditions in Scenario 3 also a high intermittence of PV profile.

All other possible cases vary between Scenario 2 and 3, hence their analysis can be considered enough to draw overall conclusions. The details of each scenario are discussed in sections V.4.1, V.4.2, V.4.3 and V.4.4.

Moreover, some common assumption is made for all scenarios and tests as detailed in the following descriptions. For the D-1 and H-1 optimizations, the cost of the PV and the ESS are estimated to be 12c€/kWh and 15c€/kWh and are computed as in III.3.2. The same selling and buying prices are applied for the day-ahead, intra-day and real-time calculations. The 24-hours are simulated in a fifth of the day that corresponds to 4.8 hours.

The control set-point is applied each 30 seconds. This frequency of control was chosen by considering: the communication delay, which takes into account the measurements reading and the control set-point application via the OPC, the response time of the ESS and the run-time of the control algorithm. In general, the sum of these three time intervals takes between 10 to 20 seconds according to the amount of variables to read and write for the communication delay and on the increasing/decreasing power step applied to the ESS.

In addition, each scenario would require a different initial and final battery's SOC in order to provide the best performances and an efficient use of components. In real applications, these values can be evaluated with weekly or monthly simulations. In this thesis, a unique value of SOC_i and SOC_f of 50.0 % was applied, in order to support all different scenarios. The energy losses of the ESS auxiliary systems are not taken into account, because the electrical-thermal model for their estimation is not analysed in the context of this thesis. Moreover, it was needed to choose the value of parameters β and γ described is section V.2.1. γ is chosen equal to 1.3, while two values of β[22] are tested, that are 0.2 in scenarios I and IV and 0.15 in scenarios 2 and 3. Hence, re-optimizations are triggered when the measured injected energy differs from the forecasted of at least ±30.0 % and/or the SOC value differs of at least ±20.0 % or ±15.0 % from the scheduled. In order to obtain same results for 24-hours and 4.8 hours tests, β was imposed equal to 0.04 in scenarios I and IV and 0.03 in scenarios 2 and 3.

V.4.1. Scenario 1 - Good PV Forecast

The first scenario considers a day with low variability in cloudiness conditions, which in consequence means scarce variability and low intermittence of the PV profile, and good *D-1* PV forecast. The data chosen represents a sunny day at the end of July. Fig. V.5 show the day-ahead and the real-time PV profiles used for this scenario, which corresponds to the scaled profile of the real system described in section V.3.

[22] If the SOC is expressed in percentage, also β have to be expressed in percentage.

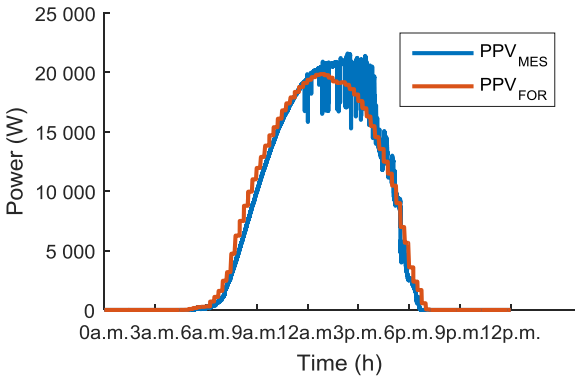

Fig. V.5 PV power profiles of forecasted data over 15 minutes and real-time measures

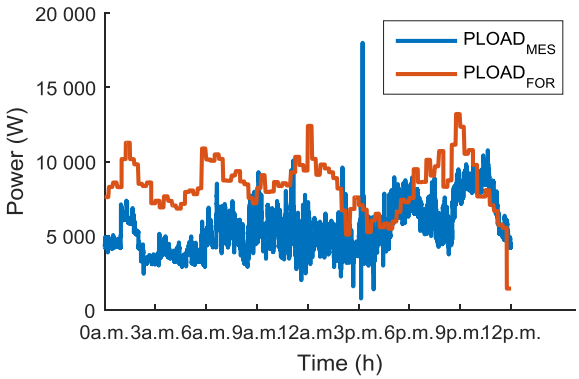

Fig. V.6 Aggregated consumption power profiles of forecasted data over 15 minutes and real-time measures

The consumption results from real-measures gathered at the MV/LV transformer at the end of July for the microgrid in the framework of IPERD project (described section V.3). The power profile used in the test is shown in blue in Fig. V.6. Because of the lack of consumption forecastalgorithms, D-1 load curve is obtained by applying the persistence concept. Hence, the averaged measures at *D-1* over 15 minutes are used as day-ahead forecast. The obtained profile is compared with measures at day D in Fig. V.6.

Comparing the chosen production and consumption, it is easy to see that in this scenario the prediction error for the entire microgrid is more due by the wrong consumption forecast. However, in order to understand the behaviour of the microgrid's components, a brief analysis of the prediction errors for both production and consumption are discussed.

Fig. V.7 and Fig. V.9 show for the selected day the absolute error between the forecasted and real values of photovoltaic and consumption powers with a 5-seconds resolution (called ε_a^{PV} and ε_a^{C}). ε_a^{PV} and ε_a^{C} are intermittent and vary between a maximal and minimal value of 3924 W and -4714 W, and 9317 W and -10927 W, respectively. This high negative peak at around 3.15 p.m. for the consumption error is nonetheless an isolated value, which may be due to a measurement error. In fact, the other peaks of negative load errors oscillate around -4000 W in late-evening hours between 10.00 p.m. and 12.00 p.m.. On the contrary, the positive error peaks oscillates around 8500 W occur between 12.00 a.m. and 12.15 a.m.. For the chosen profile, ε_a^{PV} assumes small positive value between 6.00 a.m. and 11.30 a.m. and after starts to oscillate between positive and negative values with a variable intensity.

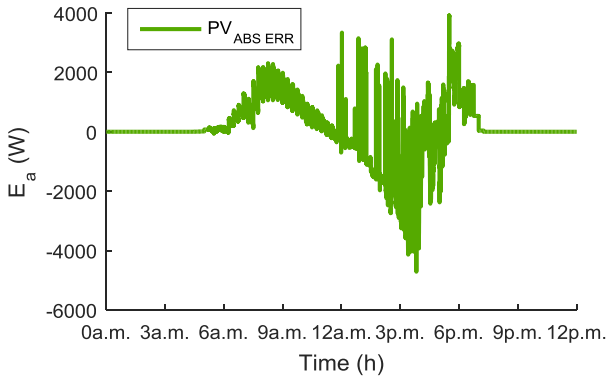

Fig. V.7 Absolute error between forecasted and real values of PV power (ε_a^{PV})

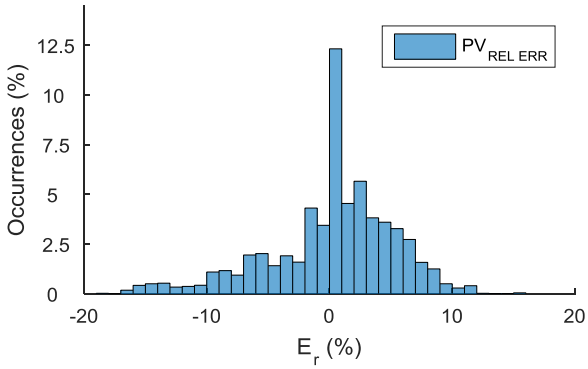

Fig. V.8 Distribution of ε_a^{PV} on microgrid P_n

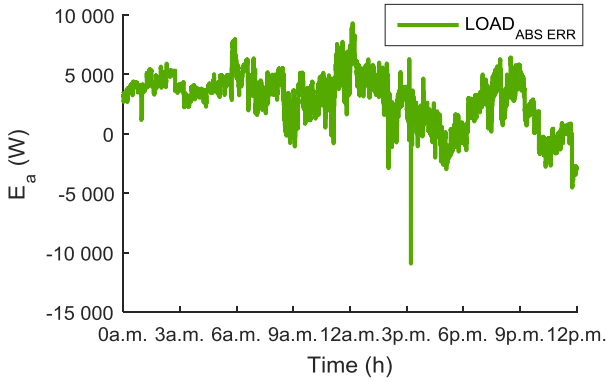

Fig. V.9 Absolute error between forecasted and real values of load power (ε_a^{C})

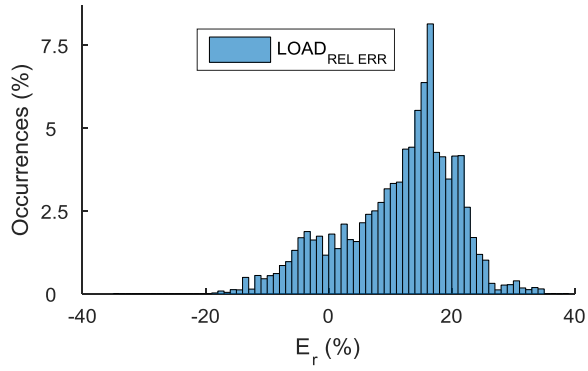

Fig. V.10 Distribution of ε_a^{C} on microgrid P_n

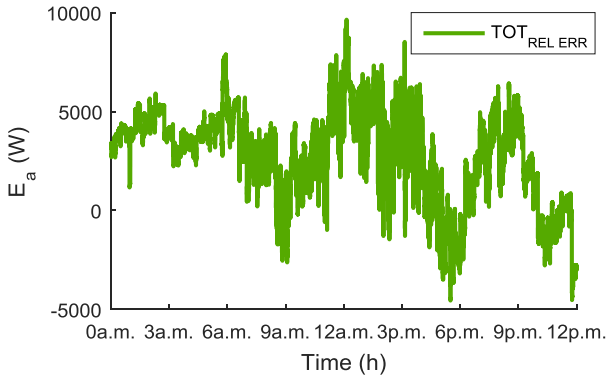

Fig. V.11 Absolute error between forecasted and real values of total microgrid power (ε_a^{PV+C})

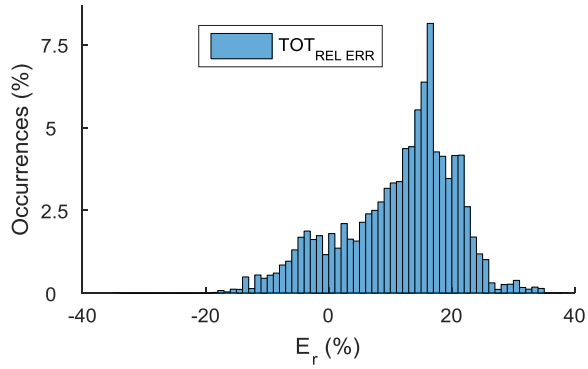

Fig. V.12 Distribution of ε_a^{PV+C} on microgrid P_n

In order to understand the global behaviour of the microgrid, the study of the combination of consumption and generation profiles is resumed by the total absolute error curve (ε_a^{PV+C}) respectively. As in consumption error analysis, the negative peak is induced by the extremely high value already found analysing the consumption. Besides, it is possible to observe the shown in Fig. V.11. The maximum and minimum value of ε_a^{PV+C} are 9641 W and -8716 W,

	< -20	**-20/-15**	**-15/-10**	**-10/-5**	**-5/0**	**0/5**	**5/10**	**10/15**	**15/20**	**> 20**
$\boldsymbol{\varepsilon_a^{PV}}$[23]	0.0 %	1.0 %	3.4 %	11.4 %	20.2 %	47.9 %	14.9 %	1.1 %	0.1 %	0.0 %
$\boldsymbol{\varepsilon_a^{C}}$	0.0 %	0.2 %	0.9 %	2.7 %	7.2 %	10.6 %	14.4 %	21.2 %	30.1 %	12.8 %
$\boldsymbol{\varepsilon_a^{PV+C}}$	0.0 %	0.3 %	1.7 %	4.3 %	8.1 %	8.5 %	13.0 %	21.0 %	26.4 %	16.8 %

Tab. V.3 Occurrences of percent values of $\boldsymbol{\varepsilon_a^{PV}}$, $\boldsymbol{\varepsilon_a^{C}}$ and $\boldsymbol{\varepsilon_a^{PV+C}}$ at various percent intervals

positive peak can be observed, where the maximal occur at around 11.50 a.m. and 12.30 a.m., and also three interval of negative peak, where the minimal occur at around 4.45 p.m. and 6.00 p.m..

The number of occurrences of various values of ε_a^{PV}, ε_a^{C} and especially ε_a^{PV+C} are more useful than extreme error values to estimate the battery solicitations which will be imposed during the real-time simulations. The parameter chosen to describe these occurrences is the distribution of ε_a^{PV}, ε_a^{C} and ε_a^{PV+C} on the microgrid test-bed rated power (P_n)[24]. For the microgrid under analysis, P_n equals to 25000 W. This parameter is preferred to the relative error essentially for two reasons. Firstly, the size and the bidirectional behaviour of the microgrid impose small values (close to zero) of the exchanged P_m^{grid} at the PCC during certain operating timeframes. It is important to stress that this attitude also suggested to analyse the fluctuations of P_m^{grid} by referring to the microgrid's rated power instead of the actual value. Secondly, it gives a more intuitive interpretation of the error value. Hence, these distributions are depicted in Fig. V.8, Fig. V.10 and Fig. V.12.

For the sake of completeness, the percent occurrences at various percent intervals between -20.0 % and 20.0 % with an increasing step of 5.0 % are resumed in Tab. V.3. As shown, around the 68.1 % of the PV errors lie in the range between -5.0 % and 5.0 %. Whereas, due to the higher error of consumption forecast, only the 54.8 % of the percent values of ε_a^{PV+C} are contained between -10.0 % and 15.0 %.

The intermittence of injected PV and absorbed consumption powers is a typical phenomenon that is often encountered. This is due by the nature of natural resource for PVs and by the nature of the small-sized load for consumptions. From the energetic point of view, the PV forecasted and the real produced energy are around 150.8 kWh and 150.1 kWh, which means a negligible reduction of 0.5 % in the injected power compared to the forecasted. The

[23] For the distribution of ε_a^{PV}, only non-zero measures of power are taken into account.

[24] Stated according to formula: $\varepsilon_r = \frac{\varepsilon_a}{P_n}$.

forecasted and the real aggregated absorbed energy are around 200.5 kWh and 130.7 kWh, meaning a 53.4 % reduction with respect to the forecasted consumption. The discussed data about produced and consumed energy are related to the 24 hours. Hence in the 4.8 hours test, the real energy consumption and production are around 26.1 kWh and 30.2 kWh.

Theses described profiles are used to run two different real-time simulations, in order to analyse different behaviours and responses of the microgrids:

- Scenario 1.a without intra-day re-optimizations, which aims to analyse the microgrid's behaviour and response while, microgrid has to respect the engaged profile;
- Scenario 1.b with intra-day re-optimizations, which aims to analyse the microgrid's behaviour and response, while on the contrary microgrid has the possibility to trade new intra-day engaged profiles.

Clearly, during the measure campaign all physical and representative quantities are collected (phase-to-phase and line-to-line voltages, line currents, active and reactive powers, contactors state, etc.). However, in the following description only fundamental measures for our observations are reported. In case of grid-connected microgrid, voltage and frequency are considered maintained and regulated by the main grid and hence they are not analysed.

Scenario 1.a without intra-day re-optimizations

Following figures show the outcomes of the real-time test without intra-day re-optimizations. Hence as mentioned, the goal is to respect the engaged profile by using the flexible components in the microgrids that in this particular case are a storage system and a photovoltaic system.

The regulation power (P_C) computed each 30 seconds is obtained as described in Tab. V.2 and is plotted in blue in Fig. V.13. The control set-point ($P_{BATT_{sp}}$) and the real measured output (P_{BATT_m}) of the battery are displayed in orange and yellow curves in Fig. V.13. The set-point power is applied every 30 sec at instant t_c. Measures are gathered each 5 seconds, therefore in following figures are used measures gathered each $t_m = t_c + 20\ sec$.

The evolution during the test of the state of charge computed by the BMS for each battery and the overall state of charge of the pack are shown in Fig. V.14. At the end of the test, the value of SOC^p reaches around 61.5 %, instead of the desired 50.0 %.

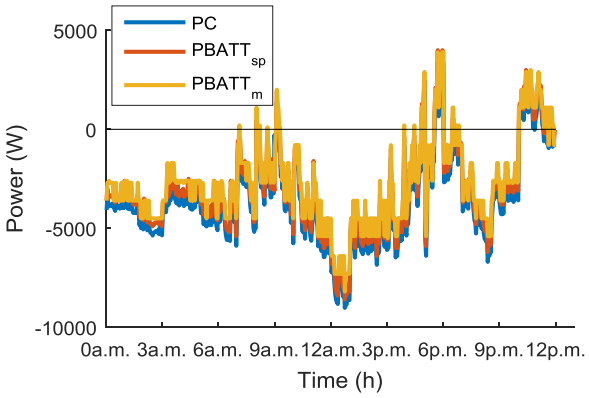

Fig. V.13 Comparison between P_C, $P_{BATT\,sp}$ and $P_{BATT\,m}$ without intra-day re-optimizations[25]

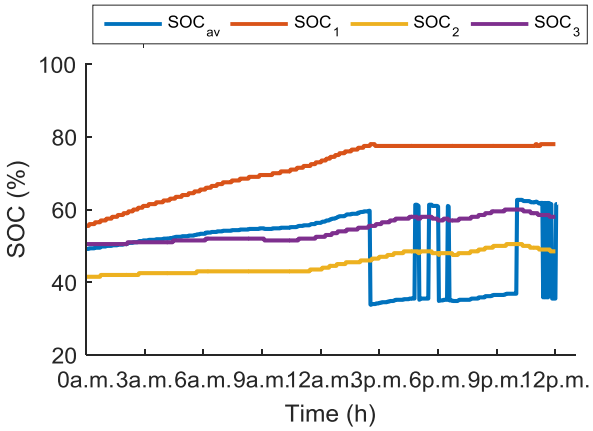

Fig. V.14 SOC^p and SOC^b for all three batteries in the ESS without intra-day optimization

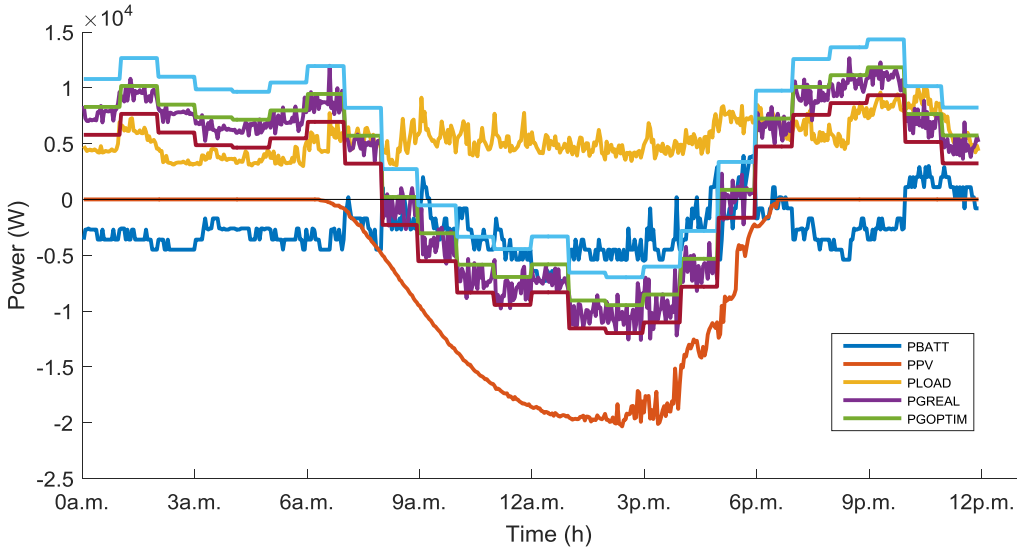

Fig. V.15 Real power profiles of photovoltaic, battery, consumption and grid exchange in t_m without intra-day re-optimizations

Fig. V.15 and Fig. V.16 show the global outcomes of this test. The first figure shows the measured powers each t_m and the second the averaged profiles over 30 seconds. In both figures, the green line shows the outcome of the *D-1* scheduling of the grid-connected microgrid. Upper and lower bounds representing the 10.0 % of the microgrid's rated power are also depicted in light-blue and red lines. As mentioned earlier, the microgrid has bidirectional power flux at the PCC. In fact, it schedules to supply energy to the main grid between 8.00 a.m. and 6.00 p.m., and to absorb it for the rest of the day. In the graphic, the orange line represents the measured power in output to the AC side of the ABB inverter.

[25] Positive values of $P_{BATT\,sp}$ and $P_{BATT\,m}$ indicate a discharging state of the battery, while negative values a charging state.

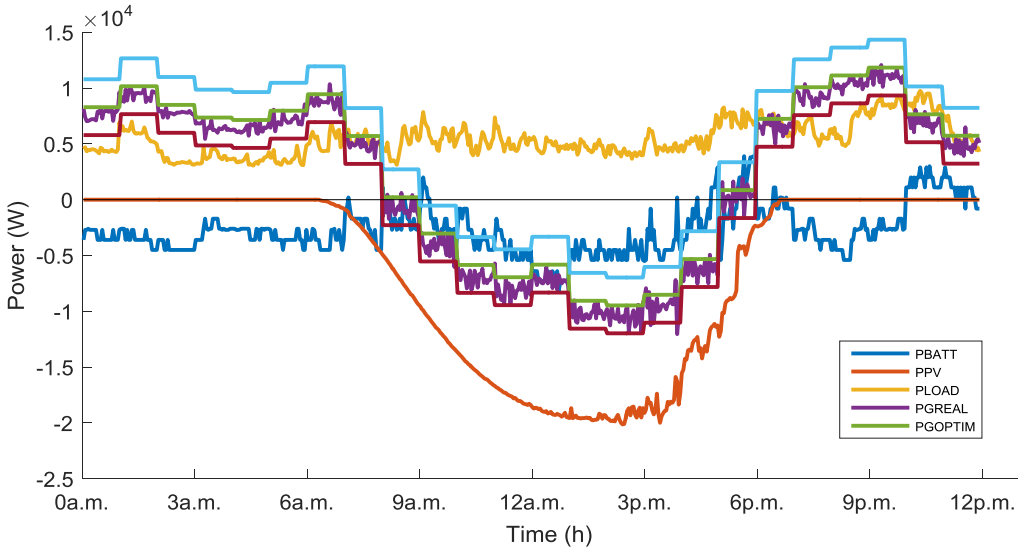

Fig. V.16 Mean profiles of photovoltaic, battery, consumption and grid exchange without intra-day optimization

Whereas, the yellow line is the simulated aggregated consumption. The violet curve is the final power exchange at the PCC.

Scenario 1.b with intra-day re-optimizations

In this second case, the outcomes of the real-time test with intra-day re-optimizations are discussed. Hence, the objective is to re-schedule the microgrid operation in order to use more efficiently the available resources and after in real-time respect the new engaged profile by using the ESS and as well as the PV if needed.

As in previous case, the control set-point and the real measured output of the battery are displayed in orange and yellow curves in Fig. V.17. The SOC^b of each battery and the SOC^p are then displayed in Fig. V.14. The microgrid's re-scheduled profile with the various intra-day re-optimizations is shown in Fig. V.19. In this figure, the name of the curves represents the time of the day in which the re-optimization is effectuated. As shown, 12 re-optimizations were applied. Before each re-optimization, the PV and consumption profiles are re-forecasted by using last 30-minutes measures and method presented in section V.2.2. The load intra-day re-forecasted profiles computed for each re-optimization are shown in Fig. V.20 (with the same colour legend applied in Fig. V.19). In this case, due to the small difference in the injected energy, the PV profile is not re-forecasted. In these two figures, the dark-green curves (named with "0") represent the day-ahead microgrid's scheduling and the day-ahead forecasted consumption.

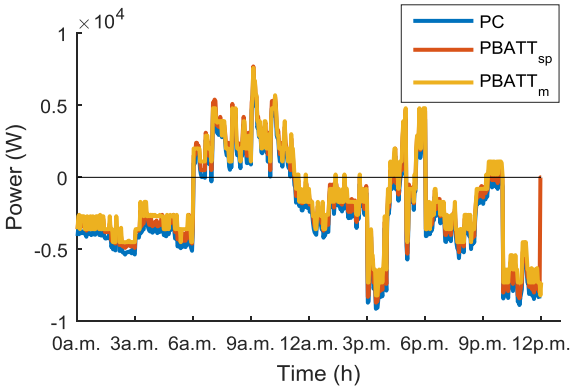

Fig. V.17 Comparison between P_C, $P_{BATT\,sp}$ and $P_{BATT\,m}$ without intra-day re-optimizations

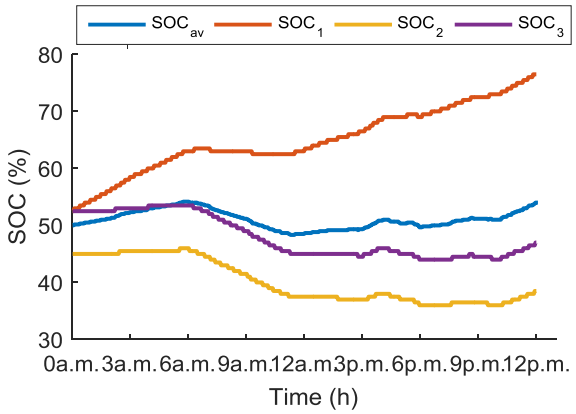

Fig. V.18 SOC^p and SOC^b for all three batteries in the ESS without intra-day optimization

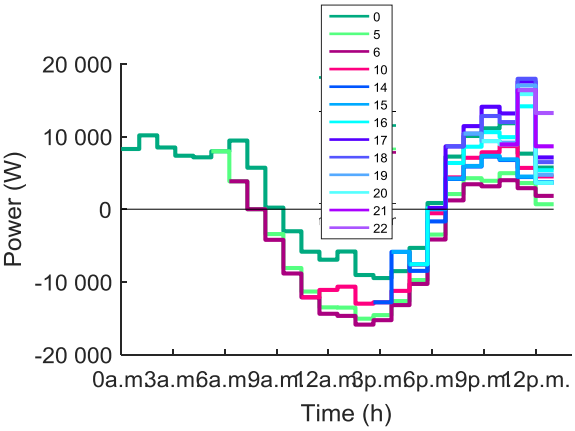

Fig. V.19 Net microgrid's power scheduled with intra-day re-optimizations

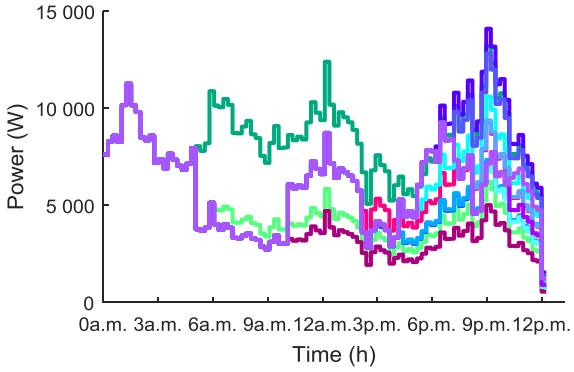

Fig. V.20 Load intra-day forecasted profiles

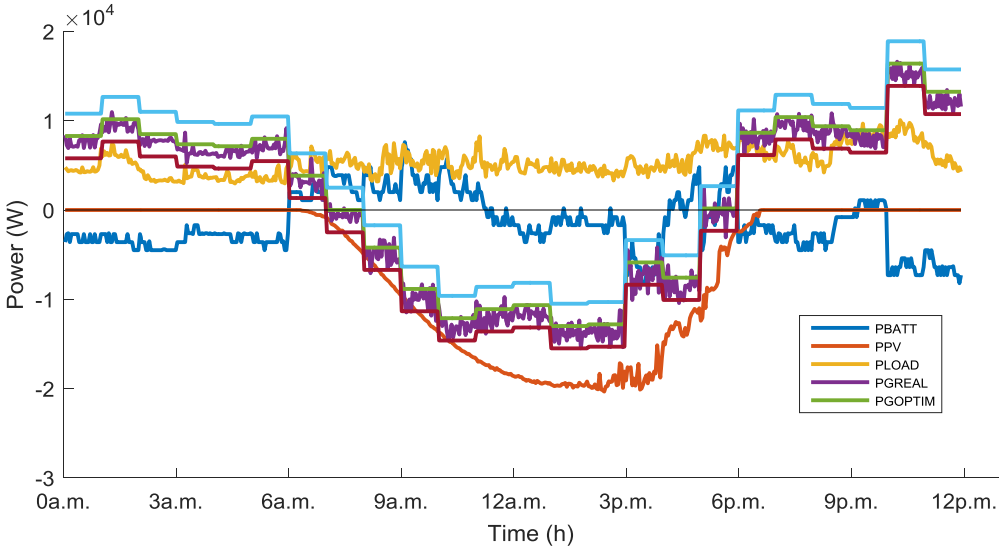

Fig. V.21 Real power profiles of photovoltaic, battery, consumption and grid exchange in t_m with intra-day re-optimizations

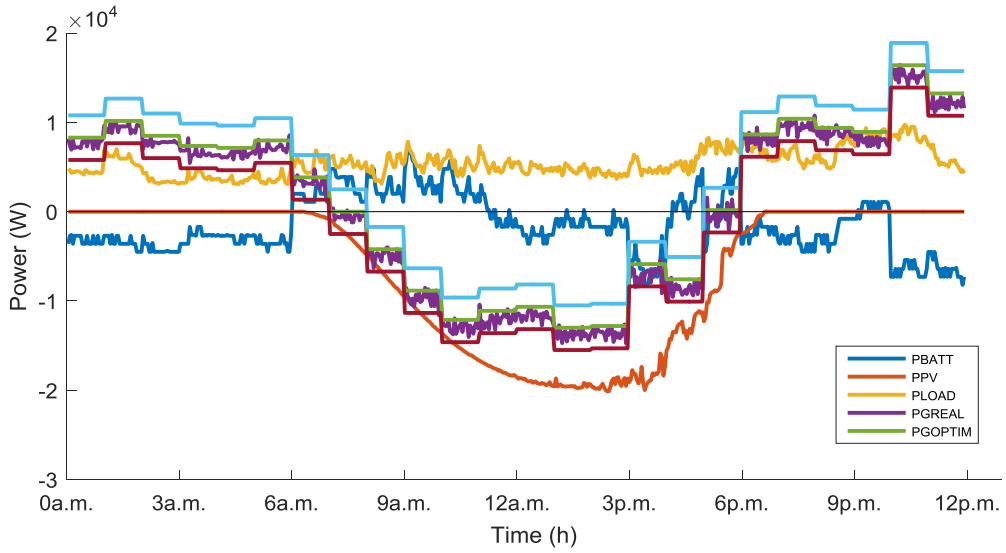

Fig. V.22 Power profiles of photovoltaic, battery, consumption and grid exchange averaged over 30 seconds with intra-day re-optimizations

Whereas in clear-violet in Fig. V.20, the final load profile obtained with the various re-forecasting is presented. The re-scheduling allows to reduce the solicitations of the ESS and to obtain a final SOC^p equal to 54.0 % (Fig. V.18). The behaviour of the components and of the entire microgrid is illustrated by reporting also in this case the actual measured values and the averaged value over 30 sec in Fig. V.15 and Fig. V.16.

The same colours code described previously is used in the graphics. However this time, the green line represents the final intra-day scheduling profile of the microgrid computed when the SOC^p differs more than 20.0 % from the previous schedule. In the rescheduled profile, due to the consumption reduction in respect of the forecasted profile, the microgrid supplies energy to the main grid between 7.00 a.m. and 6.00 p.m..

Comparison between Scenario 1 without and with intra-day re-optimizations

In both cases, the measured battery power is lower or equal to the battery control set-point which is essentially caused by the control granularity of the battery. The PV system power is never cut as the battery is able to provide the necessary support. Fig. V.14 and Fig. V.18 show the different usage of the single battery in the pack. In fact, the battery 1 is more used and stressed then battery 2 and 3. This is due to the not-homogeneous ageing of the three batteries and also from their different healthy state (in particular, out of order cells). Moreover, the battery 1 disconnects when reaches the 80.0 % of its SOC, as at 2.30 p.m., by inducing a rapid

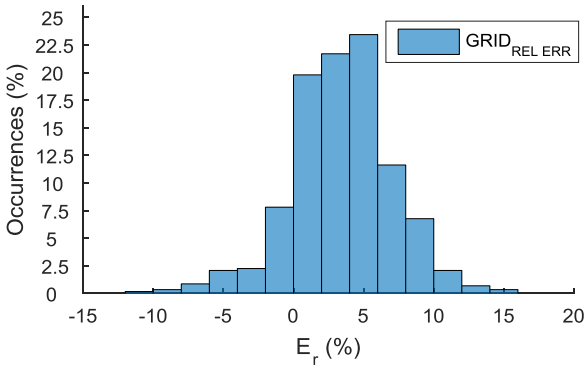

Fig. V.23 Distribution of errors between forecasted and real measured powers at PCC on microgrid P_n for case 1.a

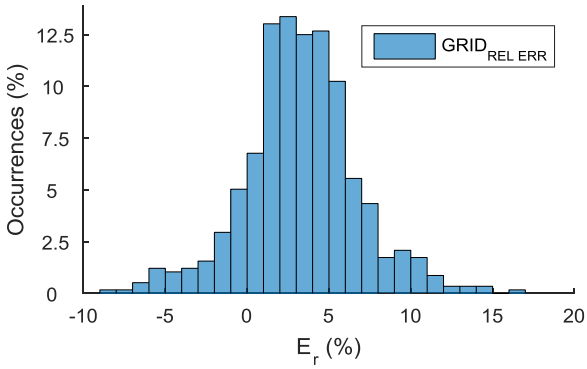

Fig. V.24 Distribution of errors between forecasted and real measured powers at PCC on microgrid P_n for case 1.b

	Case 1.a		**Case 1.b**	
	MESURE (t_m=t_c+20 sec)	**AVERAGE** (30 sec)	**MESURE** (t_m=t_c+20 sec)	**AVERAGE** (30 sec)
x ≥ -15	0.0 %	0.00 %	0.00 %	0.00 %
-15 < x ≤ -10	0.2 %	0.00 %	0.00 %	0.00 %
-10 < x ≤ -5	2.3 %	0.35 %	2.08 %	0.35 %
-5 < x ≤ 0	11.1 %	6.77 %	11.81 %	6.77 %
0 < x ≤ 5	55.2 %	69.97 %	58.33 %	69.97 %
5 < x ≤ -10	28.1 %	22.05 %	23.96 %	22.05 %
10 < x ≤ 15	3.0 %	0.87 %	3.65 %	0.87 %
x ≥ 15	0.2 %	0.00 %	0.17 %	0.00 %

Tab. V.4 Occurrences of percent values of the error between forecasted and real measured powers at PCC

loss of the pack available SOC. Furthermore, the use of re-optimization allows to reduce the battery's solicitations and to refresh the final SOC to a value closer than the imposed 50.0 %. In fact, the SOC_f is equal to 61.5% without re-optimization and 54.0 % with re-optimizations.

It is not possible to reach exactly 50.0 % of SOC because of the forecast errors in the last operating hour. In fact, the last possible re-optimization was at 10.00 p.m., due to the lack of data for *D+1*. However, in a continuous process with more days test it will be possible to reschedule the microgrid's profile by reaching a final SOC (SOC_f) closer to the imposed value.

The final power exchange at the PCC oscillates around the forecasted value. The distribution of the errors between the forecasted and the real measured powers at PCC on microgrid P_n are illustrated in Fig. V.23 and Fig. V.24 for both analysed cases.

	D-1	Case 1.a	Case 1.b
C_{DG}	16.4 €	18.2 €	18.2 €
C_{ESS}	0.7 €	10.6 €	8.2 €
$C_{g_{BUY}}$	22.4 €	20.3 €	20.5 €
$C_{g_{SELL}}$	-7.8 €	-9.2 €	-13.7 €
DC*	31.7 €	39.9 €	33.1 €
MF*	14.6 €	11.1 €	6.7 €

**MF*: Daily money flow between the µgrid and DSO (expenses and revenues); * *DC*: Daily expense or revenue of the µgrid considering the money flow with the DSOA/AGGA, the DG costs and the ESS costs

Tab. V.5 Daily economic results of Scenario 1

The percent occurrences at various percent intervals between -15.0 % and 15.0 % with an increasing step of 5.0 % are resumed in Tab. V.4. As shown in the case without re-optimization, 66.3 % of the errors are comprised between -5.0 % and 5.0 % and 96.7 % are comprised between -10.0 % and 10.0 %. Otherwise with re-optimization, the same percentage intervals comprise 70.1 % and 96.3 % of the errors. Hence in both cases, the error is almost lower than ±10.0 % of P_n by guaranteeing a good reliability.

Tab. V.5 resumes the microgrid's expenses and revenues estimated at *D-1* and obtained with a post real-time analysis. The values in the table are converted for 24 hour operation. The daily expense or revenue (DC) takes into account also C_{DG} and C_{ESS}, which are calculated considering an expense of 12.0 c€/kWh for the PV and 15.0 c€/kWh for the ESS, as introduced in section V.4. The estimated value of DC at *D-1* is lower than the real value for both cases 1.a and 1.b, due essentially to the increase of C_{ESS}. Moreover as stated above, the re-scheduling process allows a more efficient use of components which can also be observed with a DC reduction of around 15.8 % between case 1.a and 1.b. The reduction of $C_{g_{BUY}}$ and the increase of $C_{g_{SELL}}$ with respect to the estimated values at D-1 can be explained by the decrease in consumption, observed in Fig. V.6.

V.4.2. Scenario 2 - Forecasted PV Power higher than the measured one

This second case study considers a day with a high increase in the absorbed energy, which means lower available PV energy and higher energy consumption. In order to represent a significant PV variation a day with high variability in cloudiness condition is considered. The data chosen represents a cloudy day in February. Forecasted profile and measured profile over 5-sec are reported in Fig. V.25. Winter consumption profiles were not available.

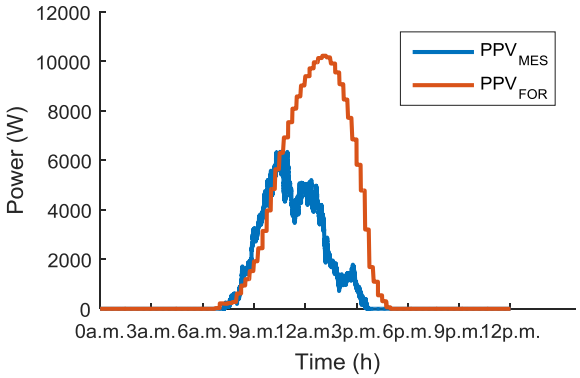

Fig. V.25 PV power profiles of forecasted data over 15 minutes and real-time measures

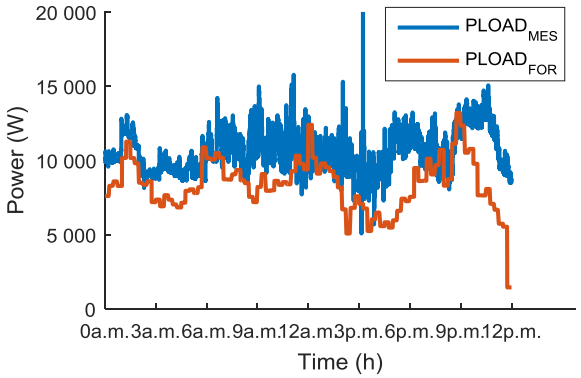

Fig. V.26 Aggregated consumption power profiles of forecasted data over 15 minutes and real-time measures

Hence, consumption profiles used in section V.4.1 were modified. In particular the same profile was applied for the forecast data. Whereas, the real-measure data were scaled of 5000 W, while maintaining the same form. Both profiles are shown in Fig. V.26.

Also for this case study, an analysis of power and energy prediction errors is presented for both production and consumption. The trends of ε_a^{PV}, ε_a^{C} and ε_a^{PV+C} for the 24-hours in analysis are shown in Fig. V.27, Fig. V.29 and Fig. V.31. ε_a^{PV} and ε_a^{C} vary between a maximal and minimal value which correspond to 8307 W and -1596 W, and 3617 W and -15227 W, respectively. Their combination of errors ε_a^{PV+C} vary between -20257 W and 2278 W. The distribution of percent error on microgrid rated power over different percent intervals are resumed in Tab. V.6 and depicted in Fig. V.28, Fig. V.30 and Fig. V.32. For the PV only around 59.5 % of errors is contained in the percent interval of ±15.0 %. Whereas, the 80.1 % of the consumption error and 63.2 % of the global error are contained in this interval. While, these percentages fall drastically to 24.4 %, 19.7 % and 15.2 % respectively, if the considered interval is ±5.0 %. Whereas from the energetic point view, the forecasted and the real injected energy by the PV system are 47.8 kWh and 22.3 kWh, respectively. Hence, the injected power was the 50.3 % lower than the amount estimated at *D-1*. The forecasted and the real aggregated absorbed energy is 200.5 kWh and 254.9 kWh that is an increase of 21.3 %. In the test, the consumption and the production are around 51.0 kWh and 4.3 kWh. As in previous section, a results comparison is made between two real-time simulations:

- Scenario 2.a without Intra-Day Re-Optimizations
- Scenario 2.b with Intra-Day Re-Optimizations

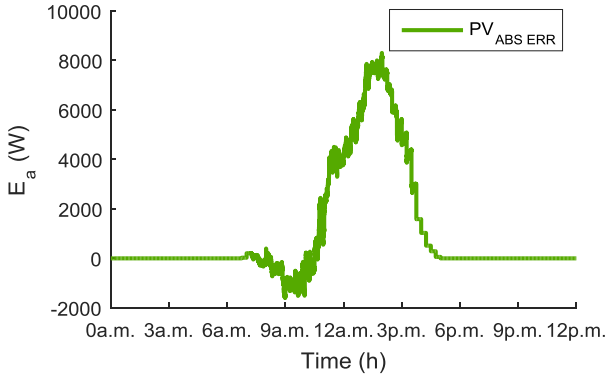

Fig. V.27 Absolute error between forecasted and real values of PV power (ε_a^{PV})

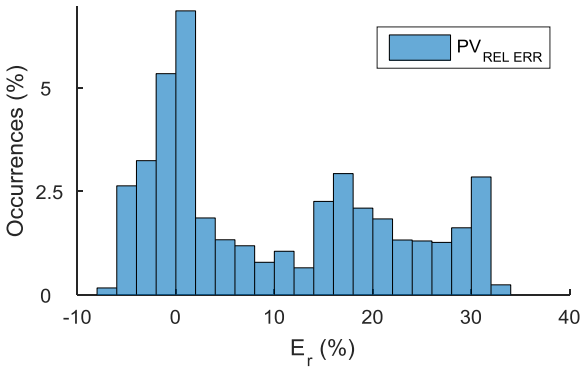

Fig. V.28 Distribution of ε_a^{PV} on microgrid P_n

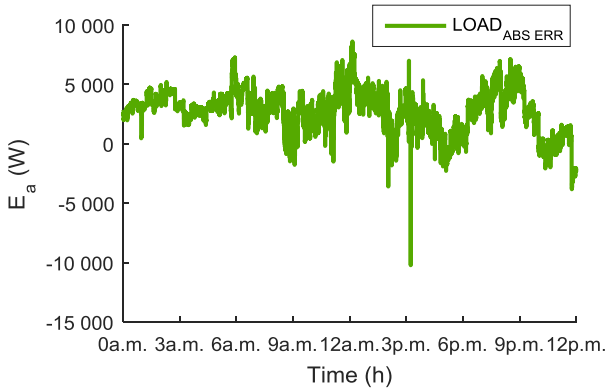

Fig. V.29 Absolute error between forecasted and real values of load power (ε_a^C)

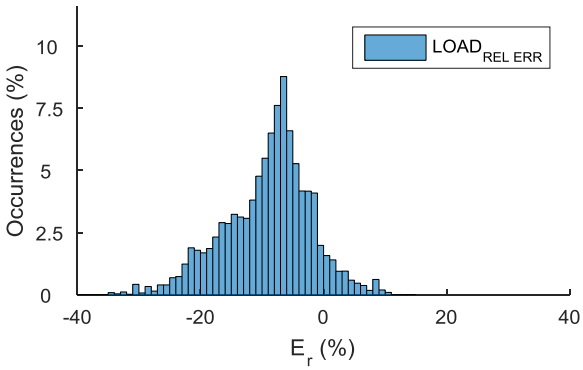

Fig. V.30 Distribution of ε_a^C on microgrid P_n

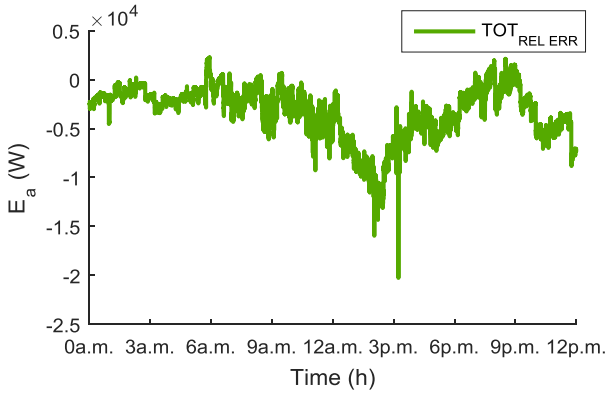

Fig. V.31 Absolute error between forecasted and real values of total microgrid power (ε_a^{PV+C})

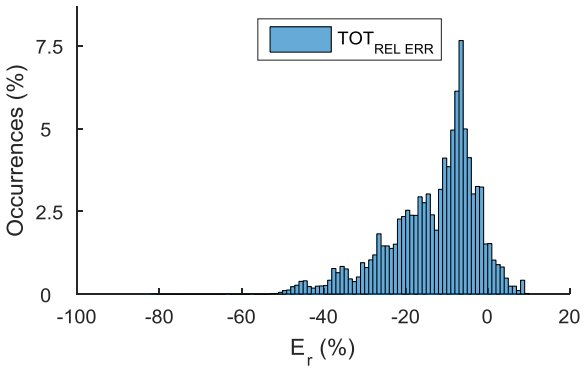

Fig. V.32 Distribution of ε_a^{PV+C} on microgrid P_n

	< -20	**-20/-15**	**-15/-10**	**-10/-5**	**-5/0**	**0/5**	**5/10**	**10/15**	**15/20**	**> 20**
$\boldsymbol{\varepsilon_a^{PV}}$	0.0 %	0.0 %	0.0 %	2.2 %	24.4 %	23.3 %	4.8 %	4.8 %	16.2 %	24.3 %
$\boldsymbol{\varepsilon_a^{C}}$	8.3 %	11.6 %	18.0 %	35.0 %	19.7 %	5.5 %	1.8 %	0.1 %	0.0 %	0.0 %
$\boldsymbol{\varepsilon_a^{PV+C}}$	23.8 %	13.0 %	14.6 %	27.6 %	15.2 %	4.8 %	1.0 %	0.0 %	0.0 %	0.0 %

Tab. V.6 Occurrences of percent values of $\boldsymbol{\varepsilon_a^{PV}}$, $\boldsymbol{\varepsilon_a^{C}}$ and $\boldsymbol{\varepsilon_a^{PV+C}}$ at various percent intervals

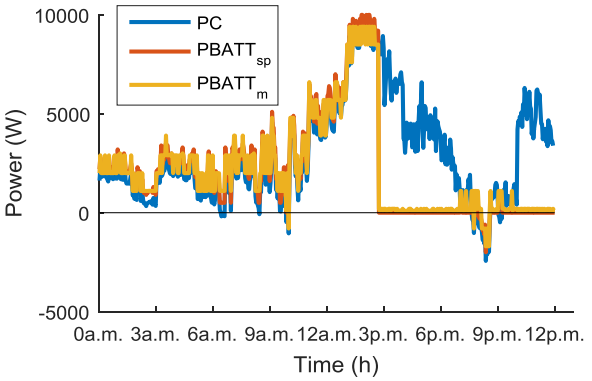

Fig. V.33 Comparison between P_C, $P_{BATT\,sp}$ and $P_{BATT\,m}$ without intra-day re-optimizations

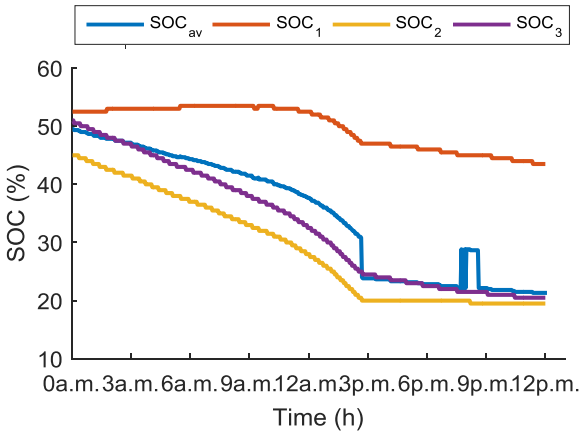

Fig. V.34 SOC^p and SOC^b for all three batteries in the ESS without intra-day optimization

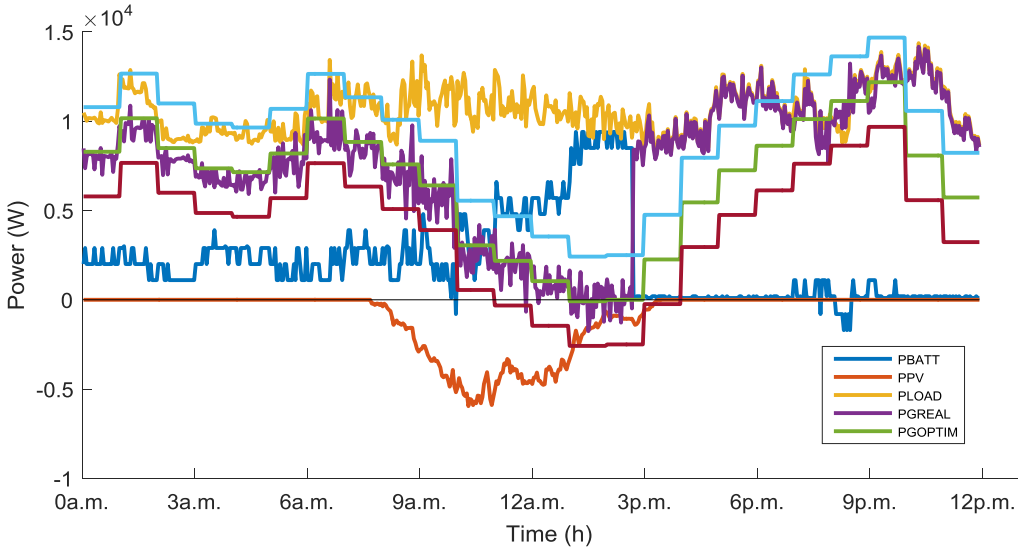

Fig. V.35 Real power profiles of photovoltaic, battery, consumption and grid exchange in t_m without intra-day re-optimizations

I. Scenario 2.b without Intra-Day Re-Optimizations

The computed control set-point of the battery and its real measured output are shown in Fig. V.33. Furthermore, the state of charge computed by the BMS for each battery and the overall SOC of the pack are illustrated in Fig. V.34. In this case study, the ESS is the unique components able to supply positive flexibility that means inject more energy. Hence, $P_{BATT\,sp}$ cannot be set to P_C between the two time intervals 2.43 p.m. – 7.00 p.m. and 9.52 p.m. – 00.00 a.m.. As shown in Fig. V.34, during these timeframes the SOC of battery 2 and 3 reaches values lower than the lower-limit set for the battery's SOC, which is 25.0 %. Battery 2 was more stressed and reached a SOC of 20.0 % which induced the opening of its contactor.

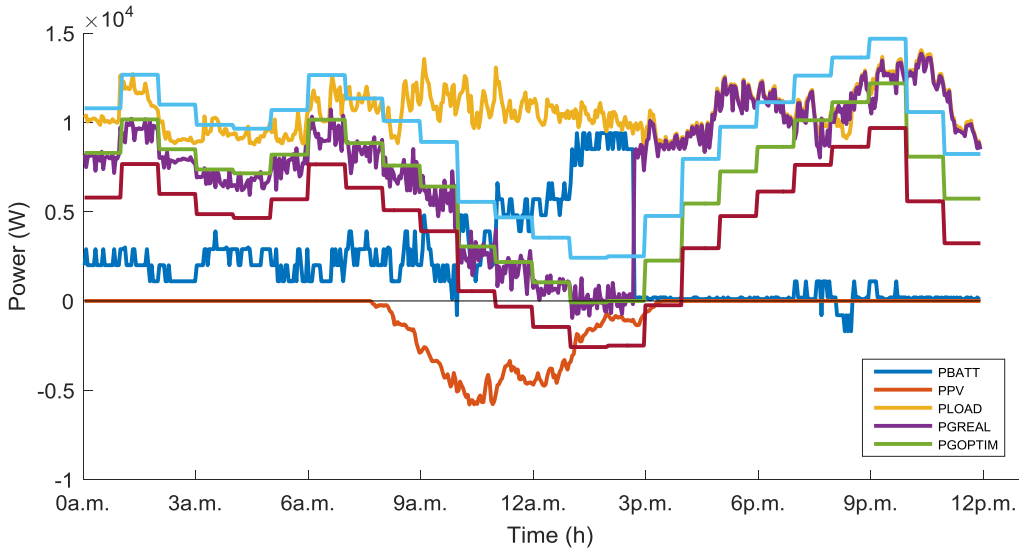

Fig. V.36 Mean profiles of photovoltaic, battery, consumption and grid exchange without intra-day optimization

Battery 3 did not reach the opening limit and continued to slowly lose its energy reaching the 20.5 % at the end of the test. The low energetic state of battery 2 and 3 induced a final pack's SOC of around 23.3 %.

In Fig. V.35 and Fig. V.36, the measured powers each t_m and the averaged profiles over 30 seconds are reported, using the same colour code described in section V.4.1. Due to the low available production, the microgrid gets a passive behaviour by mainly absorbing energy from the main grid. Starting from 2.43 p.m., the lack of positive flexibilities induces a bad control of the microgrid which does not respect the engaged profile at the PCC.

II. Scenario 2 with Intra-Day Re-Optimizations

As in previous case, P_C, $P_{BATT_{sp}}$ and P_{BATT_m} are compared in Fig. V.37. The re-scheduling process allows to reduce the amount of flexibility to control in order to respect the engaged plan. Hence in this case study, the available flexibility is enough to implement a satisfying control. The batteries' and pack's SOC are displayed in Fig. V.38.

As reported in Fig. V.39, the microgrid's operation is re-scheduled 10 times. Each time the load profile is re-forecasted and the PV profile is re-forecasted at 9.00 a.m.. A comparison between the da-ahead forecasted profile, the final re-forecasted profile and the real measured consumption is shown in Fig. V.40. Because of the low performances of the intra-day forecasting algorithm, a high error in the forecast process of both profile persists. Hence, a large support of the battery continues to be request by the control algorithm and the final SOC

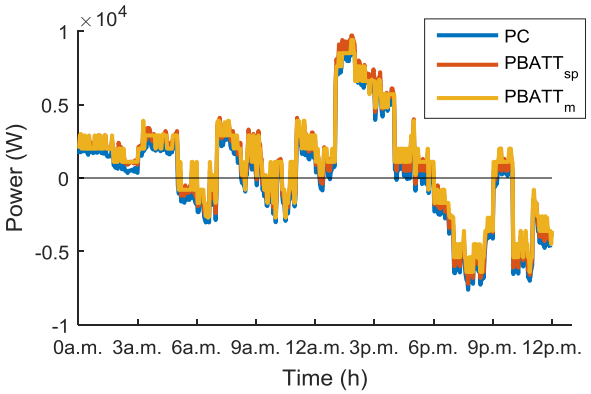

Fig. V.37 Comparison between P_C, $P_{BATT\,sp}$ and $P_{BATT\,m}$ with intra-day re-optimizations

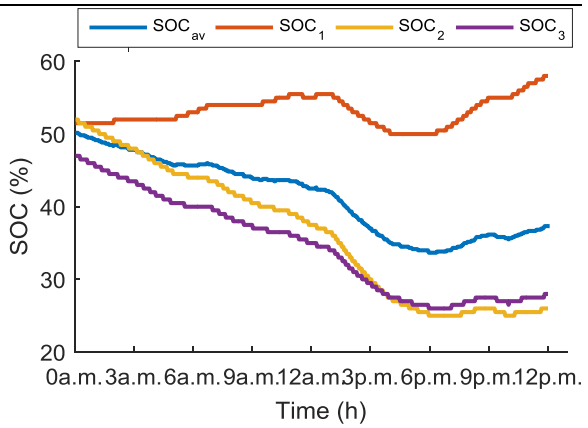

Fig. V.38 SOC^p and SOC^b for all three batteries in the ESS with intra-day optimization

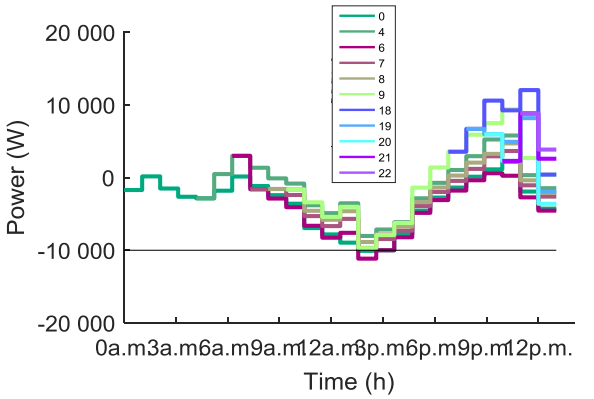

Fig. V.39 Net microgrid's power scheduled with intra-day re-optimizations

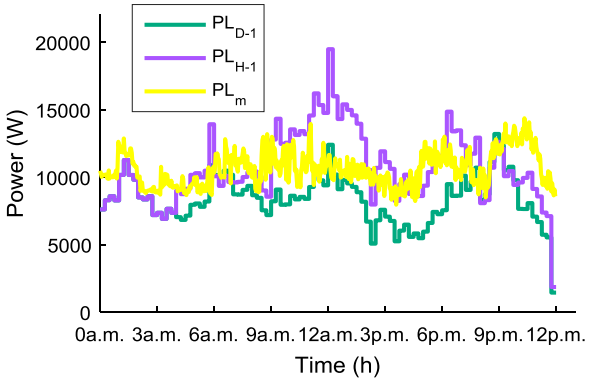

Fig. V.40 Comparison between D-1, final re-forecasted and measured consumption profiles

is equal to 37.5 % which is far from the desired value, but higher than the value reached in the previous test.

Fig. V.41 and Fig. V.42 illustrate the actual and averaged results of the test, which clearly show a more performant control thanks to the combination of re-optimization algorithm and the ESS.

Comparison between Scenario 2 without and with intra-day re-optimizations

This case studies show clearly the behaviour of the battery for low SOC and confirm the control granularity of the battery and the losses due the inverter auto-consumption (see $P_{BATT\,sp}$ and $P_{BATT\,m}$ in Fig. V.33 and Fig. V.37). Both Fig. V.34 and Fig. V.38 show a different usage of each single battery in the pack. However, in both cases battery 2 and 3 are subject to a more deep discharge, which induces a less efficient use of the ESS. This

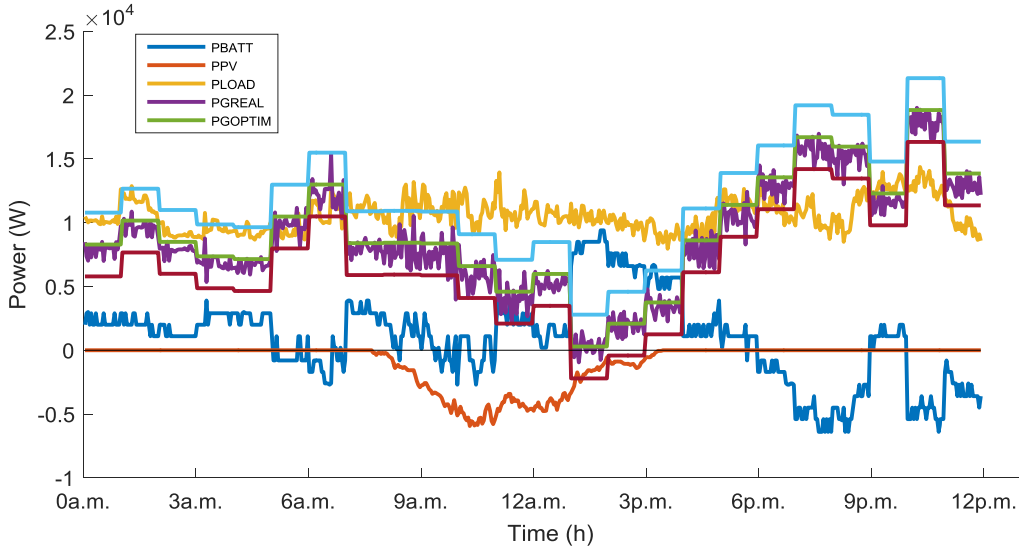

Fig. V.41 Real power profiles of photovoltaic, battery, consumption and grid exchange in t_m with intra-day re-optimizations

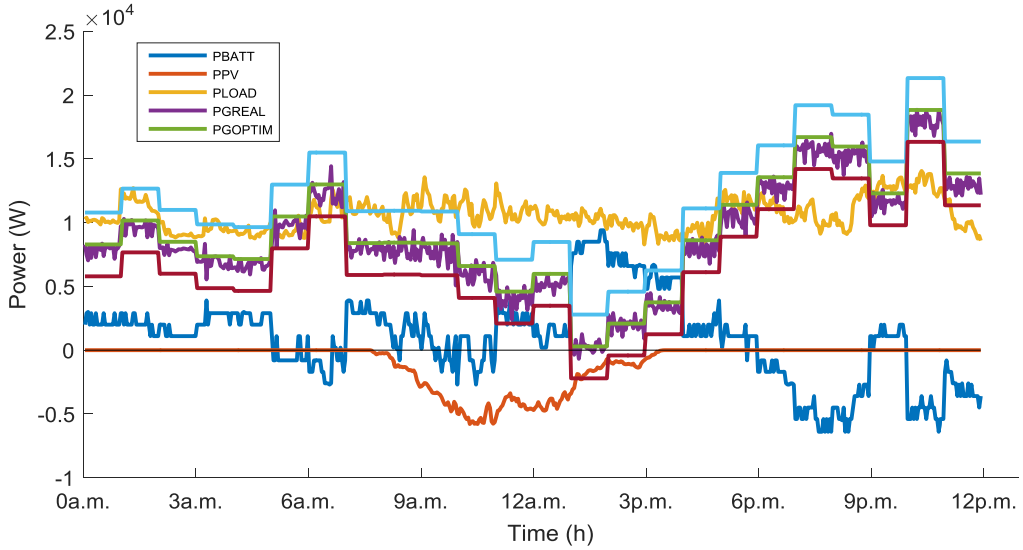

Fig. V.42 Power profiles of photovoltaic, battery, consumption and grid exchange averaged over 30 seconds with intra-day re-optimizations

behaviour is caused by the not-homogeneous healthy state of the three batteries, which induces a lower resistance of battery 2 and 3.

As in section V.4.1, the use of re-optimization allows to reduce the battery's solicitations and to restore the pack's SOC in order to reach a final value of 50.0 %. However, also if the re-schedule allows a higher SOC_f respect to the case without optimization, the low performance of the intra-day forecasting algorithm and the forecast error in the last "hour of the day" impose a SOC_f of 37.5 %. In fact, also in this case the last re-optimization that is possible to run is at 10.00 p.m..

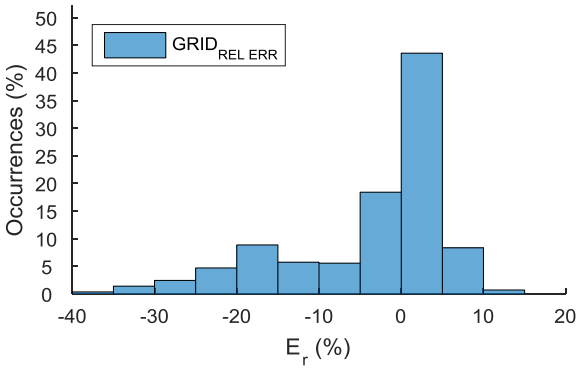

Fig. V.43 Distribution of errors between forecasted and real measured powers at PCC on microgrid P_n for case 2.a

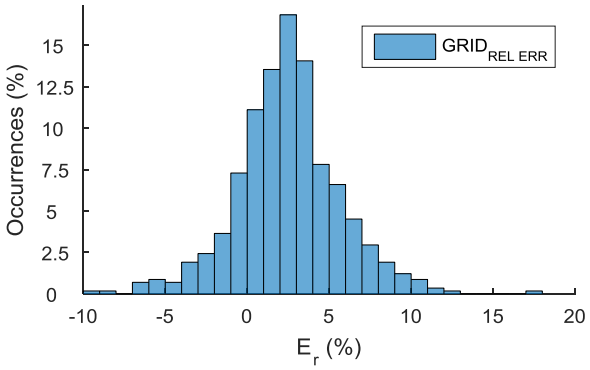

Fig. V.44 Distribution of errors between forecasted and real measured powers at PCC on microgrid P_n for case 2.b

	Without intra-day re-optimizations		With intra-day re-optimizations	
	MESURE (t_m=t_c+20 sec)	AVERAGE (30 sec)	MESURE (t_m=t_c+20 sec)	AVERAGE (30 sec)
x ≥ -15	17.7 %	17.7 %	0.0 %	0.0 %
-15 < x ≤ -10	5.7 %	6.1 %	0.0 %	0.0 %
-10 < x ≤ -5	5.6 %	3.8 %	1.9 %	0.5 %
-5 < x ≤ 0	18.4 %	17.2 %	16.0 %	12.7 %
0 < x ≤ 5	43.6 %	50.2 %	63.4 %	74.5 %
5 < x ≤ -10	8.3 %	5.0 %	17.2 %	12.2 %
10 < x ≤ 15	0.7 %	0.0 %	1.4 %	0.2 %
x ≥ 15	0.0 %	0.0 %	0.2 %	0.0 %

Tab. V.7 Occurrences of percent values of forecasted and real measured powers at PCC

The final power exchange at the PCC oscillates around the forecasted value. For both case studies, the percent distribution of these oscillations on microgrid P_n is shown in Fig. V.43 and Fig. V.44.

The distribution of these percent oscillations for various percent intervals is reported in Tab. V.7. Form these results, the 62.0 % of these oscillations are comprised between -5.0 % and 5.0 % in the first case. For the secon case, this interval comprises the 79.4 % of oscillations. However, these percentages rise to 75.9 % and 98.5 % by considering a symmetric increase of 5.0 % of this interval.

Tab. V.8 resumes the microgrid's expenses and revenues estimated at *D-1* and obtained with a post real-time analysis for 24 hours of operation. The estimated value of DC at *D-1* is lower than the real value for both cases 2.a and 2.b, due to the increase in the consumption compared to the forecasted, which increases $C_{g_{BUY}}$, and the C_{ESS} expense.

	D-1	2.a	2.b
C_{DG}	5.1 €	2.6 €	2.6 €
C_{ESS}	1.0 €	0.1 €	3.4 €
$C_{g_{BUY}}$	30.3 €	34.7 €	39.8 €
$C_{g_{SELL}}$	0.0 €	0.0 €	0.0 €
DC*	36.4 €	37.3 €	45.7 €
MF*	30.3 €	34.7 €	39.8 €

**MF*: Daily money flow between the µgrid and DSO (expenses and revenues); * *DC*: Daily expense or revenue of the µgrid considering the money flow with the DSOA/AGGA, the DG costs and the ESS costs

Tab. V.8 Daily economic results of Scenario 2

Moreover, DC is higher for case 2.b than for case 2.a. However, this parameter does not respect the expense reality. In fact first and foremost it is needed to consider that in the used model the C_{ESS} is computed only when the ESS is charging. Furthermore in case I, the ESS injects energy between 0.00 a.m. and around 2.45 p.m. and the SOC^p is not restored, which causes the reduction of $C_{g_{BUY}}$ and C_{ESS}. However, this cost will be part of the D+1 costs making this reduction a simple illusion. On the contrary in case 2.b, the ESS is charged between 6.00 p.m. – 9.00 p.m. and 10.00 p.m. – 12.00 p.m. starting to restore the SOC^p and increasing C_{ESS}.

V.4.3. Scenario 3 - Forecasted PV Power lower than the measured one

This third case study aims to analyse the impacts of a second worst case scenario on the microgrid's operation. This scenario implements a day with an increase in the local production and a reduction in the local consumption compared to the forecasted scenario. The prediction error is then caused by wrong forecast of both profiles. The PV profile represents a sunny day at the end of February, in which the meteorological conditions are particularly favourable. The day-ahead and the real-time profiles used in the test are shown in Fig. V.45. Whereas, due to a lack of consumption measures for the month of February, the data described in section V.4.2 are exploited. In order to let the PV be more predominant in the error, the measured profile was increased of 1000 W, while maintaining the same profile for the forecast, as depicted in Fig. V.46.

Also in this case, the analysis of power prediction errors is briefly presented for both production and consumption. The trends of ε_a^{PV}, ε_a^{C} and ε_a^{PV+C} are depicted in Fig. V.47, Fig. V.49 and Fig. V.51. As can be seen, the unexpected surplus in the PV production induces a significant error, which is predominant in the global error and strongly impacts the process of

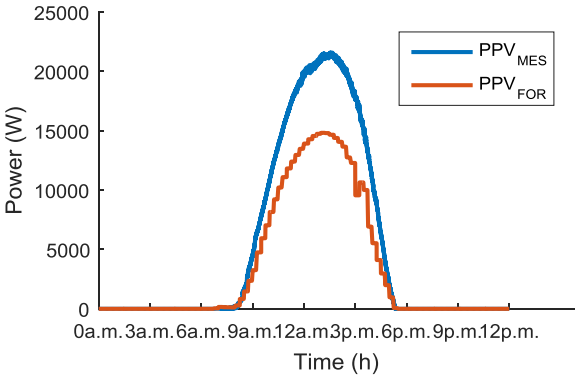

Fig. V.45 PV power profiles of forecasted data over 15 minutes and real-time measures

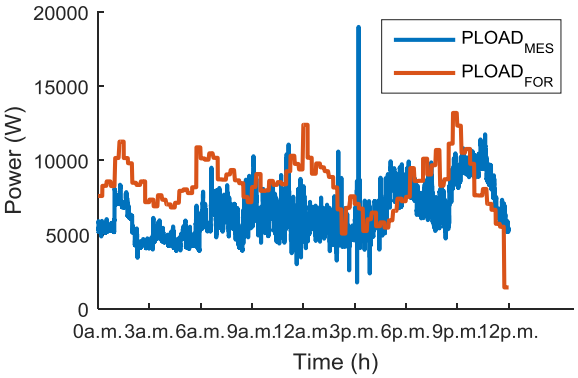

Fig. V.46 Aggregated consumption power profiles of forecasted data over 15 minutes and real-time measures

re-scheduling. The distribution of error in Fig. V.48 and the shape of ε_a^{PV}, which follows the typical shape of PV production, show that the forecast has underestimated the real available power for all hours of the day. Furthermore, the analysis of the error distribution displays that a high density of instances, around 52.6 %, are in intervals less than the -15.0 %. The remaining 47.4 % is comprised between the -15.0 % and 5.0 %, as shown in Tab. V.9. The negative peak value of ε_a^{PV} reaches around -7819 W at around 3.00 p.m.. The trend of ε_a^{C} is resumed in Fig. V.49 and Fig. V.50, but assumes the same behaviour described in section V.4.1.

It is very interesting to describe the behaviour of their combination (resumed in Fig. V.51 and Fig. V.52). As expected, there is a large positive peak with a concave downward shape between 9.00 a.m. and 4.00 p.m. which clearly indicates an increase in the production, which will necessary need a re-scheduling process and a new trade with the DSO. Moreover, two negative peak with lower absolute value and a concave upward shape are encountered between 4.30 p.m. - 6.15 p.m. and 10.00 p.m. - 11.45 p.m., due to the lower consumption. The upper and lower peaks of ε_a^{PV+C} reach respectively 14222 W and -5530 W. The upper limit is very high and pushes the percent distribution of ε_a^{PV+C} toward high percent interval as Tab. V.9. However, around 60.8 % of instances are in the interval between ± 15.0 %.

From the energetic point view, the daily forecasted and the real producible energy by the PV are 79.3 kWh and 116.9 kWh, respectively, which means an increase of the 47.4 % with respect to the amount estimated at *D-1*. For the consumption, the daily energy forecasted and the considered absorbed energy are respectively 200.5 kWh and 154.7 kWh that is a decrease

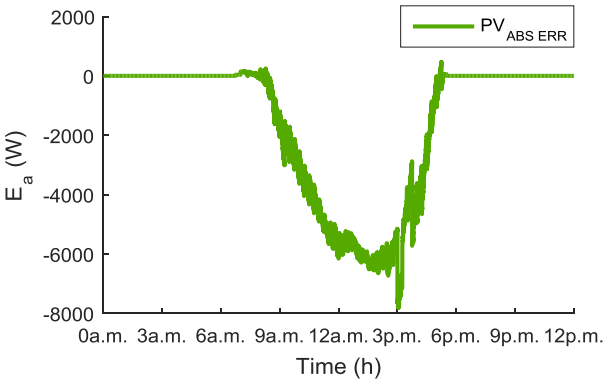

Fig. V.47 Absolute error between forecasted and real values of PV power (ε_a^{PV})

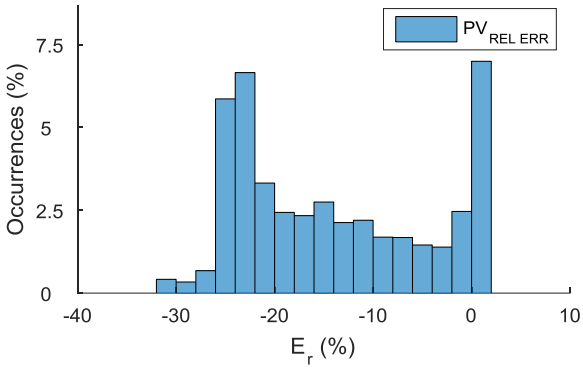

Fig. V.48 Distribution of ε_a^{PV} on microgrid P_n

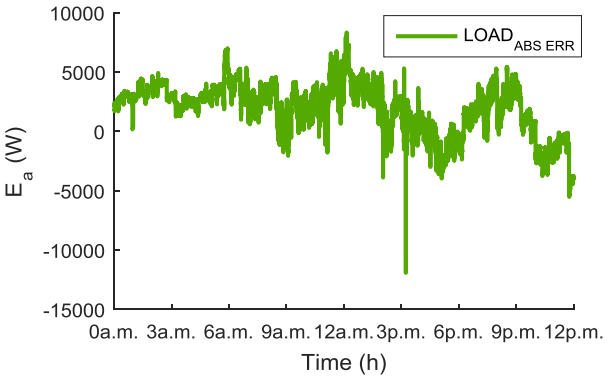

Fig. V.49 Absolute error between forecasted and real values of load power (ε_a^{C})

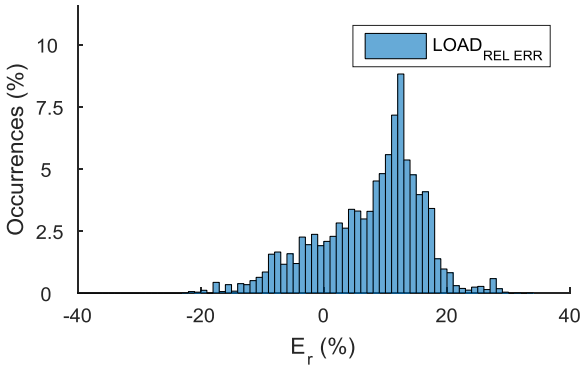

Fig. V.50 Distribution of ε_a^{C} on microgrid P_n

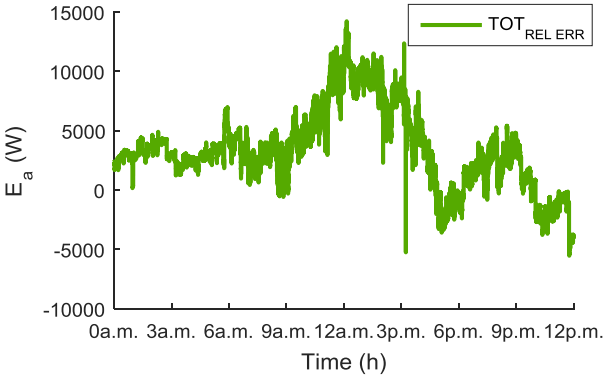

Fig. V.51 Absolute error between forecasted and real values of total microgrid power (ε_a^{PV+C})

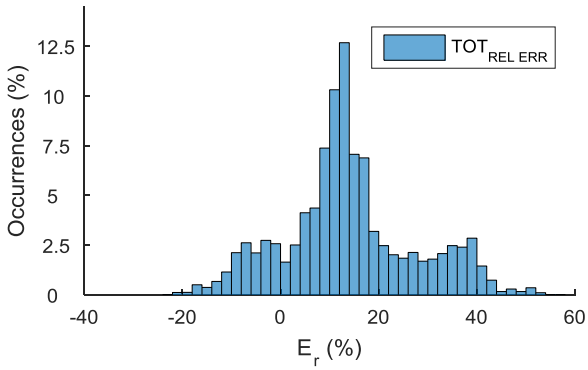

Fig. V.52 Distribution of ε_a^{PV+C} on microgrid P_n

	< -20	**-20/-15**	**-15/-10**	**-10/-5**	**-5/0**	**0/5**	**5/10**	**10/15**	**15/20**	**> 20**
$\boldsymbol{\varepsilon_a^{PV}}$	38.6 %	14.1 %	12.4 %	9.2 %	10.1 %	15.6 %	0.0 %	0.0 %	0.0 %	0.0 %
$\boldsymbol{\varepsilon_a^{C}}$	0.1 %	1.0 %	1.9 %	6.8 %	9.7 %	13.2 %	18.9 %	31.7 %	13.8 %	2.9 %
$\boldsymbol{\varepsilon_a^{PV+C}}$	0.1 %	0.9 %	1.8 %	6.1 %	6.0 %	6.0 %	14.0 %	26.8 %	13.3 %	24.9 %

Tab. V.9 Occurrences of percent values of $\boldsymbol{\varepsilon_a^{PV}}$, $\boldsymbol{\varepsilon_a^{C}}$ and $\boldsymbol{\varepsilon_a^{PV+C}}$ at various percent intervals

of 29.6 %. In the test, the consumption and the production are around 30.9 kWh and 23.6 kWh.

For this study, the described profiles are used to run three different real-time simulations:

- Scenario 3.a without Intra-Day Re-Optimizations
- Scenario 3.b with Intra-Day Re-Optimizations
- Scenario 3.c with Intra-Day Re-Optimizations and DSO Limits in Power Exchanges.

I. Scenario 3.a without Intra-Day Re-Optimizations

Fig. V.57 shows the overall measured power during the test. Whereas, the control power computed each 30 seconds is plotted in blue in Fig. V.55. As figure shows, the control set-point and the measured power at the AC side of the battery's inverter are lower than the control power between 11.30 a.m. and 1.00 p.m.. In fact during this timeframe, P_C is higher than $P_{BATT\,MAX}$, which was imposed equal to 12000 W, and reaches a maximal value of around 13400 W. Hence, a control set-point ($P_{PV\,sp}$) was applied to the PV inverter and the photovoltaic production was in part cut, as shown in Fig. V.55 and Fig. V.56. Moreover, in Fig. V.56, the orange curve is always lower than the blue curve due to the losses in the conversion stage.

Moreover, another important phenomenon on the ESS behaviour has to be observed in this timeframe. The performance of the ESS decreases for more intense solicitations by increasing the power losses and inducing a higher reduction of $P_{BATT\,m}$ compared to the imposed $P_{BATT\,sp}$. The estimated state of charge of each battery and the overall SOC of the pack are illustrated in Fig. V.54, in which it is possible to see the loss of the battery 1, due to the reaching of the upper-limit of the SOC. The SOC_f of the pack reaches around 66.2 % at the end of the test.

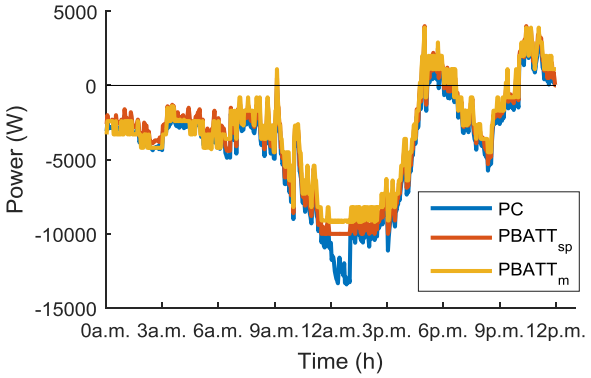

Fig. V.53 Comparison between P_C, $P_{BATT\,sp}$ and $P_{BATT\,m}$ without intra-day re-optimizations

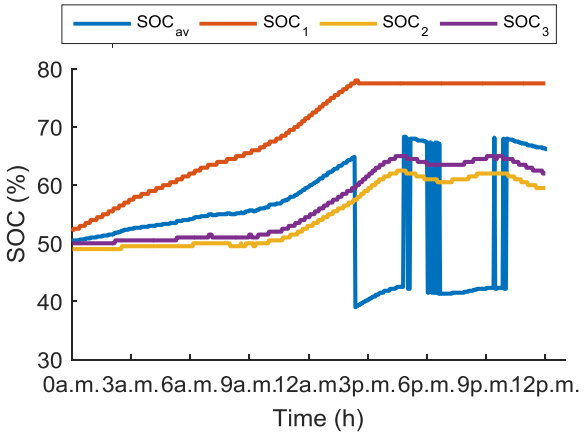

Fig. V.54 SOC^p and SOC^b for all three batteries in the ESS without intra-day optimization

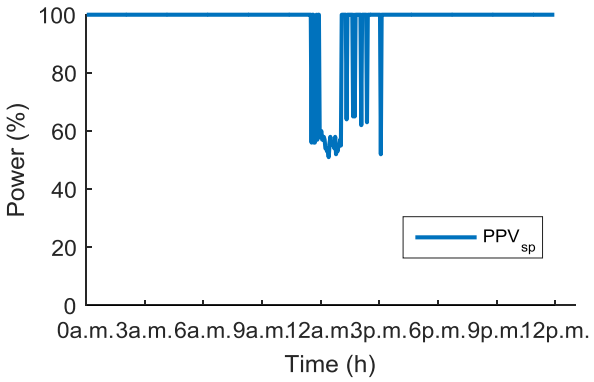

Fig. V.55 $P_{PV\,sp}$ without intra-day re-optimizations[26]

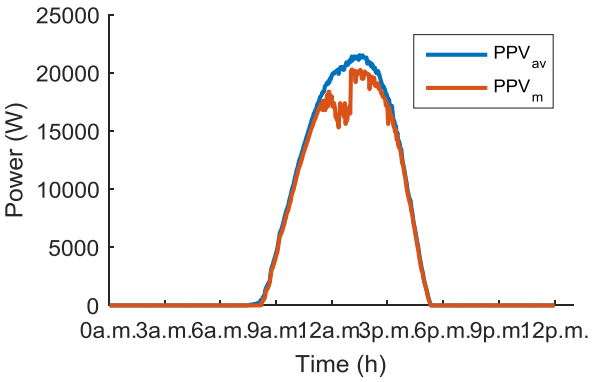

Fig. V.56 Comparison between $P_{INV\,m}$ and $P_{PV\,av}$ without intra-day re-optimizations

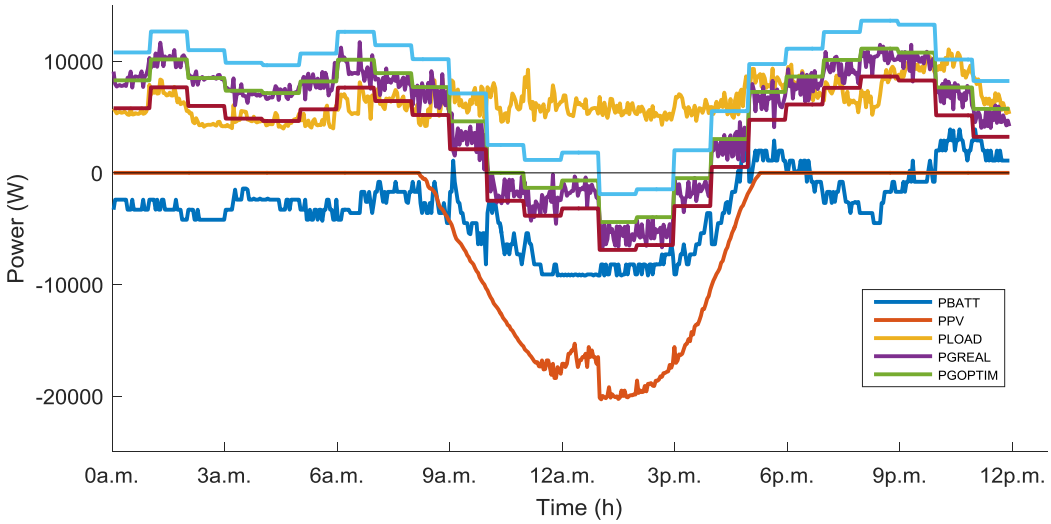

Fig. V.57 Real power profiles of photovoltaic, battery, consumption and grid exchange in t_m without intra-day re-optimizations

[26] $P_{PV\,sp}$ is expressed as function of the rated power of the inverter, which is 30 kW.

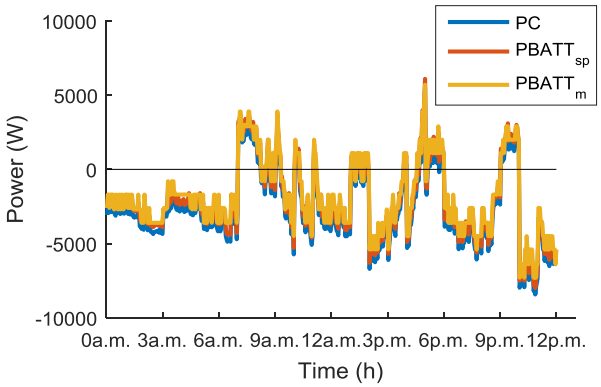

Fig. V.58 Comparison between P_C, $P_{BATT\,sp}$ and $P_{BATT\,m}$ with intra-day re-optimizations

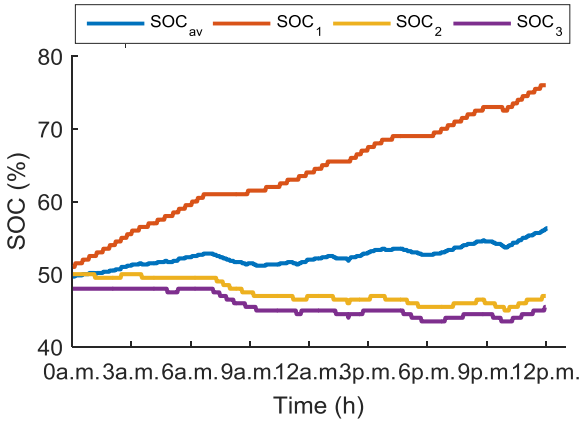

Fig. V.59 SOC^p and SOC^b for all three batteries in the ESS with intra-day optimization

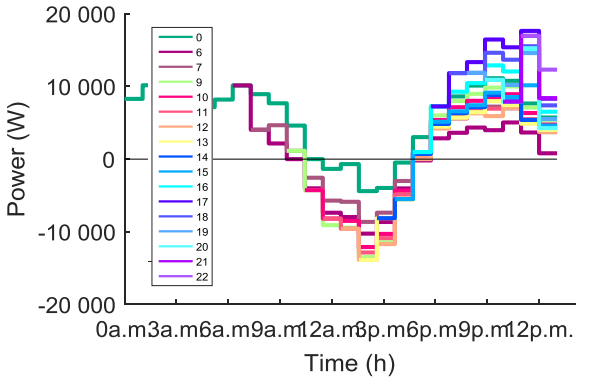

Fig. V.60 Net microgrid's power scheduled with intra-day re-optimizations

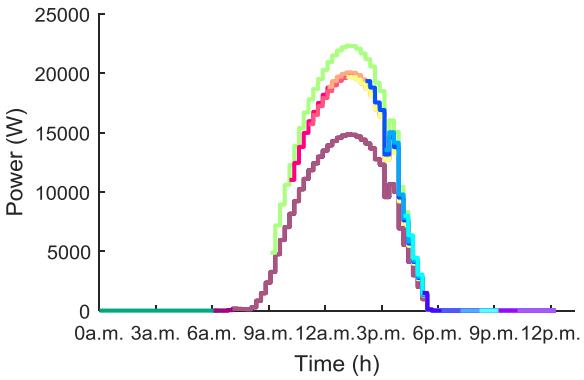

Fig. V.61 PV intra-day re-forecasted profiles

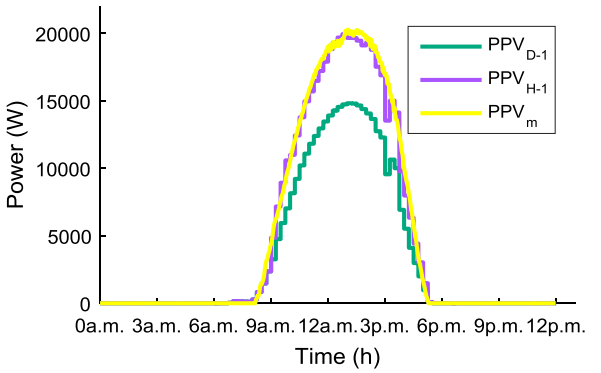

Fig. V.62 Comparison between D-1, final re-forecasted and measured PV profiles

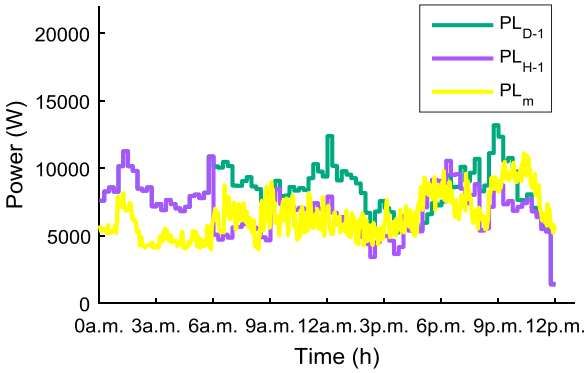

Fig. V.63 Comparison between D-1, final re-forecasted and measured consumption profiles

II. Scenario 3.b with Intra-Day Re-Optimizations

Fig. V.60 shows the 16 re-scheduling process of the microgrid, in which the microgrid becomes from a weakly to a stronger injecting source between 10.00 a.m. and 5.00 p.m.. The measured powers each t_m are illustrated in Fig. V.67.

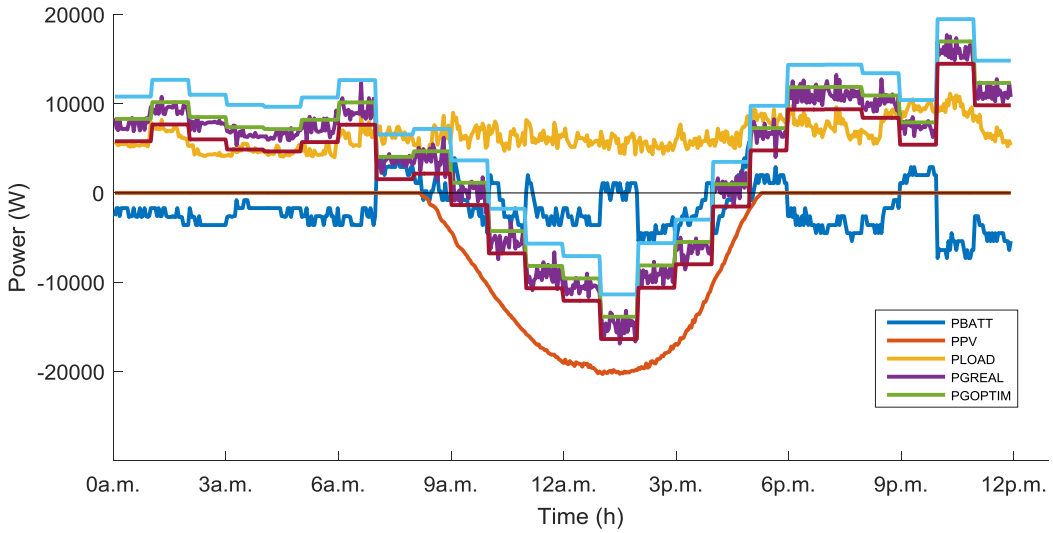

Fig. V.64 Real power profiles of photovoltaic, battery, consumption and grid exchange in t_m with intra-day re-optimizations

In this case study, the scarce variability of the irradiation guarantees a standard form of the available PV power, which allows a good performance of the persistent intra-day algorithm by obtaining a good forecast of the final profile, as shown in Fig. V.61 and Fig. V.62. While in contrast for the consumption forecast, the performances are lower due to the daily variability of the shape, as in Fig. V.63.

The re-optimization allows to reduce the need of flexibilities solicitations (Fig. V.58 and Fig. V.59) by requiring to the battery a maximal charging and discharging powers of 8000 W and 6100 W, respectively, and reaching a final SOC of around 56.3 %.

III. Scenario 3.c with Intra-Day Re-Optimizations and DSO Limits

In the previous scenario, it is considered that at the end of each re-scheduling, the DSO is informed and accepts the change. However due to security reason, such as power or voltage congestions, it may not accept the new plan and impose an injection limit.

Hence, the main goal of this case study is to analyse the reaction of the microgrid to this limit. Two limits are supposed imposed by the DSO during the hour of PV injection peak. The timeframes with injection limit are 12.00 a.m. - 1.00 p.m. and 1.00 p.m. – 2.00 p.m. and in both the imposed power limit was equal to 9000 W, which correspond around to 6.0 % and 35.1 % of the power level in the previous case.

The timeframes of re-optimization, as well as the re-forecasted profile of consumption and production, are the same discussed in previous sub-section (see Fig. V.62 and Fig. V.63).

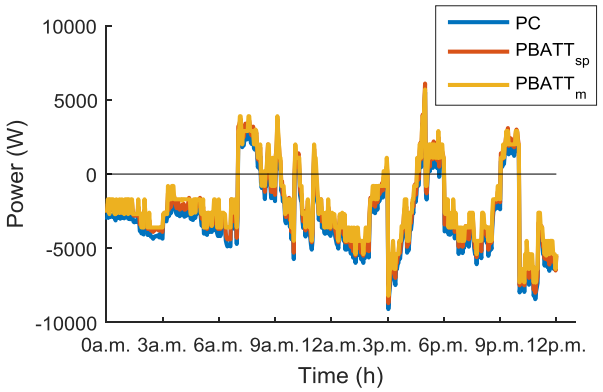

Fig. V.65 Comparison between P_C, $P_{BATT\,sp}$ and $P_{BATT\,m}$ with intra-day re-optimizations

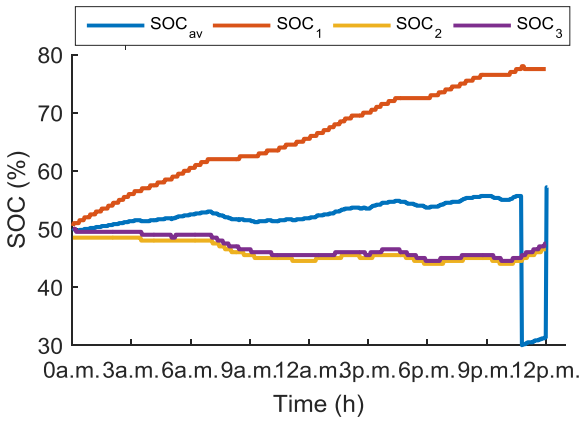

Fig. V.66 SOC^p and SOC^b for all three batteries in the ESS with intra-day optimization

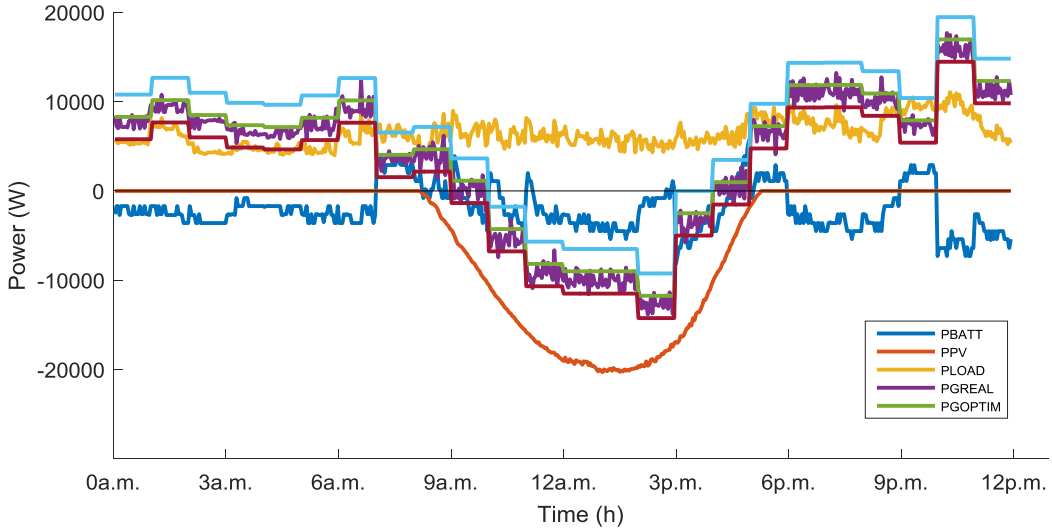

Fig. V.67 Real power profiles of photovoltaic, battery, consumption and grid exchange in t_m with intra-day re-optimizations and DSO Limits

<u>Comparison between Scenario 3 without intra-day re-optimizations, with intra-day re-optimizations and with DSO Limits</u>

Naturally, case 3.a needs a higher availability of flexibilities than case 3.b and 3.c, which leads to a less efficient use of the installed resources. In all three cases, battery 1 is subject to a deeper charge, due as in previous case by the not-homogeneous batteries' state of healthy.

In case 3.b and 3.c, the use of re-optimization reduces the battery's solicitations and try to restore the pack's SOC_f. The DSO limits does not impact considerably the microgrid's behaviour and the SOC_f suffers a small increase of 0.9 %. In all three cases flexibilities available leads to the oscillation of the power at the PCC around the forecasted values.

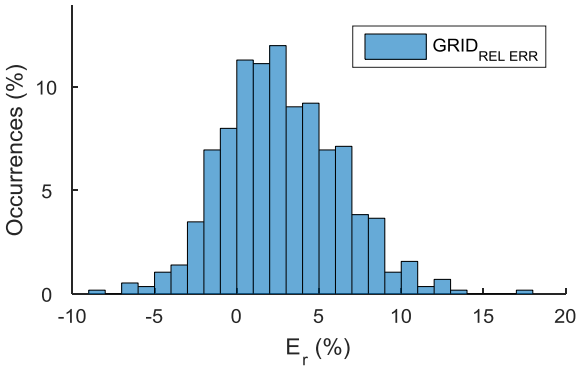

Fig. V.68 Distribution of errors between forecasted and real measured powers at PCC on microgrid P_n for case 3.a

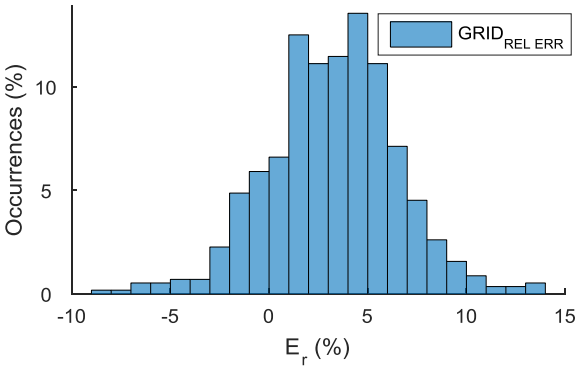

Fig. V.69 Distribution of errors between forecasted and real measured powers at PCC on microgrid P_n for case 3.c

	CASE 3.a	CASE 3.b	CASE 3.c
	MESURE (t_m=t_c+20 sec)	MESURE (t_m=t_c+20 sec)	MESURE (t_m=t_c+20 sec)
x ≥ -15	0.0 %	0.0 %	0.0 %
-15 < x ≤ -10	0.0 %	0.0 %	0.0 %
-10 < x ≤ -5	1.0 %	1.4 %	1.4 %
-5 < x ≤ 0	20.8 %	13.9 %	14.4 %
0 < x ≤ 5	52.6 %	56.4 %	55.2 %
5 < x ≤ -10	22.6 %	26.4 %	26.9 %
10 < x ≤ 15	2.8 %	1.9 %	2.1 %
x ≥ 15	0.2 %	0.0 %	0.0 %

Tab. V.10 Occurrences of percent values of forecasted and real measured powers at PCC

	D-1	**3.a**	**3.b**	**3.c**
C_{DG}	8.1 €	13.8 €	14.2 €	14.2 €
C_{ESS}	0.8 €	12.8 €	8.2 €	8.8 €
$C_{g_{BUY}}$	27.6 €	25.8 €	25.7 €	25.7 €
$C_{g_{SELL}}$	-1.6 €	-2.6 €	-7.9 €	-7.2 €
DC*	34.9 €	49.8 €	40.1 €	41.5 €
MF*	26.0 €	23.2 €	17.8 €	18.5 €

****Legend**: *MF*: Daily money flow between the µgrid and DSO (expenses and revenues); * *DC*: Daily expense or revenue of the µgrid considering the money flow with the DSOA/AGGA, the DG costs and the ESS costs

Tab. V.11 Daily economic results of Scenario 3

The percent distribution of these oscillations on microgrid P_n is shown in Fig. V.68 and Fig. V.69 for case 3.a and 3.c, which are presented in conjunction with the occurrences study for various percent intervals for all three cases and resumed in Tab. V.10. However for all three cases the applied control is quite performant and the greatest majority of the occurrences (in particular, the 97.0 %, 98.1 % and 97.9 %) is contained between ± 15.0 % with a small increase for case 3.b.

The microgrid's expenses and revenues for 24 hours of operation are resumed in Tab. V.11 for all three case studies and compared with the expected computed at *D-1*. The lower DC is found for case study 3.b, which allow to economize around 19.5 % and 3.4 % compared to case 3.a and 3.c. However, this reduction could make profitable if the DSO remunerates these flexibility services or if grid tariffs are reduced.

V.4.4. Scenario 4 - Forecasted PV Power Lower than measured one with High Intermittence

This fourth case study aims to study the performance of the developed strategy in case of high PV intermittency. As in previous case, the used scenario considers a day with an increase in the local production and a reduction in the local consumption with respect to the forecasted scenario. The PV profile represents a sunny day in September with repeated passage of small clouds. The PV profiles are depicted in Fig. V.70. For the consumption are used the same profiles described in section V.4.3 and reported again in Fig. V.71.

The trends of ε_a^{PV} and ε_a^{PV+C}, and their distributions, are shown in Fig. V.72, Fig. V.74, Fig. V.73 and Fig. V.75. The surplus in the available production induces a significant error, which this time is extremely intermittent. However, between 9.00 a.m. and 6.00 p.m., ε_a^{PV+C} follows a concave downward trend, which is function of the PV production. ε_a^{PV+C} has a maximal and minimal value of 15815 W and -6031 W, respectively.

The occurrences of percent values of ε_a^{PV} and ε_a^{PV+C} at various percent intervals reported in Tab. V.12 show that the high intermittence of the global profile induces a high heterogeneity of errors. Hence, only around 61.9 % of the percent ε_a^{PV+C} occurrences are comprised between ± 15.0 %.

For the production side, the daily forecasted and available energies are around 79.3 kWh and 115.6 kWh for 24-hour operation that corresponds to an increase of 45.9 % with respect to the estimated amount at *D-1*.

I. Scenario 4.a with high PV intermittence without intra-day re-optimizations

As in previous case, a high flexibility is required during daily hours, in particular between 8.45 a.m. and 4.45 p.m. as in Fig. V.76. The behaviour of the ESS discovered in section V.4.3 remains valid also for this scenario, as shown by orange and yellow curves.

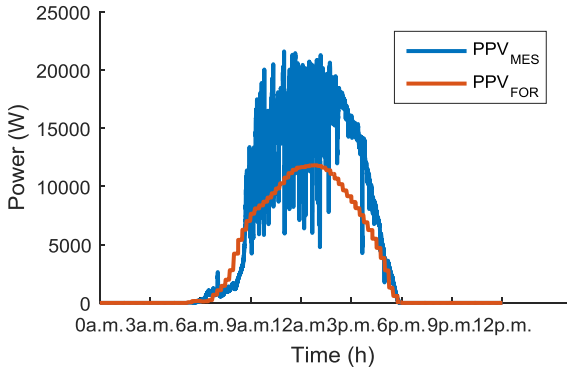

Fig. V.70 PV power profiles of forecasted data over 15 minutes and real-time measures

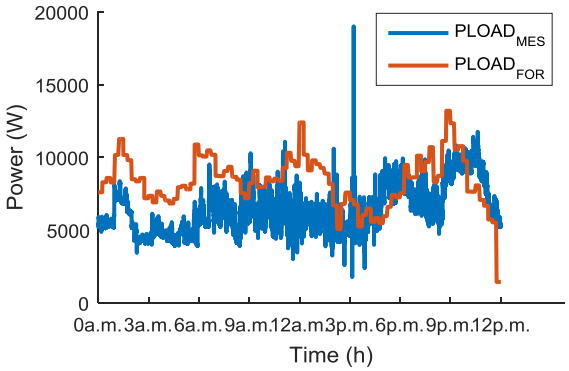

Fig. V.71 Aggregated consumption power profiles of forecasted data over 15 minutes and real-time measures

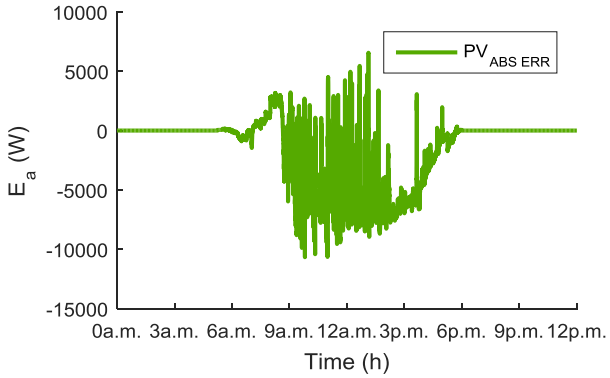

Fig. V.72 Absolute error between forecasted and real values of PV power (ε_a^{PV})

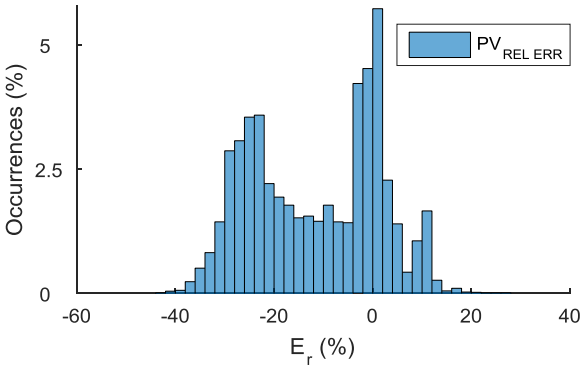

Fig. V.73 Distribution of ε_a^{PV} on microgrid P_n

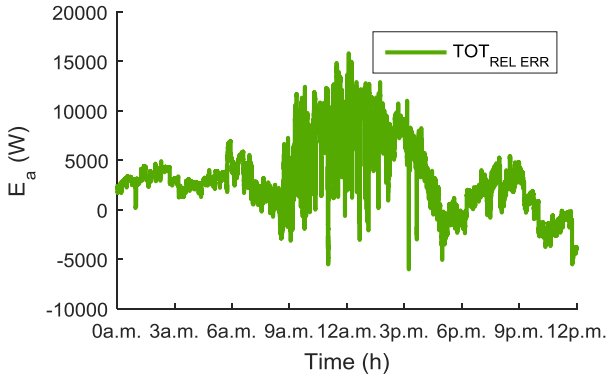

Fig. V.74 Absolute error between forecasted and real values of total microgrid power (ε_a^{PV+C})

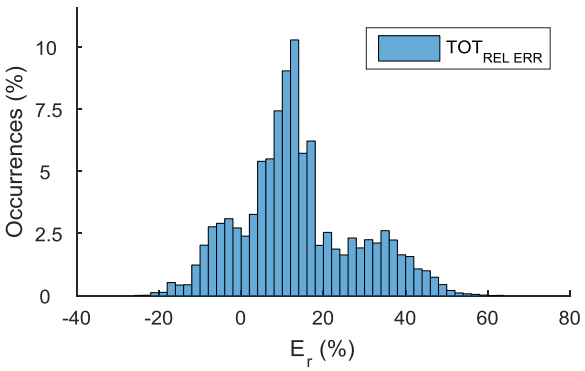

Fig. V.75 Distribution of ε_a^{PV+C} on microgrid P_n

	< -20	**-20/-15**	**-15/-10**	**-10/-5**	**-5/0**	**0/5**	**5/10**	**10/15**	**15/20**	**> 20**
$\boldsymbol{\varepsilon_a^{PV}}$	34.7	8.5	7.0	7.3	17.9	16.0	4.5	3.6	0.3	0.1
$\boldsymbol{\varepsilon_a^{PV+C}}$	0.1	1.0	1.7	6.5	7.0	8.1	15.9	22.7	10.6	26.4

Tab. V.12 Occurrences of percent values of $\boldsymbol{\varepsilon_a^{PV}}$ and $\boldsymbol{\varepsilon_a^{PV+C}}$ at various percent intervals

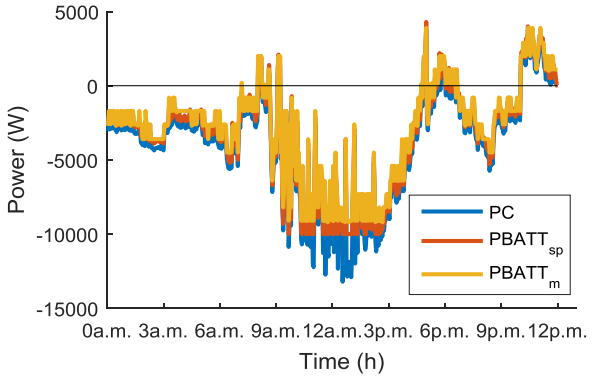

Fig. V.76 Comparison between P_C, $P_{BATT\,sp}$ and $P_{BATT\,m}$ without intra-day re-optimizations

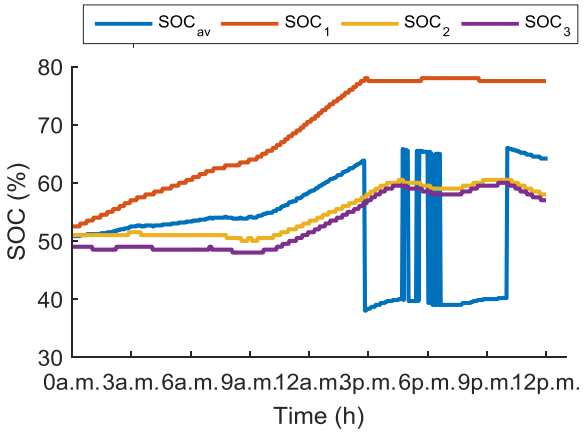

Fig. V.77 SOC^p and SOC^b for all three batteries in the ESS without intra-day optimization

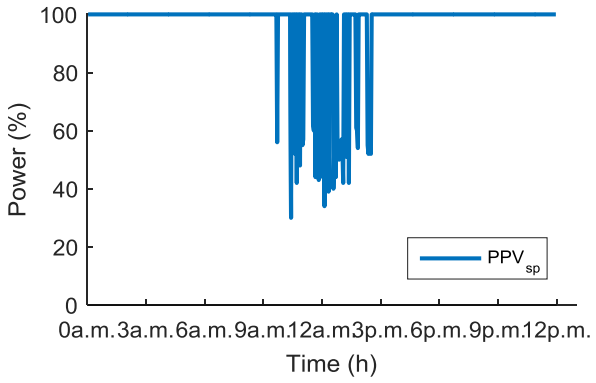

Fig. V.78 $P_{PV\,sp}$ withot intra-day re-optimizations

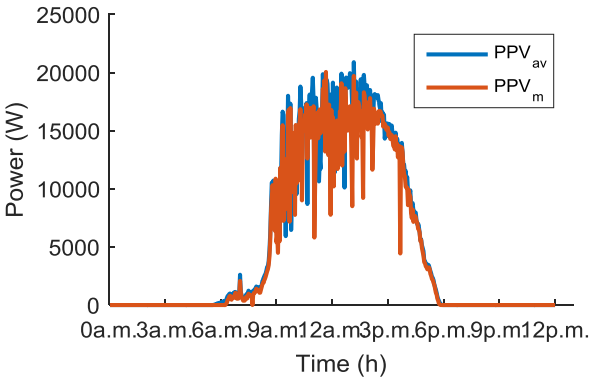

Fig. V.79 Comparison between $P_{INV\,m}$ and $P_{PV\,av}$ without intra-day re-optimizations

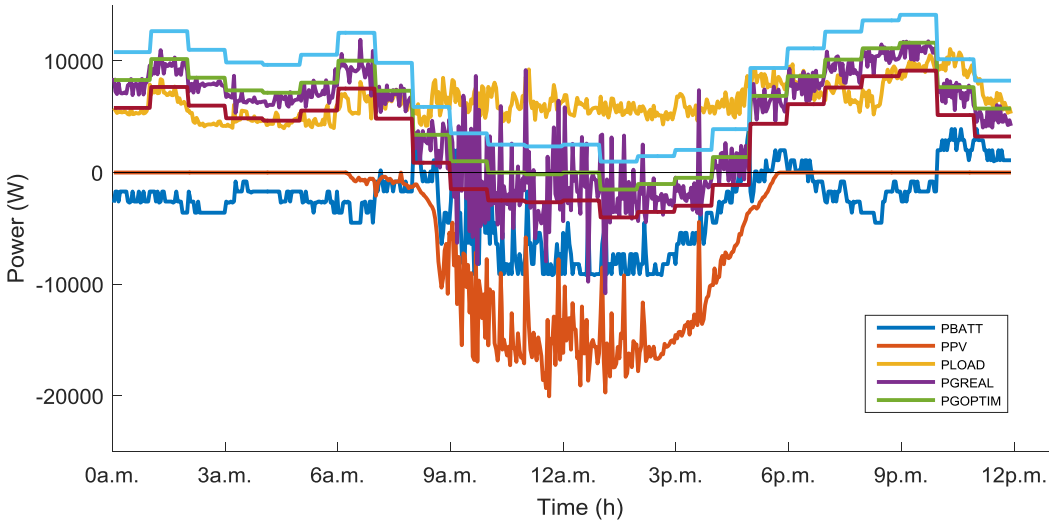

Fig. V.80 Real power profiles of photovoltaic, battery, consumption and grid exchange in t_m without intra-day re-optimizations

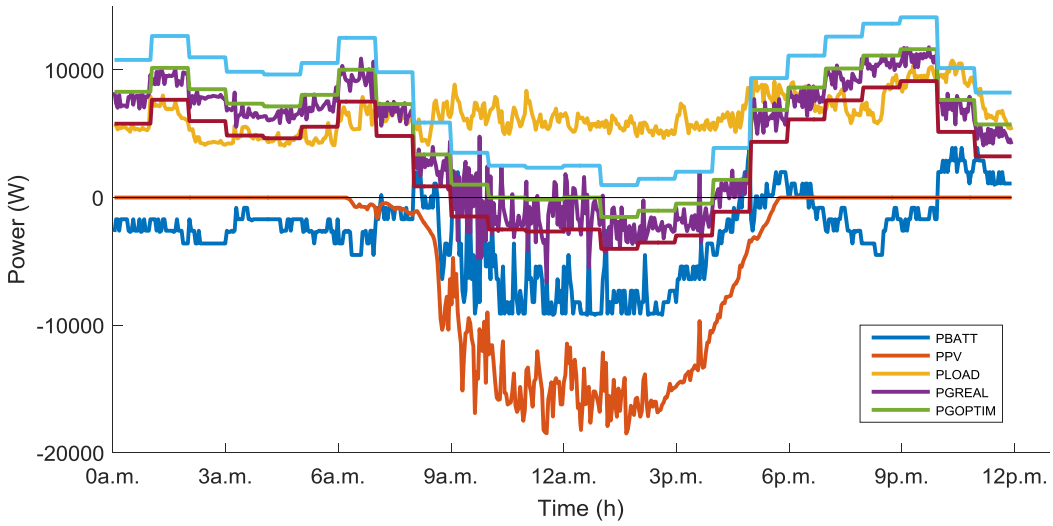

Fig. V.81 Mean profiles of photovoltaic, battery, consumption and grid exchange without intra-day optimization

Moreover, the PV was cut off in certain timeframes between 10.00 a.m. and 2.30 p.m., as illustrated in Fig. V.78 and Fig. V.79. The available production was around 23.3 kWh for a 4.8 hours test, while the injected energy was 22.7 kWh. Hence, the energy loss for cutting the PV was around 2.2 % of the available production. However considering the high increase in the available solar source, the SOC_f reaches around 64.2 % which is relatively close to the desired value.

However, the intermittency of the PV injection is much faster than the applied control. Hence, even if the intermittency of the exchanged power at the PCC is slightly smoothed, the profile remains intermittent, as shown in violet in Fig. V.80.

II. Scenario 4.b with high PV intermittence with intra-day re-optimizations

In general also in this case, the re-scheduling process consists of 13 re-optimization, as in Fig. V.84. The ESS is able to support in power and energy the operation of the microgrid, as shown in Fig. V.82 and Fig. V.83. The SOC_f reaches a final value of around 60.0 %. Hence in general it is possible to affirm that reducing the use of the ESS and avoiding the cut off of the PV make a better use of the installed resources. However, the intermittency of the injected PV continues to induce an intermittent global exchange with the host grid, as clearly illustrated in Fig. V.86 by plotting the measured powers each t_m. If the averaged profiles over 30 seconds are analysed the intermittency is evidently reduced, as Fig. V.87.

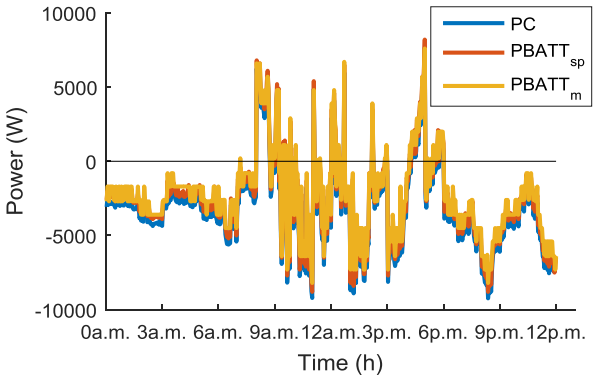

Fig. V.82 Comparison between P_C, $P_{BATT\,sp}$ and $P_{BATT\,m}$ with intra-day re-optimizations

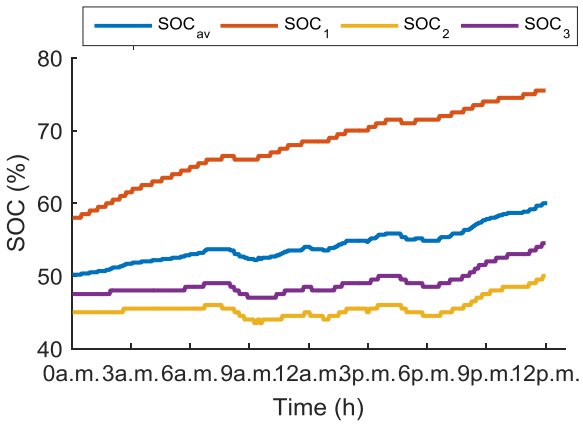

Fig. V.83 SOC^p and SOC^b for all three batteries in the ESS with intra-day optimization

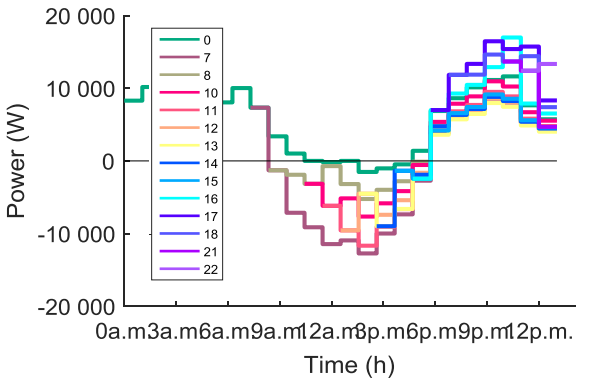

Fig. V.84 Net microgrid's power scheduled with intra-day re-optimizations

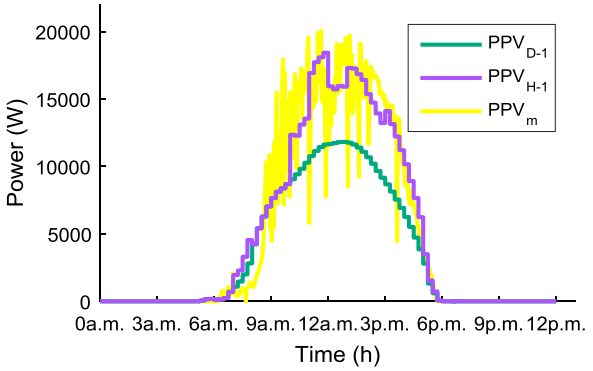

Fig. V.85 Comparison between D-1, final re-forecasted and measured PV profiles

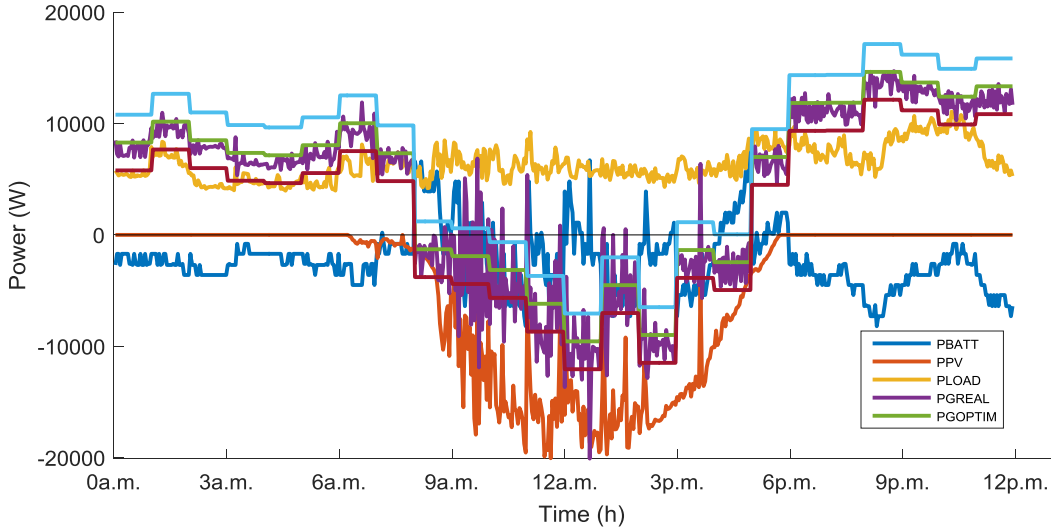

Fig. V.86 Real power profiles of photovoltaic, battery, consumption and grid exchange in t_m with intra-day re-optimizations

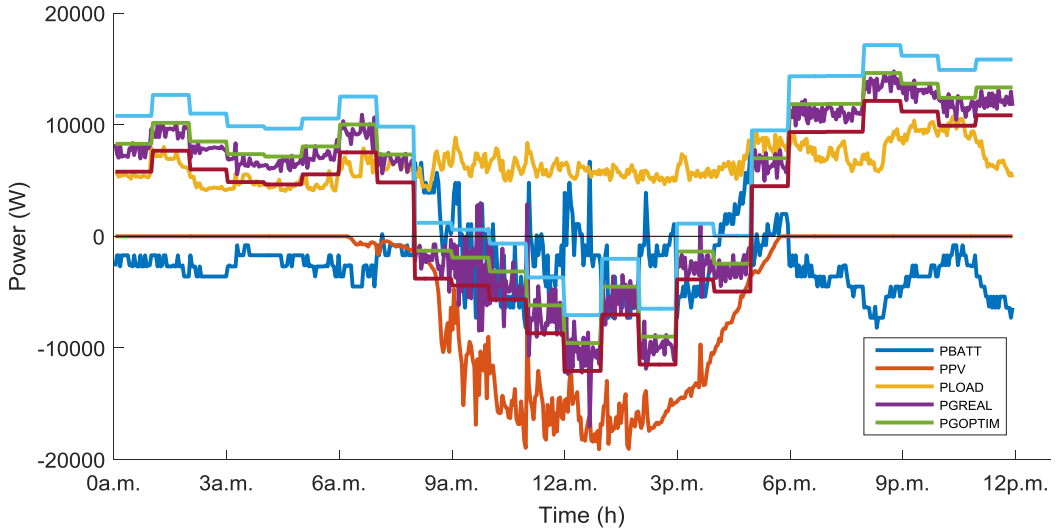

Fig. V.87 Mean profiles of photovoltaic, battery, consumption and grid exchange with intra-day optimization

Comparison between Scenario 4 without and with intra-day re-optimizations

Also the comparison between results of case 4.a and 4.b confirms the effectiveness of the re-scheduling process in order to reduce the amount of needed flexibilities, which will require an increase in installation costs obtained in previous sections. However in both cases, there is a strong oscillation of the power at the PCC around the forecasted values. The percent distribution of these oscillations on microgrid P_n is shown in Fig. V.88 and Fig. V.89 for case 4.a and 4.b.

The distributions in the two cases are a similar trend, confirmed by the occurrence study for various percent intervals presented in Tab. V.13. In fact, in both cases the instances comprises between ±5.0 % are around 63.0 %, while only around 6.0 % falls in ranges higher/lower of plus/minus 15.0 %. A slight reduction in the density of high ranges can be nonetheless observed in case I. This is probably due to the PV cut off, which in certain timeframe can help to reduce the PV variability by imposing for 30 second a constant injection[27].

[27] N. B.: This is possible only in timeframes in which the imposed power set-point to the PV inverter is lower than the available PV power.

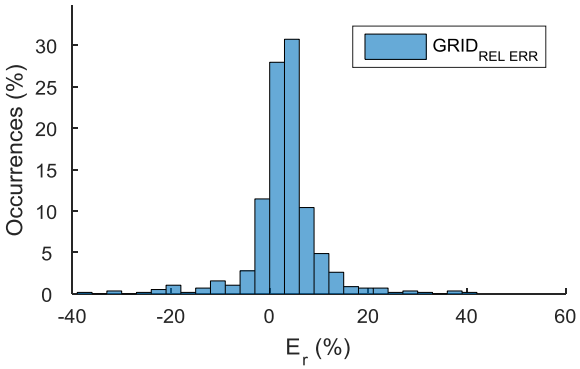

Fig. V.88 Distribution of errors between forecasted and real measured powers at PCC on microgrid P_n for case 4.a

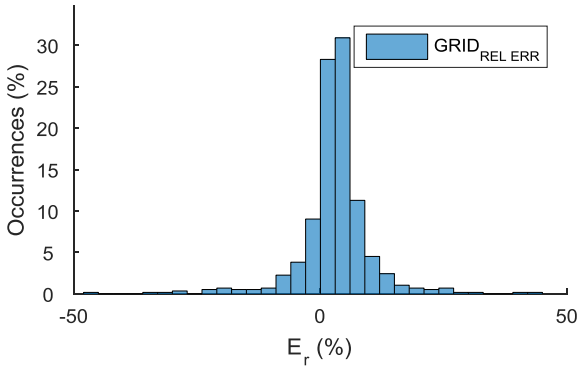

Fig. V.89 Distribution of errors between forecasted and real measured powers at PCC on microgrid P_n for case 4.b

	4.a		4.b	
	MESURE (t_m=t_c+20 sec)	AVERAGE (30 sec)	MESURE (t_m=t_c+20 sec)	AVERAGE (30 sec)
x ≥ -15	2.4 %	0.2 %	2.6 %	0.5 %
-15 < x ≤ -10	1.6 %	0.0 %	1.0 %	0.2 %
-10 < x ≤ -5	2.6 %	2.4 %	3.5 %	2.3 %
-5 < x ≤ 0	13.4 %	9.7 %	11.8 %	10.6 %
0 < x ≤ 5	50.0 %	61.8 %	51.2 %	59.9 %
5 < x ≤ -10	20.5 %	21.7 %	21.7 %	21.4 %
10 < x ≤ 15	6.1 %	2.8 %	4.5 %	3.8 %
x ≥ 15	3.5 %	1.4 %	3.6 %	1.4 %

Tab. V.13 Occurrences of percent values of forecasted and real measured powers at PCC

	D-1	**4.a**	**4.b**
C_{DG}	8.5 €	13.6 €	14.0 €
C_{ESS}	0.8 €	11.7 €	9.7 €
$C_{g_{BUY}}$	25.4 €	23.1 €	26.4 €
$C_{g_{SELL}}$	-0.5 €	-1.4 €	-6.7 €
DC*	34.2 €	47.0 €	43.4 €
MF*	24.9 €	21.7 €	19.7 €

**MF*: Daily money flow between the µgrid and DSO (expenses and revenues); * *DC*: Daily expense or revenue of the µgrid considering the money flow with the DSOA/AGGA, the DG costs and the ESS costs

Tab. V.14 Daily economic results of Scenario 4

Hence, it is possible to affirm that the control applied is slow for an intermittent profile with a second by second variation. In fact, it is needed to consider that 24-hours profiles are applied in simulations by inducing an increase in the speed of the intermittency. It is nonetheless needed to consider that the implemented strategies are oriented to higher size microgrids (between 200 kW and 2000 kW) in which the random fluctuations of both production and consumption are in part statistically reduced as function of the microgrid's size. After that, it is needed to analyse the clauses in the contract stipulated between

microgrids and network operators in order to not impose criticality in the grid operation, and consequently apply a speeder control, e.g. 10-15 seconds.

In this scenario and in Scenario 4.a, re-optimizations are triggered when SOC^p is subject to 20.0 % of variation. However, this induce a higher use of the battery, as between 0.00 a.m. and 7.00 a.m. Hence, it is more efficient to apply lower β, such as 15.5% or even 10.0 %, and run more re-optimizations in order to find the more economic operation of the microgrid and use the flexibilities in case of DSO limits or if the new traded bids are not accepted by aggregators or markets. In future studies, sensitivity analysis based on statistical data of consumption and variable generation can be introduced in order to find the best combination of β and γ.

The economic results for 24-hour operation are resumed in Tab. V.14 for both tests and are compared with results obtained in the *D-1* simulation. In case I, during 8.45 a.m. and 3.00 p.m. the PV energy is in part stored in the ESS and used in the evening hours between 10.00 p.m. and 12.00 p.m., which induces a decrease in $C_{g_{BUY}}$. On the other hand, the ESS is more stimulated, which causes the rise of C_{ESS}. Furthermore, in case II the energy injected in the host grid increases by rising $C_{g_{SELL}}$. Hence at the end, the microgrid economizes around 7.0 % in case 4.b in respect of case 4.a.

V.5. Conclusions

In real-time, generation and consumption sides are both subjected to unexpected changes. Forecast errors may induce several issues in this new paradigm where the scheduling process takes an increasing role to assure a secure and economical operation of networks. Consequently in this chapter, the intra-day dynamic scheduling and the real-time control of microgrid were discussed. Moreover, the developed energy management framework was experimentally validated on a physical microgrid by testing four scenarios.

On one hand, the day-ahead schedule may not remain optimal in real-time scenarios. Hence, microgrids have to be able to reschedule their operation in the most economical way. The outcomes of real-time tests has shown that the re-scheduling process is a fundament tool which will allow to massively integrate in a cost-efficient way both distributed generation and storage systems into the electrical system. In fact, the obtained daily expense of the microgrid has a reduction when implementing re-optimizations. This will allows to use more efficiently

all installed resources reducing installation and/or operation costs, e.g. by diminishing the size or extending the usage time of an ESS.

On the other hand, also if the intra-day rescheduling can be a source of incomes or a reduction of costs for microgrids' owners and is necessary to satisfy inflexible consumption, distribution grids operation based on active methods strictly depends on generation and consumption and requires to be monitored in real-time. Hence in case of criticalities, microgrids have to be able to respect their day-ahed engagement or to be subject to new constraints and in case of services engagement to respond to the DSO. In case of this engagement failure, the microgrid's owner could be penalized. In future works, these penalties must be taken into account in the optimization process. In this respect, results has demonstrated that microgrids are able to collaborate with DSOs and respond to their needs in case of voltage or power congestions by using installed flexibilities. Hence, the engagement in services market flexibilities or in capacity limit allocation is possible. A remuneration or a grid tariffs reduction have to be nonetheless guaranteed in order to compensate the increase in the microgrids costs, due to the less efficient operation. Furthermore, a more speed control, such as 10 or 15 seconds, can be introduced if will be needed to improve the control performance in case of small-sized microgrids and high intermittency of consumption/production profiles.

Moreover, the Naïve Predictor method was used for the intra-day re-forecast of power profile. This approach is based on persistence concept and resulted sufficiently accurate to estimate standard and not extremely variable in shape profiles, such as for PV profile in worst-case scenario 2, and its performance increase for next hours forecast. However, the introduction of more performant forecast algorithm will reduce the number of re-optimizations by decreasing the interactions with the DSOs, aggregators or markets. This will improve control performance and will reduce the amount of needed flexibilities as well as microgrids costs.

Finally, the intra-day phases and interactivity between microgrids and network and/or market operators need to be strengthened and will play a key role for a more economical and safe operation of the electrical system.

VI. CONCLUSIONS AND PERSPECTIVES

This chapter summarizes the main findings of the thesis by highlighting the most important questions addressed. Furthermore, some potential lines of research that may results from the work presented here are outlined to guide future research.

VI.1. General Conclusions

The massive integration of multi-technology small and medium sized systems generators, such as renewable-based generators, storage systems, as well as demand-response into the power system represents an important challenge for the success of the energy transition. In future power systems, these distributed systems will assume a central role due to their number and ubiquity on the national scale. Their integration into the power system will require their active participation in electricity markets and grid operation within coherent controllable entities, such as microgrid and virtual power plants. This evolution in the existing power system represents the driving-force behind the motivations of this thesis, which aims to conceptualize, develop and implement new management strategies for the future smart grid.

The different pillars of innovation, findings and conclusions, of this thesis revolve around the following three key points:

- The conceptualization and the development of a *Sliding Multi-Level Optimization Framework*,
- Case study analysis through simulations of the *Sliding Multi-Level Optimization Framework*,
- Case study analysis through real-time tests of the microgrid behaviour in the *Sliding Multi-Level Optimization Framework*.

The conceptualization and the development of a *Sliding Multi-Level Optimization Framework* is the cornerstone of this research. This optimization framework is implemented for energy management and control of a large number of small and medium sized distributed systems, through a Multi-Agent System. In chapters III and IV, efforts made have allowed to prepare the foundation for the management of this multi-component system, through a Multi-Agent System, by providing:

- the architecture of the management and control system, in particular
  - Agents' interactions,

  - communication and tasks sequence,
  - information exchanged (type, form, structure),
- and the smart algorithms for the management, namely
  - the microgrid's algorithm for day-ahead, intra-day and real-time energy management
  - the aggregator's algorithm for day-ahead and intra-day energy management for multi-microgrid systems
  - the distribution system operator's algorithm for a day-ahead and an intra-day application of congestion management.

On one hand, this part of the work shows the importance of the implementation of a structured approach to develop a collaborative, interoperable and extensible system with plug-and-play ability. A structured system is able to integrate any type of technology without requiring a modification of the structure and sequence of aggregated information exchanged between levels. The same is true as well for the smart-algorithms that make decisions in each level, except if the functionalities or the objectives need to be extended or changed. Furthermore, the distribution of information allows to reduce difficulties related to big-data manipulation. On the other hand, the simulation that have been performed highlight the effectiveness of the proposed approach also from the economic point of view by respecting in an optimal way each microgrids' self-interest. In this way, each level can be seen as a coherent structure with some degree of flexibility. Each level can adapt its global power/energy to participate in electricity and/or services market by holding responsible and empowering all distributed systems in order to ensure a reliable and economic operation of the power system.

The plug-and-play ability of microgrids and aggregators in this structured *Sliding Multi-Level Optimization Framework* is confirmed by the applications analysed for active management of distribution grids and electricity markets, in chapters IV. In particular, two mechanisms for the active management of distribution grids "*Flexibility Services Market"* and "*Capacity Limit Allocation"* are conceptualized from both technical and economical point of view and implemented in the hierarchical optimization framework developed. As mentioned, case studies for the day-ahed scheduling of multi-microgrid systems show that the optimization structure and the structure of messages exchanged between microgrids and aggregators do not need to be changed when there is a change in the strategy or in the

technologies which provide flexibility, such as distributed generators or demand-response aggregated with storage systems. Furthermore, results from simulations shows that the use of active strategies for distribution network operation can be a way to reduce or defer investments for distribution system operators and can be a source of income for microgrids. However, the implementation of active management approaches requires a high degree of complexity in its implementation compared to the fit-and-forget approach for distribution grid operation. The need to develop a reliable, scalable and interoperable information and communication infrastructure, to introduce a reliable and fast toolbox for the network analysis and to introduce as well as profound changes to the regulatory framework induces new complexities in the system.

The encouraging results obtained in simulations are emphasized by the validation of the rolling optimization process, which implements intra-day and real-time phases of microgrid energy management. Real-time tests confirm all the advantages of using microgrids as a flexible coherent structure, which can be modelled for active grid management, as hypothesized in the development and simulation phases. In addition, test outcomes show that the re-scheduling process, required by the fact that the day-ahead schedule may not remain optimal in real-time scenarios, is a fundament tool that has to be introduced in aggregators' and DSOs' operation, in order to massively integrate in a cost-efficient way both distributed generation and storage systems into the electrical system.

VI.2. Outlook on future research

The development and results presented in this thesis point the way towards new questions, technical developments and studies, which may further enhance the work presented here.

First and foremost, in this thesis the attention was focused on the development of the global framework as well as of the microgrid and aggregator levels. However, the key of this *Multi-Level Optimization Framework* lies in the tasks distribution starting from the lower level until the upper level, in which each smart-level has the same importance, like in a house of cards. Hence in future works, the lower level populated by components have to be improved in order to increase the performance of the entire system. For example, new local functionalities have to be implemented in the battery management system, such as the charge/discharge of a single battery in the pack, preferred the usage of the battery with the better state of health, and so on. In the same manner, the distribution management system may to be improved by providing new functionalities for the network analysis, based on state

estimation and forecast algorithms. In particular, a reliable and accurate algorithm able to estimate available flexibilities at different aggregation levels and in different locations in the network has to be studied and implemented. Additionally, performing algorithms for the evaluation of generation side and consumption flexibilities have to be developed to guarantee an efficient and economical use of flexibilities.

Secondly, the construction sector is pushing toward an optimized and self-sustainable operation of buildings by installing multi-source systems in order to fulfil electric and thermal demand based on different technologies, such as solar photovoltaic systems and collectors, heat pumps, cogeneration, etc.. Hence, considering the flexible and extensible nature of the architecture, the use of the framework developed could be extended to a multi-source system coupling thermal and electrical demand for a more efficient use of resources on district level and for providing services for network operators as well.

Furthermore, long-term tests and a measurement campaign performed on real large scale multi-microgrid system including different technologies for both electrical and thermal needs, such as fuel-cells, electric thermal storage heaters, concentration photovoltaics, combined heating and power systems, have to be accomplished in order to investigate further technical challenges and validate the economic benefits.

Finally, recommendations for a revised regulatory framework concerning new electricity and grid tariff for consumers and prosumers as well as new business models for old and new actors, such as aggregators, electricity retailers and distribution system operators, have to be considered.

VII. APPENDIX

Appendix A

Electricity Markets

Since the start of the deregulation process in the electricity sector in 1990, the "Electricity Market" has become a key instrument for the development of a competitive environment. In a liberalised market, different entities are responsible for the electricity generation, as well as for the operation of transmission and distribution systems. Electricity producers and electricity suppliers are the two main actors in this sector. Electricty producers, which are the generation station's owners, trade and sell their energy production in market platforms. On the contrary, the suppliers trade and buy electricity on these platforms. Subsequently, they sell electricity to the end-consumers in the retail market through approved contracts by regulators.

Electricity market transactions can be categorized into forward and spot markets. In forward markets long-term and medium-term contract are negotiated. In this market, over-the-counter bilateral contracts are signed for the supply of electricity over weeks, months, quarterly periods or years to come, at a price negotiated directly on the contract date. Forward contract cover standardized products, such as base-load or peak-load. First and foremost, forward markets, are needed to ensure the supply of the foreseeable demand. Secondly, these over-the-counter contracts have the effect to manage price risks by reducing its volatility.

On the contrary, short-term contracts are traded in spot markets. In these markets, electricity sale/purchase contracts signed are immediately effective. In France and Germany, EPEX operates the power spot market, while this role is taken by IPEX in Italy. Two types of short-term spot markets exist for selling/buying electricity: the day-ahead market and the intra-day market.

In the day-ahead market, producers, wholesalers, distributors, retailers and eligible final customers, such as large-sized industrial, submit their demand bids and supply offers in order to negotiate electricity for the next day. In this market, hourly products are traded in a daily auction and settled at the market clearing price with a merit-order criterion taking into account transmission capacity limits. In this manner, the electricity price for each hour of the following day is determined. In Italy, six zonal prices representing a portion of the transmission grid exist. The accepted supply offers are valued at the zonal clearing price, while the accepted demand bids are valued at a national single price, called "*Prezzo Unico*

Nazionale", obtained as average of the zonal prices weighted on the purchased quantity in each zone.

In intra-day markets, the same actors may trade new electricity blocks in order to adjust their scheduled injection or withdrawal by submitting additional supply offers or demand bids. In France in intra-day markets, hourly products are negotiated in a continuous-trading market until 30 minutes before of delivery. In Germany, both hourly and fifteen-minute blocks can be traded in continuous until 30 minutes before of delivery. Furthermore in Germany, fifteen-minute products can be negotiated in a daily auction as well. In Italy, the intra-day trading takes place in seven auction sessions, detailed in [191]. Supply offers and demand bids are selected with the same criterion described for the day-ahed market. Nevertheless, the clearing price is not computed and all purchases and sales are valued at the day-ahed hourly price.

Both day-ahead and intra-day markets are governed by rules. Most important market rules for France, Germany and Italy are summarized in Tab. VII.1 [192] [193].

	France	***Italy***	***Germany***
Platform	EPEXSPOT	IPEX	EPEXSPOT
Procedure	Daily auction	Daily auction	Daily auction
Tradable Contracts	1 h	1 h	1 h
Order Book closes	12 p.m.	12 p.m.	12 p.m.

(a) Day-Ahead

	France	***Italy***	***Germany***
Platform	EPEXSPOT	IPEX	EPEXSPOT
Procedure	Continuos	Daily auction	Daily auction / continuous*
Tradable Contracts	1 h	1 h	1 h / 15 min*
Trading closes	30 min before delivery	7 Sessions	30 min before delivery

(b) Intra-Ahead

Tab. VII.1 French, Italian and German market rules [194]

Appendix B

Description of the 74-Bus MV Grid

The power distribution network in analysis is a rural grid situated in the eastern part of French constituted approximately of 100 km of 20 kV lines. Six MV feeders underlie the transformer substation supplied by a HV/MV transformer with nominal power of 20 MVA. A schematic representation of the grid is depicted in Fig. VII.1. The model details related to each feeder and to the HV/MV transformer are listed in Tab. VII.2.

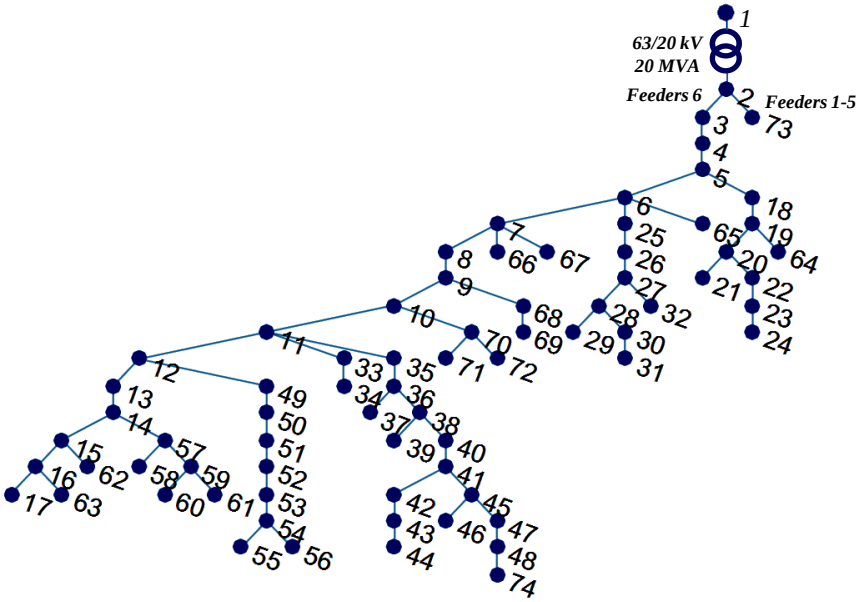

Fig. VII.1 74-Bus MV Grid

N. Line	f_{bus}	t_{bus}	r (p.u.)	x (p.u.)	b (p.u.)	V_n (kV)	I_{max} (A)
1	1	2	0.02	0.399501	0	63	183
2	3	4	0.100938	0.104975	0	20	400
3	4	5	0.0355	0.03692	0	20	400
4	5	6	0.015428	0.02415	0	20	369
5	6	7	0.063279	0.09905	0	20	369
6	7	8	0.0199	0.03115	0	20	369
7	8	9	0.044832	0.070175	0	20	369
8	9	10	0.074235	0.1162	0	20	369
9	10	11	0.062049	0.097125	0	20	369
10	11	12	0.044385	0.069475	0	20	369
11	12	13	0.04785	0.0749	0	20	369
12	13	14	0.022807	0.0357	0	20	369
13	14	15	0.087856	0.055388	0	20	197
14	15	16	0.078771	0.044975	0	20	197
15	16	17	0.122907	0.070175	0	20	197
16	5	18	0.025305	0.015665	0	20	309
17	18	19	0.084594	0.0483	0	20	197
18	19	64	0.033102	0.0189	0	20	197
19	19	20	0.317534	0.1813	0	20	197
20	20	21	0.110953	0.06335	0	20	197
21	20	22	0.091337	0.05215	0	20	197
22	22	23	0.156622	0.089425	0	20	197

23	23	24	0.094491	0.054383	0	20	197
24	6	25	0.035554	0.0203	0	20	197
25	25	26	0.113712	0.064925	0	20	197
26	26	27	0.038006	0.0217	0	20	197
27	27	28	0.132715	0.075775	0	20	197
28	28	29	0.066204	0.0378	0	20	197
29	28	30	0.045669	0.026075	0	20	197
30	30	31	0.045362	0.0259	0	20	197
31	27	32	0.063446	0.036225	0	20	197
32	6	65	0.054557	0.03115	0	20	197
33	7	66	0.012298	0.01925	0	20	369
34	7	67	0.012298	0.01925	0	20	369
35	9	68	0.056703	0.032375	0	20	197
36	68	69	0.133941	0.076475	0	20	197
37	10	70	0.032796	0.018725	0	20	197
38	70	71	0.108501	0.06195	0	20	197
39	70	72	0.152637	0.08715	0	20	197
40	11	33	0.012873	0.00735	0	20	197
41	33	34	0.017777	0.01015	0	20	197
42	11	35	0.099919	0.05705	0	20	197
43	35	36	0.099	0.056525	0	20	197
44	36	37	0.096854	0.0553	0	20	197
45	36	38	0.053638	0.030625	0	20	197
46	38	39	0.11034	0.063	0	20	197
47	38	40	0.225473	0.07735	0	20	125
48	40	41	0.152906	0.145425	0	20	125
49	41	42	0.089032	0.02165	0	20	125
50	42	43	0.175359	0.071575	0	20	125
51	43	44	0.192445	0.09275	0	20	125
52	41	45	0.094173	0.04235	0	20	125
53	45	46	0.050573	0.028875	0	20	197
54	45	47	0.15938	0.091	0	20	197
55	47	48	0.171734	0.09822	0	20	309
56	12	49	0.034635	0.019775	0	20	197
57	49	50	0.064978	0.0371	0	20	197
58	50	51	0.120455	0.068775	0	20	197
59	51	52	0.138845	0.079275	0	20	197
60	52	53	0.093176	0.0532	0	20	197
61	53	54	0.139764	0.0798	0	20	197
62	54	55	0.003632	0.001438	0	20	239
63	54	56	0.107888	0.0616	0	20	197
64	14	57	0.098387	0.056175	0	20	197
65	57	58	0.02544	0.014525	0	20	197
66	57	59	0.094709	0.054075	0	20	197
67	59	60	0.170108	0.097125	0	20	197
68	59	61	0.254089	0.145075	0	20	197
69	15	62	0.025746	0.0147	0	20	197
70	16	63	0.082449	0.047075	0	20	197
71	2	3	0	0.0001	0	20	400
72	2	73	0.03125	0.599186	0	20	800
73	48	74	0.07	0.0928	0	20	262

Tab. VII.2 Characteristics of 74-Bus MV Grid

Optimal Power Flow Results for the 74-Bus MV Grid

The detailed results of the optimal power flow solved to find the optimal solution of the Flexibility Service Market for active management of distribution grids are shown in Tab. VII.3 and Tab. VII.4 for timeframes 12 and 14, receptively.

OPTIMAL POWER FLOW in t=12						
	VOLTAGE		*GENERATION*		*LOAD*	
Bus	***Mag (p.u.)***	***Ang (deg)***	***P (MW)***	***Q (MVAr)***	***P (MW)***	***Q (MVAr)***
1	1.070	0.000	11.6163443	5.80490182	0.000	0.000
2	1.047	-2.316	-	-	0.000	0.000
3	1.047	-2.316	-	-	0.000	0.000
4	1.050	-2.069	-	-	0.038	0.008
5	1.051	-1.982	-	-	0.000	0.000
6	1.051	-1.921	-	-	0.000	0.000
7	1.054	-1.655	-	-	0.000	0.000
8	1.054	-1.572	-	-	0.000	0.000
9	1.056	-1.384	-	-	0.000	0.000
10	1.059	-1.069	-	-	0.000	0.000
11	1.062	-0.808	-	-	0.000	0.000
12	1.061	-0.820	-	-	0.000	0.000
13	1.061	-0.834	-	-	0.097	0.019
14	1.061	-0.839	-	-	0.000	0.000
15	1.061	-0.839	-	-	0.000	0.000
16	1.061	-0.838	0.09999899	0	0.000	0.000
17	1.061	-0.839	-	-	0.045	0.009
18	1.051	-1.985	-	-	0.092	0.018
19	1.050	-1.993	-	-	0.000	0.000
20	1.049	-2.021	-	-	0.144	0.029
21	1.048	-2.024	-	-	0.153	0.031
22	1.048	-2.024	-	-	0.012	0.002
23	1.048	-2.028	-	-	0.073	0.015
24	1.048	-2.029	-	-	0.073	0.015
25	1.051	-1.924	-	-	0.120	0.024
26	1.051	-1.930	-	-	0.111	0.022
27	1.051	-1.931	-	-	0.000	0.000
28	1.050	-1.934	-	-	0.031	0.006
29	1.050	-1.934	-	-	0.021	0.004
30	1.050	-1.934	-	-	0.035	0.007
31	1.050	-1.935	-	-	0.019	0.004
32	1.051	-1.932	-	-	0.059	0.012
33	1.062	-0.807	0.2500989	0	0.000	0.000
34	1.062	-0.808	-	-	0.139	0.028
35	1.067	-0.642	0.0115989	0	0.000	0.000
36	1.072	-0.480	-	-	0.000	0.000
37	1.072	-0.458	0.809599	0	0.000	0.000
38	1.074	-0.405	0.35019899	0	0.000	0.000
39	1.074	-0.406	-	-	0.049	0.010
40	1.083	-0.222	0.03134483	0	0.000	0.000
41	1.089	0.094	-	-	0.021	0.004
42	1.089	0.101	0.03368092	0	0.000	0.000
43	1.090	0.121	0.12678166	0	0.000	0.000
44	1.091	0.143	0.47508191	0	0.000	0.000
45	1.092	0.176	-	-	0.000	0.000
46	1.092	0.197	1.50429342	0	0.000	0.000
47	1.095	0.282	-	-	0.121	0.099
48	1.098	0.394	-	-	0.021	0.020
49	1.061	-0.820	-	-	0.012	0.002
50	1.061	-0.819	-	-	0.002	0.001

51	1.061	-0.817	-	-	0.012	0.002
52	1.061	-0.815	-	-	0.047	0.009
53	1.061	-0.813	-	-	0.021	0.004
54	1.062	-0.809	-	-	0.000	0.000
55	1.062	-0.809	0.15009893	0	0.000	0.000
56	1.061	-0.810	-	-	0.075	0.015
57	1.061	-0.845	-	-	0.000	0.000
58	1.061	-0.845	-	-	0.106	0.021
59	1.061	-0.848	-	-	0.000	0.000
60	1.060	-0.853	-	-	0.134	0.027
61	1.060	-0.852	-	-	0.066	0.013
62	1.061	-0.839	-	-	0.042	0.009
63	1.061	-0.838	-	-	0.035	0.007
64	1.050	-1.993	-	-	0.042	0.009
65	1.051	-1.922	-	-	0.028	0.006
66	1.054	-1.655	-	-	0.009	0.002
67	1.054	-1.655	-	-	0.007	0.001
68	1.056	-1.385	-	-	0.068	0.014
69	1.056	-1.386	-	-	0.042	0.009
70	1.059	-1.068	0.10509892	0	0.000	0.000
71	1.059	-1.068	-	-	0.007	0.001
72	1.059	-1.070	-	-	0.075	0.015
73	1.020	-7.188	-	-	15.297	3.059
74	1.100	0.499	2.37331336	0	0.000	0.000
			---	---	---	---
		Total:	17.938	5.805	17.602	3.610

Tab. VII.3 OPF Results: Application in 74-bus MV grid without aggregator

OPTIMAL POWER FLOW in t=14						
	VOLTAGE		***GENERATION***		***LOAD***	
Bus	***Mag (p.u.)***	***Ang (deg)***	***P (MW)***	***Q (MVAr)***	***P (MW)***	***Q (MVAr)***
1	1.061	0.000	4.999	3.109	0.000	0.000
2	1.049	-0.996	-	-	0.000	0.000
3	1.049	-0.996	-	-	0.000	0.000
4	1.052	-0.734	-	-	0.028	0.006
5	1.053	-0.641	-	-	0.000	0.000
6	1.054	-0.579	-	-	0.000	0.000
7	1.056	-0.311	-	-	0.000	0.000
8	1.057	-0.227	-	-	0.000	0.000
9	1.059	-0.038	-	-	0.000	0.000
10	1.062	0.278	-	-	0.000	0.000
11	1.065	0.538	-	-	0.000	0.000
12	1.064	0.531	-	-	0.000	0.000
13	1.064	0.522	-	-	0.055	0.011
14	1.064	0.519	-	-	0.000	0.000
15	1.064	0.520	-	-	0.000	0.000
16	1.064	0.522	0.100	0.000	0.000	0.000
17	1.064	0.521	-	-	0.025	0.005
18	1.053	-0.644	-	-	0.074	0.015
19	1.053	-0.649	-	-	0.000	0.000
20	1.052	-0.669	-	-	0.106	0.021
21	1.052	-0.671	-	-	0.092	0.018
22	1.052	-0.671	-	-	0.007	0.001
23	1.051	-0.674	-	-	0.057	0.011
24	1.051	-0.675	-	-	0.056	0.011
25	1.054	-0.581	-	-	0.086	0.017

26	1.053	-0.586	-	-	0.075	0.015
27	1.053	-0.586	-	-	0.000	0.000
28	1.053	-0.588	-	-	0.021	0.004
29	1.053	-0.589	-	-	0.014	0.003
30	1.053	-0.589	-	-	0.025	0.005
31	1.053	-0.589	-	-	0.014	0.003
32	1.053	-0.587	-	-	0.053	0.011
33	1.065	0.539	0.250	0.000	0.000	0.000
34	1.065	0.538	-	-	0.113	0.023
35	1.069	0.699	0.021	0.000	0.000	0.000
36	1.074	0.857	-	-	0.000	0.000
37	1.075	0.874	0.623	0.000	0.000	0.000
38	1.076	0.932	0.350	0.000	0.000	0.000
39	1.076	0.931	-	-	0.045	0.009
40	1.085	1.118	0.018	0.000	0.000	0.000
41	1.091	1.435	-	-	0.014	0.003
42	1.092	1.446	0.428	0.000	0.000	0.000
43	1.093	1.468	0.239	0.000	0.000	0.000
44	1.093	1.486	0.399	0.000	0.000	0.000
45	1.094	1.509	-	-	0.000	0.000
46	1.094	1.532	1.609	0.000	0.000	0.000
47	1.096	1.595	-	-	0.143	0.128
48	1.099	1.683	-	-	0.035	0.029
49	1.064	0.532	-	-	0.008	0.002
50	1.064	0.533	-	-	0.002	0.000
51	1.064	0.536	-	-	0.010	0.002
52	1.065	0.539	-	-	0.034	0.007
53	1.065	0.542	-	-	0.016	0.003
54	1.065	0.547	-	-	0.000	0.000
55	1.065	0.547	0.150	0.000	0.000	0.000
56	1.065	0.546	-	-	0.055	0.011
57	1.064	0.514	-	-	0.000	0.000
58	1.064	0.514	-	-	0.081	0.016
59	1.064	0.511	-	-	0.000	0.000
60	1.064	0.507	-	-	0.120	0.024
61	1.064	0.509	-	-	0.049	0.010
62	1.064	0.520	-	-	0.038	0.008
63	1.064	0.521	-	-	0.020	0.004
64	1.053	-0.649	-	-	0.023	0.005
65	1.054	-0.579	-	-	0.019	0.004
66	1.056	-0.311	-	-	0.006	0.001
67	1.056	-0.311	-	-	0.004	0.001
68	1.059	-0.039	-	-	0.044	0.009
69	1.059	-0.039	-	-	0.033	0.007
70	1.062	0.278	0.095	0.000	0.000	0.000
71	1.062	0.278	-	-	0.004	0.001
72	1.062	0.277	-	-	0.054	0.011
73	1.034	-3.858	-	-	9.130	1.826
74	1.100	1.765	1.865	0.000	0.000	0.000
			---	---	---	---
		Total:	11.146	3.109	10.890	2.299

Tab. VII.4 OPF Results: Application in 74-bus MV grid without aggregator in h=14

Appendix C

Structure and Ontology of Agents' Messages

In a heterogeneous, distributed and collaborative system such as a microgrid is necessary that all physical and virtual agents in the system are able to establish complex dialogues through a common agent communication language. The goal of a common language is to give to all agents the ability to acquire and share information without misunderstandings. As in human languages, agent communication language has to be rule-governed and signs-based by sharing a common syntax and semantic in order to describe the entire knowledge of agents. For this reason, the study of the syntax, the semantic and the content of exchanged massages in multi-agent systems is becoming more and more important.

As mentioned in section II.5.3.2, in this thesis the structure of exchanged messages and the structure of the content are based on the IEEE FIPA standards [77] and [79]. FIPA ACL is a communication language that relies on speech act theory and makes available a structure for building the messages based on a set of one or more parameters in Tab. II.5. However, a common syntax is not proposed. Hence, a common hierarchical vocabulary has defined in order to assure agent's comprehension in the multi-microgrid system.

power	:buy :sell :share		:gen_pos :gen_neg :load_pos :load_neg	:max :min
price	:buy :sell :share		:gen_pos :gen_neg :load_pos :load_neg	

Tab. VII.5 Ontology terms used in the messages among agents

Examples of MMCA's proposals to the AGGA:

```
(PROPOSE
 :sender  ( agent-identifier :name MMCA1@10.0.204.162:1099/JADE  :addresses
(sequence http://GRE041935.intra.cea.fr:7778/acc ))
 :receiver  (set ( agent-identifier :name Agg@10.0.204.162:1099/JADE  :addresses
(sequence http://GRE041935.intra.cea.fr:7778/acc )) )
 :content  "( power :buy 22.299 :share :gen_pos :max 35.0 80.0  :min 15.0 55.0
price :share :gen_pos 19.0 18.5  )"
 :reply-with  AGGA1@10.0.204.162:1099/JADE1487143052848
:language  fipa-sl
:conversation-id  Electrical-Trade-Microgrids )

   (PROPOSE
    :sender   ( agent-identifier :name MMCA4@10.0.204.162:1099/JADE   :addresses
(sequence http://GRE041935.intra.cea.fr:7778/acc ))
    :receiver  (set ( agent-identifier :name Aggregatore@10.0.204.162:1099/JADE
:addresses (sequence http://GRE041935.intra.cea.fr:7778/acc )) )
    :content   "( power :buy 38.86 :share :load_neg :max 7.3 :min 7.3 price
:share :load_neg 4.9 )"
    :reply-with   AGGA1@10.0.204.162:1099/JADE1503055470687   :language   fipa-sl
:conversation-id  Electrical-Trade-USER )
```

Examples of AGGA's answer to an MMCA:

```
(ACCEPT-PROPOSAL
 :sender  ( agent-identifier :name AGGA1@172.20.10.3:1099/JADE  :addresses
(sequence http://GRE041935.intra.cea.fr:7778/acc ))
 :receiver  (set ( agent-identifier :name MMCA4@172.20.10.3:1099/JADE
:addresses (sequence http://GRE041935.intra.cea.fr:7778/acc )) )
 :content  "power :share :load_neg 7.3  price :share :load_neg 5.0"
 :language  fipa-sl  :conversation-id  Electrical-Trade-USER )
```

Tab. VII.6 Examples of exchanged messages by using [77], [79] and the used ontology

LIST OF PUBLICATIONS

Conference Communication:

- "Control Applications for Microgrids with MAS", Quoc Tuan TRAN, Elvira AMICARELLI, Helene CLEMOT, "OPAL RT15 European User Group Event - Barcelona, Spain, May 2015".

Conference Paper:

- "Optimal energy management and control for an isolated area", Quoc Tuan TRAN, Elvira AMICARELLI, Nicolas MARTIN, Marion PERRIN, "Cigré/IEC Symposium, Development of electricity infrastructure in Sub-Saharan Africa – Cape Town, Africa, May 2015".
- "Multi-Agent System for Microgrid Resource Management with high penetration of PV Systems", Elvira AMICARELLI, Quoc Tuan TRAN, Seddik BACHA; "First International Conference on Solar Energy and Materials (ICSEMA16) – Marrakech, Marocco, March 2016".
- "Multi-Agent System for Day-Ahead Energy Management of Microgrid", Elvira AMICARELLI, Quoc Tuan TRAN, Seddik BACHA, "18th European Conference on Power Electronics and Applications - Karlsruhe, Germany, September 2016".
- "Impact of European Market Frameworks on Integration of Photovoltaics in Virtual Power Plants", Eiko KRUGER, Elvira AMICARELLI, Quoc Tuan TRAN, "16th IEEE International Conference on Environment and Electrical Engineering - Florence, Italy, June, 2016".
- "Optimization Algorithm for Microgrids Day-Ahead Scheduling and Aggregator Proposal", Elvira AMICARELLI, Quoc Tuan TRAN, Seddik BACHA, "17th IEEE International Conference on Environmental and Electrical Engineering – Milan, Italy, June 2017".
- "Flexibility Service Market for Active Congestion Management of Distribution Networks using Flexible Energy Resources of Microgrids", Elvira AMICARELLI, Quoc Tuan TRAN, Seddik BACHA, "7th IEEE International Conference on Innovative Smart Grid Technologies – Turin, Italy, September, 2017".

BIBLIOGRAPHY

[1] "World Energy Outlook 2012," International Energy Agency, OECD/IEA, Paris, 2012.

[2] "Global trends in renewable energy investments," Bloomberg - New Energy Finance, Frankfurt School - UNEP, 2015.

[3] "Monthly Energy Review," U.S. Energy Information Administration, June 2017.

[4] "THE FIRST DECADE: 2004 – 2014," REN21 - Renewable Energy Policy Network for the 21th Century, 2014.

[5] Renewable energy in Europe 2016 - Recent growth and knock-on effects, EEA Report, 2016.

[6] Eurostat, "Electricity price statistics," June 2017. [Online]. Available: http://ec.europa.eu/eurostat/statistics-explained/index.php/Electricity_price_statistics.

[7] "Renewables 2016 Global Status Report," REN21, 2016.

[8] "European Energy Industry Investments - European Parliament," Feb. 2017. [Online]. Available: http://www.europarl.europa.eu/RegData/etudes/STUD/2017/595356/IPOL_STU(2017)595356_EN.pdf.

[9] Eurostat, "Renewable energy statistics," June 2017. [Online]. Available: http://ec.europa.eu/eurostat/statistics-explained/index.php/Renewable_energy_statistics.

[10] "Technology Roadmap - Solar Photovoltaic Energy," International Energy Agency, 2014.

[11] A. M. Pavan, P. R. V. Lughi, F. Spertino and S. Vergura, "Diminishing cost of electricity from wind power and photovoltaics," in *17th International Conference on Environmental and Electrical Engineering*, Milan, Italy, 2017.

[12] "Rapporto Statistico 2014 - Solare Fotovoltaico," Gestore Servizi Energetici, 2015.

[13] P. Dondi, D. Bayoumi, C. Haederli, D. Julian and M. Suter, "Network integration of distributed power generation.," *J. Power Sources*, vol. 106, no. 1-2, pp. 1-9, Apr. 2002.

[14] "Fifth "Energy Transition" Monitoring Report. The Energy of the Future. 2015 Reporting Year – Summary," The Federal Ministry for Economic Affairs and Energy (BMWi), December 2016, [Online]. Available: https://www.bmwi.de/Redaktion/EN/Publikationen/monitor.

[15] N. Hatziargyriou, Microgrids: Architectures and Control., Wiley-IEEE Press, 2014.

[16] P. P. Barker and R. W. D. Mello, "Determining the impact of distributed generation on power systems. I. Radial distribution systems.," *IEEE Power Engineering Society Summer Meeting*, vol. 3, pp. 1645-1656, 2000.

[17] G. Lorenz and P. Mandatova, "Active Distribution System Management. A key tool for the smooth integration of distributed generation," Eurelectric, Feb. 2013.

[18] T. Erge and C. Sauer, "Final Public Report - Market Access for Smaller Size Intelligent Electricity Generation," MASSIG Project, Jul. 2010.

[19] B. Nykvist and M. Nilsson, "Rapidly falling costs of battery packs for electric

vehicles," *Nat. Clim. Change,* vol. 5, no. 4, p. 329–332, Apr. 2015 .

[20] A. Rosso, J. Ma, D. S. Kirschen and L. F. Ochoa, "Assessing the contribution ofdemand side management to power system flexibility," in *IEEE Conf. Decis.Control Eur. Control Conf*, 2011.

[21] H. Hao, Y. Lin, A. S. Kowli, P. Barooah and S. Meyn, "Ancillary service to the grid through control of fans in commercial building HVAC systems," *IEEETransactions: Smart Grid,* vol. 5, no. 4, p. 2066–2074, 2014.

[22] K. O. Aduda, T. Labeodan, W. Zeiler, G. Boxem and Y. Zhao, "Demand side flexibility: potentials and building performance implications," *Sustainable Cities and Society,* 2016.

[23] "Microgrids: Large Scale Integration of Micro-Generation to Low Voltage Grids.," ENK5-CT-2002-00610, 2003–2005.

[24] "More microgrids: Advanced Architectures and Control Concepts for More microgrids.," FP6 STREP, Proposal/Contract no.: PL019864, http://www.microgrids.eu., 2006–2009.

[25] S. Alwala, A. Feliachi and M. A. Choudhry, "Multi Agent System based fault location and isolation in a smart microgrid system.," in *Innovative Smart Grid Technologies (ISGT), 2012 IEEE PES, pp. 1-4*, 2012.

[26] I. Patrao, E. Figueres, G. Garcerá and R. González-Medina, "Microgrid architectures for low voltage distributed generation.," *Renew. Sustain. Energy Rev,* vol. 43, p. 415–424, Mar. 2015.

[27] J. J. Justo, F. Mwasilua, J. Leeb and J.-W. Jung, "AC-microgrids versus DC-microgrids with distributed energy resources: a review.," *Renew Sustain Energy Rev,* vol. 24, pp. 387-405, August 2013.

[28] Integration of Distributed Energy Resources - The CERTS MicroGrid Concept., Consortium for Electric Reliability Technology Solutions, April 2002.

[29] "More Microgrids: http://www.smartgrids.eu/node/14," [Online].

[30] "Increase Project: http://www.project-increase.eu/," [Online].

[31] S. Bracco, F. Delfino, F. Pampararo, M. Robba and M. Rossi, "The University of Genoa smart polygeneration microgrid test-bed facility: The overall system, the technologies and the research challenges," *Renew Sustain Energy Review,* vol. 18, pp. 442-459, 2013.

[32] E. Unamuno and J. A. Barrena, "Hybrid ac/dc microgrids—Part I: Review and classification of topologies.," *Renewable and Sustainable Energy Reviews,* vol. 52, p. 1251–1259, 2015.

[33] "Pilot Microgrids - CESI RICERCA DER Test Facility," [Online]. Available: http://www.microgrids.eu/index.php?page=kythnos&id=6.

[34] D. E. Olivares, A. Mehrizi-Sani, A. H. Etemadi, C. A. Canizares, R. Iravani, M. Kazerani, A. H. Hajimiragha, O. Gomis-Bellmunt, M. Saeedifard, R. Palma-Behnke, G. A. Jimenez-Estevez and N. D. Hatziargyriou, "Trends in Microgrid Control.," *IEEE Trans. Smar Grid,* vol. 5, no. 4, pp. 1905-1919, Jul. 2014.

[35] "PARADISE Project," 2014. [Online]. Available: http://www.gipsa-lab.fr/projet/PARADISE/publications.html.

[36] "European Distribution System Operators for Smart Grids. Flexibility: The role of DSOs in tomorrow's electricity market," EDSO for SmartGrids, Brussels.

[37] "Flexibility and Aggregation. Requirements for their interaction in the market," EURELECTRIC, 2014.

[38] R. M. André, G. Mendes, T. Rautiainen, E. Jiménez, C. Varandas, N. Lopes, A. Michiorri, G. Pires and P. Matos, "Customers' flexibility valued in market and regulated environment," in *2016 CIRED Workshop*, Helsinki, 2016.

[39] T. ESTERL, R. SCHWALBE, D. B. D. CASTRO, F. KUPZOG and S. KADAM, "Impact of market-based flexibility on distribution grids," in *2016 CIRED Workshop*, Helsinki, 2016.

[40] "EnergyPool: http://www.energy-pool.eu," [Online].

[41] "Voltalis: https://www.voltalis.com/," [Online].

[42] "Flexitricity: https://www.flexitricity.com," [Online].

[43] C. Eid, P. Codani, Y. Chen, Y. Perez and R. Hakvoort, "Aggregation of Demand Side flexibility in a Smart Grid: A review for European Market Design," in *Proceedings of the 12th Int. Conf. Eur.Energy Mark.; p.1–5*, Lisboa, 2015.

[44] D. F. Spulber, "Market microstructure : intermediaries and the theory of the firm, .," vol. 53, p. 240, 1999.

[45] M.-K. Codognet, "The shipper as he architect of contractual relations in access to natural gas networks," 2004.

[46] T. W. Haring, J. L. Mathieu and G. Andersson, "Comparing Centralized and Decentralized Contract Design Enabling Direct Load Control for Reserves.," *IEEE Trans. Power Syst.*, vol. 31, no. 3, p. 2044–2054, May 2016.

[47] L. Zhang, Z. Yan, D. Feng, G. Wang, S. Xu, N. Li and L. Jing, "Centralized and Decentralized Optimal Scheduling for Charging Electric Vehicles," *IEEE Transactions on Smart Grid, Special Issue: Smart Grid Technologies and Development in China*, Feb. 2014.

[48] S. D. J. McArthur, E. M. Davidson, V. M. Catterson, A. L. Dimeas, N. D. Hatziargyriou, F. Ponci and T. Funabashi, "Multi-Agent Systems for Power Engineering Applications-Part I: Concepts, Approaches, and Technical Challenges.," *IEEE Trans. Power Syst.*, vol. 22, no. 4, pp. 1743-1752, Nov. 2007.

[49] S. Russell and P. Norvig, Artificial Intelligence - A modern Approach, Second Edition: Prentice Hall, 1994.

[50] M. Wooldridge and N. R. Jennings, "Intelligent Agents: Theory and Practice.," *In Knowledge Engineering Review*, vol. 10 (2), 1995.

[51] S. Franklin and A. Graesser, "Is it an agent or just a program?," *Proc 3rd Int. Workshop Agent Theories, Architectures, and Languages. New York. Springer-Verlag*, 1996.

[52] M. Wooldridge, An Introduction to Multi-Agent Systems, JOHN WILEY & SONS, LTD, 2002.

[53] T. Logenthiran, D. Srinivasan and D. Wong, "Multi-agent coordination for DER in MicroGrid.," *IEEE International Conference on Sustainable Energy Technologies*, vol. ICSET 2008, pp. 77-82, 2008.

[54] M. Pipattanasomporn, H. Feroze and S. Rahman, "Multi-agent systems in a distributed smart grid: Design and implementation.," in *Power Systems Conference and Exposition 2009. PSCE '09. IEEE/PES, pp. 1-8*, 2009.

[55] T. Logenthiran, D. Srinivasan and A. M. Khambadkone, "Multi-agent system for

energy resource scheduling of integrated microgrids in a distributed system.," *Electric Power Systems Research,* vol. 81, p. 138–148, 2011.

[56] T. Logenthiran, D. Srinivasan, A. M. Khambadkone and H. N. Aung, "Multiagent System for Real-Time Operation of a Microgrid in Real-Time Digital Simulator.," *IEEE Transactions on Smart Grid,* vol. 3, no. 2, pp. 925-933, June 2012.

[57] C. Shao, C. Xu, S. He, X. Lin and a. X. Li, "Operation of Microgrid Reconfiguration based on MAS (Multi-Agent System).," in *TENCON 2013 - 2013 IEEE Region 10 Conference (31194), pp. 1–4.*, 2013.

[58] H. Wang, "Multi-agent co-ordination for the secondary voltage in power system contingencies.," *Proc. IEE Generation, Transmission and Distribution,* vol. 148, pp. 61-66, Jan 2001.

[59] E. M. Davidson, S. D. J. McArthur, J. R. McDonald, T. Cumming and I. Watt, "Applying Multi-Agent System Technology in Practice: Automated Management and Analysis of SCADA and Digital Fault Recorder Data.," *IEEE Transactions on Power Systems,* vol. 21, no. 2, May 2006.

[60] "FIPA - The Foundation for Intelligent Physical Agents Society.," [Online]. Available: http:/www.fipa.org/.

[61] FIPA Agent Management Specification - Standard SC00023K., http://www.fipa.org/, 2004.

[62] G. Nguyen, T. Dang, L. Hluchy, M. Laclavik, Z. Balogh and I. Budinska, "Agent platform evaluation and comparison.," Institute of Informatics Slovack Academy of Science, Pellucid 5FP IST Project IST-2001-34519, June 2002.

[63] K. Kravari and N. Bassiliades, "A Survey of Agent Platforms.," *Journal of Artificial Societies and Social Simulation,* vol. 18, 2015.

[64] M. S. Rajendram and R. K. Pandey, "Multi Agent Control for two area power system network.," in *2012 International Conference on Computing Electronics and Electrical Technologies (ICCEET), pp. 134-137*, 2012.

[65] Y. S. Foo.Eddy, H. B. Gooi and S. X. Chen, "Multi-Agent System for Distributed Management of Microgrids.," *IEEE Trans. Power Syst.,* vol. 30, no. 1, pp. 24-34, Jan. 2015.

[66] H. N. Aung, A. M. Khambadkone, D. Srinivasan and T. Logenthiran, "Agent-based intelligent control for real-time operation of a microgrid.," in *2010 Joint International Conference on Power Electronics, Drives and Energy Systems (PEDES) Power. pp. 1-6.*, India, 2010 .

[67] "JADE - JAVA Agent DEvelopment Framework (Official Web SIte) http://jade.tilab.com/," [Online].

[68] B. Balachandran, "Developing intelligent agent applications with JADE and JESS.," *Knowledge-based Intelligent Information and Engineering Systems,* vol. 5179, pp. 236-244, 2010.

[69] L. Berthelot, M. Bourdeau, O. Corby, A. Delteil and R. Dieng-Kuntz, "CoMMA Corporate Memory Management through Agents Corporate Memory Management through Agents: The CoMMA project final report.," *Research Report,* 2015.

[70] S. Chakraborty and S. Gupta, "Medical Application Using Multi Agent System - A Literature Survey," *Journal of Engineering Research and Applications,* vol. 4, no. 2, pp. 528-546, February 2014.

[71] "software, Wikipedia - Comparison of agent-based modeling," [Online]. Available: http://en.wikipedia.org/wiki/Comparison_of_agent-based_modeling_software.

[72] J. C. Collins and L. C. Lee., "Building electronic marketplaces places with the ZEUS agent tool-kit.," *Agent Mediated Electronic Commerce,* vol. 1571, p. 1–24, 1998.

[73] F. Michel, "Formalisme, outils et éléments méthodologiques pour la modélisation et la simulation multi-agents.," Ph.D. Thesis, Université Montpellier II - Sciences et Techniques du Languedoc, December 2004.

[74] N. Howden, R. Rönnquist, A. Hodgson and A. Lucas, "JACK intelligent agents-summary of an agent infrastructure.," in *5th International conference on autonomous agents*, 2001.

[75] J. Hu, A. Saleem, S. You, L. Nordström, M. Lind and J. Østergaard, "A multi-agent system for distribution grid congestion management with electric vehicles.," *Eng. Appl. Artif. Intell.,* vol. 38, pp. 45-58, Feb. 2015.

[76] "JACK (Official Web Site) http://www.agent-software.com/products/," [Online].

[77] FIPA ACL Message Structure Specification - Standard SC00061G., http://www.fipa.org/, 2002.

[78] S. D. J. McArthur, E. M. Davidson, V. M. Catterson, A. L. Dimeas, N. D. Hatziargyriou, F. Ponci and T. Funabashi, "Multi-Agent Systems for Power Engineering Applications #x2014;Part II: Technologies, Standards, and Tools for Building Multi-agent Systems.," *IEEE Trans. Power Syst.,* vol. 22, no. 4, p. 1753–1759, Nov. 2007.

[79] FIPA SL Content Language Specification - Standard SC00008I, http://www.fipa.org/, 2002.

[80] "SEAS Ontology," SEAS Project, 2016. [Online]. Available: http://ci.emse.fr/seas/.

[81] "QUDT," AMES Research Center, [Online]. Available: http://www.qudt.org/.

[82] O. Shehory, "Advanced Artificial Intelligence - IBM Research Lab in Haifa," [Online]. Available: http://u.cs.biu.ac.il/~shechory/AdvancedAI2/Lecture2-2005.pdf.

[83] F. L. Bellifemine, G. Caire and D. Greenwood, Developing Multi-Agent Systems with JADE., Wiley, February 2007.

[84] H. Pezeshki, P. Wolfs and M. Johnson, "Multi-agent systems for modeling high penetration photovoltaic system impacts in distribution networks," in *Innovative Smart Grid Technologies Asia (ISGT), 2011 IEEE PES, pp. 1-8*, 2011.

[85] O. Shehory, "Architectural Properties of Multi-Agent Systems," CMU-RI-TR-98-28 - The Robotics Institute Carnegie Mellon University, Pittsburgh, Pennsylvania 15213, Dec. 1998.

[86] D. P. Buse and Q. H. Wu, IP Network-based Multi-agent Systems for Industrial Automation - Chapter 2: Agents, Multi-agent Systems and Mobile Code., Springer, 2007.

[87] G. Rimassa, F. Bellifemine and G. Caire, "Package jade.core.behaviours," [Online]. Available: http://jade.tilab.com/doc/api/jade/core/behaviours/package-summary.html.

[88] F. Y. S. Eddy, A multi agent system based control scheme for optimization of microgrid operation., Diss. Nanyang Technological University, Jan. 2016.

[89] M. Nikraz, G. Caire and P. A. Bahri, "A Methodology for the Analysis and Design of

Multi-Agent Systems using JADE.," *International Journal of Computer Systems Science & Engineering,* vol. 21, no. 2, pp. 99-116, 2006.

[90] E. Amicarelli, T. Tran and S. Bacha, "Multi-Agent System for Day-Ahead Energy Management of Microgrid," in *Power Electronics and Applications (EPE'16 ECCE Europe), 2016 18th European Conference on,* Karlsruhe, Sept. 2016.

[91] R. Rigo-Mariani, B. Sareni and X. Roboam, "Integrated optimal design of a smart microgrid with storage," *IEEE Transactions on Smart Grid,* vol. 8, no. 4, pp. 1762-1770, 2017.

[92] H. Kanchev, D. Lu, F. Colas, V. Lazarov and B. Francois, "Energy Management and Operational Planning of a Microgrid With a PV-Based Active Generator for Smart Grid Applications," *IEEE Trans. Ind. Electron.,* vol. 58, no. 10, p. 4583–4592, Oct. 2011.

[93] M. Yazdanian and A. Mehrizi-Sani, "Distributed control techniques in microgrids," *IEEE Transactions on Smart Grid ,* vol. 5, no. 6, pp. 2901-2909, 2014.

[94] H. Pezeshki, P. Wolfs and M. Johnson, "Multi-agent systems for modelling high penetration photovoltaic system impacts in distribution networks," in *Innovative Smart Grid Technologies Asia (ISGT), 2011 IEEE PES,* 2011.

[95] A. L. Dimeas and N. D. Hatziargyriou, "Operation of a Multiagent System for Microgrid Control," *IEEE Trans. Power Syst.,* vol. 20, no. 3, p. 1447–1455, Aug. 2005.

[96] T. Nagata and K. Okamoto, "A multi-agent based optimal operation for microgrid," in *2014 IEEE International Conference on Systems, Man and Cybernetics (SMC),* 2014.

[97] Z. Vale, P. T., P. I. and H. Morais, "MASCEM: electricity markets simulation with strategic agents," *IEEE Intelligent Systems,* vol. 26, no. 2, pp. 9-17, 2011.

[98] G. Santos, T. Pinto, H. Morais, M. S. T., F. P. I., F. R. and Z. Vale, "Multi-agent simulation of competitive electricity markets: Autonomous systems cooperation for European market modeling," *Energy Conversion and Management,* vol. 99, pp. 387-399, 2015.

[99] EDF, "Particuliers EDF," [Online]. Available: https://particulier.edf.fr/fr/accueil/contrat-et-conso/options/tempo.html.

[100] D. Sera, R. Teodorescu and P. Rodriguez, " PV panel model based on datasheet values," in *IEEE International Symposium on Industrial Electronics,* 2007.

[101] Y. Riffonneau, "Gestion des flux énergétique dans un système photovoltaïque avec stockage connecter au réseau – Application à l'habitat," Thèse de doctorat. Université Joseph-Fourier-Grenoble I, 2009.

[102] Y. Riffonneau, S. Bacha, F. Barruel and S. Ploix, "Optimal Power Flow Management for Grid Connected PV Systems With Batteries," *IEEE Transactions on Sustainable Energy,* vol. 2, no. 3, pp. 309-320, Jul. 2011.

[103] Z. Wu, H. Tazvinga and X. Xia, "Optimal schedule of photovoltaic-battery hybrid system at demand side," in *13th International Conference on Control Automation Robotics Vision (ICARCV), pp. 553-558,* 2014.

[104] "ABB Solar Inverters - PVI-10.0/12.0-I-OUTD 10 to 12 kW," [Online]. Available: https://library.e.abb.com/public/b0275636e28d013e85257e1f0078eb9e/PVI-10.0-12.0_BCD.00377_EN.pdf.

[105] B. Wichert, "PV-diesel hybrid energy systems for remote area power generation — A review of current practice and future developments.," *Renew Sustain Energy Reviews*, vol. 1, no. 3, p. 209–228, 1997.

[106] P. Haessig, " Dimensionnement et gestion d'un stockage d'énergie pour l'atténuation des incertitudes de production éolienne," Thèse de doctorat. École normale supérieure de Cachan-ENS Cachan, 2014.

[107] V. Pop, H. J. Bergveld, D. Danilov, P. P. Regtien and P. H. Notten, Battery management systems: Accurate state-of-charge indication for battery-powered applications, Springer Science & Business Media, 2008.

[108] N. G. Paterakis, O. Erdinç, A. G. Bakirtzis and J. P. S. Catalão, "Optimal Household Appliances Scheduling Under Day-Ahead Pricing and Load-Shaping Demand Response Strategies," *IEEE Trans. Ind. Inform.*, vol. 11, no. 6, pp. 1509-1519, Dec. 2015.

[109] D. Tsuanyo, Y. Azoumah, D. Aussel and P. Neveu, "Modeling and optimization of batteryless hybrid PV (photovoltaic)/diesel systems for off-grid applications," *Energy*, vol. 86, pp. 152-163, 2015.

[110] C. Kost, J. Mayer, J. Thomsen, N. Hartmann, C. Senkpiel and S. Philipps, "Levelized cost of electricity renewable energy technologies," Fraunhofer Institute for Solar Energy System ISE, 2013.

[111] R. Marchesi, P. Bombarda, A. Casalegno, L. Colombo and A. Rota, "Costi di produzione di energia elettrica da fonti rinnovabili. Report ordered by AEEG to Politecnico di Milano," Politecnico di Milano - Dipartimento di Energia, 2010.

[112] B. Zakeri and S. Syri, "Electrical energy storage systems: A comparative life cycle cost analysis," *Renew. Sustain. Energy Rev.*, vol. 42, p. 569–596, Feb. 2015.

[113] R. LUTHANDER, J. WIDÉN and D. NILSSON, "Photovoltaic self-consumption in buildings: A review," *Applied Energy*, vol. 142, pp. 80-94, 2015.

[114] J. Nocedal and S. J. Wright, Numerical Optimization, New York Berlin Heidelberg: Springer-Verlag , 1999.

[115] T. H. Cormen, C. E. Leiserson, R. L. Rivest and C. Stein, Introduction to Algorithms - Thirs edition, Cambridge, Massachusetts London, England: The MIT Press, 2009.

[116] L. Khachiyan, "Polynomial algorithms in linear programming," *USSR Computational Mathematics and Mathematical Physics*, vol. 20, pp. 53-72, 1980.

[117] G. B. Dantzig and M. N. Thapa, Linear Programming - 1: Introduction, Springer-Verlag New York, January 1997.

[118] R. Banos, F. Manzano-Agugliaro, F. Montoya, C. Gil, A. Alcayde and J. Gómezc, "Optimization methods applied to renewable and sustainable energy: A review," *Renewable and Sustainable Energy Reviews*, vol. 15, p. 1753–1766, 2011.

[119] T.-H. Wu, "A note on a global approach for general 0–1 fractional programming," *European Journal of Operational Research*, vol. 101, no. 1, pp. 220-223, 1997.

[120] H. D. Sherali and P. J. Driscoll, "Evolution and state-of-the-art in integer programming.," *Journal of Computational and Applied Mathematics*, vol. 124, no. 1, pp. 319-340, 2000.

[121] "GLPK - GNU Linear Programming Kit," [Online]. Available: https://www.gnu.org/software/glpk/.

[122] "CBC - COIN-OR Branch and Cut solver," [Online]. Available: https://www.coin-

or.org/Cbc/cbcuserguide.html.

[123] "SCIP - Solver for Constraint Integer Programming," [Online]. Available: http://scip.zib.de/ .

[124] H. Morais, P. Kadar, P. Faria, Z. A. Vale and H. M. Khodr, "Optimal scheduling of a renewable micro-grid in an isolated load area using mixed-integer linear programming," *Renewable Energy,* vol. 35, no. 1, pp. 151-156, 2010.

[125] R. J. Bessa, M. A. Matos, F. J. Soares and J. A. P. Lopes, "Optimized bidding of a EV aggregation agent in the electricity market," *IEEE Transactions on Smart Grid,* vol. 3, no. 1, pp. 443-452, 2012.

[126] X. Guan, Z. Xu and Q. S. Jia, "Energy-efficient buildings facilitated by microgrid," *Energy-efficient buildings facilitated by microgrid. IEEE Transactions on smart grid,* vol. 3, no. 1, pp. 243-252, 2010.

[127] D. S. L. T., S. M. and L. F., "Day-ahead microgrid optimal self-scheduling: Comparison between three methods applied to isolated dc microgrid," in *Industrial Electronics Society, IECON 2014-40th Annual Conference of the IEEE* , Oct. 2014.

[128] E. Amicarelli, Q. T. Tran and S. Bacha, "Optimization Algorithm for Microgrids Day-Ahead Scheduling and Aggregator Proposal," in *17th IEEE International Conference on Environmental and Electrical Engineering*, Milan, Italy, June 2017.

[129] E. Krüger, "Développement d'algorithmes de gestion optimale des systèmes de stockage énergétique basés sur des modèles adaptatifs," in *Thèse de doctorat. Université Joseph-Fourier-Grenoble I*, Grenoble, 2017.

[130] N. A. Luu, Q. T. Tran and S. Bacha, "Optimal energy management for an island microgrid by using dynamic programming method," in *IEEE Eindhoven PowerTech, pp. 1-6, .*, Eindhoven - Netherlands, 2015.

[131] S. Eshghi and R. Patil, "Optimal battery pricing and energy management for microgrids," in *2015 American Control Conference*, Chicago, IL, USA, July 2015.

[132] P. Haessig, H. B. Ahmed and M. B., "Energy storage control with aging limitation.," in *2015 IEEE Eindhoven PowerTech Conference*, Eindhoven, 2015.

[133] O. K. Aduda, T. Labeodan, W. Zeiler, G. Boxem and Y. Zhao, "Demand side flexibility: potentials and building performance implications," in *Sustainable Cities and Society,* 2016.

[134] R. Missaoui, H. Joumaa, S. Ploix and S. Bacha, "Managing energy smart homes according to energy prices: analysis of a building energy management system," *Energy and Buildings*, vol. 71, p. 155–67, 2014.

[135] "OPTI Toolbox," [Online]. Available: https://www.inverseproblem.co.nz/OPTI/index.php/Main/HomePage.

[136] Rte, Panorama de l'électricité renouvelable en 2016., 2016.

[137] M. Caramia and P. Dell´Olmo, Multi-objective Management in Freight Logistics - Increasing Capacity, Service Level and Safety with Optimization Algorithms, Springer London, 2008.

[138] G. Zhang, J. Lu and Y. Gao, Multi-Level Decision Making - Models, Methods and Applications, Springer-Verlag Berlin Heidelberg, 2015.

[139] Y. Censor, "Pareto Optimality in Multiobjective Problems," *Applied Mathematics and Optimization; Springer-Verlag New York Inc,* vol. 4, pp. 41-59, 1977.

[140] R. T. Marler and J. S. Arora, "Survey of multi-objective optimization methods for engineering," *Structural and multidisciplinary optimization,* vol. 26, no. 6, pp. 369-395, 2004.

[141] D. S., Foundations of bilevel programming., Springer Science & Business Media, 2002.

[142] G. Anandalingam and T. L. Friesz, "Hierarchical optimization: An introduction," *Annals of Operations Research,* vol. 34; Issue 1, p. 1–11, December 1992.

[143] "Loi n° 2000-108 du 10 février 2000 relative à la modernisation et au développement du service public de l'électricité.," https://www.legifrance.gouv.fr/affichTexte.do?cidTexte=JORFTEXT000000750321.

[144] "Gesetz über die Elektrizitäts und Gasversorgung; Energiewirtschaftsgesetz – EnWG," Bundesministeriums der Justiz und für Verbraucherschutz, Webpage: https://dejure.org/gesetze/EnWG/11.html, 2017.

[145] "Moderne Verteilernetze für Deutschland (Verteilernetzstudie).," Bundesministeriums für Wirtschaft und Energie (BMWi), Webpage: http://www.bmwi.de/Redaktion/DE/Publikationen/Studien/verteilernetzstudie.html, 2017.

[146] S. Huang, Q. Wu, Z. Liu and A. H. Nielsen, "Review of congestion management methods for distribution networks with high penetration of distributed energy resources," in *Innovative Smart Grid Technologies Conference Europe (ISGT-Europe), 2014 IEEE PES*, 2014.

[147] P. B. Andersen, J. Hu and K. Heussen, "Coordination strategies for distribution grid congestion management in a Multi-Actor, Multi-Objective Setting," *Proc. 2012 Eur. ISGT, Berlin, Germany.*.

[148] C. Zhang, Y. Ding, N. C. Nordentoft, P. Pinson and J. Østergaard, "FLECH - A Danish market solution for DSO congestion management through DER flexibility services.," *Journal of Modern Power Systems and Clean Energy,* vol. 2; No. 2, pp. 126-133, 2014.

[149] R. A. Verzijlbergh, L. J. D. Vries and Z. Lukszo, "Renewable energy sources and responsive demand. Do we need congestion management in the distribution grid?," *IEEE Transaction on Power Systems,* vol. 29, no. 5, pp. 2119-2128, September 2014.

[150] E. Amicarelli, Q. T. Tran and S. Bacha, "Flexibility Service Market for Active Congestion Management of Distribution Networks using Flexible Energy Resources of Microgrids," in *7th IEEE International Conference on Innovative Smart Grid Technologies*, Turin, Italy, September 2017.

[151] P. Cramton, "Alternative Pricing Rules," *Power Systems Conference and Exposition,* vol. IEEE PES, 2004.

[152] S. Oren, "When is Pay-as-Bid Preferable to Uniform Price in Electricity," *Power Systems Conference and Exposition,* vol. IEEE PES, 2004.

[153] S. S. Torbaghan, N. Blaauwbroek, P. Nguyen and M. Gibescu, "Local market framework for exploiting flexibility from the end users.," vol. 2016 13th International Conference on the In European Energy Market (EEM); IEEE, pp. pp. 1-6, 2016, June.

[154] S. A.-H. Soliman and A. A.-H. Mantawy, "Modern Optimization Techniques with

Applications in Electric Power Systems (Energy Systems)," Springer, 2011.

[155] "Standard: CENELEC - EN 50160; Voltage characteristics of electricity supplied by public electricity networks," European Committee for Electrotechnical Standardization, July 2010.

[156] C. E. M.-S. Ray Zimmerman, "http://www.pserc.cornell.edu/matpower/," Nov 1, 2016. [Online].

[157] J. Currie and D. I. Wilson, "OPTI: Lowering the Barrier Between Open Source Optimizers and the Industrial MATLAB User.," *Foundations of Computer-Aided Process Operations*, Georgia, USA, 2012.

[158] "https://www.cs.virginia.edu/~whitehouse/matlab/MatlabControl.java," [Online].

[159] L. Gkatzikis, I. Koutsopoulos and T. Salonidis, "The role of aggregators in smart grid demand response markets," in *" IEEE J. Sel. Areas Commun., vol. 31, no. 7, pp. 1247–1257, Jul. 2013.*.

[160] K. L. Anaya and M. G. Pollitt, "Finding the optimal approach for allocating and releasing distribution system capacity: Deciding between interruptible connections and firm DG connections," Energy Policy Research Group - Cambridge Working Paper in Economics, October 2013.

[161] T. Boehme, G. P. Harrison and A. R.Wallace, "Assessment of distribution network limits for non-firm connection of renewable generation.," *IET Renewable Power Generation*, vol. 4, no. 1, p. 64–74, Jan. 2010.

[162] "The Role of Distribution System Operators (DSOs) as Information Hubs," EURELECTRIC, Jun. 2010.

[163] G. Valtorta, A. D. SImone and C. N. e. al., "D3.1 ADDRESS Project- Prototypes and algorithms for network management, providing the signals sent by the DSOs to aggregators and the markets, enabling and exploiting Active Demand.," Enel Distribuzione; EDF-SA; Ziv; ABB; Univ. Siena; Univ. Cassino; Kema; Vattenfall, May 2011.

[164] E. D. Olivares, A. C. Cañizares and M. Kazerani, "A centralized energy management system for isolated microgrids," *IEEE Transactions on smart grid*, vol. 5, no. 4, pp. 1864-1875, 2014.

[165] K. Hajar, A. Hably, S. Bacha, A. Elrafhi and Z. Obeid, "Optimal centralized control application on microgrids. ,," in *2016 3rd International Conference on Renewable Energies for Developing Countries (REDEC) IEEE.*, Jul. 2016.

[166] A. G. Tsikalakis and N. D. Hatziargyriou, "Centralized control for optimizing microgrids operation.," *IEEE TRANSACTIONS ON ENERGY CONVERSION*, vol. 23, no. 1, pp. 1-8, Mar. 2008.

[167] Q. Jiang, M. Xue and G. Geng, "Energy Management of Microgrid in Grid-Connected and Stand-Alone Modes," *IEEE Transactions on Power Systems*, vol. 28, no. 3, pp. 3380-3389, August 2013.

[168] Y. Riffonneau, S. Bacha, F. Barruel, Y. Baghzouz and E. Zamaï, "Optimal reactive supervision of grid connected PV systems with batteries in real conditions.," *International Review of Electrical Engineering*, vol. 7, pp. 4607-4615, 2012.

[169] C. M. Rangel, D. Mascarella and G. Joos, "Real-Time Implementation & Evaluation of Grid-Connected Microgrid Energy Management Systems," in *2016 IEEE Electrical Power and Energy Conference (EPEC)*, 2016.

[170] C. Yin, H. Wu, F. Locment and M. Sechilariu, "Energy management of DC microgrid based on photovoltaic combined with diesel generator and supercapacitor," *Energy Conversion and Management,* vol. 132, pp. 14-27, 2017.

[171] D. Ocnasu, C. Gombert, B. S., R. D., F. Blache and S. Mekhtoub, "Real-time hybrid facility for the study of distributed power generation systems," *Revue des Energies Renouvelables,* vol. 11, no. 3, pp. 343-356, 2008.

[172] H. Gaztanaga, I. Etxeberria-Otadui, B. S. and R. D., "Real-time analysis of the control structure and management functions of a hybrid microgrid system," in *IEEE Industrial Electronics, IECON 2006-32nd Annual Conference on*, Nov. 2006.

[173] S. Bacha, D. Picault, B. Burger, I. Etxeberria-Otadui and J. Martins, "Photovoltaics in Microgrids: An Overview of Grid Integration and Energy Management Aspects," *IEEE Industrial Electronics Magazine,* vol. 9, no. 1, p. 33–46, Mar. 2015.

[174] B. Wang, M. Sechilariu and F. Locment, "Intelligent DC microgrid with smart grid communications: Control strategy consideration and design," *IEEE transactions on smart grid,* vol. 3, no. 4, pp. 2148-2156, 2012.

[175] V. Kostylev and A. Pavlovski, " Solar Power Forecasting Performance – Towards Industry Standards," in *Proceedings of the 1st International Workshop on the Interation of Solar Power into Power Systems,* Aarhus, Denmark, October 2011.

[176] M. Diagne, M. David, P. Lauret, J. Boland and N. Schmutz, "Review of solar irradiance forecasting methods and a proposition for small-scale insular grids," *Renewable and Sustainable Energy Reviews,* vol. 27, pp. 65-76, 2013.

[177] S. Pelland, J. Remund, J. Kleissl, T. Oozeki and K. D. Brabandere, "Photovoltaic and Solar Forecasting: State of the Art," IEA - PVPS Task 14, Report IEA-PVPS T14-01: 2013, 2013.

[178] S. S. Soman, H. Zareipour, O. Malik and P. Mandal, "A review of wind power and wind speed forecasting methods with different time horizons," in *IEEE North American Power Symposium (NAPS)*, 2010.

[179] A. K. Srivastava, A. S. Pandey and D. Singh, "Short-Term Load Forecasting Methods: A Review," in *International Conference on Emerging Trends in Electrical, Electronics and Sustainable Energy Systems (ICETEESES–16)*, 2016.

[180] E. Perez, H. Beltran, N. Aparicio and P. Rodriguez, "Predictive power control for PV plants with energy storage," *IEEE Transactions on Sustainable Energy,* vol. 4, no. 2, pp. 482-490, 2013.

[181] F. Barruel, H. Buttin, O. Wiss, S. Grehant and J. Merten, "PRISMES: The INES Microgrid Platform," in *23rd European Photovoltaic Solar Energy Conference and Exhibition,* Valencia, Spain, Se. 2008.

[182] "User‟s Manual. Programmable Photovoltaic Array Simulation System PVAS3; Austrian Institute Of Technology," Österreichisches Forschungs- und Prüfzentrum Arsenal GmbH, Vienna, Austria, 2009.

[183] R. Kadri, H. Andrei, P. J. Gaubert, T. Ivanovici, G. Champenois and P. Andrei, "Modeling of the photovoltaic cell circuit parameters for optimum connection model and real-time emulator with partial shadow conditions," *Energy,* vol. 42, no. 1, pp. 57-67, 2012.

[184] L. Bun, B. Raison, G. Rostaing, S. Bacha, A. Rumeau and A. Labonne, "Development of a real time photovoltaic simulator in normal and abnormal operations," in

IECON 2011-37th Annual Conference on IEEE Industrial Electronics Society, Nov. 2011.

[185] "OPC Unified Architecture," Standard, OPC Foundation - The Industrial Interoperability, [Online]. Available: https://opcfoundation.org/about/opc-technologies/opc-ua/.

[186] MathWorks, "OPC Toolbox," [Online]. Available: https://fr.mathworks.com/help/opc/.

[187] "Insertion de Productions et Equilibre des Réseaux de Distribution - Pojet IPERD," [Online]. Available: https://setis.ec.europa.eu/energy-research/sites/default/files/project/docs/fiche_projet_IPERD.pdf.

[188] "steadysun," [Online]. Available: http://steady-sun.com/fr/.

[189] S. Rodat, C. Tantolin, X. L. Pivert and S. Lespinats, "Daily forecast of solar thermal energy production for heat storage management," *Journal of Cleaner Production,* vol. 139, pp. 86-98, 2016.

[190] S. Lespinats, G. Stoops, T. Pistarino and X. L. Pivert, "Forecasting the solar production from a plurality of sources," in *29th European Photovoltaic Solar Energy Conference and Exhibition (PV SEC),* Amesterdam, Pays-Bas., Septembre 2014.

[191] "Italian Spot Electricity Market," Gestore dei Mercati Energetici, [Online]. Available: http://www.mercatoelettrico.org/en/mercati/mercatoelettrico/MPE.aspx.

[192] "EPEX SPOT Operational rules," EPEX SPOT, Paris, 2016. [Online]. Available: Available: https://www.epexspot.com/en/product-info/Trading.

[193] Testo integrato della disciplina del mercato elettrico, Rome: Gestore dei Mercati Energetici, 2015.

[194] E. Krüger, E. Amicarelli and Q. T. Tran, "Impact of European market frameworks on integration of photovoltaics in virtual power plants," in *IEEE 16th International Conference on Environment and Electrical Engineering (EEEIC),* Florence, Italy, 2016.

[195] "Proposal for a "Regulation of the European parliament and of the council on the internal market for electricity"," COM(2016) 861; final 2016/0379 (COD), Brussels, 2016.

[196] T. Bongrain, "Production photovoltaïque - Le foisonnement, un outil prometteur pour l'intégration de l'énergie solaire," *Le journal des energies renouvelables*, no. 230, Novembre-Décembre 2015 .

[197] D. F. Spulber, "Market microstructure and intermediation," *Journal of Economic Perspective,* vol. 10, no. 3, pp. 135-152, Summer 1996.

[198] CEI 0-16. Reference technical rules for the connection of active and passive consumers to the HV and MV electrical networks of distribution Company, Dec. 2012.

[199] E. COMMISSION, "COMMISSION REGULATION (EU) 2015/1222 of 24 July 2015 - Establishing a guideline on capacity allocation and congestion management," Official Journal of the European Union, Jul. 2015.

[200] "Aurora Trio Three-Phase Commercial Inverter - GENERAL SPECIFICATIONS," [Online]. Available: http://new.abb.com/power-converters-inverters/solar/string/three-phase/trio-20-0kw-27-6kw.

[201] "FIAMM/Sonick," [Online]. Available: http://www.fzsonick.com/en/.